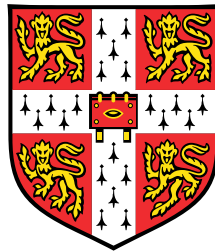


Functional heterogeneity of oligodendrocyte progenitor cells in the central nervous system



Sarah Förster

Department of Clinical Neurosciences
University of Cambridge

This dissertation is submitted for the degree of
Doctor of Philosophy

St. Catharine's College

April 2018

Summary

Functional heterogeneity of oligodendrocyte progenitor cells in the central nervous system

Sarah Förster

Oligodendrocytes (OL) are the myelinating cells of the central nervous system (CNS), whose function is to optimise neuronal transmission and preserve axonal integrity. Oligodendrocytes are derived from a stem cell population, called oligodendrocyte progenitor cells (OPCs). OPCs and their progeny (together termed oligodendrocyte lineage cells (OLCs)) have been implicated in the pathophysiology of various diseases including not only demyelinating diseases (eg. multiple sclerosis (MS) or Pelizaeus-Merzbacher disease (PMD)), but also psychiatric disorders (eg. schizophrenia or Rett syndrome (RTT)). Regardless of the type of disease, understanding the fundamental biology of OLCs is pivotal to develop therapeutic strategies.

In the mouse embryonic forebrain, OPCs are generated in consecutive waves from distinct brain regions along a spatiotemporal gradient; with ventral OPCs emerging before dorsal OPCs. The developmentally distinct OPCs, and their progeny, persist in the brain throughout life. To investigate whether ventrally and dorsally derived OLCs fulfil different functions in the adult brain, dorsally derived OPCs were ablated in development using a *Sox10*-driven diphtheria toxin fragment A (DTA) mouse model. As dorsally derived OPCs populate the cortex, locomotor coordination and cognition were investigated following dorsal OPC ablation. Mice ablated of the dorsal OPC population do not show a significant deficit in learning and attentional function. In contrast, ablated mice exhibit an impaired locomotor coordination, while general vigilance, gait, balance and sensation are comparable to control groups. The locomotor coordination disabilities are a result of alterations of brain, not spinal cord homeostasis, as only a minor number of OLCs in the spinal cord are affected by the ablation model. In addition, no signs of neuronal cell death or chronic inflammatory response were detected in response to the ablation. As the oligodendrocyte numbers are similar between control and ablated animals, the locomotor coordination phenotype can also not be explained by reduced numbers of oligodendrocytes.

However, clustering analysis following single-cell Drop-sequencing uncovered a heterogeneity of OL subpopulations in the brain. Whilst some OL subpopulations are of mixed developmental origin, others are exclusively formed by either ventrally or

dorsally derived OLs. In the absence of dorsal OPCs, ventral OPCs are not capable of forming dorsal oligodendrocyte subpopulations.

In conclusion, our results unveil the influence of the developmental origin of OPC on their differentiation potential and demonstrate a functional heterogeneity of oligodendrocyte subpopulations in homeostatic brain function.

Declaration

I hereby declare that except where specific reference is made to the work of others, the contents of this dissertation are original and have not been submitted in whole or in part for consideration for any other degree or qualification in this, or any other university. This dissertation is my own work and contains nothing which is the outcome of work done in collaboration with others, except as specified in the text and Acknowledgements. This dissertation contains fewer than 65,000 words including appendices, bibliography, footnotes, tables and equations and has fewer than 150 figures.

Sarah Förster

April 2018

Acknowledgements

I have heard many people saying how tough a PhD can be. Surely I also had these tough phases, but after (almost) completing it, I can say that I really enjoyed my PhD. This would have been impossible without such an intriguing project and the help of all the wonderful people in my life.

First and foremost I would like to acknowledge Robin. Originally I planned to carry out haematology research during my PhD. But an inspiring talk about the regenerative potential of OPCs made me go into the field of neuroscience (even though I had never even heard of an OPC before). I never regretted it even for a minute, which is mostly thanks to Robin. Thank you for your support, expertise and enthusiasm. Thank you for your trust, allowing me the freedom to explore and discover the field of OPC heterogeneity.

Thank you to the Wellcome Trust and St. Catharine's College for funding my work and research trips.

I also would like to thank Abbe for entrusting me with continuing her project, even though it turned out to be a different project than we originally planned. But there is no doubt, that your encouragement and help at the beginning gave me the best start possible. You definitely gave me the feeling that I will manage to do a PhD, which I am most grateful for. Your positive attitude to also appreciate the little progress in science inspired me, even after you left the lab.

Obviously this PhD would have been much tougher without the outstanding support of my wonderful lab members. You are an incredible group to work with, thank you for all the lab meetings, lunch time chats and pub nights. I am happy to be a member of the Franklin family. Even though you were all so important for the progress of my PhD, I would like to specifically mention Ludo, Natalia, Alerie, Mickey and Björn, who spent hours discussing my project and/or teaching me. Thanks a lot! Lots of you are not only my work colleagues, but became very good friends over the years. Ludo, Natalia, Alerie, Myf, Björn, Chris, Mickey and Roey, thank you so much for all the fun and laughs outside the lab. I will never forget our great travels to conferences,

dinners, college formals, pub nights and evenings in the lab. So many great adventures we shared.

I would like to thank my collaborators, Eosu, Christopher, Marcus, Elisa and David (and their supervisors) for their experimental support and fruitful discussions.

Almost on this day 4 years ago, I met Anna and Loukia for the first time. Thanks to the challenges we had to face in our first year, we became a strong team very soon after. I am immensely proud of what we have achieved in the past 4 years and could not have asked for better companions in the PhD programme. We were always wondering why they picked us, as we are so different. But I think they made the right choice allowing us to become such good friends. Looking forward to more celebrations, dinners and trips together!

A big part of my spare time I spent with my dear college friends Ciara, Helene, Vruti, Sebastian, Fran (I know you are not from Catz, but you kind of are now) and Anna (you belong to the Catz group as well). I had so much fun exploring college life with you. Whether it was college sport, parties or formals; I always had an enjoyable time. Thank you for teaching me various aspects of British culture, language and TV; I had to catch up a lot. In addition I would like to especially thank Fran for putting up with every day during my write up period. So happy I had somebody to talk to in the evening to participate in normal life (this is obviously not the only reason why sharing a flat with you is great). I am sure you are also glad to hear that the kitchen will be free of computers again!

It would be wrong to not acknowledge my friends from my undergraduate studies, Lissi, Vroni, Olga, Claudia, Julia, Jana, Sandra, Moritz and Jakob. Even though they were obviously not able to support me on a daily basis, knowing that I had their friendship and support behind me meant a lot. The trips to meet up with all of you empowered me, allowing me to come back to science with a fresh mind. We started this crazy journey of becoming scientists together, and I am very proud of what we all have achieved.

Last but not least, I would like to especially acknowledge my parents. Without their outstanding support I would not be where I am now. Mama, Papa, vielen Dank für eure Unterstützung in all den Jahren. Ohne euch wäre der PhD nicht möglich gewesen. Zu wissen, dass ihr immer für mich da seid, mir helft, wo ihr nur könnt, mir Mut zuspricht in schlechten Zeiten und immer an mich glaubt, gibt mir mehr Kraft, als ihr euch vorstellen könnt. Der PhD ist auch euer Werk.

Abstract

Oligodendrocytes (OL) are the myelinating cells of the central nervous system (CNS), whose function is to optimise neuronal transmission and preserve axonal integrity. Oligodendrocytes are derived from a stem cell population, called oligodendrocyte progenitor cells (OPCs). OPCs and their progeny (together termed oligodendrocyte lineage cells (OLCs)) have been implicated in the pathophysiology of various diseases including not only demyelinating diseases (eg. multiple sclerosis (MS) or Pelizaeus-Merzbacher disease (PMD)), but also psychiatric disorders (eg. schizophrenia or Rett syndrome (RTT)). Regardless of the type of disease, understanding the fundamental biology of OLCs is pivotal to develop therapeutic strategies.

In the mouse embryonic forebrain, OPCs are generated in consecutive waves from distinct brain regions along a spatiotemporal gradient; with ventral OPCs emerging before dorsal OPCs. The developmentally distinct OPCs, and their progeny, persist in the brain throughout life. To investigate whether ventrally and dorsally derived OLCs fulfil different functions in the adult brain, dorsally derived OPCs were ablated in development using a *Sox10*-driven diphtheria toxin fragment A (DTA) mouse model. As dorsally derived OPCs populate the cortex, locomotor coordination and cognition were investigated following dorsal OPC ablation. Mice ablated of the dorsal OPC population do not show a significant deficit in learning and attentional function. In contrast, ablated mice exhibit an impaired locomotor coordination, while general vigilance, gait, balance and sensation are comparable to control groups. The locomotor coordination disabilities are a result of alterations of brain, not spinal cord homeostasis, as only a minor number of OLCs in the spinal cord are affected by the ablation model. In addition, no signs of neuronal cell death or chronic inflammatory response were detected in response to the ablation. As the oligodendrocyte numbers are similar between control and ablated animals, the locomotor coordination phenotype can also not be explained by reduced numbers of oligodendrocytes.

However, clustering analysis following single-cell Drop-sequencing uncovered a heterogeneity of OL subpopulations in the brain. Whilst some OL subpopulations are

of mixed developmental origin, others are exclusively formed by either ventrally or dorsally derived OLs. In the absence of dorsal OPCs, ventral OPCs are not capable of forming dorsal oligodendrocyte subpopulations.

In conclusion, our results unveil the influence of the developmental origin of OPC on their differentiation potential and demonstrate a functional heterogeneity of oligodendrocyte subpopulations in homeostatic brain function.

Table of contents

Acknowledgements	vii
Abstract	ix
List of figures	xv
List of tables	xvii
1 Introduction	1
1.1 The cells of the central nervous system	1
1.1.1 Neurons	1
1.1.2 Astrocytes	3
1.1.3 Microglia	5
1.2 Oligodendrocyte lineage cells (OLCs)	6
1.2.1 Markers and characteristics of OLCs	6
1.2.2 Functions of OPCs	9
1.2.3 Functions of oligodendrocytes	11
1.3 Myelination	14
1.3.1 Developmental myelination	15
1.3.2 Myelin plasticity	22
1.3.3 Myelination in ageing	25
1.4 Heterogeneity of oligodendrocyte lineage cells	28
1.4.1 OPC heterogeneity	28
1.4.2 Oligodendrocyte heterogeneity	34
1.5 Regulation of neuronal conduction and transmission	37
1.6 The role of OLCs in diseases	39
1.7 Objectives	42

2	Materials and Methods	45
2.1	Animal models	45
2.2	Animal husbandry	47
2.3	Isolation of primary cells	47
2.4	Flow cytometry	48
2.5	Western Blot	49
2.6	Perfusion and Dissection	50
2.7	Preparation of cryosections	50
2.8	Immunohistochemistry	51
2.9	Confocal Microscopy and Image Analysis	52
2.10	Resin embedding and preparation of semi-thin sections	53
2.11	Electron Microscopy (EM)	53
2.12	Magnetic resonance imaging (MRI)	53
2.13	10X Genomics Single-Cell RNA-Sequencing	54
2.14	Behavioural experiments	56
2.14.1	Cohort Breeding	56
2.14.2	Assessment of general vigilance	57
2.14.3	Assessment of locomotor coordination	58
2.14.4	Assessment of sensory function	60
2.14.5	Assessment of cognitive function	60
2.15	Statistics	63
3	Functional consequences of dorsal OPC ablation <i>in vivo</i>	67
3.1	Mouse models	67
3.2	Efficiency of dorsal OPC ablation model	69
3.3	Ablation of dorsal OPCs causes locomotor disabilities in adult mice	71
3.4	Ablation of dorsal OPCs does not result in cognitive impairment in adult mice	79
3.5	Conclusion and discussion chapter 3	83
4	Off-target effects of the DTA ablation system	87
4.1	Neurons are not affected by the DTA ablation model	87
4.2	Ablation of dorsal OPCs does not influence axonal health	88
4.3	Astrocytes are not affected by the DTA ablation model	90
4.4	Microglia are not affected by dorsal OPC ablation	90
4.5	<i>Emx1</i> ⁺ cells are present in the spinal cord	92
4.6	Conclusion and discussion chapter 4	94

5	Effects of DTA ablation on oligodendrocyte lineage cells	97
5.1	Ablation of dorsal OPCs leads to an expansion of OPCs, but not oligodendrocytes	97
5.2	Ablation of dorsal OPCs does not cause white matter hypomyelination	99
5.3	Conclusion and discussion chapter 5	102
6	Intrinsic heterogeneity of ventral and dorsal OLCs	105
6.1	Ventral and dorsal OPCs have the same propensity to differentiate . .	105
6.2	Differences in gene expression of ventral and dorsal oligodendrocytes	109
6.3	Ventral and dorsal oligodendrocytes form similar myelin	110
6.4	Ventral and dorsal oligodendrocytes form similar nodal structures . .	114
6.5	Conclusion and discussion chapter 6	116
7	Discussion	119
7.1	Importance of studying OLC heterogeneity	119
7.2	Heterogeneity of the oligodendrocyte lineage	121
7.2.1	Ventral and dorsal oligodendrocytes are functionally heterogeneous	121
7.2.2	How do developmentally distinct oligodendrocytes acquire intrinsic heterogeneity?	122
7.3	Functional heterogeneity of other cell lineages in the brain	123
7.3.1	Heterogeneity of astrocytes	123
7.3.2	Heterogeneity of neurons	123
7.3.3	Common developmental origin of neurons and glia cells . . .	124
7.4	Does the heterogeneity of developmentally distinct oligodendrocytes cause the locomotor phenotype?	125
7.5	Can general effects of the ablation model cause the locomotor phenotype? 131	
7.5.1	Increase of OPCs might contribute to the locomotor phenotype	131
7.5.2	Off target effects of the DTA ablation system	133
7.6	Summary - Working model	133
	References	135
	Appendix 1	157

List of figures

1.1	Modulation of neuronal transmission by astrocytes	4
1.2	Modulation of neuronal transmission by microglia	6
1.3	The oligodendrocyte lineage: OPCs differentiate into mature oligodendrocytes	8
1.4	Remyelination	11
1.5	Modulation of neuronal transmission by oligodendrocyte lineage cells	12
1.6	Transcription factors and signalling pathways involved in OPC differentiation	16
1.7	The process of myelination	18
1.8	Age-dependent changes of myelination	26
1.9	Developmental origin of OPCs	29
1.10	Modulation of neuronal transmission by the complex interaction network of brain cells	38
2.1	Breeding strategies of animal cohorts	56
2.2	Experimental set-up of behavioural experiments	62
2.3	Test parameters continuous performance test	64
3.1	<i>Emx1-Cre/Sox10-DTA</i> mouse model	68
3.2	<i>Emx1-Cre/Sox10-tdTomato</i> mouse model	68
3.3	Whole brain ablation efficiency of <i>Emx1-Cre/Sox10-DTA</i> model	69
3.4	Forebrain ablation efficiency of <i>Emx1-Cre/Sox10-DTA</i> model	71
3.5	Ablation of dorsal OPCs causes locomotor impairments	73
3.6	Ablation of dorsal OPCs specifically causes locomotor coordination impairment	76
3.7	Locomotor coordination impairment phenotype is subtle	78
3.8	No sustained attention deficits in ablated animals	81
3.9	Increasing the difficulty level of rCPT did not show a sustained attention deficits in ablated animals	83

4.1	Neuronal number is unaffected by dorsal OPC ablation	88
4.2	Axonal health is unaffected by dorsal OPC ablation	89
4.3	WM astrocyte numbers are unaffected by dorsal OPC ablation	92
4.4	Microglia numbers are unaffected by dorsal OPC ablation	93
4.5	<i>Emx1</i> ⁺ cells are present in the spinal cord	94
5.1	Expansion of OPCs in ablated animals	98
5.2	Oligodendrocyte numbers are unaffected in ablation model	100
5.3	Normal myelination in WM tracts of ablated animals	101
6.1	Ventral and dorsal OPCs have the same propensity to form oligodendrocytes	107
6.2	Ventral and dorsal OPCs have the same propensity to retain OPC fate	108
6.3	Ventral and dorsal oligodendrocytes show distinct gene expression profiles	112
6.4	Ventral and dorsal oligodendrocytes form similar myelin	114
6.5	Ventral and dorsal oligodendrocytes form similar nodal structures	115
7.1	Neuro- and gliogenesis in embryonic progenitor zones	124
7.2	Function of dorsally derived oligodendrocytes	126

List of tables

1.1	Proportion of new-born oligodendrocytes in the adult brain	23
1.2	Heterogeneity of developmentally distinct OPCs	31
1.3	Heterogeneity of white and grey matter OPCs	33
1.4	Age-dependent factors of myelination failure	40
1.5	Involvement of OPCs in psychiatric disorders	42
2.1	Mouse lines	45
2.2	Flow cytometry antibodies	48
2.3	Western blot antibodies	50
2.4	Immunohistochemistry antibodies	52
4.1	Expression pattern of <i>Sox10</i> in the CNS	96
4.2	Expression pattern of <i>Emx1</i> in the CNS	96
7.1	Formulation of PFA	157
7.2	Formulation of glutaraldehyde	157
7.3	Formulation of Half	158
7.4	Formulation of transport medium	159
7.5	Formulation of dissociation solution	159
7.6	Formulation of trituration solution	159
7.7	Formulation of mowiol	159
7.8	Formulation of resin	160
7.9	Formulation of western blot running buffer	160
7.10	Formulation of western blot transfer buffer	160

Chapter 1

Introduction

1.1 The cells of the central nervous system

The central nervous system (CNS) is primarily composed of two main categories of cells, neurons and glia cells. Neurons are capable of initiating and transmitting electrical signals (or action potentials) coding for information, representing the foundation for any locomotor or cognitive activity executed by the CNS. Consequently, neurons were believed to be the only functional cell type in the CNS up until the nineteenth century. However, in 1856, Rudolf Virchow described a population of connective cells in the CNS which he termed glia cells (cited in (Somjen, 1988)). Following the development of various new staining techniques, Santiago Ramon y Cajal and his student Pio del Rio Hortega subsequently divided glia cells into astrocytes, microglia and oligodendrocytes (del Río Hortega, 1928). The latest glia cell type, the oligodendrocyte progenitor cell (OPC), was identified by Martin Raff and colleagues in 1983 (Raff, Miller, & Noble, 1983). Since the discovery of glia cells, their importance has ascended from a more supportive role as brain 'glue' to the status of key players in CNS physiology. Indeed, numerous studies have highlighted the importance of the interaction between glia cells and neurons to optimise neuronal action potential transmission, thereby facilitating ideal CNS function. As malfunction of any glia cell type leads to neurological diseases, the detailed understanding of how glia cells optimise neuronal function is pivotal to the development of therapeutic strategies.

1.1.1 Neurons

Neurons are electrically excitable cells that transmit information via electrical and chemical signals. In a non-activated state, ion pumps ensure a constant resting mem-

brane potential of -70mV by shuttling sodium ions outwards, and simultaneously potassium ions into the cell. In addition to ion pumps, ion channels gating the flow of sodium and potassium ions are located in the neuronal cell membrane. Upon an activating stimulus, including pressure, stretch and chemical substances, an action potential is initiated by sodium ion influx causing a depolarisation of the neuron. Subsequent repolarisation is achieved by an outflow of potassium ions, eventually leading to a reestablishment of the membrane resting potential. The action potential is propagated along the axon towards the synapse by the depolarisation of neighbouring ion channels, ultimately resulting in the release of neurotransmitters to either activating or inhibiting adjacent neurons (Hodgkin & Huxley, 1990).

Neurons are an incredibly heterogeneous cell population, existing in a number of different shapes and sizes, traditionally classified either by their morphology or function. The great heterogeneity of neurons is established during development when neurons are specified from radial glia cells, a stem cell population in the ventricular zone of the CNS (Miyata et al., 2004; Noctor, Martínez-Cerdeño, Ivic, & Kriegstein, 2004). Different types of neurons are generated in distinct locations in the ventricular zone due to gradients of morphogens (such as sonic hedgehog (SHH) or bone morphogenic proteins (BMPs)) establishing territories of transcription factor expression, each associated with specification of a particular type of neurons (Briscoe, Pierani, Jessell, & Ericson, 2000). In addition to location, timing of neuronal specification contributes to neuronal heterogeneity in the CNS (Desai & McConnell, 2000).

In the adult, neurons are classically categorised based on their morphology into type 1 and type 2 neurons. Whilst type 1 neurons have a long projection axon (eg. spinal motor neuron), type 2 neurons only have a short axon projecting locally (eg. granule cell). Additionally, other neurons with distinct locations and shapes exist in the CNS, including basket, pyramidal and Purkinje cells. To identify a specific neuron subtype *in vivo*, the spiking pattern can be recorded electrophysiologically. In general, neurons are subdivided into regular (tonic) spiking, bursting or fast spiking. Functionally neurons can be classified according to the direction of information transmission into afferent, efferent and interneurons. Afferent (or sensory neurons) convey information from tissues and organs into the CNS, whereas efferent neurons send signals in the opposite direction. Interneurons connect neurons within a specific CNS region. Furthermore neurons can be classified by their effect on other neurons into excitatory neurons, releasing glutamate (an activating neurotransmitter) or inhibitory neurons, releasing gamma-aminobutyric acid (GABA) (an inhibiting neurotransmitter). Altogether about 90% of the neurons present in the CNS fall into these two categories, whereas the remaining neurons release other neurotransmitters such as acetylcholine

or glycine. However, the above mentioned classifications cannot fully describe the complexity of neurons within the CNS. Novel techniques, such as Patch-seq, combining the analysis of molecular, morphological and physiological characteristics of a single cell, are helping to reveal the true heterogeneity of the neurons (Fuzik et al., 2016).

In order to execute highly complex locomotor and cognitive tasks, neurons form sophisticated networks in the CNS. The neuronal transmission within each network needs to be precisely timed to optimise CNS function. Glia cells and microglia play an important role in preserving neuronal health and integrity as well as tweaking neuronal transmission (see Section 1.1.2, Section 1.1.3 and Section 1.2.3).

1.1.2 Astrocytes

Astrocytes represent the most abundant type of glia cells, populating the whole CNS in a non-overlapping manner (Bushong, Martone, Jones, & Ellisman, 2002). Astrocytes are localised in close proximity to both blood vessels and neuronal synapses (forming the so-called tripartite synapse), enabling them to fulfil unique functions due to their special interactions in the CNS (Figure 1.1).

Their close proximity to blood vessels results in an important role for astrocytes in providing nutrients and antioxidants to neurons (Allaman, Bélanger, & Magistretti, 2011). For example, astrocytic glycogen use can sustain neuronal activity during hypoglycemia and periods of high neuronal activity (Suh et al., 2007). In addition, due to providing a link between neuronal synapses and blood vessels, astrocytes are capable of regulating local blood flow in response to neuronal activity. By releasing prostaglandins (PGE), nitric oxide (NO), and arachidonic acid (AA) from astrocytes, CNS blood vessel diameter is modulated (Attwell et al., 2010; Gordon, Howarth, & Macvicar, 2011). Lastly, even though the blood brain barrier (BBB) is established before the formation of astrocytes in the CNS, maintenance of the BBB in an adult animal is significantly influenced by astrocytes (Daneman & Prat, 2015) (Figure 1.1).

Astrocytes play a key role in the modulation of neuronal transmission through various mechanisms (W. S. Chung, Allen, & Eroglu, 2015). Firstly, astrocytes take part in neurotransmitter recycling, for example by taking up glutamate, released during neuronal transmission, thus preventing neuronal excitotoxicity (N. B. Hamilton & Attwell, 2010). After the uptake into astrocytes, glutamate is converted into its precursor glu-

tamine and recycled back to synapses for reconversion into active transmitters (van den Berg & Garfinkel, 1971; Ottersen, Zhang, & Walberg, 1992; Rothman, De Feyter, de Graaf, Mason, & Behar, 2011). Secondly, astrocytes also directly regulate synaptic transmission (W. S. Chung et al., 2015) through the release of gliotransmitters (glutamate, GABA, D-serine) from astrocytes in response to neuronal activity (W. S. Chung et al., 2015). Finally, astrocytes take part in synaptogenesis, by releasing molecular signals such as thrombospondin (Christopherson et al., 2005) and synaptic pruning, by tagging synapses for elimination by microglia (Stevens et al., 2007; Schafer et al., 2012) (Figure 1.1).

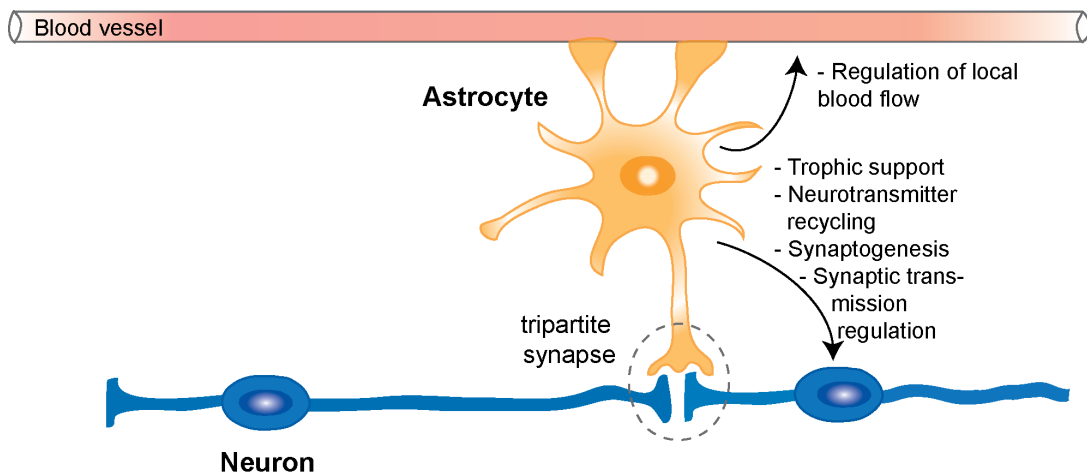


Fig. 1.1 Modulation of neuronal transmission by astrocytes.

Since the late nineteenth century, astrocytes have been divided into two main subtypes, protoplasmic and fibrous astrocytes based on their distinct morphology, location and gene expression. Protoplasmic astrocytes reside in the grey matter and do not express much glial fibrillary acidic protein (GFAP). The processes of protoplasmic astrocytes have been found in close contact to synapses and blood vessels. In comparison, fibrous white matter astrocytes express GFAP and their processes interact with nodes of Ranvier and blood vessels (Ramón y Cajal, n.d.; Eng, Vanderhaeghen, & Gerstl, 1970). As GFAP is not expressed by all astrocytes, other markers including glutamine synthetase (GS) (Norenberg, 1979), S100 calcium-binding protein β (S100 β) (Landry, Ivy, Dunn, Marks, & Brown, 1989), hepatic and glial cell adhesion molecule (HEPACAM) (Y. Zhang et al., 2016) and aldehyde dehydrogenase 1 family member L1 (ALDH1L1) (Neymeyer, Tephly, & Miller, 1997) are also used to identify astrocytes in the CNS. Besides the two classic astrocyte types, more specialised astrocytes can be found, including Bergmann glia in the cerebellum or Müller cells of the retina.

Further gene expression studies revealed a developmental heterogeneity of astrocytes, with regionally allocated astrocyte subtypes in the CNS fulfilling distinct functions to support neuronal transmission (Hochstim, Deneen, Lukaszewicz, Zhou, & Anderson, 2008; Tsai et al., 2012; Molofsky et al., 2014) (see Discussion 7.3.1).

1.1.3 Microglia

Microglia are specialised myeloid cells residing in the CNS, accounting for 5-20% of the total non-neuronal cell population within the CNS parenchyma. Even though originally defined as a type of glial cell, microglia are very different from astrocytes and oligodendrocytes, especially with respect to their developmental origin. Originating from primitive macrophages in the yolk sac (Ginhoux et al., 2010; Kierdorf et al., 2013; Schulz et al., 2012), which enter the blood circulation and colonise the neuroepithelium, microglia appear in the CNS from embryonic day (E) 9.0 (Alliot, Godin, & Pessac, 1999).

The main function of microglia is the surveillance of the CNS environment to detect perturbations. When identifying signs of pathogenic invasion or tissue damage, microglia become activated, change their morphology from a ramified to a more spindle shape, and secrete an array of immunomodulatory molecules, helping to resolve the injury. Additionally, microglia contribute to CNS homeostasis by phagocytosis of damaged cells, DNA fragments, protein aggregates and foreign material (reviewed in (Ransohoff & El Khoury, 2015)). The immunomodulatory function in homeostasis is unique to microglia cells, hence presenting another distinguishing factor between microglia and true glia cells (astrocytes and oligodendrocytes). Recent studies revealed that the surveillance of microglia goes beyond their well established immune functions, as they play fundamental roles in shaping neuronal circuits in the uninjured CNS. In steady state, microglia constantly monitor their environment by extending processes to neuronal synapses, contributing to synapse remodelling and pruning (Tremblay, Lowery, & Majewska, 2010; Paolicelli et al., 2011; Schafer et al., 2012). Furthermore, neuronal excitability is controlled by microglia through the neuronal anion transmembrane gradient (Coull et al., 2005). Microglia have been also shown to regulate the neuronal progenitor cell (NPCs) pool by engulfing NPCs during development (Cunningham, Martínez-Cerdeño, & Noctor, 2013). Lastly, microglia have been shown to secrete neurotrophic factors that protect neurons from death after injury (Lalancette-Hébert, Gowing, Simard, Weng, & Kriz, 2007) (Figure 1.2).

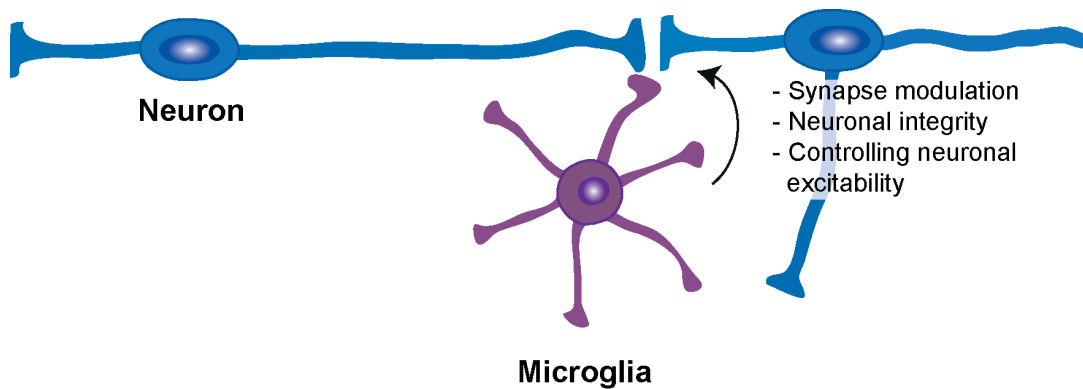


Fig. 1.2 **Modulation of neuronal transmission by microglia.**

In early studies on microglia, regional differences in their density and morphology had been noticed. As an example, the hippocampus is populated by five times as many microglia when compared to the cerebellum and its resident microglia are more ramified in comparison to all other assessed brain regions (Lawson, Perry, Dri, & Gordon, 1990). In addition to morphological heterogeneity, differences in gene and protein expression were demonstrated in microglia from the same brain region (de Haas, Boddeke, & Biber, 2008; Keren-Shaul et al., 2017; Grabert et al., 2016). Microglia also vary in their proliferative capacity *in vitro*, with the fold expansion of microglia isolated from the subventricular zone (SVZ) being 20 times greater than microglia isolated from any other brain regions (Marshall, Demir, Steindler, & Laywell, 2008).

1.2 Oligodendrocyte lineage cells (OLCs)

1.2.1 Markers and characteristics of OLCs

In the adult CNS, OPCs are distributed evenly across both white and grey matter, estimated to make up 5-8% of all brain cells (Pringle, Mudhar, Collarini, & Richardson, 1992) (Figure 1.3). The term oligodendrocyte progenitor cell does not describe its full potential. Instead, OPCs should be called adult stem cells because they can (1) self-renew, (2) have the ability to maintain a cell population throughout life and (3) are multipotent (Crawford, Stockley, Tripathi, Richardson, & Franklin, 2014). OPCs have been shown to demonstrate lifelong proliferation (Young et al., 2013) and to sustain constant numbers throughout life (Rivers et al., 2008), even after an injury of the oligodendrocyte lineage, demonstrating the self-renewal and lineage-maintaining capacity of OPCs. *In vitro* studies demonstrated that OPCs can give rise to astrocytes

and oligodendrocytes (Raff, Miller, & Noble, 1983), however it was shown that OPCs almost exclusively form oligodendrocytes *in vivo* (Rivers et al., 2008; Young et al., 2013; Hughes, Kang, Fukaya, & Bergles, 2013). In response to a demyelinating injury, OPCs can also differentiate into Schwann cells *in vivo* (Zawadzka et al., 2010).

OPCs are identified by a variety of molecular markers including general neural progenitor markers (Nestin and Vimentin (Lendahl, Zimmerman, & McKay, 1990)) or OPC specific surface molecules A2B5, neural/glia antigen 2 (NG2), myelin transcription factor 1 (MYT-1) and platelet derived growth factor receptor α (PDGFR α) (Raff, Abney, Cohen, Lindsay, & Noble, 1983; J. G. Kim & Hudson, 1992; Redwine & Armstrong, 1998; Sim, Zhao, Penderis, & Franklin, 2002). It should be noted that the majority of these markers are also expressed in other cell types, therefore a combination of markers is essential to unambiguously identify an OPC (Figure 1.3).

The differentiation of OPCs into oligodendrocytes is gradual; gene expression changes cause OPCs to form pre-myelinating oligodendrocytes (Trapp, Nishiyama, Cheng, & Macklin, 1997). Pre-myelinating oligodendrocytes are morphologically distinguished from OPCs by their increased number of processes. To identify a pre-myelinating oligodendrocyte, the surface markers ectonucleotide pyrophosphatase/phosphodiesterase 6 (ENPP6) (Xiao et al., 2016), O4 (Sommer & Schachner, 1981) and 2',3'-cyclic-nucleotide 3'-phosphodiesterase (CNPase) (Poduslo & Norton, 1972) can be used. Pre-myelinating oligodendrocytes form progressively more complex process networks and eventually mature myelin sheaths, thus becoming a mature oligodendrocyte (Figure 1.3). Mature sheath-forming oligodendrocytes typically express the marker proteins myelin basic protein (MBP) (Sternberger, Itoyama, Kies, & Webster, 1978), myelin/oligodendrocyte glycoprotein (MOG) (Linnington, Webb, & Woodhams, 1984), myelin-associated glycoprotein (MAG) (Sternberger, Quarles, Itoyama, & Webster, 1979), myelin regulatory factor (MYRF) (Cahoy et al., 2008) and proteolipid protein (PLP) (Sobel, Greer, Isaac, Fondren, & Lees, 1994) (Figure 1.3).

Other markers such as the transcription factors oligodendrocyte lineage transcription factor 2 (OLIG2) (Zhou, Wang, & Anderson, 2000) and SRY-related HMG-box10 (SOX10) (Kuhlbrodt et al., 1998; Stolt et al., 2002) are expressed by all OLCs, namely OPCs, oligodendrocytes and all differentiation stages in between. Therefore, these markers are termed oligodendrocyte lineage markers, and do not allow the distinction of a specific oligodendrocyte lineage cell type.

The close contact between oligodendrocytes and axons through the myelin sheath enables oligodendrocyte lineage cells to play an exceptional role in the modulation of neuronal conduction and transmission (see Section 1.2.2 and Section 1.2.3).

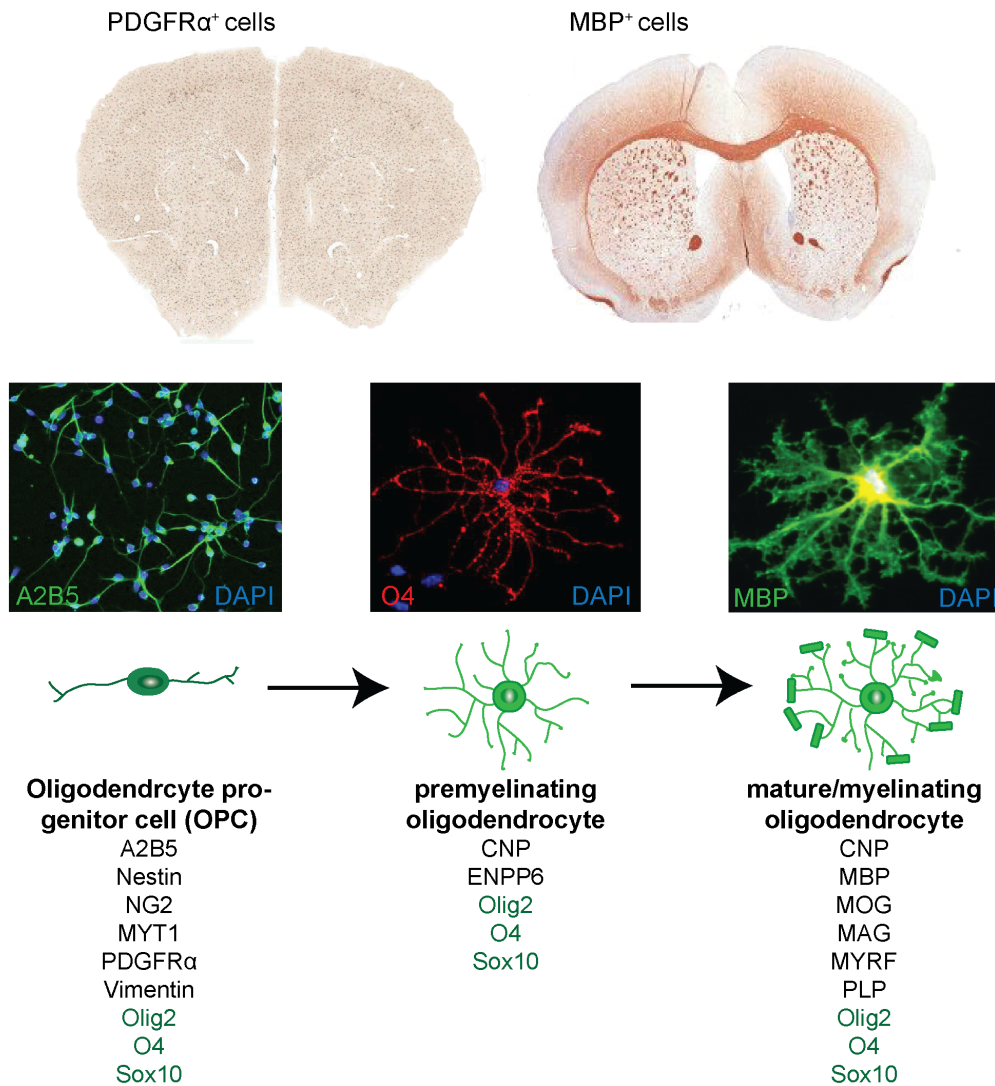


Fig. 1.3 OPC differentiation into mature oligodendrocytes. (Top left) *In situ* hybridisation for PDGFR α illustrating the distribution of PDGFR α positive OPCs in the adult CNS. OPCs are evenly spread across the white and grey matter. Image source: Allen Brain Atlas, mouse brain. (Top right) *In situ* hybridisation for MBP illustrating the distribution of MBP positive mature oligodendrocytes in the adult CNS. The majority of mature oligodendrocytes populate the white matter areas including the corpus callosum, anterior commissure and optic nerve. Image source: Allen Brain Atlas, mouse brain. (Bottom) Schematic representation of OPC differentiation. Commonly used marker proteins are indicated below the individual differentiation steps. Biomarkers highlighted in green label the whole oligodendrocyte lineage

1.2.2 Functions of OPCs

The fact that OPC numbers remain stable throughout life led to the hypothesis that OPCs fulfil additional functions in the brain besides only providing a source of oligodendrocytes in development. Indeed, OPCs also have a very important function in remyelination, a process restoring functional myelin sheaths after myelin loss. In response to oligodendrocyte injury or death, local resident microglia and astrocytes recognise the injury and release a plethora of immunomodulatory molecules, activating adjacent cells, including OPCs. OPC activation is associated with an increased sensitivity to growth factors as well as changes in gene expression (eg. *Nkx2.2* (Fancy, Zhao, & Franklin, 2004) and *Sox2* (Zhao et al., 2015)). Subsequently, OPCs proliferate, migrate to the site of CNS damage and differentiate into oligodendrocytes capable of creating new myelin sheaths, representing a robust ability of the CNS to repair itself (reviewed in (Franklin & Ffrench-Constant, 2017)) (Figure 1.4).

In addition to providing a source of oligodendrocytes under physiological and pathophysiological conditions, OPCs might play a role in regulating the plasticity of neuronal synapses through neuron-OPC synapses. After the first postnatal week, glutamatergic and GABAergic synapses between neurons and OPCs can be seen in white matter (Kukley, Capetillo-Zarate, & Dietrich, 2007; Ziskin, Nishiyama, Rubio, Fukaya, & Bergles, 2007) and grey matter (*inter alia*: (Bergles, Roberts, Somogyi, & Jahr, 2000; Mangin, Kunze, Chittajallu, & Gallo, 2008; Y. Tanaka et al., 2009; Mangin, Li, Scafidi, & Gallo, 2012)) brain regions. Studies have shown that nearly all OPCs form up to 70 synaptic connections with neurons (Lin et al., 2005), which are lost upon differentiation into oligodendrocytes (De Biase, Nishiyama, & Bergles, 2010; Kukley, Nishiyama, & Dietrich, 2010), indicating that the functional role of these neuron-glia synapses is specific to the OPC population. It is well established that neuronal activity, and concomitantly released neurotransmitters, modulate OPC behaviour (Yuan, Eisen, McBain, & Gallo, 1998; Káradóttir, Hamilton, Bakiri, & Attwell, 2008; Gibson et al., 2014), demonstrating a potential mechanism by which myelination is regulated in the CNS (see Section 1.3.1). While the role of synaptic input of neurons onto OPCs is beginning to be understood, the question remains whether OPCs also influence neuronal function via the synapse. Recently, Sakry and colleagues demonstrated a bidirectional cross-talk between neurons and OPCs for the first time (Sakry et al., 2014). In detail, under physiological conditions, NG2 is cleaved by the γ -secretase ADAM10 in a neuronal activity dependent manner by which the ectodomain is shed into the extracellular matrix.

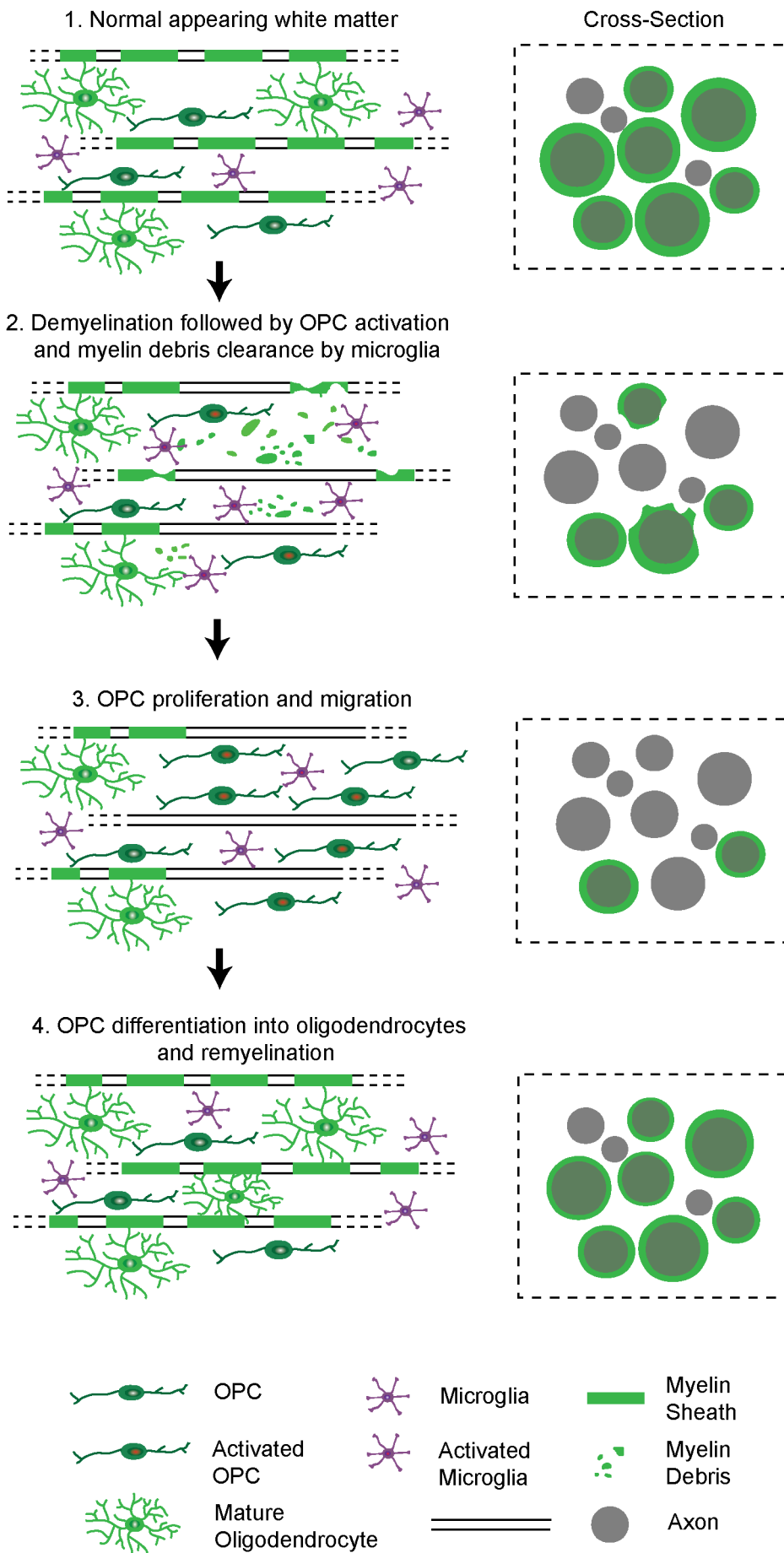


Fig. 1.4 Schematic representation of the process of remyelination. In response to myelin loss, local OPCs become activated, proliferate and migrate towards the lesion area. Subsequently, OPCs differentiate into oligodendrocytes, capable of remyelination of naked axons. Figure modified from (Franklin & Ffrench-Constant, 2008).

The inhibition of this process as well as the knockout of NG2 *in vivo* (NG2 knockout mice) diminishes AMPA- and NMDA- dependent current amplitudes in the pyramidal neurons of the somatosensory cortex. The alteration of neuronal circuit function in the somatosensory cortex leads to altered somatosensory behaviour in NG2 knockout mice (Sakry et al., 2014). In addition, a further potential link between the presence of OPCs and neuronal activity in homeostasis has been uncovered. The genetic ablation of NG2⁺ cells in the mouse cortex causes deficits in excitatory glutamatergic neurotransmission and reduces extracellular glutamate uptake by astrocytes, eventually inducing a depressive-like behaviour (Birey et al., 2015). However, as NG2 is not only expressed in OPCs, but also in microglia and pericytes, the observed effects cannot unambiguously be attributed to OPCs. An OPC specific knockout of NG2 would resolve whether microglia and pericytes contribute to the described changes in neuronal transmission. Even though the two mentioned studies begin to elucidate an effect of OPCs on neuronal activity, a more detailed analysis of how OPCs modulate neuronal activity remains to be performed (Figure 1.5).

1.2.3 Functions of oligodendrocytes

In evolution, the demand for more complex brain activity created the need to speed up neuronal conduction. Initially, an increase of action potential conduction was achieved by a gain in axon diameter. However, as the skull provides a natural restriction of extensive growth of the brain, it is believed that myelin evolved to increase action potential conduction in the limited available space. The myelin ensheathment of axon segments is referred as myelination. Myelinated axon segments (or internodes) alternate with unmyelinated segments (nodes of Ranvier) at which an accumulation of voltage-gated sodium channels allows for action potential propagation. Myelin insulates the internodal axon segments to decrease membrane capacitance and increase membrane resistance, thereby facilitating fast saltatory propagation of action potentials. Saltatory conduction causes a 10-fold increase in the speed of neuronal conduction (Salami, Itami, Tsumoto, & Kimura, 2003). The conduction speed along an axon can be significantly modulated by the length and the thickness of the myelin sheath (see Section 1.3.1) (Figure 1.5).

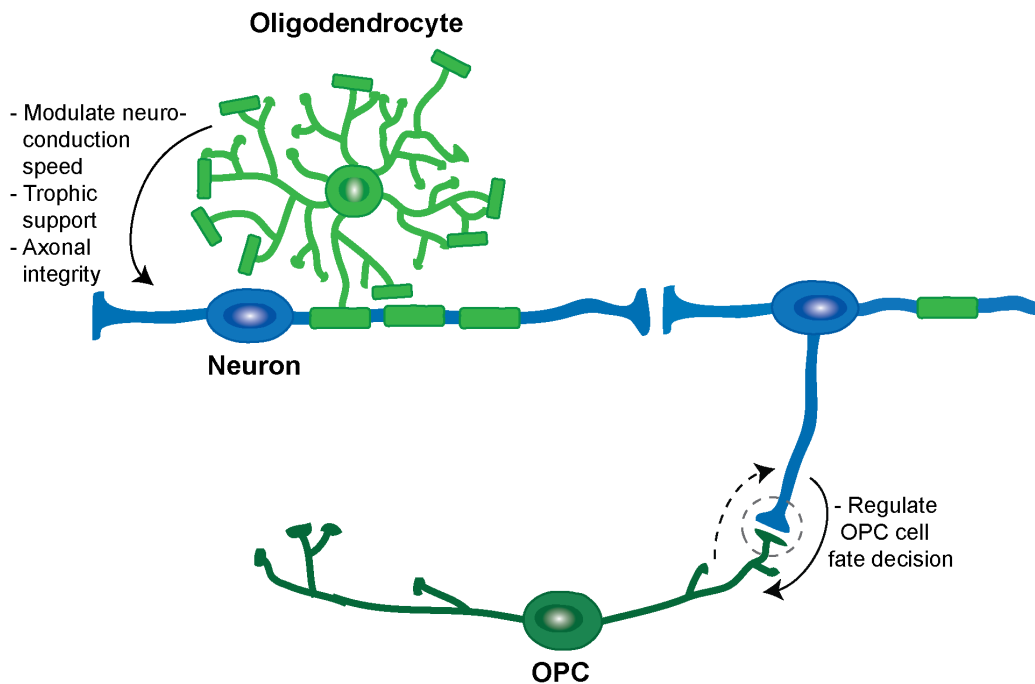


Fig. 1.5 **Modulation of neuronal conduction by oligodendrocyte lineage cells.**

In addition to facilitating saltatory conduction of action potentials, it was hypothesised that the myelin sheath reduces the energy consumption of an axon by restricting the area at which an action potential can be generated to the nodes of Ranvier, thereby decreasing the ATP requirement for the restoration of the ion gradient following an action potential (Nave, 2010) (see Section 1.1.1). However, calculations by Harris and Attwell demonstrated that myelination does not in general confer a reduction in energy consumption of axons. After taking into account the energy consumption of action potential firing, myelination and myelin maintenance, energy savings due to myelination is dependent on the firing rate. For myelination to confer energy saving, the firing rate would need to be approximately the inverse square of the diameter, and therefore would most likely be higher than the measured mean firing rates of different axon classes (Harris & Attwell, 2012). Whilst the calculations presented in this paper are based on experimental values of the optic nerve, the results might look different in other CNS white matter regions which are characterised by axons with different diameter, internodal lengths and firing rates (Figure 1.5).

In the CNS, axons often extend over long distances, rendering the provision of nutrients from the neuronal cell body to the axon difficult. Therefore, an additional mechanism of nutrient supply exists by which energy-rich molecules (eg. lactate) are

transferred from the oligodendrocyte to the axon to fuel the axonal compartment for mitochondrial ATP production (Y. Lee et al., 2012; Trevisiol et al., 2017). A recent publication elucidated the molecular mechanism showing how oligodendrocytes and axons are metabolically coupled. The activation of oligodendroglial NMDA receptors, mimicking neuronal activity, led to an increased expression of GLUT1 transporter on the cell membrane of oligodendrocytes, resulting in an increased uptake of glucose and lactate release by the oligodendrocytes. Mice lacking oligodendroglial NMDA receptors develop late-onset axon degeneration, demonstrating the importance of the metabolic support of the oligodendrocytes to the axons (Saab et al., 2016). In accordance, experimental manipulation of small cytoplasmic channels in the otherwise compacted myelin sheath, connecting the oligodendroglial soma to the innermost layer of myelin, further substantiated the importance of oligodendroglial metabolic support to the axons. It has been reported that the myelin channels are kept in place by a fine balance between the expression of the two myelin proteins, MBP and CNP (Snaidero et al., 2017). Knockout of CNP tips the weight towards an excess of MBP, known to facilitate compaction of the myelin sheath by connecting myelin sheaths laterally, resulting in closure of myelin channels (Snaidero et al., 2017). In CNP knockout animals, axons die due to the lack of nutritional support by the oligodendrocyte (Lappe-Siefke et al., 2003). However, yet again mathematical calculations show that the axon can take up enough glucose to produce all ATP needed for neuronal conduction and transmission (Harris & Attwell, 2012). Assuming that the calculations are correct, why the axon is still taking up energy rich molecules from the oligodendrocyte remains to be elucidated (Figure 1.5).

In contrast to the loss of CNP, the knockout of MBP does cause severe myelination defects. Besides a pronounced hypomyelination, myelin sheaths which are formed are not compacted (Readhead & Hood, 1990; C. M. Smith, Cooksey, & Duncan, 2013). Even though the dysmyelination in MBP-KO mice does not yield into axonal degeneration, alterations in multiple axonal processes, including axonal transport, cytoskeleton formation and metabolism, were observed (C. M. Smith et al., 2013). Why the lack or altered myelination in MBP-KO mice does not result in axon degeneration can only be speculated. The provision of neurotrophic factors provided by the oligodendrocyte itself protects the axon from death (C. M. Smith et al., 2013). Indeed, early *in vitro* co-culture and conditional medium experiments showed that local OLCs secrete factors enhancing neuronal survival (Sortwell et al., 2000; Wilkins, Chandran, & Compston, 2001; Dai et al., 2003). Careful molecular analysis revealed neurotrophins (such as brain-derived neurotrophic factor (BDNF) and neurotrophin-3 (NT-3)) (Byravan, Foster,

Phan, Verity, & Campagnoni, 1994; Dai, Qu, & Dreyfus, 2001), glial cell line-derived neurotrophic factor (GDNF) (Wilkins, Majed, Layfield, Compston, & Chandran, 2003), insulin like growth factor 1 (IGF-1) (Wilkins et al., 2001) and tumour growth factor β (TGF β) (da Cunha, Jefferson, Jackson, & Vitković, 1993; Poulsen et al., 1994) as examples of trophic factors secreted by OLCs. In addition, OLCs also express the receptors for the above mentioned trophic factors, which can affect OLCs proliferation, differentiation and survival (McKinnon, 1993; Barres et al., 1994; Cohen, Marmur, Norton, Mehler, & Kessler, 1996). Therefore, neurotrophic factors secreted by the OLCs do not only affect neurons, but also create a paracrine feedback loop on OLCs behaviour. As an additional layer of regulation, neuronal signals (eg. glutamate or carbachol (acetylcholine receptor agonist)) were shown to modulate the expression of neurotrophic factors in OLCs (Dai et al., 2001) (Figure 1.5).

The investigation of effects of the knockout of PLP, an integral protein of the myelin sheath, revealed a role for oligodendrocytes in the local regulation of axonal function. In mice lacking PLP, substantial axon degeneration occurs even in the presence of normal myelin sheaths that exhibit only subtle abnormalities in compaction (Griffiths et al., 1998). It was shown that in the absence of PLP the fast axonal transport is impaired, resulting in axonal loss (Edgar et al., 2004). Hence, the loss of PLP protein has primarily consequences on the axon itself, which cannot be overcome by the positive effects of the myelin sheath.

In accordance, MAG, a non-compact myelin protein, has been reported to have an effect on the axon, whilst it is less important for the myelin sheath formation. MAG-deficient mice are fully myelinated with only subtle abnormalities in the myelin sheaths, but show decreased axon calibers due to reduced phosphorylation of neurofilaments and neurofilament spacing (Montag et al., 1994; Garcia et al., 2003).

1.3 Myelination

As a link between oligodendrocytes and neurons, myelination undoubtedly represents an important tool to provide support to neurons and improve neuronal conduction. However, not every axon in the CNS is myelinated. How is an axon chosen for myelination? Why do some axons need oligodendrocyte support more than others (see Section 1.3.1)? Compelling evidence shows that myelination continues well into adulthood. But how does myelination influence adult brain function (eg. learning) (see

Section 1.3.2)? And is impaired myelination a primary cause for disease and ageing (see Section 1.3.3)?

1.3.1 Developmental myelination

The process of myelination

The process of myelination consists of multiple steps (1) OPC expansion and migration, (2) initiation of OPC differentiation into oligodendrocytes and (3) myelin wrapping (including Node of Ranvier formation and myelin compaction) (Figure 1.7).

As a first step, OPCs are specified from radial glia cells in the mouse CNS starting from E12.5 (Pringle & Richardson, 1993; Kessaris et al., 2006) (see Section 1.4.1). Subsequently, the newly-formed OPCs undergo extensive proliferation and migrate along vasculature, eventually populating the whole CNS (Tsai et al., 2016). *In vivo* imaging showed that OPCs maintain unique territories by self-avoidance, and OPC cell loss through death or differentiation triggers rapid migration and proliferation of adjacent cells to restore their density (Hughes et al., 2013). Through these mechanisms, the number of OPCs is kept constant at 5-8% in the adult murine brain (Pringle et al., 1992).

After the OPC network within the CNS parenchyma is established, an OPC can undergo two different fates, either remaining in the stem cell state or differentiating into oligodendrocytes. However, to date no differentiation initiation factor has been identified, but multiple hypotheses have been proposed. One hypothesis says that there is simply an internal clock, dictating when an OPC will start differentiating (Klingseisen & Lyons, 2017). Indeed, a paper investigating the fate of OPCs after cell division showed that there is a critical time window in which cell fate is determined as OPCs differentiated at a similar rate (Hill, Patel, Goncalves, Grutzendler, & Nishiyama, 2014). But as not all OPCs differentiate *in vivo*, an orchestrating signal coordinating the number of differentiating OPCs must exist. A second hypothesis suggests that contact-inhibition of neighbouring OPCs triggers differentiation upon full establishment of the OPC network (Klingseisen & Lyons, 2017). However, as oligodendrocyte numbers reach a plateau and no significant amount of oligodendrocyte cell death has been detected post development, there must be a stop signal inhibiting constant OPC differentiation at high OPC densities in an adult animal. Alternatively, it seems likely that the cell fate decision to self-renew or differentiate must be tightly coupled to

neuronal development. Multiple neuronal proteins (eg. PSA-NCAM (Nait Oumesmar et al., 1995; Fewou, Ramakrishnan, Büssov, Gieselmann, & Eckhardt, 2007), Jagged (Wang et al., 1998)) actively inhibit OPC differentiation. Therefore, potentially a release from inhibitory factors, rather than a release of differentiation factors causes the initiation of OPC differentiation.

A complex network of signalling pathways and transcription factors have been revealed controlling OPC differentiation, which still remains to be fully elucidated. Whilst OLIG1/OLIG2 (Lu et al., 2002; Zhou & Anderson, 2002), SOX10 (Stolt et al., 2002), NKX2.2 (Qi et al., 2001), MYRF (Emery et al., 2009), YY1 (He et al., 2007), SIP1 (Weng et al., 2012), TCF4 (Fancy et al., 2009) and ZFP191 (Howng et al., 2010) are positive regulators of OPCs differentiation, HES5 (Kondo & Raff, 2000) and SOX5/6 (Stolt et al., 2006) negatively regulate OPC differentiation (the list of transcription factors is not exhaustive). The expression of these transcription factors are regulated by epigenetic factors and extracellular signals via various signalling pathways. The AKT/mTOR (Flores et al., 2008; Tyler et al., 2009), p38/MAP (Haines, Fragoso, Hossain, Mushynski, & Almazan, 2008; Fragoso et al., 2007), ERK/MAPK pathway (Fyffe-Maricich, Karlo, Landreth, & Miller, 2011) and nuclear receptor (NR) signalling (de la Fuente et al., 2015) have been identified as important drivers of differentiation, whereas NOTCH (Wang et al., 1998; Y. Zhang et al., 2009), WNT (Fancy et al., 2009), BMP (Weng et al., 2012), FGF (McKinnon, Matsui, Dubois-Dalcq, & Aaronson, 1990; Goddard, Berry, Kirvell, & Butt, 2001) and PDGFR α pathway signalling (Fruttiger et al., 1999; Zhu et al., 2014) inhibit OPC differentiation (Figure 1.6).

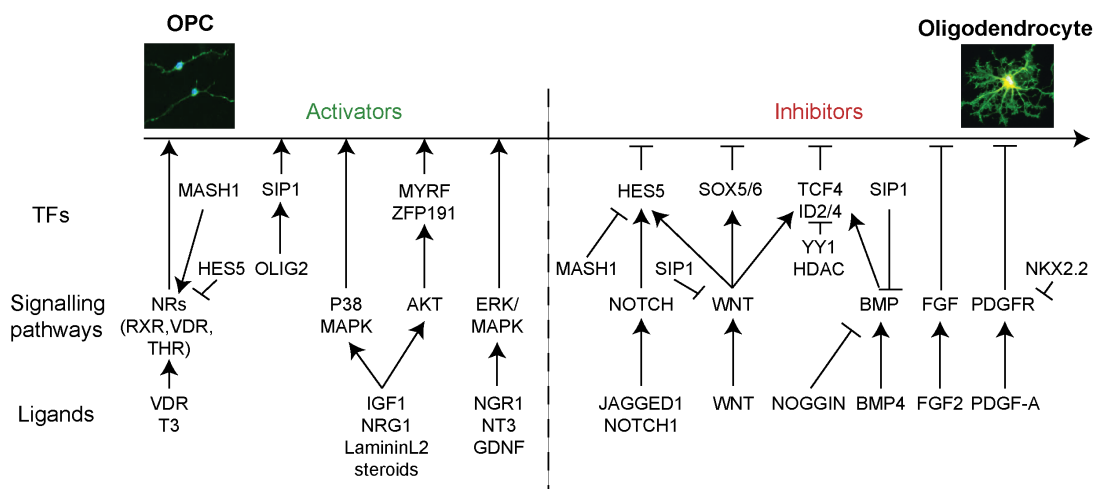


Fig. 1.6 Overview of transcription factors and signalling pathways involved in OPC differentiation.

As for the epigenetic factors, microRNAs, in particular miRNA-219 and miRNA-338 (Dugas et al., 2010), actively repress HES5, SOX5/6 and the PDGFR α signalling pathways. Furthermore, HDAC1 and HDAC2 regulate OPC differentiation by disrupting the canonical Wnt-signalling pathway, usually blocking OPC differentiation when active (Ye et al., 2009) (Figure 1.6). Some of these differentiation factors are currently being trialled for treatment of demyelinating diseases (see Section 1.6).

The first mature oligodendrocytes can be detected at birth and P6 in the spinal cord and brain, respectively (Foran & Peterson, 1992). As for OPCs, the number of oligodendrocytes in the CNS are tightly regulated by the limited amount of survival and proliferation factors, including platelet-derived growth factor A (PDGF-AA), insulin-like growth factor 1 (IGF1) (Barres et al., 1992; Barres & Raff, 1994), fibroblast growth factor 2 (FGF 2) (McKinnon et al., 1990) and neurotrophin 3 (NT 3) (Barres & Raff, 1994). An excess of oligodendrocytes is counteracted by an increase in apoptosis (Calver et al., 1998).

Most oligodendrocytes generate between 20 and 60 myelinating processes (Chong et al., 2012). *In vivo* live imaging in zebrafish showed that oligodendrocytes form their myelin sheaths, located at the tip of myelinating processes, in a synchronous fashion in a time window of only 5 hours (Czopka, Ffrench-Constant, & Lyons, 2013). Once a particular axon has been engaged by a myelin sheath, dramatic changes in the plasma membrane architecture are induced. Careful electron microscopic (EM) analysis of the myelination process revealed a two motion model of myelination: whilst the leading edge of the inner tongue, the myelin membrane closest to the axon, is continuously wrapped around the axon, the already established myelin membrane layers extend laterally towards the future node. During this lateral extension, the edges of the myelin sheaths remain in contact with the axon and move in a helical manner towards the future node, where they align and form the characteristic paranodal loops (Snaidero et al., 2014). The turnover of filamentous (F)-actin (meaning its assembly and disassembly) was determined as a driving force of myelin sheath wrapping, and subsequent spreading and adhesion of the myelin sheath to the axon (Nawaz et al., 2015). Early pulse-labelling studies demonstrated that most membrane components of the myelin sheath are synthesised in the soma of oligodendrocytes, and thus need to be transported to the growth tip (Gould & Dawson, 1976), most likely through the cytoplasmic channels between the myelin sheaths. An exception is the MBP protein, whose mRNA is transported to the myelin sheath (Lyons, Naylor, Scholze, & Talbot, 2009) where the protein is translated locally (Laursen, Chan, & Ffrench-Constant, 2011).

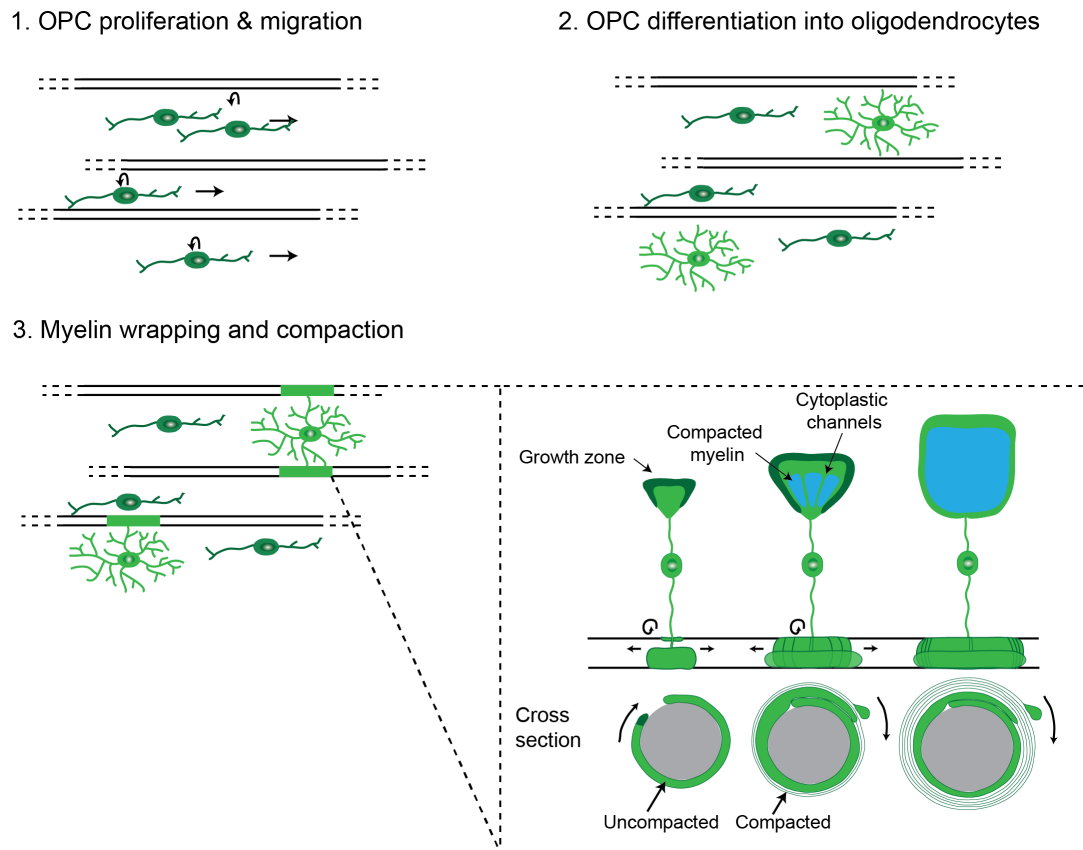


Fig. 1.7 Schematic representation of the the process of myelination. In development, following the specification of OPCs from radial glia cells, OPCs undergo an extensive expansion before migrating throughout the CNS parenchyma to establish an even distribution. Subsequently, OPCs differentiate into mature oligodendrocytes and establish physical contact with an axon. After an axon has been engaged by a myelin sheath, the inner lamellae of the myelin sheath is wrapped around the axon, whilst the sheath also extends laterally. Simultaneously the compaction of the myelin sheath proceeds from the outer most to the inner most myelin lamella. Figure modified from (Snaidero et al., 2014).

In a final step, the node of Ranvier is established by ion channel clustering (mostly sodium and potassium channels) through the interaction of axonal and glial adhesion molecules, as well as extracellular matrix proteins (Rasband & Peles, 2015). Simultaneously, the layers of myelin sheath membranes are compacted by dimerisation of MBP protein deposited in adjacent myelin layers, thereby acting as a molecular zipper (Aggarwal et al., 2013). The compaction of the myelin sheaths proceeds from the most outer to the inner layer (Snaidero et al., 2014), with the exception of the inner-most myelin lamellae remaining non-compacted, providing a platform for neuron-glia communication (see Section 1.2.3).

Beyond the remarkable ultrastructure of the myelin sheath (eg. the organisation of paranodes and nodes, the compaction, the cytoplasmic channels), myelin itself has unique characteristics regarding its molecular composition and stability. In comparison to other membranes, 70-80% of the myelin sheath contains lipids (by dry weight) and only a small proportion of proteins, of which MBP and PLP are the most abundant. Furthermore, the myelin sheath is a poorly hydrated structure containing only 40% water. Another defining feature of the myelin sheath is its remarkable stability. The half-life of myelin membrane components is in the order of weeks to months. As an example, cholesterol, one of the most abundant lipid components of the sheath, has an estimated half-life of 7-8 months (M. E. Smith & Eng, 1965), likewise myelin proteins were found to be one of the most long lived proteins in a mouse (Toyama et al., 2013).

Myelination of the CNS follows a spatiotemporal pattern with the spinal cord being myelinated earlier than the brain. In the spinal cord, the process of myelination proceeds from rostral to caudal spinal cord areas, with an earlier start of myelination in the ventral funiculus in comparison to the dorsal funiculus (Foran & Peterson, 1992). In contrast, in the brain caudal areas are myelinated before rostral areas, and central brain areas are myelinated before peripheral brain areas (Kinney, Brody, Kloman, & Gilles, 1988; Foran & Peterson, 1992; Deoni et al., 2011). In the adult, distinct CNS areas are myelinated to a different extent. Whilst most of the white matter tracts in the CNS (corpus callosum (CC), anterior commissure (AC), optic nerve, white matter of spinal cord) are almost fully myelinated, grey matter axons are sparsely myelinated (Tomassy et al., 2014).

Regulation of myelination

How is myelination regulated? What causes an axon to be myelinated and to what extent?

Multiple *in vitro* studies provide compelling evidence that only a permissive structure (eg. cylindrical polystyrene nanofibers, glass micropillars or beads) is required for myelination by an oligodendrocyte (S. Lee et al., 2012; Mei et al., 2014; Bechler, Byrne, & Ffrench-Constant, 2015; Redmond et al., 2016). Even though the oligodendrocytes are clearly capable of myelination without an inducing signal, an axon selection signal for myelination must exist *in vivo* as not all axons are myelinated in the CNS (Remahl & Hildebrand, 1982; Tomassy et al., 2014; Micheva et al., 2016). EM studies suggested the axon's diameter is an important determinant of myelination, based on the observation that the smallest axons within an CNS region are never

myelinated (critical axon diameter for myelination depends on CNS area and age (Remahl & Hildebrand, 1982)). The hypothesis that the axon's diameter is an important determinant of myelination is supported by the finding that the artificial increase in the axon diameter by PTEN knockout causes axons to be myelinated in a normally unmyelinated area (Goebbels et al., 2017). However, the PTEN knockout also leads to altered gene expression and ectopic OPC proliferation/differentiation. Therefore, the increased myelination could also be attributed to changes in the oligodendrocyte lineage. In addition, there is a significant overlap in myelinated and unmyelinated axon diameters in the CNS (Remahl & Hildebrand, 1982), suggesting that the axon's diameter is not regulating axon selection. The reason why oligodendrocytes never myelinate small axons *in vivo* remains to be elucidated. Potentially, the high curvature of small diameter axons physically inhibits the myelination by an oligodendrocyte. In addition, in order for the hypothesis that the axon's diameter regulates axon selection to hold true, neuronal signals capable of regulating the axon diameter need to be identified. So far, only the establishment of axon-oligodendrocyte contact was shown to increase the axon diameter (Colello, Pott, & Schwab, 1994; Sánchez, Hassinger, Paskevich, Shine, & Nixon, 1996; Brady et al., 1999), suggesting that all axons are the same diameter until engaging with oligodendrocytes.

OPCs can receive inputs from neurons (Barres, Koroshetz, Swartz, Chun, & Corey, 1990; Wyllie, Mathie, Symonds, & Cull-Candy, 1991; Steinhäuser, Jabs, & Kettenmann, 1994; Jabs, Kirchhoff, Kettenmann, & Steinhäuser, 1994), provoking a sodium current after depolarisation (Chittajallu, Aguirre, & Gallo, 2004; Káradóttir et al., 2008), eventually modulating OPC proliferation, differentiation and myelination *in vivo* (Li, Brus-Ramer, Martin, & McDonald, 2010; Makinodan, Rosen, Ito, & Corfas, 2012; Gibson et al., 2014; Mensch et al., 2015). While these studies provide a link between neuronal activity and oligodendrocyte lineage progression, it was questioned whether neuronal activity also takes part in axon selection for myelination. Hines and colleagues showed that oligodendrocytes initially extend myelin sheaths to many axons, but after initial axon wrapping, activity-dependent vesicle secretion from axons promotes extension and stabilisation of only a proportion of sheaths. The remaining myelin sheaths were retracted in the absence of neuronal activity (Hines, Ravanelli, Schwindt, Scott, & Appel, 2015). However, neuronal activity is only required for myelination in a subtype of neurons (Koudelka et al., 2016). Mechanisms by which myelination of other subtypes of neurons are regulated remains to be elucidated.

Neuronal activity cannot be the only determinant of myelination, as a patchy

myelination pattern along a single axon (Tomassy et al., 2014; Micheva et al., 2016) cannot be explained by neuronal activity, which is expected to be homogenous within the same axon. But why would an axon only be partially myelinated? Intriguingly, even though single oligodendrocytes can form up to 60 myelin sheaths, an oligodendrocyte lays down only a single myelin sheath per axon (Young et al., 2013). The biological function of this observed phenomena remains to be elucidated; however, it is hypothesised that this is a mechanism by which oligodendrocytes coordinate the timing of neuronal conduction of a neuronal circuit. Partial myelination can potentially facilitate fine tuning of the neuronal circuit coordination. Indeed, studies reported myelination to be a tool of adjusting neuronal conduction to ensure the coordination of signals transmitted along axons with varying length in one neuronal circuit (Salami et al., 2003; Seidl, Rubel, & Barría, 2014). The feedback mechanism to achieve tailored myelination of single axons needs to be investigated.

Taken together, new mechanisms remain to be discovered which explain the complex *in vivo* myelination pattern. Questions that remain unanswered include (1) why are more white matter axons myelinated than grey matter axons?, (2) why are some grey matter axons only partially myelinated? and (3) why are the smallest axons within a tissue not myelinated at all? Answering these questions will help to reveal new regulators of axon selection for myelination.

Another research area focuses on the question of why myelin is exclusively formed around the axon. A study by Redmond and colleagues provided insights into how axon selective myelination is achieved (at least for a subset of neurons) for the first time. Neurons express the inhibitory molecule JAM2 specifically on the soma and dendrites, which is sufficient to prevent myelin wrapping (Redmond et al., 2016). JAM2 was also found to only be important for a small subset of neurons (Redmond et al., 2016). Whether other additional inhibitory molecules are expressed alongside JAM2 or on different neuronal subtypes remain to be identified. Furthermore, why oligodendrocytes spare other cellular processes (eg. processes of astrocytes or OPCs) from myelination remains an intriguing question.

In the brain, a great heterogeneity of established myelin sheaths, regarding the number of myelin sheaths per oligodendrocyte, sheath length and thickness, can be observed (see Section 1.4.2). The number of myelin sheaths formed per oligodendrocyte typically ranges from 10 to 60, and myelin sheath length ranges from $20\mu\text{m}$ to $200\mu\text{m}$ (Chong et al., 2012). Electron microscopy measurements revealed a strong correlation

between myelin thickness and axon diameter *in vivo* (Williams & Wendell-Smith, 1971), with a calculated optimal conduction velocity at a g-ratio of 0.77 (Chomiak & Hu, 2009). Are the myelin sheath properties established by the oligodendrocyte itself? Independent of neuronal signals, oligodendrocytes can sense the axon diameter, as nanofibres below $0.3\mu\text{m}$ in diameter are not myelinated *in vitro* (S. Lee et al., 2012). In the same *in vitro* culture system, oligodendrocytes isolated from the cortex or the spinal cord recapitulated the average *in vivo* myelin sheath length (Bechler et al., 2015). Furthermore, the competition between individual oligodendrocytes has been proven to be an important determinant of myelin sheath length (Chong et al., 2012). In contrast, Almeida and colleagues showed that axons are regulating the myelination potential of a single oligodendrocyte. Increasing the number of axons in the spinal cord resulted in an association of a single oligodendrocyte with a higher number of axons, while oligodendrocyte numbers stayed stable (Almeida, Czopka, Ffrench-Constant, & Lyons, 2011). The observation that neuronal activity can tweak sheath thickness (Gibson et al., 2014), length (elongation (Goebbels et al., 2010) and shortening (Mills et al., 2015)), and the number of myelin processes formed (Czopka et al., 2013) suggests that there is also an element of neuronal activity influencing myelin properties, potentially fine-tuning the myelin sheath properties to optimise neuronal conduction.

1.3.2 Myelin plasticity

The great majority of myelinating oligodendrocytes are formed in early postnatal periods (Kang, Fukaya, Yang, Rothstein, & Bergles, 2010). However, OPCs are still engaging in dynamic behaviour in the adult brain. Using live 2-photon imaging of the cortex, Hughes and colleagues estimated that about 3% of NG2⁺ OPCs are involved in physiological processes (eg. cell death, proliferation and differentiation) per day. This keeps OPC numbers stable by balancing OPC loss through cell death or differentiation ($1.2 \pm 0.1\%$ per day) with cell addition through proliferation ($1.5 \pm 0.1\%$ per day) (Hughes et al., 2013). Using EdU labelling studies it was demonstrated that all OPCs proliferate in the adult brain (Clarke et al., 2012; Young et al., 2013), but their cell cycle time is dramatically increased with age (Young et al., 2013). In contrast, earlier studies assessing OPC proliferation using BrdU suggested the co-existence of a proliferative and a quiescent OPC population in the brain (Rivers et al., 2008; Psachoulia, Jamen, Young, & Richardson, 2009; Guo et al., 2010). However, work from Young and colleagues demonstrated cell toxicity of BrdU used in these studies, resulting in inaccurate conclusions on the proliferative capacity of OPCs (Young et al., 2013). Whereas a small proportion of astrocytes is formed from OPCs

in adult mice (S. H. Chung, Guo, Jiang, Pleasure, & Deng, 2013), adult OPCs mostly differentiate into oligodendrocytes (Dimou, Simon, Kirchhoff, Takebayashi, & Götz, 2008; Psachoulia et al., 2009; Hughes et al., 2013; S. H. Chung et al., 2013; Young et al., 2013). Studies assessing the proportion of new-born oligodendrocytes in the adult brain reveal different numbers (Table 1.1). Nonetheless, two general conclusions can be drawn from the analysis of all the datasets: (1) more new-born oligodendrocytes can be observed in the white matter when compared to grey matter areas and (2) the proportion of proliferating OPCs remains stable with ageing, however the rate of OPC maturation decreases. Immunofluorescence and electron microscopy analysis confirmed that the adult-born oligodendrocytes form processes as well as compact myelin sheaths (Kang et al., 2010; Young et al., 2013) (see Section 1.8). However, the myelin sheaths formed by adult-born oligodendrocytes are shorter when compared to developmental myelination (Young et al., 2013).

New-born OLs	Brain region	Labelling period	Mouse Model	References
90%	CC	P30-P120	<i>Pdgfra-CreER</i>	(Kang et al., 2010)
29%	CC	P45-P255	<i>Pdgfra-CreERT2</i>	(Rivers et al., 2008)
50%	CC	P60-P102	<i>Pdgfra-CreERT2</i>	(Young et al., 2013)
61%	CC	P70-P130	<i>Pdgfra-CreER</i>	(Kang et al., 2010)
81%	CC	P75-P140	<i>Olig2-CreERTM</i>	(Dimou et al., 2008)
82%	CC	P180-P245	<i>Olig2-CreERTM</i>	(Dimou et al., 2008)
18%	CC	P240-P340	<i>Pdgfra-CreERT2</i>	(Psachoulia et al., 2009)
50%	Cortex	P30-P120	<i>Pdgfra-CreER</i>	(Kang et al., 2010)
35%	Cortex	P70-P130	<i>Pdgfra-CreER</i>	(Kang et al., 2010)
20%	Cortex	P75-P140	<i>Olig2-CreERTM</i>	(Dimou et al., 2008)
12%	Cortex	P180-P245	<i>Olig2-CreERTM</i>	(Dimou et al., 2008)

Table 1.1 **Proportion of new-born oligodendrocytes in the adult brain.** OLs = oligodendrocytes, CC = corpus callosum, P = postnatal day.

But what is the role of newly generated OPCs in the adult brain? Do they replace old myelin sheaths (myelin remodeling) or do they add new myelin sheaths (*de novo* myelination)? These hypotheses are not mutually exclusive.

In some brain areas, such as the cortex and subcortical white matter, the majority of neurons have been shown to be unmyelinated or only partially myelinated, even in the adult animal (Tomassy et al., 2014). Consequently, new-born oligodendrocytes could simply myelinate previously unmyelinated areas of an axon to perhaps fine-tune

neuronal conduction or facilitate circuit plasticity, important for learning.

An increasing body of literature demonstrates experience-dependent plasticity in human brains in adulthood. All these studies use magnetic resonance imaging (MRI) to evaluate changes in grey and white matter. In particular, fractional anisotropy (FA) is used to determine changes in the brain microstructure. Multiple studies reported an increase in the FA in response to motor learning (Bengtsson et al., 2005; Boyke, Driemeyer, Gaser, Büchel, & May, 2008; Scholz, Klein, Behrens, & Johansen-Berg, 2009; Taubert et al., 2010) or cognitive tasks (Keller & Just, 2009; Takeuchi et al., 2010; Schlegel, Rudelson, & Tse, 2012) (reviewed in: (Zatorre, Fields, & Johansen-Berg, 2012)). As an example, a significant increase in FA could be detected in right posterior intraparietal sulcus (IPS) of human adults after a 6 week juggling training period, indicating a change in white matter (Scholz et al., 2009). However, as changes in the FA measurement can be caused by changes in myelination, axon diameter, axon density, fibre organisation or a combination of all of these factors, it is not possible to pinpoint what structural event underlies a change in FA. Therefore, carrying out combined MRI and histological analysis in animal models is important to shed light on the molecular mechanisms underlying the experience-dependent white matter changes. Markham and colleagues reported a 10% increase in the CC volume in adult rats when exposed to an enriched environment. Histological analysis revealed that the reported increase in white matter volume was not due to a change in myelin, but rather due to an increase in the number of astrocytic cell processes and branching of unmyelinated axons (Markham, Herting, Luszbek, Juraska, & Greenough, 2009). In contrast, the increase in FA in rats performing the morris water maze or single pellet reaching task was associated with an increased staining for myelin basic protein, hinting towards the production of new oligodendrocytes (Blumenfeld-Katzir, Pasternak, Dagan, & Assaf, 2011; Sampaio-Baptista et al., 2013). Using a genetically modified mouse line, in which the differentiation of new oligodendrocytes is blocked by the knockout of MYRF, McKenzie and colleagues demonstrated very elegantly that newly-generated oligodendrocytes are required to learn a motor skill (eg. running on a complex wheel) in mice (McKenzie et al., 2014). The formation of new oligodendrocytes, which is initiated by motor learning not exercise, happens very rapidly (2-4 hours) after the training of the motor task begins (Xiao et al., 2016). The rapidity of the formation of new oligodendrocytes would suggest a close relationship between neuronal activity and oligodendrogenesis. In summary, *de novo* myelination is required for motor learning in adulthood, demonstrating the need for the formation of new oligodendrocytes in the adult brain. Conversely, a lack of neuronal activity due to social deprivation of adult

mice, causes hypomyelination in the medial prefrontal cortex, a region important in social function (Liu et al., 2012)

An alternative possibility is that adult-born oligodendrocytes are necessary to replace oligodendrocytes due to loss of function or cell death. In favour of this hypothesis is that new oligodendrocytes are even formed in brain areas, *inter alia* the optic nerve, which are fully myelinated in the adult animal (Young et al., 2013). However, until now no evidence of oligodendrocyte cell death in the adult brain has been published. Indeed, it is not clear whether myelinating oligodendrocytes can be replaced without compromising axonal integrity. In contrast, occasional retraction of myelin sheaths by mature oligodendrocytes was observed, without cell death (Fernández-Gamba et al., 2012; Makinodan et al., 2013; Czopka et al., 2013). In an *in vitro* co-culture system of rat neurons and oligodendrocytes, cellular stress induced by 3-nitropropionic acid (3-NP) (Fernández-Gamba et al., 2012) or N-methyl-D-aspartate (NMDA) (Makinodan et al., 2013) caused reversible retraction of myelin sheaths. Retraction of myelin sheaths from around axons has also been observed in zebrafish *in vivo*, but at a very low rate and mostly shortly after initial myelination (Czopka et al., 2013). Further studies are needed to investigate if myelin turnover drives the production of new-born oligodendrocytes in adult animals, with particular focus on the extent of myelin sheath retraction (in particular in mammals) and mature oligodendrocyte apoptosis.

1.3.3 Myelination in ageing

While the white matter content of the brain increases into adulthood, with a peak of myelination in the 4th decade of life in humans, a significant decline in white matter can be detected in aged individuals using MRI (reviewed in (Madden, Bennett, & Song, 2009)) (Figure 1.8). The degeneration of white matter is more pronounced in certain brain regions, leading to the "last in, first out" hypothesis, stating that neuronal tracts which were myelinated last, are more susceptible to age-related degeneration (Raz et al., 2005; Bender, Völkle, & Raz, 2016). These studies are supported by the notion that the number of myelin proteins in the brain decreases with progressive age (Xie, Zhang, Fu, & Chen, 2013). The reduced number of myelin proteins, including the compaction protein MBP, might explain the myelin breakdown, characterised by the severe decompaction of the myelin lamellae without changes to the g-ratio, detected in aged rats (Xie, Liang, Fu, Zhang, & Chen, 2014). The degree to which age-related myelin loss is due to primary oligodendrocyte dysfunction, as opposed to being a

consequence of axon loss, remains to be determined. However, changes within the oligodendrocyte lineage are starting to be discovered, hinting towards an active role of OLCs in ageing.

Interestingly, myelin loss with ageing is not likely to be due to the loss of OPCs as studies in mice have demonstrated that stable numbers of OPCs are maintained well into old age (Sim et al., 2002). However, the cell cycle time of aged OPCs shows a 4-8 fold increase (depending on brain region) when compared to adult OPCs (Psachoulia et al., 2009). Whilst there is no doubt over age-associated cell cycle elongation, the quantification needs to be considered with caution as BrdU was shown to cause OPC apoptosis, therefore disrupting the OPC proliferation potential (Young et al., 2013). In contrast to stable OPC numbers, oligodendrocyte numbers decrease with age in the order of 27% between 20 and 90 years of age (Pelvig, Pakkenberg, Stark, & Pakkenberg, 2008) (Figure 1.8).

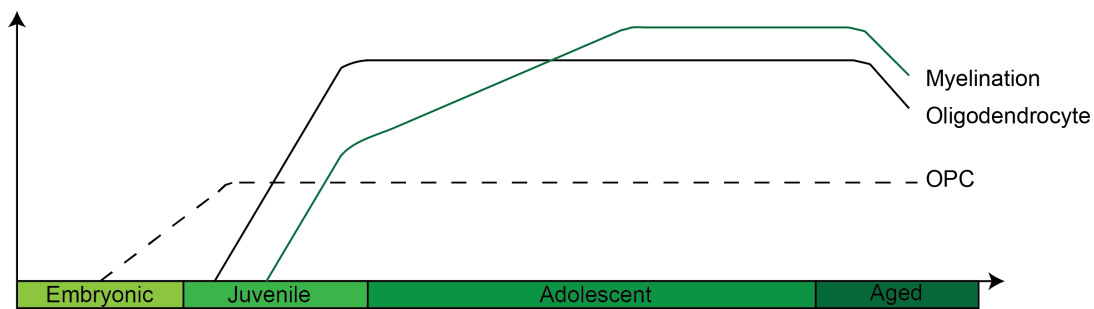


Fig. 1.8 Schematic representation of the numbers of oligodendrocytes and OPCs as well as the overall myelination levels across the lifetime of an individual.

This might be explained by a switch from asymmetric (an OPC generates one OPC and one oligodendrocyte upon division) to symmetric (an OPC generates two OPCs upon division) OPC proliferation, reducing the number of oligodendrocytes (Boda et al., 2015). However, this switch in OPC proliferation mode is still a hypothesis as there are controversial opinions as to whether asymmetric cell OPCs cell division exists (Sugiarto et al., 2011; Hughes et al., 2013; Boda et al., 2015; Klingseisen & Lyons, 2017). In agreement with the age-associated decrease in oligodendrocytes numbers, the percentage of newly formed oligodendrocytes negatively correlates with the animal's age (Table 1.1). These differences in oligodendrogenesis are region-specific, as, for example, in the hippocampus there is more oligodendrogenesis detectable in the dorsal areas when compared to the ventral areas. This difference reflects an increased survival of newly born dorsal oligodendrocytes, because OPC proliferation rates are comparable in the dorsal and ventral hippocampus in the aged animals (Yamada & Jinno, 2014). However, the argument that the mode of OPC proliferation is responsible for reduced

oligodendrocyte numbers necessitates a constant oligodendrocyte turn over in the brain, for which there is no experimental evidence yet (Section 1.3.2).

Multiple molecular changes within the OPC and oligodendrocyte population have been detected with ageing, which are likely to partially explain the decline in oligodendrocyte numbers in the aged brain. Besides the before mentioned increase in cell cycle time, the gene and protein expression profile of OPCs changes dramatically with progressive age (Roey Baror and Alerie Guzman de la Fuente, Franklin laboratory, University of Cambridge, unpublished data), leading to a reduced differentiation capacity of old OPCs into oligodendrocytes (Björn Neumann, University of Cambridge, Franklin laboratory, unpublished data). In addition, OPCs show an abnormal regulation of differentiation inhibitors through epigenetic mechanisms. Shen and colleagues performed a global analysis of epigenetic markers in the genome of young and old mice. They were able to detect an abnormal loss of repressive histone methylation and an increase in acetylation in aged OLCs, which are due to the decline in function of the histone modification enzymes (Shen, Liu, Li, Wolubah, & Casaccia-Bonnet, 2008). In young mice, down regulation of OPC differentiation inhibitors (eg. HES5, SOX5/6, ID4 (see Section 1.3.1)) is associated with the recruitment of histone deacetylases (HDACs) to the promoter regions of these genes (Marin-Husstege, Muggironi, Liu, & Casaccia-Bonnet, 2002). However, in old mice, HDAC recruitment is inefficient, resulting in the accumulation of transcriptional inhibitors and impaired OPC differentiation (Shen, Liu, et al., 2008; Shen, Sandoval, et al., 2008). In addition, microarray analysis of the rat optic nerve at different ages showed that transcripts involved in immune response and neurotransmitter transport processes are up regulated in aged animals, whereas the biosynthesis of lipids is significantly decreased with ageing (Xie, Fu, et al., 2014), likely being an explanation of the myelin breakdown observed in the aged CNS (Xie, Liang, et al., 2014).

In addition to the intrinsic changes in the OLCs with ageing, various extrinsic factors inhibiting OPC differentiation have been identified, which will be discussed in Section 1.6. Whether and to what extent aged oligodendrocyte lineage cells show other hallmarks of ageing (López-Otín, Blasco, Partridge, Serrano, & Kroemer, 2013) needs to be investigated. For example, it is highly likely that actively differentiating, post-mitotic OPCs show the greatest vulnerability to this oxidative-induced damage, acquiring DNA damage in their lifetime (Tse & Herrup, 2017). The combination of intrinsic and environmental changes resulting in decreased OLC function in an aged individual primes the CNS for myelin diseases (see Section 1.6).

1.4 Heterogeneity of oligodendrocyte lineage cells

Given the functional heterogeneity of neurons (eg. firing patterns, connectome), neuronal circuits most likely require specific support in terms of nutrients, neurotrophic factors, neuronal conductance and transmission. But how is this individual support achieved in the CNS? The OLCs undoubtedly have a big impact on the modulation of neuronal conduction and neuronal welfare. Therefore, different subpopulations of OPCs and oligodendrocytes might facilitate the individual, regional support of neuronal circuits. So far, OPC heterogeneity with regards to their developmental origin (ventral versus dorsal OPCs) and their location (white matter versus grey matter OPCs) have been identified. However, the question of whether OPC heterogeneity has any consequences on CNS function remains and current studies are beginning to investigate whether OLC heterogeneity is important in physiological brain function.

1.4.1 OPC heterogeneity

Heterogeneity of the developmental origin of OPCs

During embryonic development of the CNS, OPCs are generated from radial glia cells in multiple localised areas. The heterogeneity of OPCs based on their embryological origin is known as developmental heterogeneity. In the murine spinal cord, most OPCs stem from the pMN domain of the ventral ventricular zone, beginning from embryonic day 12.5 (E12.5) and subsequently populate the entire neural tube (Pringle & Richardson, 1993; Fogarty, Richardson, & Kessaris, 2005). Additionally, a minority of OPCs are generated from progenitors in the dorsal dP3, dP4, dP5 and dP6 progenitor domains beginning at E16.5 (Cai et al., 2005; Vallstedt, Klos, & Ericson, 2005; Fogarty et al., 2005). In the adult mouse, OPCs from ventral and dorsal regions are intermixed, with a heavy predominance of pMN-derived (ventral) cells (85-90%). OPCs stemming from dorsal progenitors mostly populate the dorsal and lateral funiculus (Crawford, Tripathi, Richardson, & Franklin, 2016) (Figure 1.9).

The developmental heterogeneity of OPCs has also been described in the murine telencephalon, in which OPCs arise from three distinct regions in a spatiotemporal manner. The earliest OPCs develop from the medial ganglionic eminence (MGE) and the anterior entopeduncular (AEP) region in the ventral developing telencephalon starting from E11.5. Subsequently, at E16.5, a second population of OPCs are formed from the ventral lateral and caudal ganglionic eminence (LGE, CGE). Both OPC populations spread from ventral to dorsal, eventually populating the whole telencephalon. After birth, the third population of OPCs arises in the developing cortex,

which populate exclusively the dorsal parts of the telencephalon (Kessaris et al., 2006). Interestingly, during postnatal development, the first population of OPCs from the MGE-AEP region is eliminated, leaving the adult brain populated by OPCs derived from the ventral LGE-CGE region and the dorsal cortex (Kessaris et al., 2006). In the adult telencephalon, dorsal derived OLCs mainly populate the cortex (50% dorsal OLCs, 50% ventral OLCs) and the corpus callosum (CC) (25% dorsal OLCs, 25% ventral OLCs), whereas the anterior commissure (AC), the pre-optic tract (POA) and the lateral olfactory tract (LOT) are almost exclusively populated by ventral OLCs (Kessaris et al., 2006) (Figure 1.9).

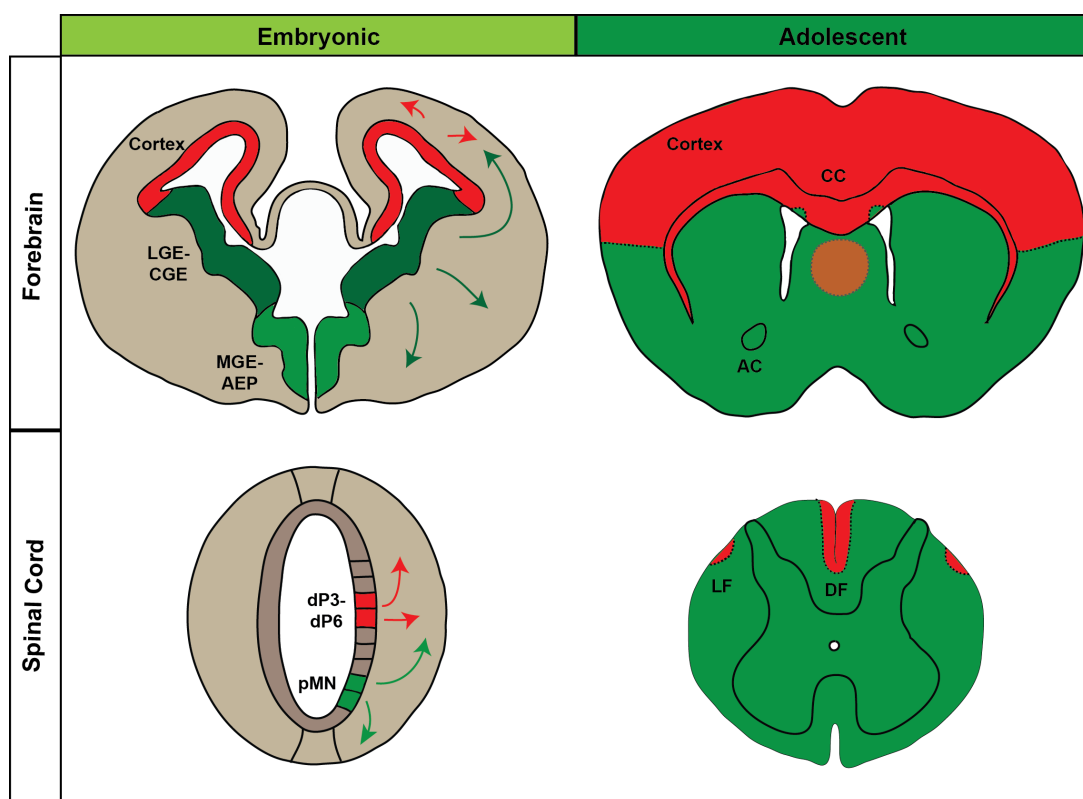


Fig. 1.9 **Developmental origin of OPCs.** MGE = medial ganglionic eminence, AEP = anterior entopeduncular, LGE = lateral ganglionic eminence, CGE = caudal ganglionic eminence, CC = corpus callosum, AC = anterior commissure, p = progenitor domain, MN = motor neuron, dP = dorsal progenitor domain, DF = dorsal funiculus, LF = lateral funiculus. Figure partially adopted from (Rowitch & Kriegstein, 2010).

The discovery of the developmental OPC heterogeneity in the CNS prompted the question of whether the developmentally distinct OPCs populations are functionally heterogeneous or only a requirement of evolution to accommodate the rapid growth of the CNS.

Arguing for an existence of a developmental heterogeneity is the finding that

molecular cues needed for OPC specification differ between the developmental origins. Whereas ventral OPCs need Shh-signalling, Shh is redundant for dorsal OPC specification (Cai et al., 2005). In contrast, the induction of FGF signalling as well as the inhibition of WNT and BMP signalling pathways have been speculated to play an important role in the specification and timing of appearance of dorsal OPCs (Chandran et al., 2003; Vallstedt et al., 2005; Langseth et al., 2010) (Table 1.2). Likewise, in favour of the hypothesis of developmental OPC heterogeneity, dorsal derived OPCs exhibit a myelination preference for dorsal areas in the CNS (Kessaris et al., 2006; Tripathi et al., 2011a). As an example, in the course of spinal cord development, the dorsal funiculus is initially populated by ventrally-derived oligodendrocytes, but is eventually comprised of more than 80% of dorsally-derived oligodendrocytes in an adult animal. The fact that ventrally derived oligodendrocyte numbers decrease after P13, whereas dorsally derived oligodendrocyte numbers stay constant, strongly argues for a selective advantage of dorsally derived oligodendrocytes in the dorsal funiculus of the spinal cord (Tripathi et al., 2011a). Similar competition between ventrally and dorsally derived oligodendrocytes can be observed in the cortex and CC in the murine forebrain (Kessaris et al., 2006) (Table 1.2).

Following the discovery of a potential competition between ventral and dorsal derived OLCs, the authors hypothesised that the developmentally distinct OPC populations might differ in their capability to respond to neuronal electrical stimulation. This hypothesis was further confounded by the findings that neuronal activity influences OPC behaviour (Li et al., 2010; Makinodan et al., 2012; Gibson et al., 2014; Mensch et al., 2015), and OPCs heterogeneity with regard to the responsiveness to neuronal stimulation was identified (Káradóttir et al., 2008). However, no difference in the electrical conductivity of ventral and dorsal derived OPCs has been observed (Tripathi et al., 2011a) (Table 1.2).

To test whether ventral OPCs can functionally compensate for the absence of dorsal oligodendrocytes, the transcription factor OLIG2 was knocked out in dorsal OPCs in the embryo, causing a block in dorsal OPC differentiation, without influencing OPC numbers. The specific knockout of OLIG2 in dorsal OPCs led to a reduction in myelination in the CC, suggesting a functional difference of ventral and dorsal OLCs (Yue et al., 2006). In contrast, the individual ablation of the developmentally-distinct OPC populations in the telencephalon by region-specific expression of diphtheria toxin A (DTA) neither caused a reduction in total OLCs at postnatal day 12 (P12) nor in myelination in adult mice (Kessaris et al., 2006), concluding that different OLCs can

functionally compensate for each other. The contradictory results of the two studies could be explained by the different target cell population ablated, OPCs (Kessar et al., 2006) and oligodendrocytes (Yue et al., 2006) (Table 1.2).

OPCs not only have an important function in developmental myelination, but also mediating remyelination in response to a demyelinating injury. By tracing the response of dorsal OPCs to a demyelinating insult in the spinal cord, it was shown that dorsal OPCs significantly contribute to remyelination by providing newly formed oligodendrocytes in the lesion (Zhu et al., 2011). In accordance, Crawford et al. demonstrated that the dorsal OPC response is more pronounced to a focal demyelination insult due to a significant increase in proliferation of dorsal OPCs when compared to ventral OPCs (Crawford et al., 2016) (Table 1.2). This is highly suggestive of a greater remyelination potential of dorsal OPCs, however, effective remyelination by dorsal OPCs remains to be proven by electron microscopy in this model.

Differences	Similarities
Region of origin in forebrain	Identical electrical properties
OPC specification signals	Comparable myelination capacity
Distinct CNS populating pattern in adult animal	
Increased remyelination capacity of dorsal OPCs	

Table 1.2 **Are developmentally distinct OPCs heterogeneous?** Summary of differences and similarities of developmentally distinct OPCs.

The developmental origin of OPCs has been proven to be functionally important in the response to a demyelinating injury in the CNS. However, how ventral and dorsal OLCs differ from each other in terms of their gene/protein expression and cellular behaviour remains to be elucidated. Accordingly, whether these differences of ventral and dorsal OLCs influence physiological brain function differently needs to be investigated (see Section 1.7).

Heterogeneity of white matter and grey matter OPCs

Proliferation capacity

In vivo proliferation studies revealed that white matter OPCs proliferate more rapidly than grey matter OPCs, due to grey matter OPCs showing longer cell cycle times (Dawson, Polito, Levine, & Reynolds, 2003; Dimou et al., 2008; Rivers et al., 2008;

Young et al., 2013). However, even though the OPCs cell cycle time increases with progressive age, independent of location in the brain, grey matter OPCs show a smaller net increase in cell cycle time (Young et al., 2013). The increased propensity of white matter derived OPCs to proliferate has been recapitulated *in vitro*, exhibiting a threefold to fourfold greater proliferative response to PDGF-AA than those in grey matter (Hill, Patel, Medved, Reiss, & Nishiyama, 2013). Tissue pieces from white matter transplanted into grey matter areas of brain slices retained their greater proliferative response to PDGF-AA, suggesting that NG2⁺ cells in the white matter have an intrinsically higher proliferative capacity than those in grey matter (Hill et al., 2013) (Table 1.3).

Differentiation potential

Work by Dimou and colleagues set out to address the specific question of grey matter versus white matter heterogeneity with regard to their differentiation potential. An OLIG2 -fate mapping strategy demonstrated that white matter OPCs have a higher tendency to differentiate into mature oligodendrocytes than OPCs from grey matter regions (white matter: 40.6%, grey matter: 11%), however this did not address the central issue of whether this difference is due to an extrinsic or intrinsic difference between the two populations (Dimou et al., 2008). Consequently, a follow up study sought to address this question by transplanting OPCs derived from both grey and white matter in to the antithetical region. White matter derived cells were able to differentiate more robustly when transplanted into both white and grey matter, than grey matter derived cells when transplanted into white matter, arguing for an intrinsic heterogeneity of white and grey matter OPCs (Viganò, Möbius, Götz, & Dimou, 2013) (Table 1.3).

Ion channel expression

Chittajallu and colleagues performed a detailed characterisation of ion channels in neonatal OPCs, thereby identifying differing profiles of Na⁺ and K⁺ channel expression in white and grey matter OPCs. With respect to voltage gated potassium channels, there is a marked increase in the expression of KDR (slow-inactivating delayed-rectifier) and Kir (inward-rectifier) potassium channel in grey matter OPCs, when compared to white matter OPCs. The expression of KA (fast-inactivating A-type) potassium channel is comparable between the two OPC subpopulations (Chittajallu et al., 2004). The difference in potassium channel expression is of particular interest as their levels of expression is correlated with the maturation of oligodendrocyte lineage cells

(Sontheimer, Trotter, Schachner, & Kettenmann, 1989; Kettenmann, Blankenfeld, & Trotter, 1991; Neusch, Rozengurt, Jacobs, Lester, & Kofuji, 2001). Therefore this apparent difference in the potassium channel expression between grey and white matter may suggest some difference in fate capacity (Table 1.3).

In addition, within the cortical grey matter, a subpopulation of OPCs cells express sodium channels, rendering it possible for a subpopulation of OPCs to elicit a spike following depolarisation (Chittajallu et al., 2004). Similarly, in the grey matter of the rat hippocampus, OPCs were shown to receive both glutaminergic and GABAergic signals (Bergles et al., 2000). Together, these data suggest a unique feature of a subpopulation of grey matter OPCs to respond to neuronal activity. However, Karadottir and colleagues found two distinct subpopulation of OPCs in the white matter of early postnatal rat cerebellum; one subpopulation received both excitatory and inhibitory synaptic inputs and, most significantly, were able to fire action potentials. The second subpopulation received no such inputs and were unable to form action potentials (Káradóttir et al., 2008). This suggests that the ability to spike may not be a distinguishing feature of white versus grey matter, but rather of two sub populations within both grey matter and white matter which play functionally distinct roles in these regions (Table 1.3).

Differences	Similarities
White matter OPCs proliferate faster (due to shorter cell cycle times)	Comparable KA channel expression in white and grey matter OPCs
White matter OPCs differentiate more into mature astrocytes	Comparable Na ⁺ channel expression in white and grey matter OPCs
White matter OPCs express less KDR and Kir channels	

Table 1.3 **Are white and grey matter OPCs heterogeneous?** Summary of differences and similarities of white and grey matter OPCs.

In summary, compelling evidence demonstrates the heterogeneity of white and grey matter OPCs with regards to their proliferation, differentiation and expression of potassium channels. However, to what extent these differences in OPC behaviour are important for intact CNS function remains to be elucidated.

1.4.2 Oligodendrocyte heterogeneity

Morphological heterogeneity

The first description of oligodendrocyte heterogeneity was provided by del Río Hortega who identified 4 different classes of oligodendrocytes based on their morphology through careful microscopic observations of the brain. Oligodendrocytes categorised in class 1 (CI) are found both in white and grey matter, and are typically characterised by a high number (5-20) of thin processes extended to small, thinly-myelinated axons. In comparison, class 2 (CII) oligodendrocytes have fewer, but thicker processes and are exclusively found in the white matter. Oligodendrocytes categorised in class 3 (CIII) and class 4 (CIV) can be mostly found in the white matter of the brain stem and spinal cord areas with thick axons. In comparison to CI and CII oligodendrocytes, they are less abundant and extend fewer processes (del Río Hortega, 1928). Following this initial classification of oligodendrocytes, additional morphological subclasses have been identified in various CNS regions (Monteiro, 1983; Ogawa, Eins, & Wolff, 1985; Butt & Ransom, 1989; Friedman, Hockfield, Black, Woodruff, & Waxman, 1989; Bjartmar, Hildebrand, & Loinder, 1994; Butt, Colquhoun, Tutton, & Berry, 1994; Butt, Ibrahim, Ruge, & Berry, 1995; Weruaga-Prieto, Egli, & Celio, 1996; Murtie, Macklin, & Corfas, 2007).

Molecular heterogeneity

In addition to the morphological classification, oligodendrocytes can also be distinguished based on expression levels of carbonic anhydrase II (CAII). Oligodendrocytes expressing CAII typically form numerous myelin sheaths supporting small diameter axons (therefore corresponding to CI and CII oligodendrocytes according to de Río Hortega), whereas oligodendrocytes lacking the expression of CAII had fewer myelin sheaths myelinating larger diameter axons (therefore corresponding to CIII and CIV oligodendrocytes according to de Río Hortega) (Butt et al., 1995). Whilst the function of CAII in the production of bicarbonate during hydration of carbon dioxide (Geers & Gros, 2000), and its importance in oligodendrocyte maturation has been demonstrated (Cammer, Zhang, & Cammer, 1993), its functional role in oligodendrocyte heterogeneity has not been proven yet.

The intracellular localisation of MBP was also reported to be heterogeneous in oligodendrocytes. Out of all oligodendrocytes imaged, some expressed MBP only in the plasmalemma, some expressed MBP in the plasmalemma and cytoplasm, and 50% expressed MBP in the plasmalemma, cytoplasm and nucleus (Hardy, Lazzarini, Col-

man, & Friedrich, 1996). As the shuttling of MBP protein between the nucleus and the cytoplasm seems to be directed, a unique function of nuclear MBP is anticipated, but to date not proven.

Functional heterogeneity

As the different morphological subclasses of oligodendrocytes are mostly found in specific brain regions, the question remained whether the differences in morphology observed reflect intrinsic heterogeneity or are dictated by either axon properties (e.g. axon diameter, surface molecules expressed on axons) or extrinsic environmental cues in specific brain regions.

The prevailing view is that axons provide molecular cues necessary for oligodendrocyte myelination, appropriate sheath lengths and thickness. This view is supported by the notion that myelin sheath length and thickness strongly correlate with the axon's diameter (Donaldson & Hoke, 1905; RUSHTON, 1951; Williams & Wendell-Smith, 1971; Murray & Blakemore, 1980).

To challenge the dogma, Bechler et al. analysed the compact myelin sheath formation of cortical and spinal cord OPCs without contribution of axons in a microfiber assay. In comparison to cortical oligodendrocytes, oligodendrocytes from the spinal cord formed myelin sheaths which were twice as long, whereas the number of sheaths formed per oligodendrocyte was similar (Bechler et al., 2015). The same difference in sheath length formation between spinal cord and cortical oligodendrocytes was observed *in vivo* (Chong et al., 2012). This demonstrates that the oligodendrocyte itself determines its myelinogenic potential (generation and coordination of the number and length of myelin internodes), hinting at an important role of the developmental origin (cortical versus spinal cord OPCs) or extracellular priming of OPCs as a source of oligodendrocyte heterogeneity.

The development of a MBP-GFP (membranous bound) reporter mouse line, only sparsely labelling about 1% of oligodendrocytes in the brain, allowed the imaging of the myelin sheaths formed by a single oligodendrocyte. The 3D reconstruction of the images revealed a heterogeneity of oligodendrocytes in their myelin sheath formation capacity with regards to the number of myelin sheaths formed per oligodendrocyte (between 10 and 60 myelin sheaths per oligodendrocyte) and myelin sheath length (between 20 μ m and 200 μ m). This heterogeneity is not region-specific, but can be detected in the same local CNS region, even along axons with similar properties (Chong et al., 2012), suggesting that oligodendrocyte heterogeneity does not exist, at

least not with regards to their myelin sheath length. Indeed, using an *in vitro* co-culture with neurons, Chong and colleagues were able to demonstrate that the density of oligodendrocytes and therefore the competition between oligodendrocytes, regulates their myelin formation (Chong et al., 2012). This competition was driven by the expression of the inhibitory molecule NOGO-A expressed on OPCs and oligodendrocytes (Chong et al., 2012). How oligodendrocyte density is regulated in the brain to explain the morphological subclasses of oligodendrocytes defined by del Rio Hortega and colleagues remains to be determined. Additionally, in a study by Vinet and colleagues, oligodendrocyte density only partially correlates with morphology complexity in the murine hippocampus (Vinet et al., 2010).

Therefore, to unambiguously prove the existence of oligodendrocyte heterogeneity, specific functions of distinct oligodendrocytes would need to be demonstrated. Recent studies observed particular distribution patterns of oligodendrocyte subpopulations in brain tissue, hinting towards a unique function of individual oligodendrocyte subtypes. Using a CNP-GFP line, three subclasses of oligodendrocytes with increasing degrees of ramification have been identified in the murine hippocampus (Vinet et al., 2010). Distribution analysis of these oligodendrocyte subtypes revealed that different oligodendrocyte subpopulations reside in distinct territories. Similar results have been found in a single-cell RNA sequencing analysis of the oligodendrocyte lineage in ten different regions (including many regions in the forebrain, but also the spinal cord) of the mouse juvenile and adult CNS (Marques et al., 2016). This study revealed 12 distinct OLC populations marking the differentiation stages of OPCs into oligodendrocytes. Half of the identified populations are mature oligodendrocytes. In the juvenile mouse, all CNS regions are comprised of oligodendrocytes from at least 2 different oligodendrocyte populations. Whereas one mature oligodendrocyte population was present in all CNS regions, the other identified oligodendrocyte populations are prevalent in certain CNS regions only. However, in the adult brain regions studied (cortex and CC), the diversity of oligodendrocyte populations is reduced, with only two oligodendrocyte populations present (Marques et al., 2016).

Recently, compelling evidence for functional heterogeneity of oligodendrocytes has been published. Using three different viruses to label oligodendrocytes, and neuronal axon projections of motor and sensory neurons in the CC, the preference of colossal oligodendrocytes to myelinate projections of motor neurons or sensory neurons was assessed. Their analysis revealed that colossal oligodendrocytes can be classified into three categories: those that preferentially myelinate axons from the

motor cortex, those that preferentially myelinate axons from the sensory cortex and those that myelinate axons from both brain regions without preference (the latter represent 75% of all oligodendrocytes assessed). However, it is conceivable that the 25% of oligodendrocytes showing a preference towards specific axons are adult-born oligodendrocytes, specifically myelinating an axon based on activity (Osanai et al., 2017).

In summary, various studies point towards oligodendrocyte heterogeneity in the CNS. However, the gold standard for proving heterogeneity unambiguously is demonstrating specific functions of the distinct subpopulations. Therefore, further studies looking into functional oligodendrocyte heterogeneity need to be conducted.

1.5 Regulation of neuronal conduction and transmission

All the distinct cell types in the CNS are in close reciprocal cross-talk, ultimately optimising neuronal transmission. The OLCs play an important role in modulating neuronal conduction. Through myelination, oligodendrocytes can adjust the speed of neuronal conduction, ensure axonal integrity and provide nutritional support (see Section 1.2.3). In turn, the impact of OPCs specifically on neuronal firing is just beginning to be elucidated (see Section 1.2.2).

Besides OLCs, astrocytes can also directly regulate neuronal transmission by modulating synaptic transmission (synaptogenesis, neurotransmitter recycling and synaptic transmission) via the tripartite synapse and by providing trophic support to the axon through gap junctions (see Section 1.1.2). In addition, astrocytes can indirectly regulate neuronal networks by affecting OPC behaviour (migration, proliferation and differentiation). In development, OPCs use the astrocyte-derived extracellular matrix as a substrate for their movement (Schnädelbach & Fawcett, 2001). Further supporting the role of astrocytes in influencing OPC behaviour, a vast body of literature uncovered that astrocytes secrete several molecules, including PDGF-AA (Raff, Lillien, Richardson, Burne, & Noble, 1988), BMP (See et al., 2004), LIF (Gard, Burrell, Pfeiffer, Rudge, & Williams, 1995) and CNTF (Stankoff et al., 2002), which control the balance between OPC self-renewal and differentiation into mature oligodendrocytes. Oligodendrocytes and astrocytes are directly connected via gap junctions, allowing a close interaction between the two cell types. Not only are the gap junctions important

for the supply of nutrients and lipids to the oligodendrocyte (Camargo et al., 2017), the maintenance of the gap junctions is also required for timing of myelination (Tress et al., 2012). Co-cultures of astrocytes and oligodendrocytes revealed further that astrocyte proximity, in a contact-independent manner, induces profound gene expression changes in the oligodendrocytes, in particular the expression of several myelin-related and cytokine receptor genes (Iacobas & Iacobas, 2010) (Figure 1.10).

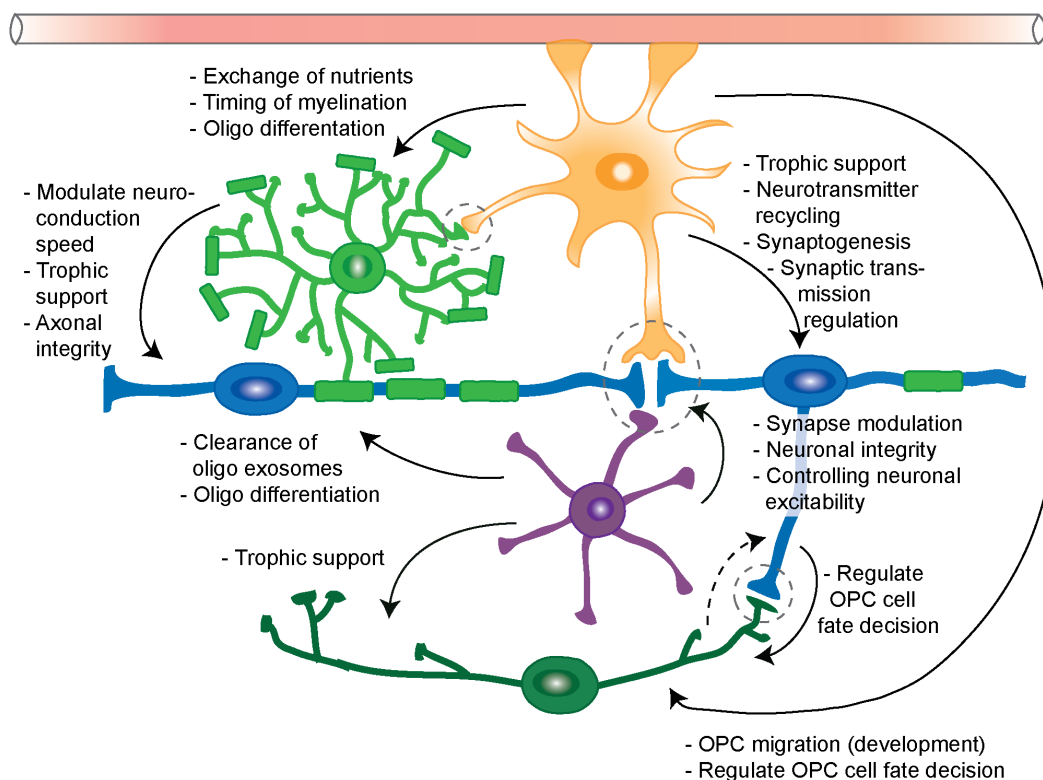


Fig. 1.10 Modulation of neuronal conduction and transmission by the complex interaction network of glia cells and microglia.

Lastly, microglia are involved in shaping synapses (synaptic pruning) and controlling neuronal excitability, thereby directly modulating neuronal transmission. Neurotrophic molecules transferred from microglia to neurons further sustain neuronal integrity (see Section 1.1.3). However, as well as astrocytes, microglia can influence neuronal conduction by indirectly acting on OLCs (Figure 1.10). Molecules secreted by microglia can influence OPC behaviour, as for example activin-A secreted by microglia increases oligodendrocyte numbers following a demyelinating insult (Miron et al., 2013). Early studies using microglia and oligodendrocyte co-cultures showed that microglia stimulate gene expression of myelin related genes in oligodendrocytes (S. P. Hamilton & Rome, 1994). Later on the PDGF α -, NF κ B- and AKT-signalling

pathway, *inter alia*, have been shown to be important in this process (Nicholas, Wing, & Compston, 2001; Nicholas, Stevens, Wing, & Compston, 2002). Furthermore, microglia are an important source of iron (X. Zhang, Surguladze, Slagle-Webb, Cozzi, & Connor, 2006; Cheepsunthorn, Palmer, & Connor, 1998), which is required for myelination (Badaracco, Siri, & Pasquini, 2010), but cannot be synthesised in oligodendrocytes itself. Finally, by taking up exosomes containing myelin debris secreted by oligodendrocytes, microglia assist in myelin turnover (Fitzner et al., 2011).

The brain is a fine-balanced system of various brain cells working together, in which different neuronal circuits might have very specific requirements at their environment. Therefore, there are likely to be regional differences in the extent and mechanisms of support by different cells types.

1.6 The role of OLCs in diseases

Cells of the oligodendrocyte lineage are implicated in a plethora of diseases, ranging from leukodystrophies (genetic disorders affecting the growth or maintenance of the myelin sheath) and demyelinating diseases (acquired diseases defined by the destruction of the myelin sheath) to psychiatric disorders.

A lack or loss of myelination in the CNS has detrimental consequences, not only in the short term because of impaired neuronal conduction, but also long term due to neuron degeneration (see Section 1.2.3). The latter represents a major problem as there is only a limited pool of neuronal stem cells in two very localised brain areas, which are not capable of repopulating the brain with newly born neurons. To counteract neuronal loss, stem cell transplantation is the only conceivable treatment option.

The causes of the lack of myelination can be separated into hereditary and acquired diseases. Hereditary demyelinating diseases include Pelizaeus-Merzbacher disease (PMD) and Krabbe disease (both categorised as leukodystrophies), caused by hereditary mutations in genes that affect development or growth of the myelin sheath (Boespflug-Tanguy, Labauge, Fogli, & Vauris-Barriere, 2008). As an example, PMD was causally associated with a mutation of PLP1 (see Section 1.2.3), leading to severe neurological disability including involuntary eye movement (nystagmus), muscle weakness (spastic quadriparesis), incoordination of muscle movements (ataxia) and cognitive impairment (Pelizaeus, 1985; Merzbacher, 1910). As treatment options for leukodystrophies, stem cell transplantation and *ex vivo* gene correction technologies are currently being developed.

In contrast, multiple sclerosis (MS), the most well-known acquired demyelination disorder, is an autoimmune disease in which macrophages mistakenly attack the myelin sheaths around axons (McFarland & Martin, 2007). In response to oligodendrocyte injury or death due to an autoimmune reaction, local OPCs proliferate, migrate to the site of CNS damage and differentiate into oligodendrocytes, which are capable of creating new myelin sheaths. This process is known as remyelination, and can result in a complete reconstruction of the myelin sheath (Franklin & Goldman, 2015) (see Section 1.2.2 and Figure 1.4). However, particularly with ageing, this process fails due to intrinsic changes in the OPC population (see Section 1.3.3). These changes have been shown to be reversible (Ruckh et al., 2012), rendering OPC reactivation as an important therapeutic option (Table 1.4). Together with intrinsic changes (see Section 1.3.3), extrinsic alterations in the brain environment are responsible for age related remyelination decline. The impairment of aged macrophages to clear myelin debris, an inhibitory signals for myelination (Kotter, Li, Zhao, & Franklin, 2006), as well as to express remyelination associated growth factors and initiate an early inflammatory response, together leads to a delay in OPC activation (Zhao, Li, & Franklin, 2006). Upon demyelination, axons enhance the expression of polysialylated neural cell adhesion molecule (PSA-NCAM), a molecule that inhibits myelination, rendering the remyelination of demyelinated axons more difficult (Charles et al., 2000). Finally, the accumulation of inhibitory mediators, such as hyaluronan (Back et al., 2005) and fibronectin aggregates (Back et al., 2005), within the extracellular environment has been shown to contribute to OPC differentiation failure (Table 1.4).

Intrinsic	Extrinsic
Changes in the gene or protein expression profile of OPCs	Reduced myelin debris clearance
Aberrant epigenetic control	Reduced OPC activation
Increased OPC cell cycle time	Aberrant expression of neuronal inhibitory mediators
Reduced OPC differentiation	Extracellular accumulation of inhibitory mediators

Table 1.4 Intrinsic and extrinsic causes of remyelination failure in aged animals.

While the death of neurons will inevitably stop the action potential activity in any neural network, minimal myelination defects (i.e. enough to cause a conduction delay of just one millisecond) will significantly impact the synchrony of a neural network and cause neurological deficits including cognitive impairment (Pajevic, Basser, &

Fields, 2014). Therefore, cognitive impairment recognised in demyelinating diseases (eg. MS) or other degenerative diseases (eg. Alzheimer's disease, dementia) might be caused by myelin loss or abnormalities as opposed to primary axonal pathology.

Investigating the role of glia in psychiatric disorders is impeded by the lack of availability of appropriate rodent models for psychiatric diseases. Nonetheless, some progress regarding OLCs involvement in development of psychiatric diseases has been made. Recently, a primary role of glia cells in the pathophysiology of psychiatric diseases has been revealed (Birey et al., 2015; Windrem et al., 2017). For instance, the ablation of NG2⁺ OPCs causes depression like symptoms in mice (Birey et al., 2015). In addition, following the transplantation of glia progenitor cells derived from iPS cells of schizophrenia patients, mice showed reduced prepulse inhibition and abnormal behaviour, including excessive anxiety, antisocial traits, and disturbed sleep, which are typical symptoms of schizophrenia (Windrem et al., 2017).

The cause of schizophrenia is not yet fully understood, however, some susceptibility genes have already been identified. Disrupted-in-schizophrenia 1 (DISC1) is one of the genes involved in schizophrenia development; DISC-1 mutant mice show an increase in schizophrenia-like behaviours (Hikida et al., 2007). It was demonstrated that DISC1 expression blocks OPC differentiation by regulating the transcription of *Sox10* and *Nkx2.2*, hinting towards a role of OLCs in DISC-1 driven schizophrenia (Hattori et al., 2014).

The over expression of another well-known myelin protein, PLP1, leads to reduced conduction velocity, despite only small changes in myelination, resulting in a schizophrenia-like behaviour including reduced prepulse inhibitions, spatial learning deficits and working memory deficit (H. Tanaka et al., 2009). Erb-B2 Receptor Tyrosine Kinase 4 (ERBB4), the receptor for NRG1, has also been shown to be involved in the pathology of schizophrenia. Oligodendrocyte-specific ERBB4 knockout mice show cellular abnormalities, including less complex oligodendrocyte morphology and thinner myelin sheaths, as well as behavioural changes with increased anxiety and enhanced sensation to amphetamine (Roy et al., 2007). Another psychiatric disease, in which the contribution of glia is extensively studied, is Rett syndrome (RTT) caused by a mutation in the methyl-CpG binding protein 2 (MeCP2) gene (Amir et al., 1999). While astrocytes and microglia seem to be the main players in RTT pathogenesis, the knockout of MeCP2 specifically in oligodendrocytes caused a mild RTT-syndrome phenotype. Restoration of MeCP2 expression in oligodendrocytes in MeCP2-null mice significantly improved locomotor deficits and hindlimb clasping phenotype, although only slightly prolonging their lifespan (Nguyen et al., 2013) (Table 1.5).

Mouse model	Phenotype	Psychiatric disorder	Reference
DISC1 KO	OPC differentiation ↓	Schizophrenia	(Hattori et al., 2014)
PLP1 OE	Axonal diameter ↓ Abnormal paranodes Conduction velocity ↓ Anxiety ↑	Schizophrenia	(H. Tanaka et al., 2009)
ERBB4 KO	Simple OL morphology G-ratio ↑ Conduction velocity ↓ Anxiety ↑ Hypersensitivity to AMP	Schizophrenia	(Roy et al., 2007)
MeCP2 KO	Vigilance/activity ↑ Severe hindlimb clasping	Rett syndrome	(Nguyen et al., 2013)
MeCP2 OE	Locomotor coordination ↑ Body weight ↑	Rett syndrome	(Nguyen et al., 2013)

Table 1.5 **The role of OLCs in the pathology of psychiatric disorders.** Gene expression changes in all mouse models are specific to oligodendrocytes. AMP = amphetamine, OE = over expression, OL = oligodendrocyte, KO = knockout

In summary, the role of the OLCs in neurological diseases is wide ranging, with huge scope for new therapeutic avenues. However, improved understanding of OPC biology is required to facilitate development of such therapeutics.

1.7 Objectives

OLCs carry out important functions in supporting neuronal integrity and optimising neuronal conduction. The lack of OLC support leaves a neuron more susceptible to degeneration, thus explaining the implication of OLC malfunction in various neurological diseases (see Section 1.6), and rendering the basic understanding of OLC function in the CNS pivotal.

In the CNS, the neuronal population is highly heterogeneous with respect to their function. Subpopulations of neurons exhibit distinct firing patterns, connectomes and effects on other neurons. Consequently, distinct neuronal subtypes and their respective neuronal circuits most likely have specific requirements from their environment. As OLCs provide vital, multifaceted support to the neuron, potentially subpopulations of the OLCs facilitate the individual, regional support of neuronal circuits.

The OLCs can be divided into two subpopulations based on their developmental origin, ventrally-derived OLCs and dorsally-derived OLCs. The functional importance of the developmental origin of OLCs has been shown in their response to a demyelinating injury. Whether the developmentally distinct OLCs fulfil different functions in the brain under steady state conditions will be investigated in this thesis.

In particular, the following key hypotheses will be explored:

1. Ventral and dorsal OLCs are intrinsically different.
2. Ventral and dorsal OLCs differently support neuronal circuits.
3. Ventral and dorsal OLCs cannot functionally compensate for one another.

Chapter 2

Materials and Methods

2.1 Animal models

In this thesis, three different mouse lines were used (Table 2.1)

(1) A generic reporter mouse line *Sox10-loxP-eGFP-PolyA-STOP-loxP-tdTomato* (hereafter called: *Sox10-eGFP-tdTomato*).

(2) A Cre-reporter mouse line driven by the *Emx1*-promoter (hereafter called: *Emx1-Cre*) to differentially label dorsally-precursor cells.

(3) A DTA-carrying reporter mouse line *Sox10-loxP-eGFP-STOP-loxP-DTA* (hereafter called: *Sox10-eGFP-DTA* to ablate oligodendrocyte lineage cells (OLCs).

Mouse line	Abbreviation	Reference
Sox10-loxp-eGFP-PolyA-STOP-loxp-TdTomato	Sox10-eGFP-tdTomato	(Kessaris et al., 2006) (Tripathi et al., 2011b)
Emx1-Cre-recombinase	Emx1-Cre	(Kessaris et al., 2006)
Sox10-loxP-GFP-polyA-STOP-loxP-DTA	Sox10-eGFP-DTA	(Kessaris et al., 2006)

Table 2.1 Overview of mouse lines.

All of the mouse lines were a kind gift by William Richardson, UCL London. A brief summary of the generation of these transgenic mouse lines is provided below.

The *Sox10-eGFP-tdTomato* reporter mouse line was generated using a fragment of a P1-derived artificial chromosome (PAC) coding for the genomic sequence of *Sox10*. The *Sox10* genomic region spanning exons 3 to exon 5 was replaced with

loxP-eGFP-poly(A)-loxP-TdTomato by homologous recombination in *Escherichia coli* (*E. coli*) (Chapter 1, Figure 3.2). The inserted transgene also carries a chloramphenicol resistance cassette (CmR) which was removed after selection of successful recombined bacterial clones. After linearisation and purification of the modified PAC DNA, the DNA was injected into pronuclei of fertilised mouse eggs. Successful random integration into the genome was confirmed by PCR and southern blot (Tripathi et al., 2011a) (Chapter 1, Figure 3.2). The *Sox10* expression of the transgene recapitulated the endogenous *Sox10* expression, as in the absence of Cre-recombinase 96% of the OLCs stained with SOX10 antibody also expressed GFP (Tripathi et al., 2011a). An additional immunostaining with OLIG2 confirmed that 92% of all OLCs are labelled by the *Sox10-eGFP-tdTomato* reporter mouse line (Tripathi et al., 2011a). The labelling of other cells outside the CNS has not been investigated.

In order to differentially label ventrally- and dorsally-derived OLCs in the brain, *Sox10-GFP-TdTom* mice were crossed to *Emx1-Cre* mice (Kessaris et al., 2006). To create the *Emx1-Cre* mouse line, a PAC clone containing the genomic DNA of *Emx1* was selected. Next, codon-improved Cre recombinase (iCre) was fused to the initiation codon of *Emx1* using a PCR-based approach, thereby removing the first exon of the *Emx1* coding region and replacing it with iCre. PAC modifications were carried out in *E. coli*. Pronuclear injection was performed as described for the *Sox10-eGFP-tdTomato* reporter mouse line (Kessaris et al., 2006). *Emx1* is expressed by the late emerging, cortical precursors of the developing forebrain and hence *Emx1* is not solely confined to oligodendrocyte lineage cells. The recombination efficiency in double transgenic *Sox10-eGFP-tdTomato/Emx1-Cre* animals is close to 100% (Tripathi et al., 2011a).

To study the specific function of dorsally-derived, *Emx1*⁺ OLCs in the brain, dorsally-derived OPCs were ablated by crossing the *Emx1-Cre* line to the *Sox10-loxP-GFP-poly(A)-loxP-DTA* mouse line (hereafter called *Sox10-eGFP-DTA*) (Kessaris et al., 2006). The *Sox10-eGFP-DTA* mouse line was generated similarly to the *Sox10-eGFP-tdTomato*. The *Sox10* genomic region spanning exons 3 to exon 5 was replaced with a *lox-eGFP-polyA4-lox-DTA* cassette by homologous recombination in *E. coli* (Chapter 1, Figure 3.1). Pronuclear injection was performed as described for the *Sox10-eGFP-tdTomato* reporter mouse line (Kessaris et al., 2006). The *Sox10* expression of the transgene recapitulated the endogenous *Sox10* expression, as 98% of the OLCs stained with SOX10 antibody also expressed GFP (Kessaris et al., 2006). Efficiency of the *Sox10*-driven ablation system was demonstrated by crossing the *Sox10-eGFP-DTA* to an *Olig2-Cre* line. As expected, no GFP⁺ or SOX10⁺ cells were detected in the

CNS of double transgenic neonatal animals. How efficiently $Emx1^+$ OLCs are ablated in *Sox10-eGFP-DTA/Emx1-Cre* animals will be discussed in Chapter 1 (see Chapter 1, Section 3.2).

2.2 Animal husbandry

Mice were housed in the Innes Building animal facility at the Department of Veterinary Medicine, University of Cambridge, according to Home Office requirements under project license 70/7715. All animals were fed a standard diet and were kept under a 12h dark, 12h light cycle in individually ventilated cages. Breeding colonies were maintained by mating transgenic mice to wild type B6CBA-F1 mice, supplied by Harlan Laboratories, UK. For genotyping, 2mm ear biopsies were collected and analysed by Transnetyx genotyping service, Cordova, Tennessee, US. Animals aged between postnatal day 0 (P0) and P5 are termed neonates, whilst adult animals are between two and four months old. Animals which are more than nine months old are termed aged/old.

2.3 Isolation of primary cells

Neonatal or adult mice were sacrificed by decapitation or lethal injection of pentobarbitone (Pentobarbitone, Animalcare), respectively. The brains were removed quickly and placed into ice-cold transport medium (Half + 2% B27 (Gibco) + 1% Pen/Strep (Gibco) + 500nM NAC (Sigma)) (proprietary formulation of Half, see appendix). Brains were cut into 1mm^3 and washed twice with HBSS- (without Mg^{2+} and Ca^{2+}) (Gibco) to restore physiological pH. To pellet the brain pieces between the washes, samples were spun at 100g at RT for 1min. Neonatal brains were dissociated in 1ml dissociation solution (Half + 24mg/ml papain (Worthington) + 160 $\mu\text{g}/\text{ml}$ DNase 1 Type IV (Sigma) + 500nM NAC (Sigma)) per brain on the shaker at 37°C for 30min. To ensure complete digestion of adult brains, adult brains were dissociated in 4ml dissociation solution per brain on the shaker at 37°C for 40min. To stop papain digestion, each sample was washed once with HBSS- and subsequently spun at 200g at RT for 5min. Next, samples were triturated in trituration solution (HALF + 2% B27 (Gibco) + 2% Sodium pyruvate (Gibco) + 500nM NAC (Sigma)) until a single cell solution was obtained. Cells were filtered through a 70 μm nylon cell strainer (Falcon) to remove large cell debris and undigested brain tissue. Following filtration,

single cells were separated from myelin debris using a 22.5% Percoll gradient. To obtain the Percoll gradient, the filtered single cell solution was thoroughly mixed with 12ml of isotonic Percoll solution (10.8ml Percoll (GE Healthcare) + 1.2ml 10x PBS (Gibco)). Next, the final volume was adjusted to 47.5ml using DMEM/F12 (Gibco) per sample. The Percoll gradient was centrifuged at 800g at RT without breaks for 20mins. Subsequently, the cell debris was discarded, the cell pellet was washed with HBSS- and spun at 350g at RT for 5min.

2.4 Flow cytometry

Total brain cells were isolated as mentioned above. After isolation, cells were stained with Zombie Violet (Biolegend) in PBS for 15min at RT to identify live cells. To wash the cells, the cell pellet was resuspended in PBS and the sample was spun at 350g for 5min (standard settings for PBS/PBS + 0.5% bovine serum albumin (BSA, Sigma) washes if not indicated otherwise). Subsequently, cells were stained with primary antibodies (Table 2.2) in PBS + 0.5% BSA for 30min at 4°C. After a wash in PBS + 0.5% BSA, cells were stained with secondary antibodies (Table 2.2) diluted in PBS + 0.5% BSA for 15min at RT. After a wash in PBS + 0.5% BSA, cells were fixed with 4% paraformaldehyde (PFA, see appendix) for 10min at RT. An excess of PFA was removed by two washes in PBS + 0.5% BSA. Cell suspensions were filtered through a nylon mesh filter (50µm, Sysmex) prior to flow cytometry analysis. For flow cytometry analysis the LSR Fortessa (BD Biosciences, San Jose, CA), equipped with a 355nm, 405nm, 488nm, 561nm, and 640nm lasers was used at the Cell Phenotyping Hub at the Addenbrooke's Hospital Cambridge. Data was analysed using FlowJo software (Tree Star).

Antigen	Clone/Code	Species	Company	Dilution
Primary-coupled antibodies				
CD11b-PerCp-Cy5.5	M1/70	rat	Biolegend	1:1000
O4-Biotin	O4	mouse	Miltenyi Biotec	1:20
PDGFR α – PeCy7	APA5	rat	eBioscience	1:1440
Primary-uncoupled antibodies				
MOG	AF2439	goat	R&D systems	1:40
Secondary antibodies				
anti-goat Alexa 647	A11057	donkey	Thermo Scientific	1:500
BV785-Streptavidin	402549	n/a	Biolegend	1:800

Table 2.2 **Antibodies used for flow cytometry.**

2.5 Western Blot

Whole brain samples were lysed in IP lysis buffer (Thermo Scientific) supplemented with 0.1% Halt protease and phosphatase inhibitor (Thermo Scientific). The protein concentration of the samples were determined using the BCA Assay Kit (Thermo Scientific) following the manufacturer's instructions. In short, samples were incubated with BCA reagents for 30min at 37°C and protein concentration was measured using a spectrophotometer.

Subsequently, lysates were mixed with NuPAGE sample LDS loading buffer (4x) (Invitrogen) supplemented with 1X NuPAGE Reducing Agent (10X) (Invitrogen). All samples were boiled at 95°C for 10mins. 20µg per sample in a volume of 40µl was loaded on a NuPAGE Novex 4-12% Bis-Tris gel (Invitrogen). Gels were run at 200V for 32min in a mini gel tank (Thermo Scientific), filled with 1x Bolt™ MOPS SDS running buffer (in distilled H₂O) (Thermo Fisher). As a protein ladder, the Precision Plus standard protein ladder (Bio-Rad) was used.

Once the proteins were separated, gels were transferred onto nitrocellulose membranes (GE Healthcare Amersham™ Hybond ECL™ membrane, 0.45µm), which were pre-incubated with methanol (Sigma) for 5min. Semi-dry transfer was run in a mini gel tank (Thermo Scientific) using 1x Bolt™ transfer buffer (in distilled H₂O) (Thermo Fisher) supplemented with 10% methanol (Sigma) and 0.1% Bolt™ Antioxidant (Thermo Fisher) for 60min at 20V.

After transfer, the nitrocellulose membranes were blocked in 1x Odyssey blocking solution (TBS, Licor) (in TBS-T (TBS + 0.1% Tween (Sigma))) for 1h at RT on the shaker. Primary antibodies (Table 2.3) diluted in Odyssey blocking solution were incubated on the shaker at 4°C overnight. Three washes with TBS-T for 10mins at RT on shaker were done to remove the excess of the primary antibody (standard settings for TBS-T washes if not indicated otherwise). Subsequently, nitrocellulose membranes were incubated with secondary antibodies (Table 2.3) diluted in Odyssey blocking solution on the shaker for 1.5hrs at RT. Nitrocellulose membranes were washed with TBS-T three times, and stained with actin-peroxidase (Sigma) (1: 25 000 in TBS-T) for 20min at RT. After two final washes with TBS-T, fluorescent signals were detected using the Odyssey apparatus (Licor) with an exposure time of 2mins. Subsequently, actin-peroxidase was developed by incubating the nitrocellulose membranes with Amersham™ ECL™ Western Blotting Analysis System (GE Healthcare). The chemoluminescence of the peroxidase reaction was detected using the Odyssey apparatus (Licor) with an exposure time of 2mins. Band intensities of the developed Western blots were determined with Odyssey software (Licor).

Antigen	Clone/Code	Species	Company	Dilution
Primary antibodies				
Actin-oxidase	A5441	mouse	Sigma-Aldrich	1:5000
CASPR1	AB34151	rabbit	Abcam	1:1000
MAG	AB89780	mouse	Abcam	1:500
MBP	MCA4095	rat	Serotec	1:500
MOG	AF2439	goat	R&D systems	1:20000
PLP	AB28486	rabbit	Abcam	1:1000
Pan-NAV	ASC-003	rabbit	Alomone Laboratories	1:200
Secondary antibodies				
anti-mouse 800	926-32212	donkey	Licor	1:15000
anti-rabbit 800	926-32213	donkey	Licor	1:15000
anti-goat 800	926-32214	donkey	Licor	1:15000
anti-mouse 680	926-68022	donkey	Licor	1:15000
anti-rat 680	926-68076	goat	Licor	1:15000

Table 2.3 **Antibodies used for western blot.**

2.6 Perfusion and Dissection

Mice were anaesthetised with 3% isoflurane in 2% oxygen. When unconscious, mice were injected (intraperitoneally) with a lethal dose of pentobarbitone (Pentoject, Animalcare). Once fully anaesthetised, evident by a lack of response to deep pain and absent corneal reflexes, the mice were placed in dorsal recumbency, the thoracic cavity opened and the left cardiac ventricle pierced with a 23g butterfly catheter attached to a pump. The left atrium was cut open and the mouse was transcordially perfused with either 4% PFA or 4% glutaraldehyde, depending on the further processing of the samples (for the formulation of PFA and glutaraldehyde, see appendix).

2.7 Preparation of cryosections

For immunohistochemistry, mice were perfused with 4% cold PFA for 3mins, using approximately 55ml of PFA. The spinal cord or brain was cautiously dissected from the vertebral canal or skull respectively. The tissue was placed in 4% PFA for a further 2hrs at RT, transferred to 20% sucrose solution (Fisher Chemicals, S8600) (in distilled H₂O) for cryoprotection and stored at 4°C for 24-48hrs, before embedding in optimal

cutting temperature (OCT) medium (RA Lamb, UK). Tissues were stored at -80°C until further processed.

$10\mu\text{m}$ thick sections were obtained using a cryostat. Slides were collected on poly-l-lysine coated glass slides (ThermoFisher), air dried and stored at -80°C until stained.

2.8 Immunohistochemistry

For staining, slides were air-dried, washed once with PBS for 10min at RT on the shaker (standard settings for PBS/ H_2O washes if not indicated otherwise), and incubated with blocking solution (10% normal donkey serum (Sigma) (in PBS) supplemented with 0.1% Triton (Sigma)) for 1h at RT. After blocking, slides were incubated with primary antibodies (Table 2.4) (diluted in blocking solution) for 12 hours at 4°C . Excess antibodies were removed by three PBS washes, and secondary antibodies (Table 2.4) (diluted in blocking solution) were applied for 1h at RT. After two PBS washes, slides were washed three times with deionised H_2O , the second H_2O wash containing Hoechst 33258 nuclear stain (1:10000, 10mg/ml, Biotium). Slides were mounted with coverslips using Mowiol and stored at 4°C until imaging (formulation of Mowiol, see appendix).

In case a nuclear antigen was to be detected, a permeabilisation step was performed prior to blocking. Slides were placed in antigen retrieval buffer solution (Dako, S2369, diluted 1:10 in distilled H_2O) which was preheated to 95°C and incubated for 10mins at 75°C . Following two PBS washes, slides were blocked and incubated with antibodies as described above.

In case a primary antibody raised in mouse was to be used, the staining protocol was adapted to prevent unspecific binding of the primary antibodies in mouse tissue. For this protocol, slides were air dried, washed in PBS, and incubated with blocking solution (10% normal donkey (Sigma, D9663), 0.1% Triton (Sigma, 78287) in PBS) for 1hr at RT. Subsequently slides were incubated with the mouse-on-mouse (MOM) kit according to manufacturer's protocol (Vector laboratories). In short, slides were incubated with MOM reagent (in PBS) for 1hr at RT. Subsequently, slides were washed twice with PBS for 2min, before incubation with MOM protein solution (in PBS) for 5min at RT. Next, slides were incubated with primary antibodies (Table 2.4) diluted in MOM protein solution for 12hrs at 4°C . The following day, excess primary antibodies were removed by three PBS washes, before slides were incubated with the secondary antibodies (Table 2.4) (diluted in PBS + 0.1% Triton (Sigma)) for 1hr at RT. After two

PBS washes, slides were washed three times with deionised H₂O, the second H₂O wash containing Hoechst 33258 nuclear stain (1:10000, 10mg/ml, Biotium). Slides were mounted with coverslips using Mowiol and stored at 4°C until imaging.

In case a primary antibody raised in mouse detecting a nuclear antigen was to be used, the two staining protocols above were combined. Initially, slides were treated with antigen retrieval (as described above) before they were blocked with 10% normal donkey serum (in PBS) supplemented with 0.1% Triton. After that, the protocol for staining mouse primary antibodies was applied.

Antigen	Clone/Code	Species	Company	Dilution
Primary antibodies				
CC1	OP80	mouse	Calbiochem	1:100
CD68	MCA1957	rat	Serotec	1:200
GFP	GFP-1020	chicken	Aves Labs	1:1000
GFAP	Z0334	rabbit	DAKO	1:1000
IBA1	019-19741	rabbit	Wako	1:1000
NeuN	Millipore	mouse	MAB377	1:50
NG2	AB5320	rabbit	Millipore	1:500
SMI32	801701	mouse	Biologend	1:500
tdTOMATO	AB8181-200	goat	Sicgen Antibodies	1:100
Secondary antibodies				
anti-chicken Alexa 488	703545155	donkey	Jackson Laboratories	1:500
anti-goat Alexa 568	A11057	donkey	Thermo Fisher	1:500
anti-rabbit Alexa 647	A31573	donkey	Thermo Fisher	1:500
anti-mouse Alexa 647	A31571	donkey	Thermo Fisher	1:500

Table 2.4 **Antibodies used for immunohistochemistry.**

2.9 Confocal Microscopy and Image Analysis

Image acquisition was performed using a Leica SP5 Confocal microscope. Cell counts were obtained from 3-6 biological replicates, 3-4 sections per brain or spinal cord per biological replicate. Cell Profiler (Version 2.2.0) and Cell profiler analyst (Version 2.2.1) were used for image analysis, cell counting and measurement of the size of the selected area.

2.10 Resin embedding and preparation of semi-thin sections

For semi-thin resin sections and electron microscopy, mice were perfused with 4% glutaraldehyde for 4min, using approximately 75ml glutaraldehyde. Tissue was post-fixed in 4% glutaraldehyde at 4°C overnight. The brains were rinsed in PBS and the corpus callosum was dissected. The tissue was further processed in 2% osmium tetroxide overnight at 4°C. The following day the tissue was initially washed three times with deionised H₂O for 10min at RT and eventually dehydrated in a series of ethanol washes (1x 70% EtOH for 15min, 1x 95% EtOH for 15min and 3x 100% EtOH for 10min (Sigma)). The tissue was then washed twice in propylene oxide for 15min. Next, the samples were transferred into a one to one mix of propylene oxide and resin (50% resin, 34% dodecenyl succinic anhydride (DDSA), 16% methyl nadic anhydride (MNA), 2% 2,4,6-Tris(dimethylaminomethyl)phenol (DMP-30), all (v/v), TAAB Laboratories) and incubated for at least 3hrs at RT. The solution was changed to pure resin overnight. The resin solution was replaced with fresh resin the next morning. Lastly, the samples were placed into flat bottom sample containers, submerged with fresh resin and incubated for 2 days at 60°C. The samples were stored at RT prior to further processing.

2.11 Electron Microscopy (EM)

Resin-embedded samples were cut into 0.75µm sections using a microtome. Sections were collected on poly-l-lysine coated glass slides (Sigma) and dried at 60°C. Pre-warmed glass slides were stained with 1% toluidine blue for approximately 5sec at 60°C. Excessive staining solution was rinsed off the slides with distilled water. On the sections, the corpus callosum was localised using light microscopy, and suitable areas of the corpus callosum were selected for electron microscopy. Ultra-thin sections of selected corpus callosum areas were cut onto copper grids and stained with uranyl acetate (carried out by Dr Daniel Morrison). The sections were examined with a Hitachi H-600 Transmission Electron Microscope.

2.12 Magnetic resonance imaging (MRI)

For MRI analysis, brains were perfused and dissected as mentioned above, except that the animals were perfused for 8min, using approximately 150ml of 4%PFA.

MRI acquisition was carried out by Joe Guy (former PhD student at the Franklin laboratory, University of Cambridge, UK).

In brief, brains were immersed in 10% formalin containing 2mM Gadovist (Bayer AG) for a minimum of 3 days to shorten T1 time of the MRI. Brains were then suspended in a susceptibility-matched fluoropolymer (Fomblin, Solvay S.A) and scanned using a Varian 9.4T MRI scanner with a 400mT/m 205/120/HD gradient insert (Magnex Scientific Ltd). Multiple acquisitions (12-16) were taken overnight with a 3D gradient-spoiled gradient-echo sequence with TR = 20 ms, TE = 5 ms, NEX = 4, and flip angle set to the Ernst angle (approximately 40°). Brains were scanned using a 40mm Millipede coil at 62.5 μ m isotropic for brains 1-6 and 60 μ m isotropic for brains 7-10.

Images were co-registered to a central time point using a 3.5D optimised automatic registration algorithm with 9 degrees of freedom, windowed sinc interpolation, and a normalised cross correlation cost function with a Powell's calling Brent's search algorithm. Surface coil-acquired images were additionally processed using a nonparametric intensity nonuniformity normalisation algorithm (Tustison et al., 2010) for bias field correction.

2.13 10X Genomics Single-Cell RNA-Sequencing

Cell isolation, Drop-sequencing and data analysis were carried out by Elisa Floriddia and David van Bruggen (Castelo-Branco laboratory, Karolinska Institute, Stockholm, Sweden).

In brief, mice were perfused using oxygenated artificial cerebrospinal fluid solution (aCSF; 87 mM NaCl, 2.5mM KCl, 1.25 mM NaH₂PO₄, 26 mM NaHCO₃, 75 mM sucrose, 20 mM glucose, 0.5 mM CaCl₂, and 4 mM MgSO₄), before the brains were dissected and cut into 300 μ m sections using a vibratome. The corpus callosum and the motor cortex were dissected from the tissue slices and dissociated using Adult Brain Dissociation Kit (Miltenyi Biotec), accordingly to the manufacturer's guidelines. The single cell suspension was filtered through a 30 μ m filter (Partec) and resuspended in aCSF + 1% BSA, before FACS-Sorting. GFP+ and tdTOMATO+ cells were FACS sorted using the BD Influx System (BD Biosciences) and collected in aCSF + 1%BSA. Next, the collected cells were briefly spun down and suspended in 30 μ l of aCSF + 1%BSA. The volume was optimised by the manufacturer (10X Genomics) to achieve single cell resolution and recovery of 3000 cells per sample.

After assessing cell viability using the Countess Automated Cell Counter (Thermo

Scientific), single cells suspension was mixed with gel beads creating Gel Bead-In-EMulsions (GEMs) (10x Genomics). Each GEM contains one cell and primers consisting of (1) an Illumina R1 sequence, (2) a unique 16 bp barcodes, (3) a 10 bp random primers and (4) poly-dT primer sequence. Next, reverse transcription in the GEMs produces barcoded, full-length cDNA from poly-adenylated mRNA. After reverse transcription, GEMs were broken and the barcoded cDNAs were recovered. Excess of primers and biochemical reagents were removed using silane magnetic beads (10x Genomics).

The full-length cDNA was amplified by PCR to generate enough template for the library construction. To optimise the cDNA amplicon size, cDNA was enzymatically fragmented. Only amplicons of the size between 200 to 9,000bp were selected. The library was constructed adding the R (Read) 1 (added during the barcoding step), P (Primer) 5, P7, a sample index, and R2 primer sequences via End Repair, A-tailing, adaptor ligation, and PCR. The P5 and P7 sequences were used in Illumina bridge amplification. R1 and R2 were standard Illumina sequencing primer sites used in paired-end sequencing. Following cDNA library preparation, the library was sequenced using Illumina sequencing.

Following sequencing, outliers were removed using the 10X genomics pipeline based on the number of detected molecules per cell (how many individual mRNA molecules were detected) and detected genes per cell. After removing outlier, molecule counts were ranging from 484 to 35759 per cell and gene counts were ranging from 301 and 5507 per cell. The generous cut offs were implemented to avoid the elimination of the OPC cells expected in the dataset, which were generally small cells with a low abundance of transcripts. The combined dataset of the several 10x runs comprised a total of 11549 cells and 27998 genes. Mitochondrial genes were omitted from the dataset to avoid potential bias in downstream analysis.

In order to generate a representation of the data the most variable genes were selected using the coefficient of variation, wherein the variance of a gene was adjusted as a function of the magnitude of expression. The average expression for a given expression magnitude was modelled using support vector regression (SVM) and then selected genes that exhibited a variation above the predicted variation for the magnitude of expression of the gene. Dimensional reduction was performed by applying the non-negative matrix factorisation using the NNLM package in R (version 0.4.1). The data output of the dimensional reduction was used as input for the t-distributed stochastic neighbour embedding (tSNE) algorithm using the R-tsne package in R (version 0.13). t-SNE is a machine learning algorithm for non-linear dimensionality reduction, embedding high-dimensional data into a space of two dimensions (dimension 1 =

tSNE-1, dimension 2 = tSNE-2), which can then be visualised in a scatter plot.

2.14 Behavioural experiments

2.14.1 Cohort Breeding

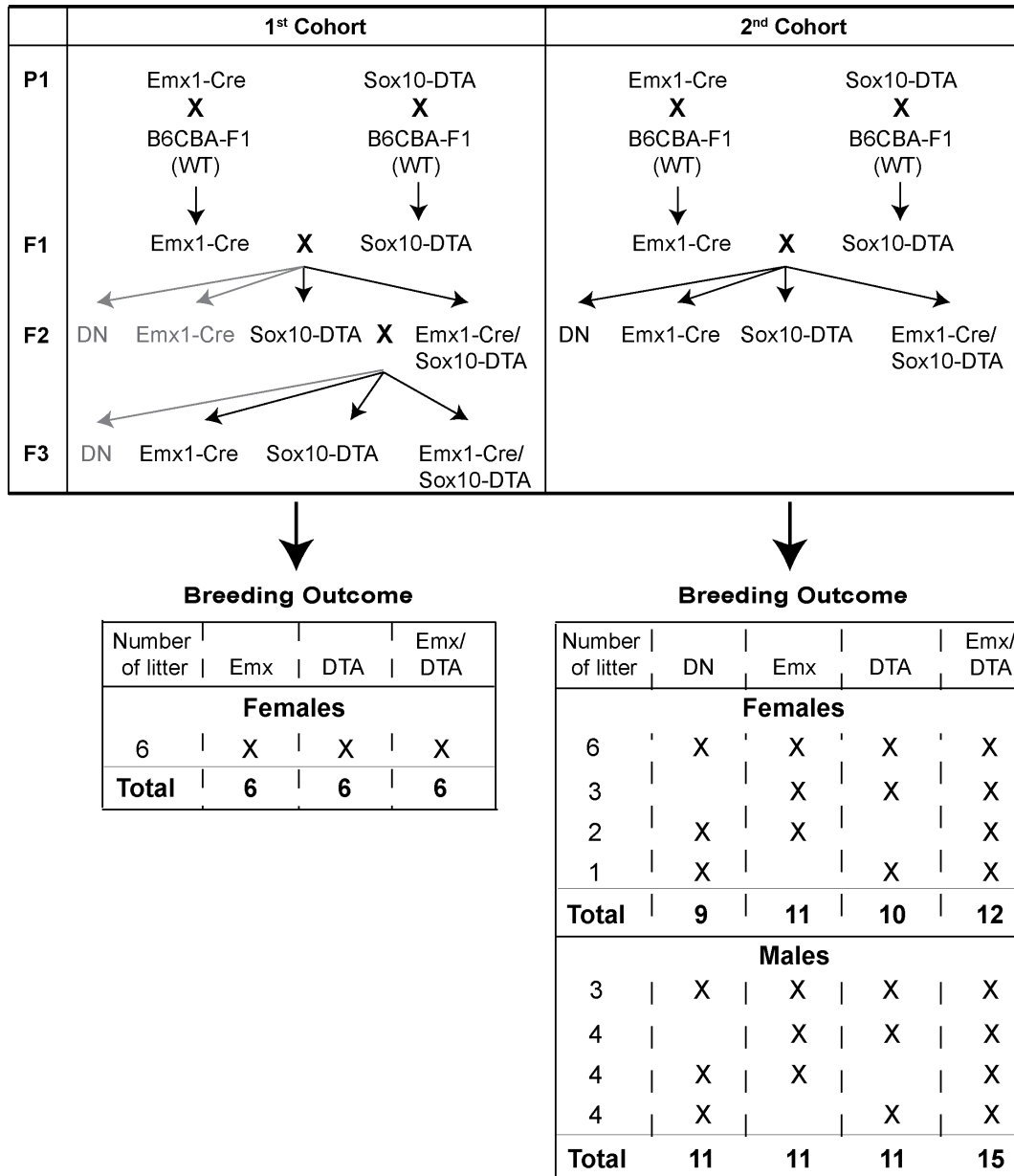


Fig. 2.1 **Breeding strategy of cohorts for behavioural testing.** (Top) Breeding strategies for the 1st and 2nd cohort has been outlined. (Bottom) Overview of the the breeding outcome. Listed are the number of litters containing litter mates with the indicated genotypes. All of the animals listed were combined into one male or female cohort (see total numbers of animals per cohort).

To breed cohorts, initially *Emx1-Cre* and *Sox10-DTA* animals were outbred to *B6CBA-F1* (WT) mice, to create a breeding stock of *Emx1-Cre* and *Sox10-DTA* (F1 generation) with maximal variance of their genetic pool. In the 1st cohort, *Emx1-Cre* were subsequently crossed to *Sox10-DTA* (F2 generation), from which in turn *Sox10-DTA* were crossed to *Emx1-Cre/Sox10-DTA* to achieve the highest number of *Emx1-Cre/Sox10-DTA* animals in the final breeding cohort (F3 generation). The final cohort consisted of six female animals of each genotype (*Emx1-Cre*, *Sox10-DTA* and *Emx1-Cre/Sox10-DTA*), each genotype triplet being litter mates and were born within two weeks (Figure 2.1). As double negative (DN) animals were included into the 2nd cohort, the breeding strategy had to be adopted. From the F1 generation, *Emx1-Cre* mice were crossed to *Sox10-DTA* mice. The number of breeding pairs in the F1 generation was calculated to get eight to ten animals per genotype (double negative (DN), *Emx1-Cre*, *Sox10-DTA* and *Emx1-Cre/Sox10-DTA*), which were litter mates and born within two weeks. Due to smaller than expected litter sizes and apparent infertility of some animals, the desired cohort size was not achieved. Therefore, the litters with *Emx1-Cre/Sox10-DTA* and only two respective single transgenic control were also considered (Figure 2.1). The final female cohort consisted of nine DN, eleven *Emx1-Cre*, ten *Sox10-DTA* and twelve *Emx1-Cre/Sox10-DTA* animals, out of which each *Emx1-Cre/Sox10-DTA* had at least two single-transgenic litter mate controls. All litters were born within two weeks. The female animals of both cohorts were used to test for their general vigilance, locomotor coordination as well as sensory function. In contrast, the final male cohort consisted of eleven *Double negative*, eleven *Emx1-Cre*, eleven *Sox10-DTA* and 15 *Emx1-Cre/Sox10-DTA* animals, out of which each *Emx1-Cre/Sox10-DTA* had at least two single-transgenic litter mate controls. All litters were born within to weeks. Male animals of the 2nd cohort were used to test cognitive function.

2.14.2 Assessment of general vigilance

Open Field Test

Mice were acclimatised to the test room for an hour. Subsequently, individual mice were placed in the middle of a 50cm² white plastic box (Figure 2.2A), and their behaviour was recorded for 5min. The open field test does not require any training. To assess general vigilance, the time spend at the walls versus the centre of the testing chamber was measured. In addition, the number of mouse droppings in the test box after the completion of the test was counted, as an indicator of stress/anxiety levels of the animals.

Rearing Test

Mice were acclimatised to the test room for 15min. Subsequently, individual animals were placed in a transparent plastic tube (diameter: 15cm, height: 30cm) (Figure 2.2B), and video-recorded for 1min. The rearing test does not require any training. The rearing test was quantified by counting how many times mice reared both freely and at the wall of the plastic tube. The rearing test was used as approximation of the hind limb strength, for which no more specific test exists.

2.14.3 Assessment of locomotor coordination

Prior to any training or test run, animals have been acclimatised to the test room for 15min.

Rotarod

The rotarod test was designed to assess general locomotor coordination of mice. The rotarod test does not require any training. For testing, the rotarod (Ugo Basile, Figure 2.2C) was set to acceleration mode, consistently accelerating from 4rpm to 40rpm over the course of 5min. Mice were placed on the rod facing forwards, while the rod was constantly rotating at 4rpm. After 10sec in which the mice have been correctly placed, the acceleration mode was started. If the mouse fell within 5sec the trial was restart as falling was most likely due to poor placement. If the mouse fell within 10sec the time and speed of rotation was noted and the mouse was allowed for two more trials. If the mouse fell after 10sec the speed at which mouse fell off and reason for end of trial (falling, jumping or passive rotation) were recorded. In addition, the first full passive rotation was recorded. A trial was ended early if an animals did three consecutive full passive rotations. The experiment was repeated three times, with at least 15min between trials.

Balancing beam

The balancing beam assesses general locomotor coordination; however, to complete this complex task, also sensory function and balance need to be intact. To a degree, anxiety can also be investigated in this test by counting the number of stops a mouse takes on the beam. For the balancing beam test mice have been trained once a day (2-3 test runs per session) for one week. Before every run, mice were placed in a temporary cage for 1min. To get used to the set-up of the beam (Figure 2.2D), a mouse was placed 20cm in front of the dark box. When the mouse reached the dark box, it was

allowed to remain in there for 2min. For all following training sessions, the mouse was placed at the beginning of the beam and was allowed to remain in the box for 1min after successfully crossing the beam. Finally, the animal was placed back into their home cage for at least 15min, before a new run was started as described above. At the end of the training phase, mice walked across the beam independently when placed on the beam. After completing the training phase, animals were tested on 3 alternate days (2 runs per session). All test runs were video-recorded to calculate the time a mouse needed to cross the beam (time a mouse stood still on the beam was not recorded), the number of stops while crossing the beam as well as to assess gait retrospectively.

Horizontal ladder

The horizontal ladder test primarily assesses general locomotor coordination, but also an intact sensation and normal vigilance/anxiety are needed to successfully walk across the ladder. For the horizontal ladder test, mice have been trained once a day (2-3 test runs per session) for two weeks. Before every run, mice were placed in a temporary cage for 1min. To get used to the set-up of the ladder (Figure 2.2E), a mouse was placed on the ladder and was left to freely walk on its first encounter. In the second training run, animals were placed on the ladder 20cm in front of the dark box. When the mouse reached the dark box, it was allowed to remain in there for 2min. For all following training sessions, the mouse was placed at the beginning of the ladder and was allowed to remain in the box for 1min. After every run the animal was placed back into their home cage for at least 15min, before a new run (as described above). At the end of the training phase, mice walked across the ladder independently when placed on the ladder. After completing the training phase, the experiment was repeated 3 times on the test day. All test runs were video-recorded to assess the time a mouse needed to cross the beam (time a mouse stood still on the ladder was not recorded), the number of steps by a single hind leg an animal needed to cross the ladder and the number of slip-offs or misses of paw placement retrospectively.

Vertical beam

The vertical beam test assesses the level of bradykinesia (slowness of movement). The vertical beam test does not require training. Before every run, mice were placed in a temporary cage for 1min. Subsequently, individual mice were placed on the side at the top end of the vertical beam (Figure 2.2F). After completing one run, animals have been placed back in their home cage for at least 15min, before a new run (as described above). The mice have been tested 3 alternate days (2 runs per session). After

secure placement, the way of descent was video-recorded. Walking down the beam was classified as successful descent, whereas sliding down or jumping off the beam were classified as unsuccessful descents. For quantification, the number of steps taken with the hind paws were counted.

Gait analysis

To assess balance and general gait of the mice, a gait analysis on a horizontal plane was performed. For the gait analysis, mice were trained once a day (2-3 test runs per session) for two weeks. Before every run, mice were placed in a temporary cage for 1min. To visualise the gait of the mice, the paws of mice were dipped into watery ink, before walking across a white paper into a dark box (Figure 2.2G). At the end of the training phase, mice walked across the white paper. At the day of testing, three runs were recorded with at least 15min between each run. The gait was assessed by measuring the stride length and stride width as well as the diagonal distance between front paws. Measurements were only taken if the animal walked at a constant speed for at least three body lengths (approximately 30cm).

2.14.4 Assessment of sensory function

Von-Frey test

To measure cutaneous sensation of the hind paws, the von-Frey test was carried out. The von-Frey test does not require training. On the test day, mice were acclimatised to the test chamber (Ugo Basile, Figure 2.2H) for 1hr. After the mice settled in the test chamber, a hind paw was touched with continuous force using the electronic von-Frey apparatus (Ugo Basile) until the animal pulled away the paw. The maximum force needed to provoke a withdrawal response to the stimulus was recorded. From each animal 5 measurements were taken.

2.14.5 Assessment of cognitive function

To assess sustained attention the continuous performance test (rCPT) was performed (C. H. Kim et al., 2015). In addition to assessing the sustained attention, also inhibitory control, intact visual perception/processing and learning/memory were indirectly assessed by the rCPT test. The rCPT test was carried out by Christopher Heath and Eosu Kim (Bussey laboratory, University of Cambridge, Cambridge, UK).

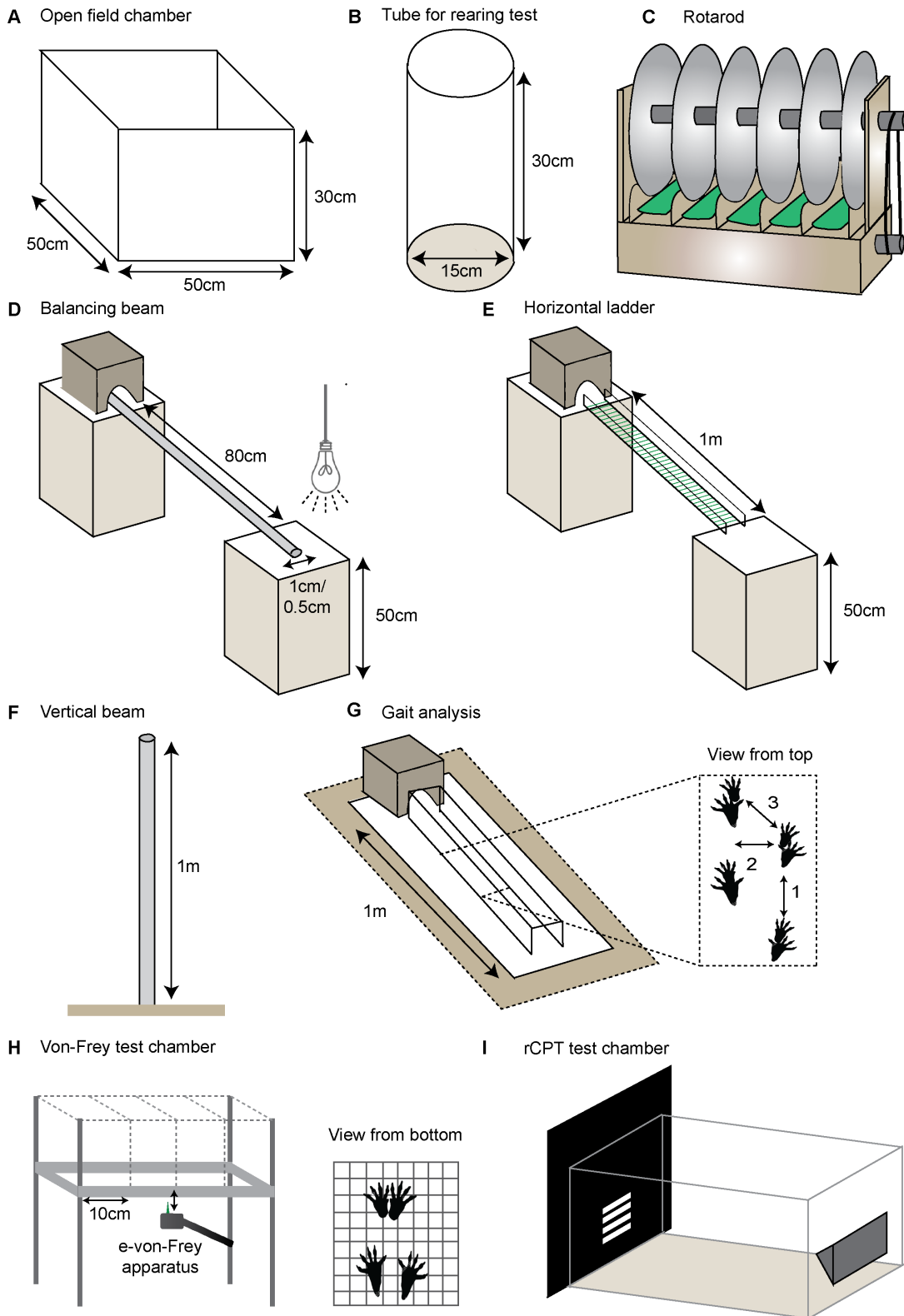


Fig. 2.2 Experimental set-up of behavioural experiments. (A) Open field test: The dimensions of the open field chamber were 50cm x 50cm x 30cm. The chamber was made up of white plastic to avoid any disturbance of the animal. (B) Rearing test: The tube was 30cm high and has a diameter of 15cm. The tube was made up of transparent plastic to allow video recording. (C) Rotarod test: The rotarod was purchased from Ugo Basile. The equipment was kindly lent by the Barker laboratory, University of Cambridge, UK. (D) Balancing beam test: A metal beam (length: 1m, diameter: 10mm or 5mm) was fixed on top of two boxes, 50cm above the table surface. Surrounding the beam, mats have been placed to cushion any falls. A lamp was used to shine light above the start point and serves as an aversive stimulus. A dark box was placed on the opposite side to attract the mouse to the finish point. (E) Horizontal ladder test: A ladder (length: 1.4 m, width: 10cm) with regular rungs was placed on top of two boxes, 50cm above the table surface. A dark box was placed on the other box to attract the mouse to the finish point. (F) Vertical beam test: A metal beam (length: 1m, diameter: 20cm) was placed vertically on the table top. Surrounding the beam, mats have been placed to cushion any falls. (G) White paper (length: 1m, width: 30cm) was placed on the table top. To force the mice to walk in a straight line, a tunnel was placed on top of the white paper. A dark box was placed at the end of the paper to attract the mouse to the finish point. (H) Von-Frey test: Mouse enclosure boxes (dimensions: 10cm x 15cm, Ugo Basile S.R.L.) were placed on top of a perforated metal platform (open grid of square holes 5x5 mm; intervening metal grid is 1mm wide, Ugo Basile). The electronic (e) von-Frey device was purchased from Ugo Basile. The equipment was kindly lent by the Fawcett and Coleman laboratory, University of Cambridge, UK. (I) rCPT test: The chamber was equipped with a touch screen on one end and a reward delivery magazine on the other. The apparatus shown in **A, D, E, F** and **G** were built on site.

For full details of test apparatus and training see original publication (C. H. Kim et al., 2015) (note that some test parameters have been changed in this experiment). In brief, the animals were acclimatised to the test chamber (Figure 2.2I) twice for 20min. Following habituation, mice underwent four stages of rCPT training, with animals only allowed to enter the next stage of training after the criterion of each stage was reached within a 45min session (Figure 2.3 A). In stage 1, animals were trained to touch a white square on the screen which was shown for 10sec (stimulus duration time). After a touch response was made, the white stimulus square was removed from the display and the animals were rewarded with a pellet. The collection of the pellet initiated an inter-trial interval (ITI) of 2sec. Following the ITI, a new trial began with the presentation of the white square. If no touch response to the white square was detected, the ITI was initiated after the stimulus duration time ended. In stage 2, the white square was replaced by the 'target' stimulus (horizontally black and white striped square) and the stimulus duration time was shortened to 2sec. In stage 3, a 'non-target'

stimulus (a white snowflake on black background) was introduced which was shown in 50% of the trials. A touch of the 'non-target' stimulus resulted in removal of the stimulus from the screen and the initiation of a correction trial. On a correction trial the non-target stimulus was always shown until the mouse showed no response to the non-target stimulus to discourage the animal from a non-selective response to a stimulus. In stage 4, the snowflake 'non-target' stimulus was replaced by four other 'non-target' stimuli ((1) diagonally black and white striped square (top left to bottom right), (2) diagonally black and white striped square (top right to bottom left), (3) black and white circled square and (4) vertically black and white striped square). As in stage 3, the probability of showing a 'target' versus any 'non-target' stimulus was 50%. The animals also entered into a correction trial with random 'non-target' stimulus representation if any 'non-target' stimulus was touched (Figure 2.3 A).

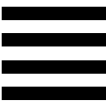
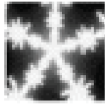
Based on the performance of an animal in the rCPT test, four measures were assessed: response to the 'target' stimulus (called hit), no response to 'target' stimulus (called miss), response to 'non-target' stimulus (called false alarm) and no response to 'non-target- stimulus (called correct rejection). From these parameter the hit rate (HR) and the false alarm rate (FAR) can be calculated. However, the HR and FAR do not always give relying information about the performance of an animal, because selective versus non-selective responses cannot always be separated. Therefore, based on the HR and FAR, the sensitivity (d'), referring to the perceptual discriminability between 'target' and 'non-target' stimulus, and response bias (c), referring to willingness to respond, were calculated (Figure 2.3 B).

After the training period testing parameters were changed to challenge the animal. The stimulus duration time was shortened to 1.5, 1.0 and 0.5sec, reducing the amount of time a stimulus was shown on the screen. In addition, the probability of showing a 'target' versus any 'non-target' stimulus was reduced to 30%, making it easier to identify a non-selective responses of the animals (Figure 2.3 A).

2.15 Statistics

In all the graphs data are presented as mean \pm standard deviation (SD). Statistical analysis was performed using Graphpad Prism (Version 7). The data was analysed for normal distribution using D'Agostino-Pearson omnibus and Shapiro-Wilk normality test.

A

Stage	'target' stimulus	'non-target' stimulus	SD [sec]	ITI [sec]	'target' stimulus probability	Criterion
1	 White square	n/a	10	2-3	n/a	Consume 80 rewards within a 45min session
2		n/a	4	2-3	n/a	Consume 80 rewards within a 45min session
3			4	2-3	50	$d' \geq 0.6$ for two consecutive sessions
4		   	4	2-3	50	$d' \geq 0.6$ for two consecutive sessions
Short SD	see stage 4	see stage 4	0.5 1.0 1.5 2.0	2-3	50	n/a
Reduced PS	see stage 4	see stage 4	2	2-3	30	n/a

B

$$\text{Hit rate (HR)} = \frac{\text{Hit}}{\text{Hit} + \text{Miss}}$$

$$\text{False alarm rate (FAR)} = \frac{\text{False alarm}}{\text{False alarm} + \text{Correct rejection}}$$

$$\text{Sensitivity (d')} = z(\text{HR}) - z(\text{FAR})$$

$$\text{Willingness (c)} = \frac{z(\text{HR}) - z(\text{FAR})}{2}$$

Fig. 2.3 Test parameters for continuous performance test. (A) rCPT parameters used in training (row 1-4) and further tests (row 5-6). **(B)** Equations for the calculation of hit rate (HR), false alarm rate (FAR), sensitivity (d') and willingness (c). SD = Stimulus duration, ITI = inter-trial interval, PS = probability of 'target' stimulus

A two-tailed unpaired Student t-test was performed to assess the statistical significance between two groups. In case a normal distribution of the data was not given, a Mann-Whitney test was performed. When comparing more than two groups, one-way Anova test was used followed by a Tukey's posthoc test. If the sample was not normally distributed, a Kruskal-Wallis test combined with a Dunn's posthoc test was carried out. In case a data set had two or more variables a two-way Anova was performed. If an interaction of the variables in the data set was detected in the two-way Anova, the variables were analysed separately by one-way Anova combined with Tukey's postdoc test. If the sample was not normally distributed, a Kruskal-Wallis test (ranks) was carried out. To test the association between the frequency of two categorical variables a χ^2 test was performed. In each figure legend the number of biological replicates (number of animals), the statistical test and the significance levels are indicated. Data was considered significant at a p-value below 0.05. Significance levels are presented graphically as: * = $p < 0.05$, ** = $p < 0.01$, *** = $p < 0.001$ and **** = $p < 0.0001$

Chapter 3

Functional consequences of dorsal OPC ablation *in vivo*

During embryonic development, OPCs arise from distinct telencephalic areas in a spatiotemporal gradient from ventral to dorsal. The identification of the two developmental origins of OPCs raised the question whether ventral and dorsal OPCs, and their progeny, fulfil distinct functions in the brain. To date, no functional difference in ventral and dorsal OPCs has been demonstrated in brain homeostasis.

3.1 Mouse models

To investigate the functional importance of the developmental origin of OLCs on physiological brain function, dorsal OPCs were ablated using a transgenic mouse model (*Emx1-Cre/Sox10-DTA*, abbreviated as *Emx/DTA*) (see Materials and Methods, Section 2.1). In this mouse model, a transgene, containing the green fluorescent reporter protein (GFP) and diphtheria toxin fragment A (DTA) under the control of the *Sox10* promoter, has been randomly inserted into the genome. To control the expression of DTA, a STOP codon flanked by *loxP*-sites has been inserted after the GFP. Therefore, without the presence of Cre-recombinase, all cells of the oligodendrocyte lineage express GFP, but not DTA. To facilitate a specific ablation of dorsal OPCs, the reporter mouse line is crossed with an *Emx1-Cre* mouse line (abbreviated as *Emx*), in which the Cre-recombinase expression is controlled by the *Emx1* promoter (Figure 3.1). During brain development, *Emx1* is exclusively expressed in the dorsal telencephalon marking, *inter alia*, dorsal brain progenitor cells (Simeone et al., 1992). As the expression of the *Sox10* and *Emx1* promoter are constitutive, dorsal OPCs are ablated immediately after formation in development. The DTA ablation strategy

has been proven to be very efficient (Yamaizumi, Mekada, Uchida, & Okada, 1978) and cell specific as DTA exhibits no bystander effect on neighbouring cells (Uchida, Pappenheimer, & Harper, 1972).

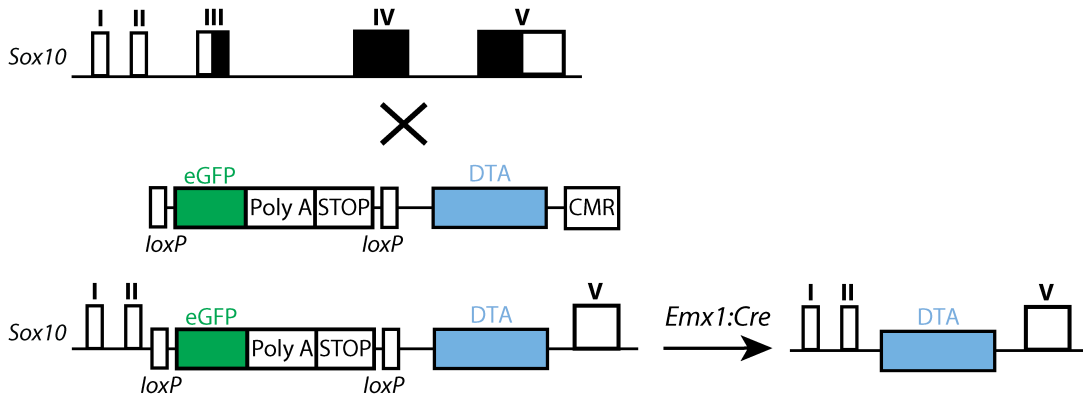


Fig. 3.1 Schematic representation of the *Emx1-Cre/Sox10-DTA* ablation model. Hereafter the ablation model will be abbreviated as *Emx/DTA*.

To distinguish ventral and dorsal OLCs in the brain the *Emx1-Cre/Sox10-GFP-tdTomato* (abbreviated as *Emx/tdTom*) mouse model has been used (see Materials and Methods, Section 2.1). The *Sox10-GFP-tdTomato* mouse line is created by random integration of a transgene, containing the two fluorescent reporter proteins GFP and tdTOMATO under the control of the *Sox10* promoter, into the genome. To control the expression of tdTOMATO in OLCs, a STOP codon flanked by *loxP*-sites has been inserted after the GFP. This reporter mouse line is crossed to the *Emx1-Cre* mouse line. In double transgenic animals, all OLCs of dorsal origin express tdTOMATO, whereas all OLCs of ventral origin keep expressing GFP (Figure 3.2). As control animals, single transgenic *Emx1-Cre* (abbreviated as *Emx*), *Sox10-DTA* (abbreviated as *DTA*) or *Sox10-tdTomato* (abbreviated as *tdTom*) were used.

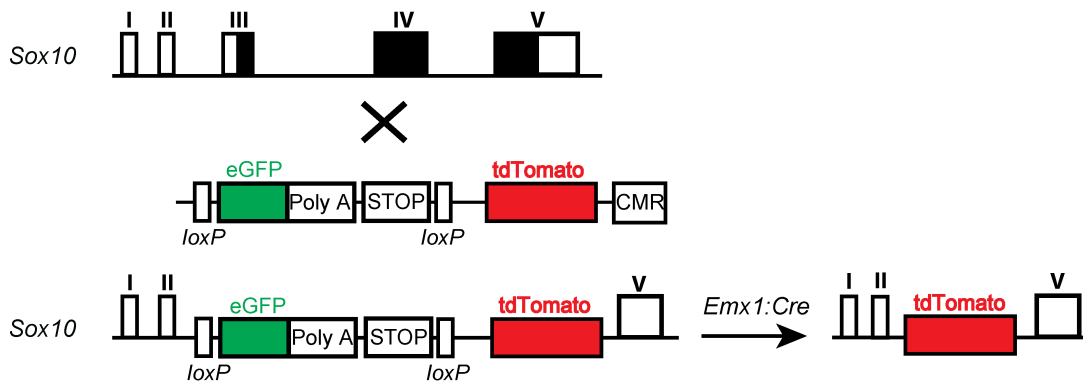


Fig. 3.2 Schematic representation of *Emx1-Cre/Sox10-tdTomato* reporter model. Hereafter, the reporter mouse line is abbreviated as *Emx/tdTom*.

3.2 Efficiency of dorsal OPC ablation model

To assess the efficiency of the DTA ablation model of dorsal OPC, flow cytometry analysis of whole brain samples of adult control and ablated animals was performed (Figure 3.3 A). In the control group (*Emx/tdTom*), 7.6% of the total brain cells expressed the OLC marker *Sox10*, splitting evenly in half between cells of the ventral and dorsal origin. After ablation, only 0.05% of the total 9.5% SOX10⁺ OLCs expressed tdTOMATO, resulting in an ablation efficiency of 98% (3.78% tdTomato⁺ cells in *Emx/tdTom* versus 0.05% tdTomato⁺ cells in *Emx/tdTom/DTA* animals) (Figure 3.3 B).

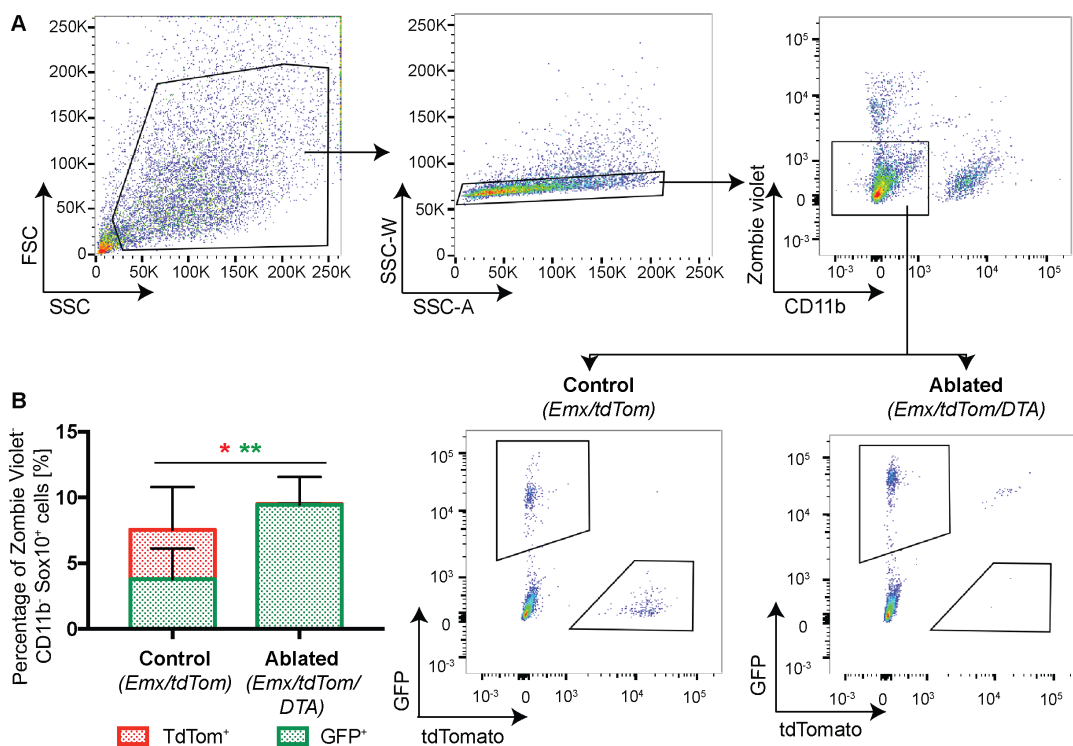


Fig. 3.3 **Efficiency of dorsal OPC ablation model in the whole brain:** (A) Gating strategy for flow cytometry analysis. Starting with whole brain samples, doublets were excluded from the analysis. Subsequently, to minimise false-positive events, Zombie Violet⁺ dead cells and CD11b⁺ microglia were excluded from the analysis. Finally, the total OLCs population (SOX10⁺, CD11b⁻) was divided into GFP⁺ and tdTOMATO⁺ OLCs. (B) Percentage of GFP⁺ (ventral) and tdTOMATO⁺ (dorsal) OLCs out of the total living SOX10⁺ OLCs in control and ablated animals. In comparison to control animals, significantly fewer tdTOMATO⁺ dorsal OLCs were detected in ablated animals (n = 6, unpaired t-test, * = p<0.05, ** = p<0.01).

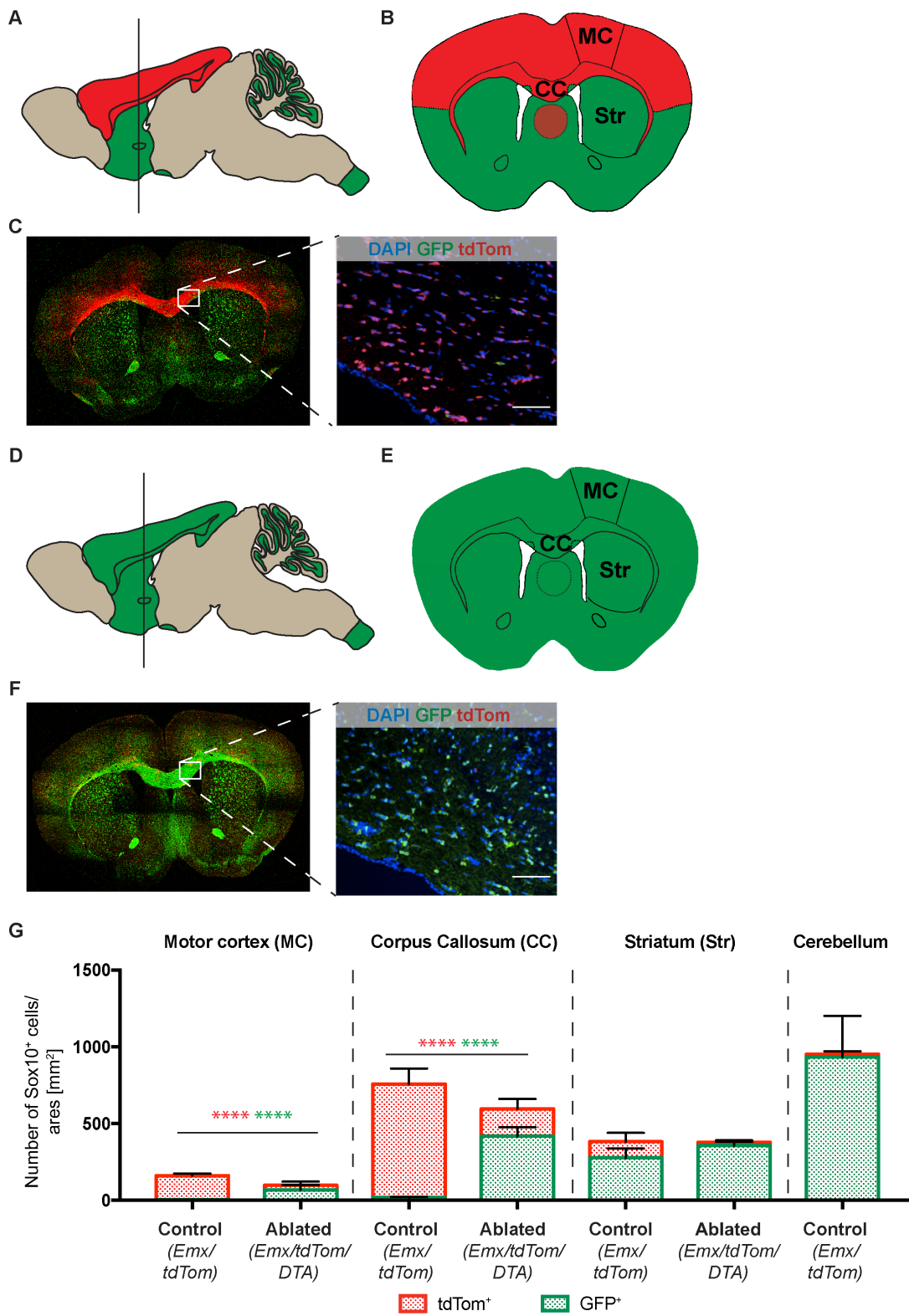


Fig. 3.4 Efficiency of dorsal OPC ablation model in the forebrain: (A) Schematic representation of a sagittal view of the brain of an *Emx/tdTom* animal. Line indicates the plane for the coronal view in (B). (B) Schematic representation of a coronal view of the brain of an *Emx/tdTom* animal. Brain areas assessed by immunohistochemistry are indicated. MC = motor cortex, CC = corpus callosum, Str = striatum. (C) Representative whole brain image of a *Emx/tdTom* animal. Images on the right shows a magnified view of the corpus callosum. Scale bar = 100 μ m. (D) Schematic representation of a sagittal view of the brain of a *Emx/tdTom* animal. Line indicates the plane for the coronal view in (E). (E) Schematic representation of a coronal view of the brain of a *Emx/tdTom* animal. Brain areas assessed by immunohistochemistry are indicated. MC = motor cortex, CC = corpus callosum, Str = striatum. (F) Representative whole brain image of a *Emx/tdTom* animal. Images on the right shows a magnified view of the corpus callosum. Scale bar = 100 μ m. (G) Number of GFP⁺ ventral and tdTOMATO⁺ dorsal OLCs in control and ablated animals. In ablated animals significantly fewer tdTOMATO⁺ dorsal OLCs were detected in all brain areas assessed (Control: n = 3, Ablated: n = 4, unpaired t-test, * = p<0.05, *** = p<0.001, **** = p<0.0001).

In addition to flow cytometry analysis, the number of ventral and dorsal SOX10⁺ OLCs was counted in frozen brain sections of adult mice (Figure 3.4). In CC and cortex of control animals on average 97.9% of all SOX10⁺ cells are of dorsal origin (CC: 737.7 tdTOMATO⁺ versus 177.0 GFP⁺ cells per area, cortex: 156.6 tdTOMATO⁺ versus 3.3 GFP⁺ cells per area) whereas only 30.7% of SOX10⁺ cells express tdTOMATO after ablation (29.8 tdTOMATO⁺ versus 68.6 GFP⁺ cells per area) (Figure 3.4 G). In contrast to the CC and cortex, the percentage of dorsal OLCs in the striatum (27.4%) was smaller in control animals. Following the ablation of dorsal OLCs using DTA expression the number of tdTOMATO⁺ SOX10⁺ cells was reduced to 5.7% (Figure 3.4 G). In summery, across all assessed brain regions, the ablation efficiency of dorsal OPCs was 72.6% (Figure 3.4 G).

In the cerebellum, only the minority of SOX10⁺ cells express tdTOMATO (Figure 3.4 G), indicating that the dorsal OLCs are mainly restricted to the forebrain.

3.3 Ablation of dorsal OPCs causes locomotor disabilities in adult mice

As dorsal OLCs cells mostly populate dorsal areas in the telencephalon, processes that are mediated by the dorsal telencephalon are likely to be most affected by the

ablation. Predominant areas in the dorsal telencephalon are the motor cortices M1 and M2, whose function can be assessed by various locomotor tests in mice.

To obtain an overview of the locomotor abilities of *Emx1-Cre/Sox10-DTA* ablated animals, the performance of six female *Emx1-Cre/Sox10-DTA* ablated animals in common locomotor tests was compared to single transgenic *Emx1-Cre* and *Sox10-DTA* animals (six animals per group) of the same sex (for cohort details see Materials and Methods, Section 2.1). As the animal's weight is very important for the performance in any locomotor test, the weight of all tested animals was monitored throughout the testing period. No significant difference in the average weight of the animal groups was detected (Figure 3.5 A).

First, the cohort of female animals were tested on the rotarod, a test often used to investigate general motor coordination. To quantify the performance of animals on the rotarod, the rotation speed at which the mice passive rotate for the first time (an initial sign of loosing locomotor control) and eventually fall off the rod was assessed. When compared to the control groups (*Emx1-Cre* and *Sox10-DTA*), animals ablated of dorsal OPCs showed a similar performance on the rotarod (Figure 3.5 B,C). The balancing beam test is described as being more sensitive in detecting locomotor coordination abilities than the rotarod test (?). Indeed, mice ablated of the dorsal OPC population needed significantly longer to cross the balancing beam in comparison to the two control groups. Ablated animals showed a significantly higher number of foot faults with their hind paws, low tail carriage and occasionally an unusual gait (Figure 3.5 D-F). Additionally, mice lacking dorsal OPCs performed significantly less well in the vertical beam test, which assesses bradykinesia (slowness of movement). The impaired ability of the animals ablated of dorsal OPCs to coordinate quick locomotor movements manifested as a sliding of the hind paws on the beam, rather than a normal walking gait observed in control animals. Consequently, to quantify the behaviour on the vertical beam test, the number of steps taken with the hind limbs were counted, revealing that mice lacking dorsal OPCs took significantly fewer steps when compared to the control groups (Figure 3.5 G). Finally, to estimate the forelimb strength and front paw coordination, the hanging bar test was carried out, revealing a significant decrease in the time an ablated mouse can hang from the bar compared to the control groups (Figure 3.5 H). In summary, the battery of locomotor tests suggests an impairment of locomotor coordination in mice lacking dorsal OPCs.

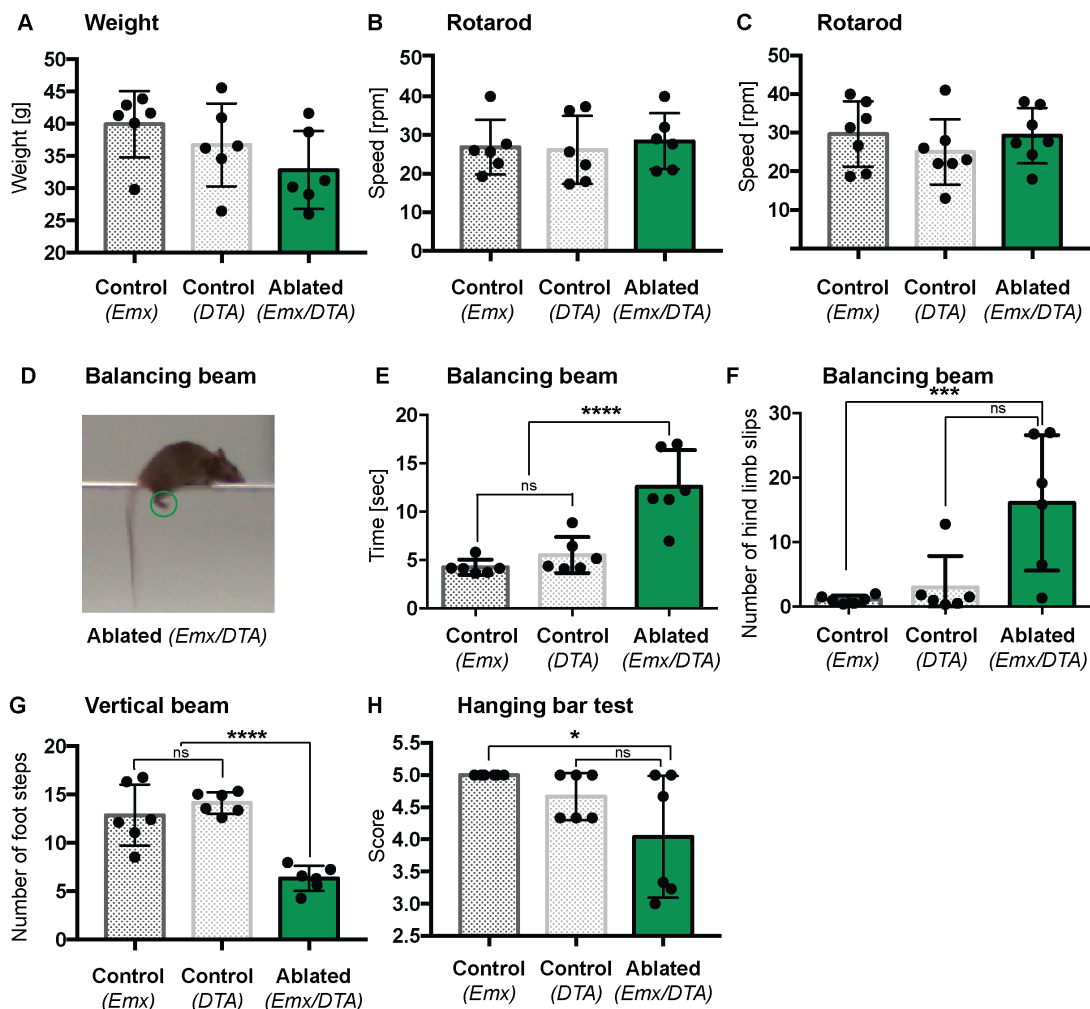


Fig. 3.5 Ablation of dorsal OPCs causes locomotor disabilities in adult mice: (A) Body weights of animals: There was no significant difference between control and ablated group (Kruskal-Wallis). (B,C) Rotarod test (5rpm to 40rpm, acceleration mode) quantified by speed at which mice showed first passive rotation (B) or fell off (C): There were no significant differences between control and ablated group (One-way Anova). (D-F) Balancing beam test: (D) Representative picture of an ablated animal walking across the beam. Circle highlights a typical foot fault. (E,F) Balancing beam test was quantified by time mice needed to cross the beam (E) and number of foot faults (F). Mice ablated of dorsal OPCs cross the beam significantly more slowly (E), show a significantly higher number of foot faults (F) and an abnormal gait (low tail carriage, hopping gait, slipping (D)) ((E): One-way Anova, Tukey's test, **** = $p < 0.0001$, (F): Kruskal-Wallis, Dunn's test: *** = $p < 0.001$). (G) Vertical beam test quantified by the number of foot steps taken with hind paws. Mice ablated of dorsal OPCs slide down the beam which is represented by a significantly lower amount of foot steps taken with the hind paws per animal (One-way Anova, Tukey's test, **** = $p < 0.0001$). (H) Hanging bar tests quantified by time mice are hanging on the bar (Score: 1 = 1-5 sec, 2 = 6-10 sec, 3 = 11-20 sec, 4 = 21-30 sec, 5 = >30 sec). Ablated animals fell off the horizontal bar significantly earlier when compared to control animals (Kruskal-Wallis, Dunn's test: * = $p < 0.05$). For all experiments 6 animals per group were used.

In order to successfully complete a locomotor test, mice not only need to be able to coordinate the locomotor movement, they also need to have physiological muscle strength, balance, sensation and vigilance (including motivation and a lack of anxiety). Consequently, to investigate whether the impaired performance on the horizontal and vertical beam was indeed caused by a locomotor coordination impairment, a second cohort of female animals was bred up to undergo further testing. In this second female cohort, twelve female *Emx1-Cre/Sox10-DTA* ablated animals were compared to the single transgenic *Emx1-Cre* and *Sox10-DTA* animals (eleven and ten animals per group, respectively) as well as double negative (DN) animals (9 animals per group) of the same sex (for cohort details see Materials and Methods, Section 2.1). The weight of all animals assessed was monitored over the entire test period and was not significantly different (Figure 3.6 A).

The most commonly used test to determine general vigilance is the open field test which can be assessed in multiple ways. For instance, measuring the amount of time an animal spends in the centre versus in close proximities to the walls of the test chamber provides an indication on the animal's anxiety levels. However, as depicted in (Figure 3.6 B), mice lacking the dorsal OPC population spent the same amount of time at the wall of the open field chamber as their control counterparts. In addition, the number of mouse droppings, another surrogate indicator of anxiety, was comparable between the animal groups tested (Figure 3.6 C).

The testing of the first cohort of female animals revealed that (1) the front limb muscle strength was reduced in ablated animals (Figure 3.5 H) and (2) the locomotor coordination impairments manifested itself in the hind limbs (Figure 3.5 E,G), creating the need for measuring hind limb strength. However, no specific test to assess hindlimb strength of mice is available. Therefore, a rearing test as an approximation of hind limb muscle strength can be used, based on the hypothesis that an abnormal muscle strength will show reduced rearing behaviour. Mice ablated of the dorsal OPCs reared as often as control animals, suggesting normal muscle strength in the hind limbs of ablated animals (Figure 3.6 D).

To assess gait and balance, a gait analysis test on a horizontal surface was performed. Ablated mice exhibited a walking behaviour indistinguishable from control animals (*data not shown*), arguing for no impact of the ablation of dorsal OPCs on balance. In addition, further gait analysis revealed that stride length, stride width and paw placement were not significantly different between the genotype groups analysed (Figure 3.6 E-G).

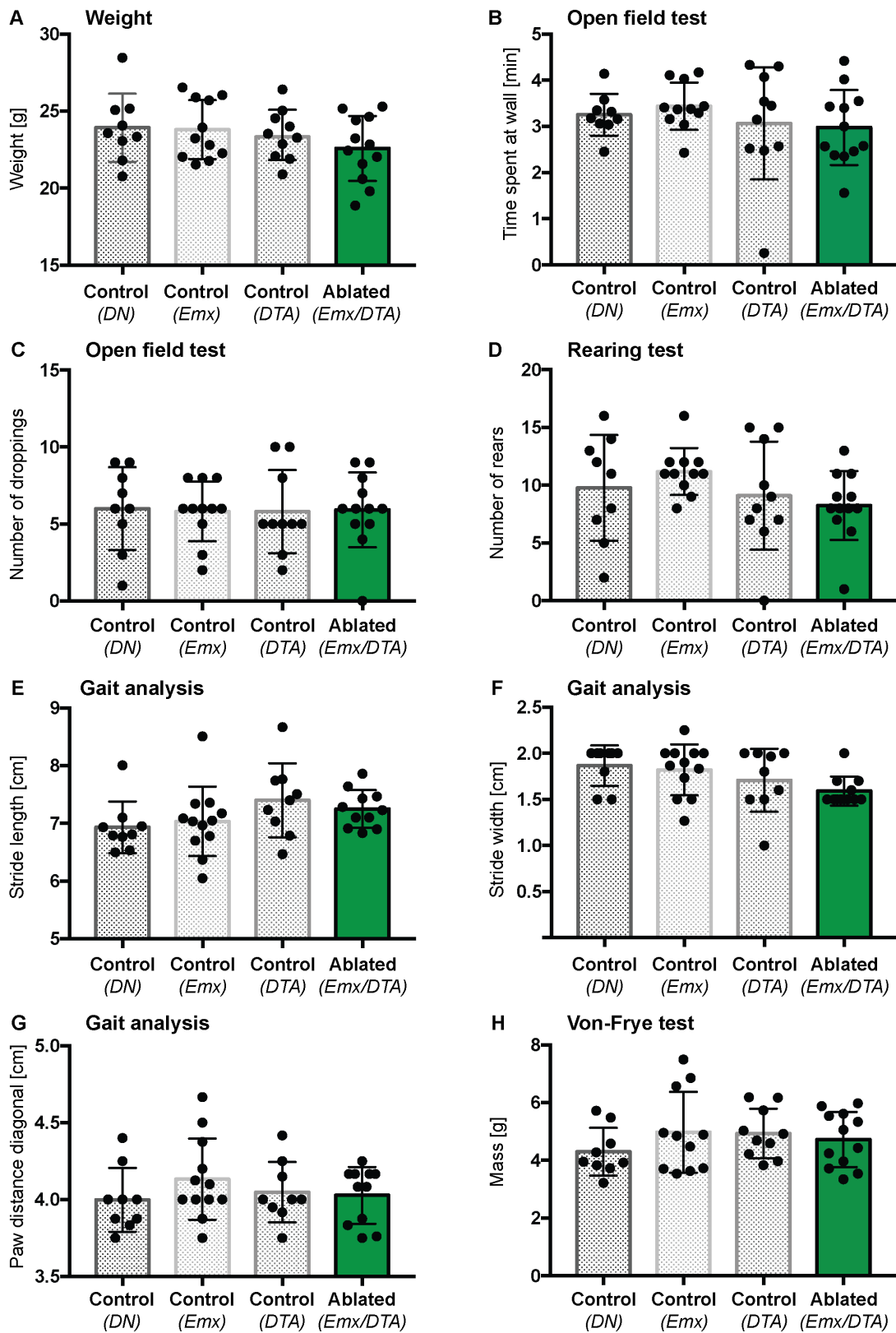


Fig. 3.6 Ablation of dorsal OPCs specifically causes impairment of locomotor coordination: (A) Weights of animals: There was no significant difference between control and ablated group (Kruskal-Wallis). (B,C) Open field test quantified by the proportion of time an animal spends in the centre versus in close proximity to the walls of the testing chamber (B) and number of mouse droppings (C). No difference in general vigilance of ablated and control animals was detected ((B): One-way Anova, (C): Kruskal-Wallis). (D) Rearing test quantified by the number of rears per minute. Ablated animals showed similar rearing behaviour to control animals (One-way Anova). (E-G) Gait analysis quantified by measuring stride length (E), stride width (F) and the diagonal distance of paw placement (G). No difference in gait was observed between ablated and control animals (Kruskal-Wallis). (H) Von-Frye test of sensation of hind paws quantified by the force needed to evoke an animal's response. Ablated animals exhibited the same level of sensation when compared to the control animals (One-way Anova). For all experiments, n = 12 of *Emx/DTA*, n = 11 of *Emx*, n = 10 of *DTA* and n = 9 of double negative (DN) animals.

Finally, sensation in the hind paws of mice ablated of dorsal OPCs was assessed using the von-Frey test. No intergroup difference in the the forces needed to evoke an animal's withdrawal response was detected, indicating that sensation is not affected by the ablation of dorsal OPCs (Figure 3.6 H). The results shown in Figure 3.6 did not reveal an effect of the ablation of dorsal OPCs on general vigilance, balance, gait and sensation. This infers that only locomotor coordination was impaired in the ablated animals.

To further validate the locomotor coordination phenotype caused by the ablation of dorsal OPCs, the horizontal ladder test and balancing beam test were performed. Unexpectedly, the horizontal ladder test did not show a significant difference between ablated and control mice (Figure 3.7 A-C). Regardless of the genotype, mice need approximately the same time to cross the ladder with the same number of steps (steps made with one hind paw were counted) (Figure 3.7 A,B). In addition, to assess locomotor coordination disabilities in more detail, the number of times an animal slipped off, misplaced a paw or completely missed a rung of the ladder was counted. Most of the paw misplacements were observed with the front paws. No significant increase in the number of slips off a rung, paw misplacements or misses of a rung was detected in ablated animals, when compared to the control groups (Figure 3.7 C). However, careful observation of the gait of the animals while walking on the horizontal ladder revealed occasionally an abnormal hopping gait. In comparison to control animals, ablated animals showed an increase in the number of steps executed in the abnormal hopping gait (Figure 3.7 C).

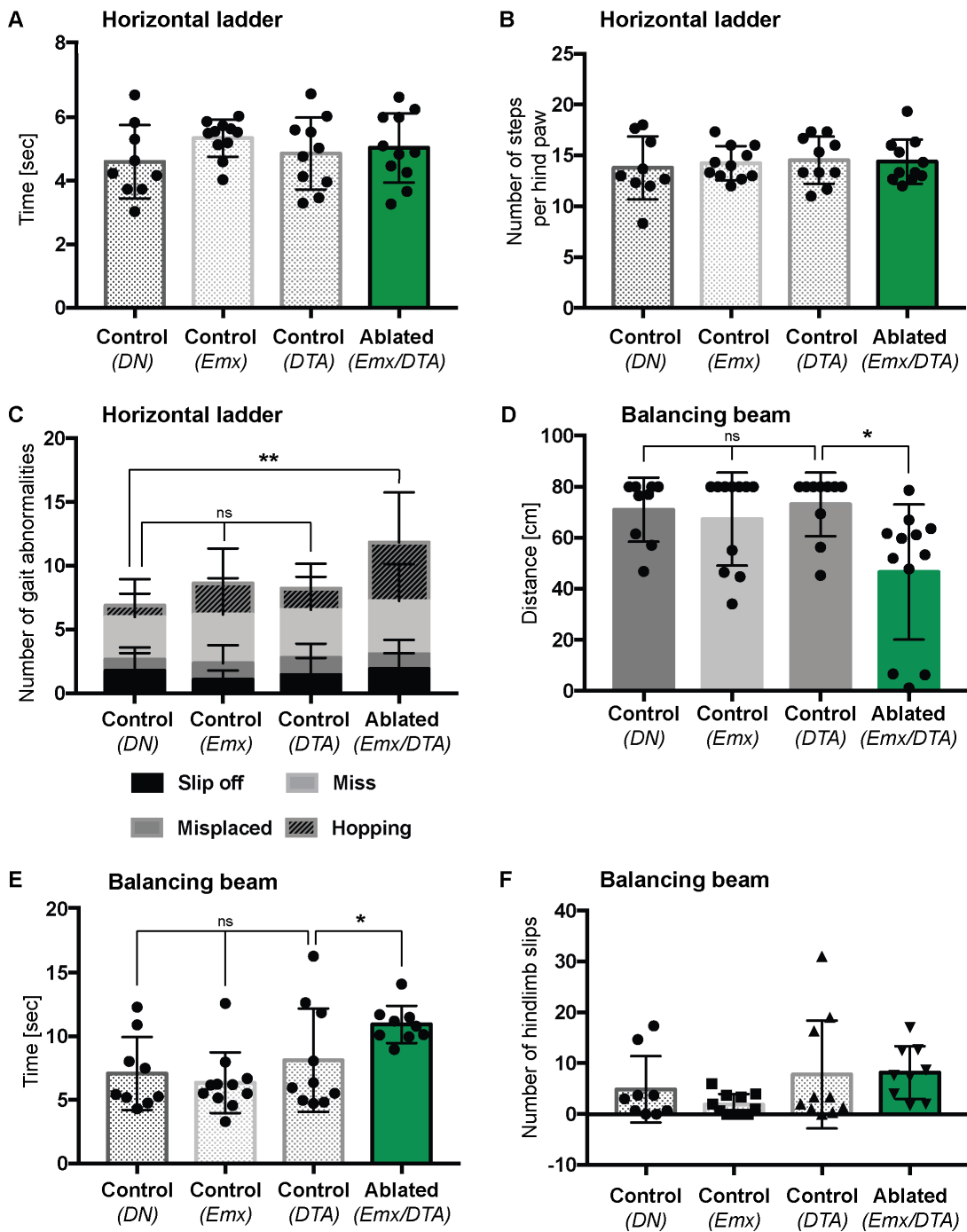


Fig. 3.7 Locomotor coordination impairment is specific to particular locomotor tests. (A-C) Horizontal ladder tests quantified by the time mice needed to cross the ladder (A), steps made with an individual hind paw to cross the ladder (B) and number of gait abnormalities (slips: limb was placed on a rung, slipped off when weight bearing; misplacement: limb was placed on a rung, but before it was weight bearing it was quickly lifted and placed on another rung or limb aimed for one rung, but was then placed on another rung without touching the first one, miss: limb completely missed a rung and hopping gait: to make a step animal simultaneously lifted both hind paws) (C). No difference in the performance of ablated animals in the horizontal ladder can be detected, with the exception of the number of steps executed in the abnormal hopping gait. Ablated animals show a significant increase in the occurrence of the hopping gait when compared to control animals (One-way Anova, except (C): Kruskal-Wallis). (D-E) Balancing beam test quantified by the distance mice walked on the balancing beam (maximum is 80cm) (D), the time mice needed to cross the beam (E) and the number of foot faults (F). Ablated animals show a significant reduction in distance walked on the balancing beam, with 25% of the animals not being able to walk on the beam at all (D). In addition, mice ablated of dorsal OPCs crossed the beam significantly slower (E), but showed no increased number of foot faults (F) ((D) χ^2 , * = $p < 0.05$, (E) Kruskal-Wallis, * = $p < 0.05$, (F) Kruskal-Wallis). For all experiments, $n = 12$ of *Emx/DTA*, $n = 11$ of *Emx*, $n = 10$ of *DTA* and $n = 9$ of double negative (DN) animals.

In contrast, the repetition of the balancing beam test confirmed a reduced locomotor coordination (also observed in first female cohort (Figure 3.5 D-F)). The average distance walked on the beam is significantly reduced in the group of ablated animals, demonstrating that ablated animals fell off the beam significantly earlier than control animals (Figure 3.7 D). In addition, out of the 12 ablated mice (*Emx/tdTom/DTA*), 25% of the animals were unable to cross the balancing beam (Figure 3.7 D), excluding them from further analysis. When only considering the animals completing the task, the time control animals needed to cross the beam was significantly faster when compared to the ablated animals (Figure 3.7 E). Furthermore, *Emx/tdTom/DTA* animals showed significant difficulties staying on the beam, a low tail carriage, occasionally an unusual gait (*data not shown*), but no increase in foot faults (Figure 3.7 F). However, a direct comparison of the first and the second female cohort exposed an overall better performance of the second female cohort. While in the first female cohort significant differences in the balancing beam task could be identified on the 10mm diameter beam, ablated animals of the second female cohort only performed significantly worse on the 5mm diameter beam.

3.4 Ablation of dorsal OPCs does not result in cognitive impairment in adult mice

Another important process involving the cerebral cortex is cognition. Consequently, to understand whether the ablation of dorsal OPCs also causes cognitive disabilities, the performance of the male animals of the second cohort of mice in the continuous performance test (rCPT) was evaluated. In this cohort, the performance of ten male *Emx1-Cre/Sox10-DTA* ablated animals was compared to the respective single transgenic *Emx1-Cre* and *Sox10-DTA* animals (nine and seven animals per group, respectively) as well as nine double negative animals of the same sex (for cohort details see Materials and Methods, Section 2.1). All the work described in this section has been carried by Eosu Kim and Christopher Heath (laboratory of Prof Tim Bussey, University of Cambridge).

As with the locomotor tasks, successfully completing the rCPT involves multiple competencies. The rCPT is mainly focused on evaluating sustained attention as it requires the animals to observe the experimental screen to respond to the stimuli shown. Besides positively responding to a "target" stimulus (called a hit), the animal needs to resist responding to an incorrect ("non-target") stimulus, which requires inhibitory control, another element of 'executive function'.

In addition to assessing the sustained attention and inhibitory control, the rCPT also requires intact visual perception/processing (identifying the stimuli on the experimental screen) and learning/memory (distinguishing a "target" stimulus from a "non-target" stimulus and memorising this information over the course of the experiment) (C. H. Kim et al., 2015).

In the initial training phase, the animals learn to distinguish a "target" from a "non-target" stimulus and how to respond to a stimulus. The ability of the animals to learn the task can be determined by assessing how many training sessions an individual animal needs to successfully complete a training stage by meeting the set criteria. The session to criterion ratio (n) was similar between all the groups (Figure 3.8 A). Furthermore, no effect of the genotype on the baseline weight or response to food restriction was detected (Figure 3.8 B,C).

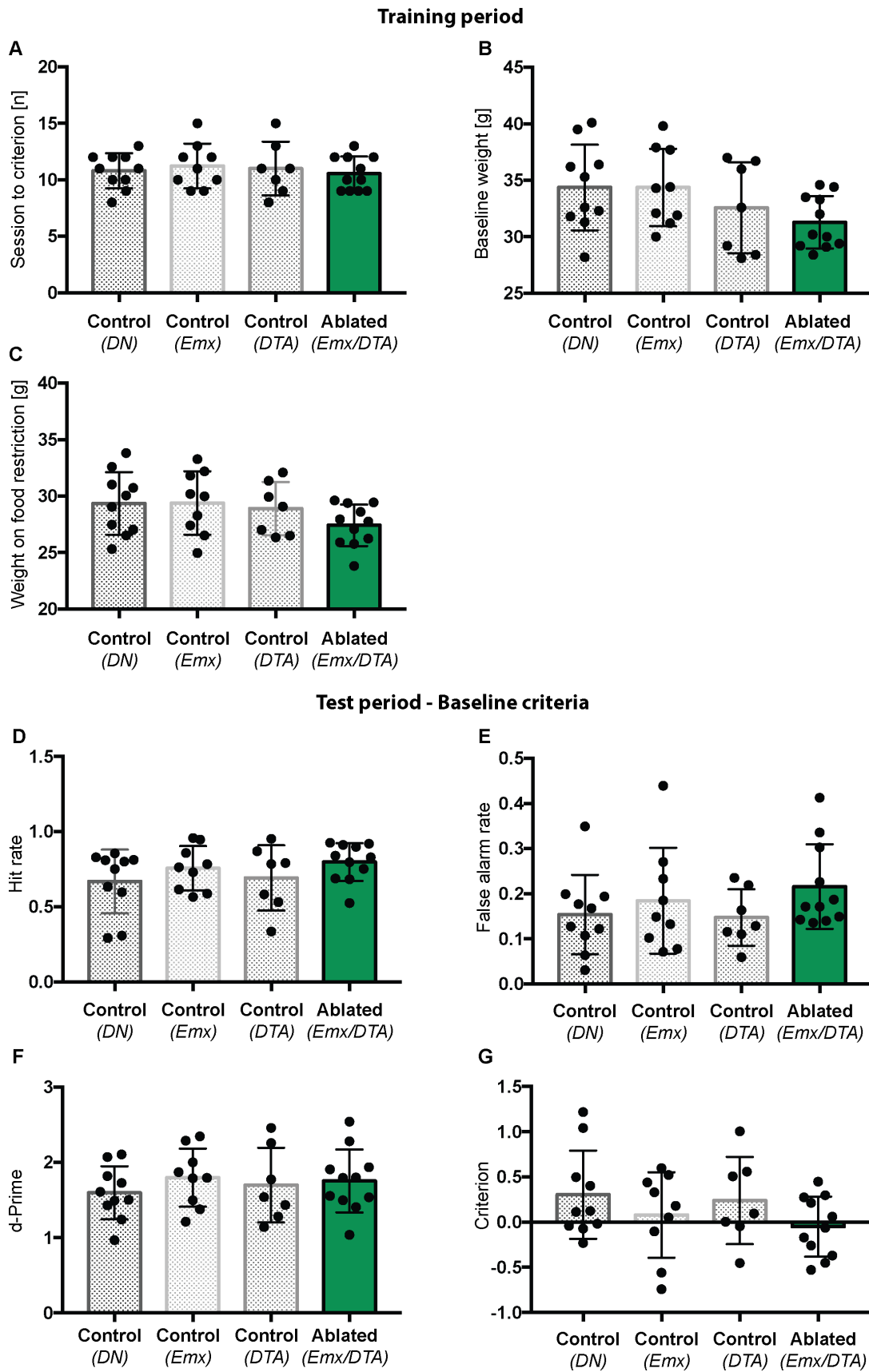


Fig. 3.8 No sustained attention deficits detected in ablated animals. (A-C) Training period: (A) Session to criterion ratio (n) as a measurement of the ability of an animal to learn the rCPT task. Ablated animals master the task after a similar amount of training as control animals (One-way Anova). (B,C) Weights of animals before (B) and after (C) food restriction. No difference in the average weight of the genotypes was detected (One-way Anova). (D-G) Testing period at baseline settings: rCPT test performance quantified by the calculation of hit rate (HR) (D), false alarm rate (FAR) (E), d-prime (d') (F) and criterion (c) (G). Animals ablated of the dorsal OPC population perform similarly to the control animals (One-way Anova). For all experiments, n = 10 of *Emx/DTA*, n = 9 of *Emx*, n = 7 of *DTA* and n = 11 of double negative (DN) animals.

In a test session, animals are shown 160 stimuli ("target" and "non-target" to equal proportion) over the course of 45 minutes. Based on the response to the stimuli, a hit rate (HR, ratio of correct responses to "target" stimulus to total number of "target" stimuli presented) and false alarm rate (FAR, ratio of responses to "non-target" stimulus to total number of "non-target" stimuli presented) are calculated (for details see Materials and Methods, 2.3 B). Using baseline test parameters (see Materials and Methods, 2.3 A), no effect of the genotype on HR and FAR was detected (Figure 3.8 D,E). In accordance, no group effect on the perceptual discriminability between "target" and "non-target" stimuli (d' measurement) or response likelihood (C measurement) was found (Figure 3.8 F,G).

In order to challenge the animals, the time for which a stimulus was shown (stimulus duration, SD) to the animal was reduced (see Materials and Methods, 2.3 A). Across all tested groups, a reduction in SD times caused a decrease in HR, indicating that the animals positively identified fewer "target" stimuli (Figure 3.9 A). Furthermore, animals were also less likely to respond to a "non-target" stimuli when SD times are reduced (Figure 3.9 B). The comparable degree of decrease in FAR and HR explains the overall decreased ability of discriminating "target" from "non-target" stimulus (d' measurement) and increased threshold to respond to a stimulus (c measurement) (Figure 3.9 C,D). However, there was no statistically significant difference between the tested animal groups (Figure 3.9 A-D).

Finally, another way of increasing the complexity of the rCPT task is to reduce the probability of presenting the "target" stimulus (relative to "non-target" stimuli). On the whole, the change in the ratio of "target" to "non-target" stimulus resulted in a slight decrease of HR and a subtle increase of FAR when compared to baseline

measurements

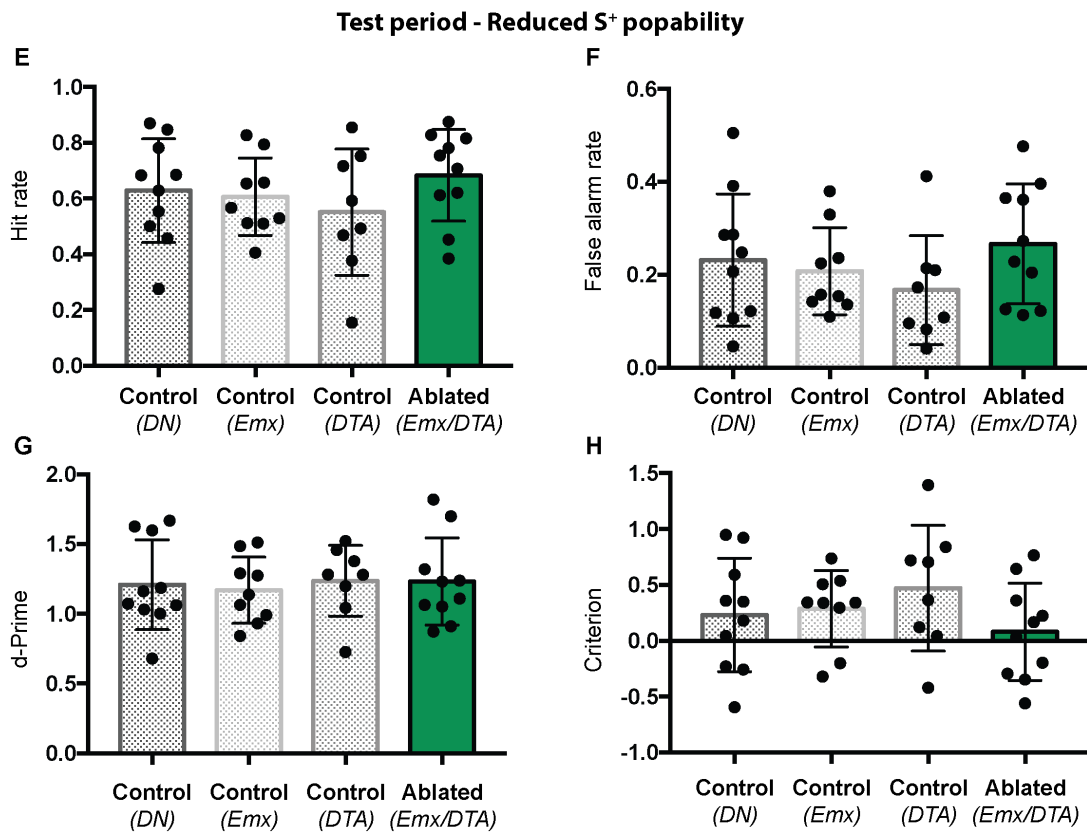
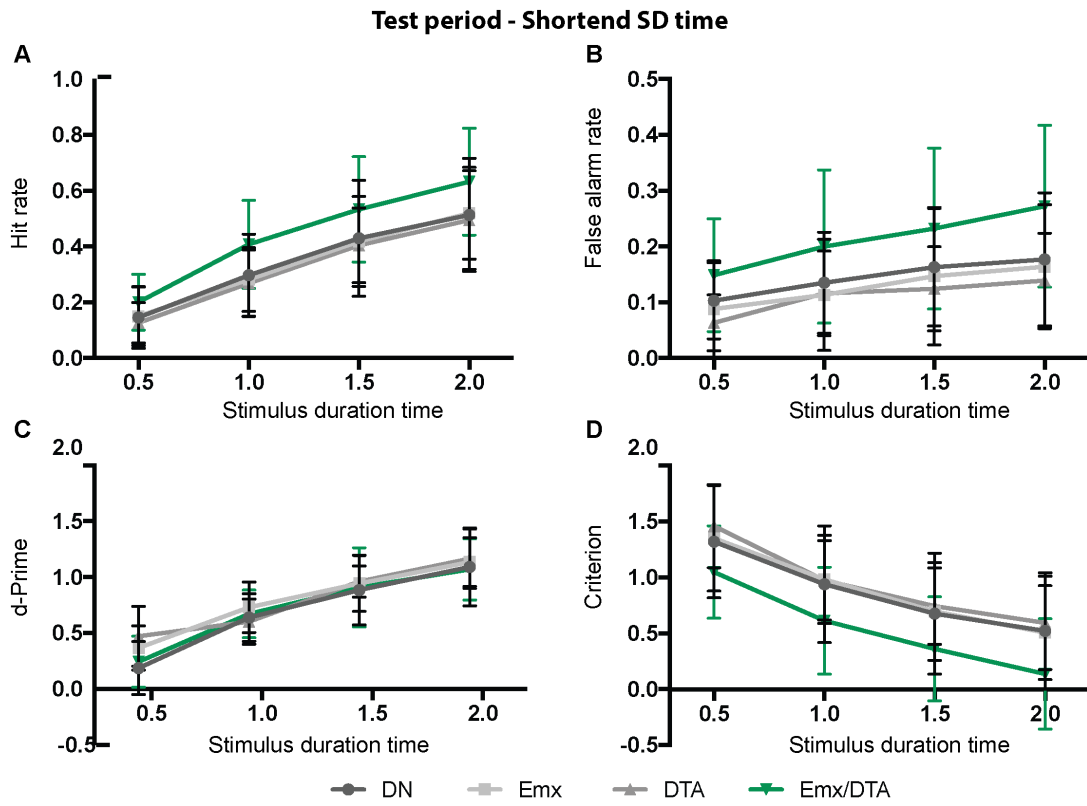


Fig. 3.9 Increasing the difficulty level of rCPT did not reveal a sustained attentional deficit in ablated animals. (A-H) rCPT test performance quantified by the calculation of hit rate (HR) (A,E), false alarm rate (FAR) (B,F), d-prime (d') (C,G) and criterion (c) (D,H). (A-D) Test period with shortened stimulus duration (SD) times. Animals ablated of the dorsal OPC population perform similarly to the control animals (One-way Anova). (E-H) Test period with reduced probability of "target" stimulus presentation (ratio "target" to "non-target" stimuli: 30:70). No significant difference between ablated and control groups in the rCPT test performance can be detected (One-way Anova). For all experiments, $n = 10$ of *Emx/DTA*, $n = 9$ of *Emx*, $n = 7$ of *DTA* and $n = 11$ of double negative (DN) animals.

(Figure 3.8 D,E), indicating that the animals struggle to discriminate between "target" to "non-target" stimuli, which is reflected in the decreased d-Prime value (Figure 3.9 E-G). Consequently, the threshold at which an animal willingly responds to a stimulus increases (Figure 3.9 H). With respect to the intergroup difference, mice ablated of the dorsal OPC population performed as well as the control animals (Figure 3.9 D-H).

3.5 Conclusion and discussion chapter 3

In this chapter, the functional consequences of the ablation of dorsal OPCs are presented. Following the ablation of dorsal OPCs in development, impairments in performing specific locomotor tasks (balancing beam test and vertical beam test) in ablated animals were shown (Figure 3.5, Figure 3.7). These disabilities are caused by a locomotor coordination problem of ablated animals, as their vigilance, including motivation and anxiety, gait, balance and sensation are equal to the control animals (Figure 3.6). However, the reduced performance of ablated animals in the locomotor tests, might also be partially explained by the reduced muscle strength detected (Figure 3.5 H). Unexpectedly, a difference in muscle strength was only detected in the front limbs, not hind limbs, even though coordination problems were always only observed in the hind limbs. A possible explanation for this discrepancy might be that the hip of a mouse is wider than its shoulder therefore rendering it easier to place the front paws correctly on a similar diameter beam. Alternatively, the rearing test used to approximate hind limb muscle strength might not be sufficiently sensitive to pick up small differences.

Generally, the locomotor phenotype observed in ablated animals is subtle, as neither the rotarod nor the horizontal ladder (with the exception of the the number of

steps executed in the abnormal hopping gait) revealed a difference in the performance of the tested animals. The subtlety of the observed results are expected because (1) the ablation of the dorsal OPCs population did not reveal a major phenotype in the normal housing environment (Kessar et al., 2006) and (2) ventral and dorsal OPCs share lots of similarities, including the capability of oligodendrocyte formation. Accordingly, the subtlety of the locomotor phenotype might also explain the over-all better performance of the second female cohort (Figure 3.7) when compared to the first female cohort. Due to the set up of the test battery performed with the second female cohort, the animals experienced more training, potentially increasing their locomotor coordination abilities.

In contrast to a disability in locomotor coordination, no differences in the performance in the rCPT task could be detected. In a broader sense, this result is indicative of no cognitive impairment due to the ablation of dorsal OPCs. However, to unambiguously prove that dorsal OPC ablation has no influence on cognition the following hypotheses would need to be disproven: (1) The cohort size used in rCPT test is sufficient to reveal statistically significant differences (as the CPT test does not work with negative feedback or punishment, the variability in the test can be high depending on the mouse strain). To disprove the first hypothesis, the statistical power of the study was calculated. According to the presented results of the rCPT test (Figure 3.8 and 3.9), the average difference between the double negative and the ablated group is 20%. The calculated power of the presented study, assuming an average cohort size of 10 animals, is 0.45. The estimated number per animals per group to reach an adequate statistical power of 0.8 is 24 animals per group. This indicates, that the number of animals assessed is too small for the difference between control and ablated animals to become significant. Due to the high requirements of the cohort (only males, litter mates, age), at least 80 breeding females would be required to breed up a colony of animals with 24 animals per group, which is incompatible with the animal breeding ethics. Based on the experimental set-up presented above, it cannot be confidently concluded that there is no intergroup difference in sustained attention. (2) The DTA-ablation efficiency is region-specific. The regional-specificity of DTA ablation is very unlikely, as multiple telencephalon regions have been tested, all showing the same ablation efficiency (Figure ??). However, the ablation efficiency in cortical areas involved in cognition remains to be investigated. (3) The performances of ablated animals is not impaired in other cognitive function tests (eg. novel object recognition). Given the subtlety of the locomotor defects in ablated animals, small differences in the cognitive performance of ablated animals would be expected. Therefore, it is possible that other

cognitive tests specifically assessing distinct aspects of cognition, such as memory or learning, may uncover disabilities due to the ablation of dorsal OPCs.

Chapter 4

Off-target effects of the DTA ablation system

The specific ablation of dorsal OPCs causes locomotor coordination defects in mice (Chapter 3). In addition to OLCs, astrocytes, microglia and certainly neurons play key roles in modulating neuronal transmission. Consequently, off-target effects of the DTA ablation system on each cell type need to be assessed to exclude that the locomotor phenotype observed is not due to leakiness or off-target effects of the *Sox10-DTA/Emx1-Cre* ablation model. The execution of a locomotor task involves multiple brain areas, including the motor cortex (MC), somatosensory cortex (SC), corpus callosum (CC) and striatum (Str). Therefore, potential effects of the DTA ablation system were studied in all aforementioned brain areas. Whilst the cerebellum is additionally important in motor control, it has been excluded from the analysis as it is exclusively populated by OLCs of ventral origin (*Figure 3.4 G*).

4.1 Neurons are not affected by the DTA ablation model

To identify neurons, the neuronal marker NeuN was used, staining the majority of neuronal subtypes. Only neuronal subtypes in the cerebellum, retina and olfactory bulb are not labelled by NeuN, making it a suitable marker for the purpose of this study. No significant difference in the total number of NeuN⁺ neurons was detected in the motor cortices (MC) (*Emx/tdTom*: 57.4% versus *Emx/tdTom/DTA*: 44.4%), somatosensory cortex (SC) (*Emx/tdTom*: 57.2% versus *Emx/tdTom/DTA*: 46.7%), or in the basal ganglia (BG) (*Emx/tdTom*: 46.3% versus *Emx/tdTom/DTA*: 40.0%) (*Figure 4.1*).

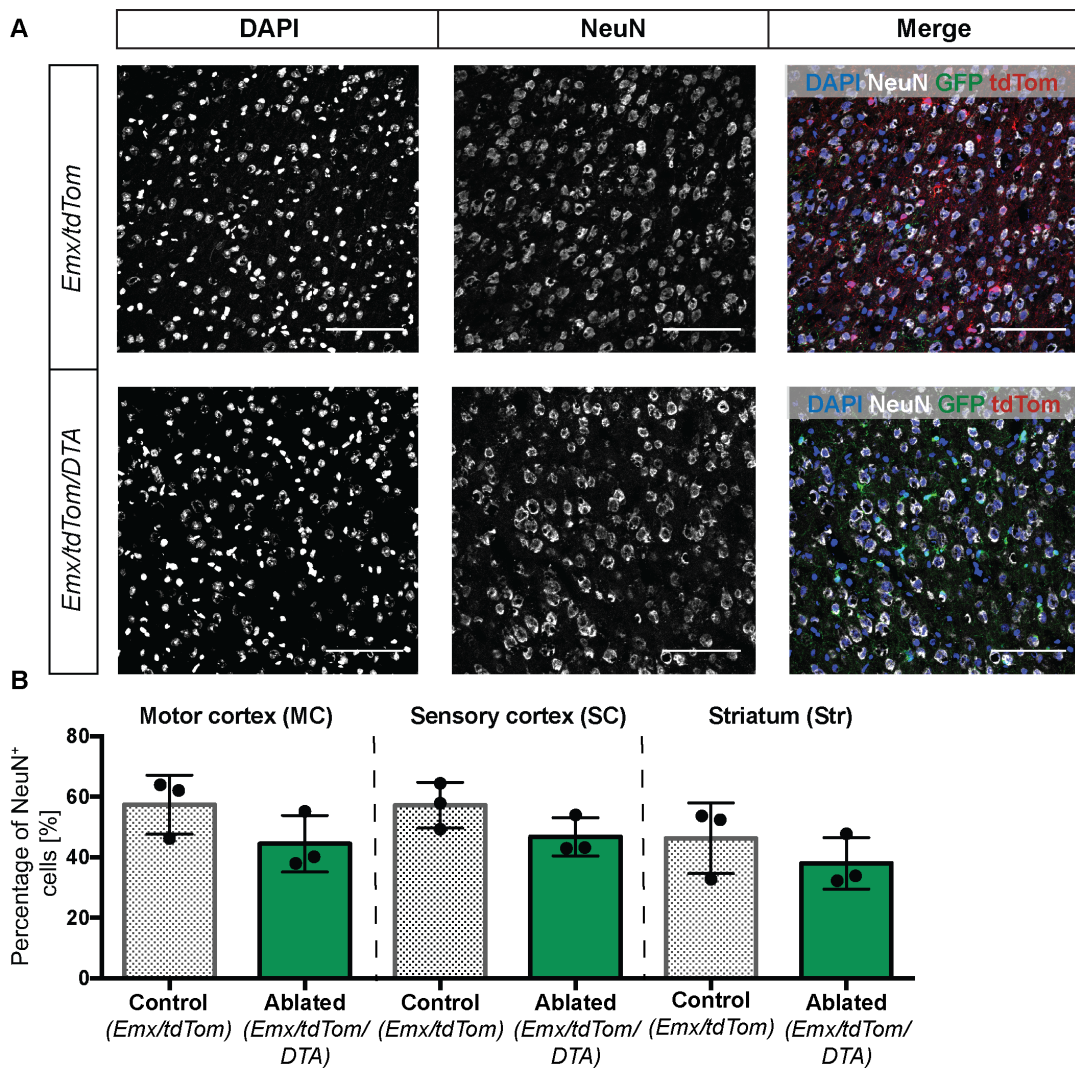


Fig. 4.1 Neurons are not affected by the DTA ablation model. (A) Representative images of the NeuN IHC staining of the MC in *Emx/tdTom* control and *Emx/tdTom/DTA* ablated animals. (B) Quantification of IHC staining. Percentage of NeuN⁺ cells (out of total DAPI⁺ cells) in *Emx/tdTom* control and *Emx/tdTom/DTA* ablated animals. The number of NeuN⁺ cells is similar between control and ablated animals (n = 3, Unpaired t-test). Scale bar = 100 μ m, IHC = immunohistochemistry

4.2 Ablation of dorsal OPCs does not influence axonal health

Through the myelination of an axon, oligodendrocytes not only accelerate neuronal conduction, but also supply the axon with important nutrients and neurotrophic factors (see Introduction, Section 1.2.3). Therefore, axonal health in the cortex might be compromised as a result of dorsal OPC ablation. One way to assess axonal health is to

measure the amount of unphosphorylated neurofilament, a major component of the axonal cytoskeleton. SMI32 is an antigen recognising the unphosphorylated epitope of the neurofilament heavy chain (NF-H).

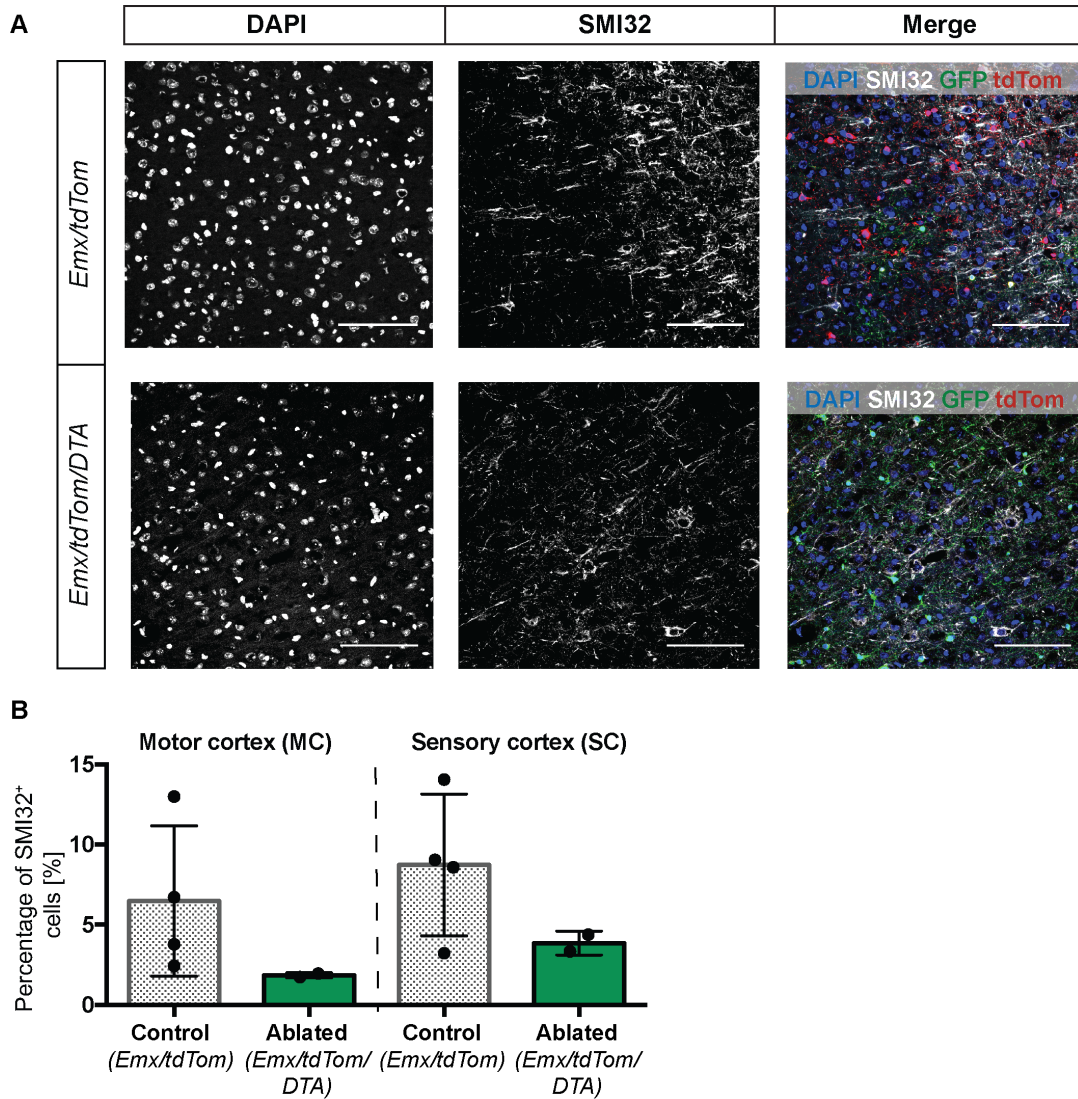


Fig. 4.2 Ablation of dorsal OPCs does not affect axonal health. (A) Representative images of the SMI32 IHC staining of the MC in *Emx/tdTom* control and *Emx/tdTom/DTA* ablated animals. (B) Quantification of IHC staining. Percentage of SMI32⁺ cells (out of total DAPI⁺ cells) in *Emx/tdTom* control and *Emx/tdTom/DTA* ablated animals. A trend towards a reduced SMI32 staining in ablated animals can be noted (Control: n = 4, Ablated: n = 2, no statistics performed due to small n-number). Scale bar = 100 μ m, IHC = immunohistochemistry

In comparison to control animals, there is no significant change in SMI32 staining in the motor cortices (MC) (*Emx/tdTom*: 4.3% versus *Emx/tdTom/DTA*: 2.8%) or somatosensory cortex (SC) (*Emx/tdTom*: 7.0% versus *Emx/tdTom/DTA*: 3.9%) in

ablated animals (Figure 4.2). However, due to the high variability of SMI32 staining in control animals, a change in the number of SMI32⁺ in ablated animals cannot be confidently excluded (see Section 4.6).

4.3 Astrocytes are not affected by the DTA ablation model

As astrocyte precursor cells can express *Sox10* and subsets of astrocytes have also been reported to express *Emx1*, astrocytes are the most likely cell population to be affected by off-target effects of the DTA ablation system. Counting of GFAP⁺ astrocytes in the CC revealed that there is no significant difference in astrocyte numbers between control and ablated animals (*Emx/tdTom*: 325.6 GFAP⁺ cells/area [mm²], *Emx/tdTom/DTA*: 298.7 GFAP⁺ cells/area [mm²]) (Figure 4.3 A,B). Additionally, the measurement of GFAP protein using whole brain western blot analysis confirmed no difference in the total amount of GFAP protein in control and ablated animals (Figure 4.3 C). As GFAP only stains astrocytes residing in the white matter, the number of grey matter astrocytes was assessed using the pan-astrocyte markers glutamine synthetase (GS) and aquaporin 4 (AQU4). No significant difference in the total amount of GS and AQU4 protein was detected in whole brain lysates of control and ablated animals (Figure 4.3 D,E).

4.4 Microglia are not affected by dorsal OPC ablation

The expression of *Emx1* and *Sox10* in microglia is not expected. However, microglia numbers and their activation status might be affected by any disturbance to the brain parenchyma caused by the DTA ablation. With an average of 9.4% of IBA1⁺ microglia in the cortices (*Emx/tdTom*: 7.6%, *Emx/tdTom/DTA*: 11.3%), 9.0% of microglia in the striatum (*Emx/tdTom*: 7.0%, *Emx/tdTom/DTA*: 11.0%) and 6.2% of microglia in the corpus callosum (*Emx/tdTom*: 6.2%, *Emx/tdTom/DTA*: 6.3%), no significant difference of IBA1⁺ microglia was detected in any brain area assessed (Figure 4.4) In addition, no indicator of an ongoing inflammation as a result of the DTA ablation was identified, as microglia of control and ablated animals have a ramified shape with no expression of the activation marker CD68 (*data not shown*).

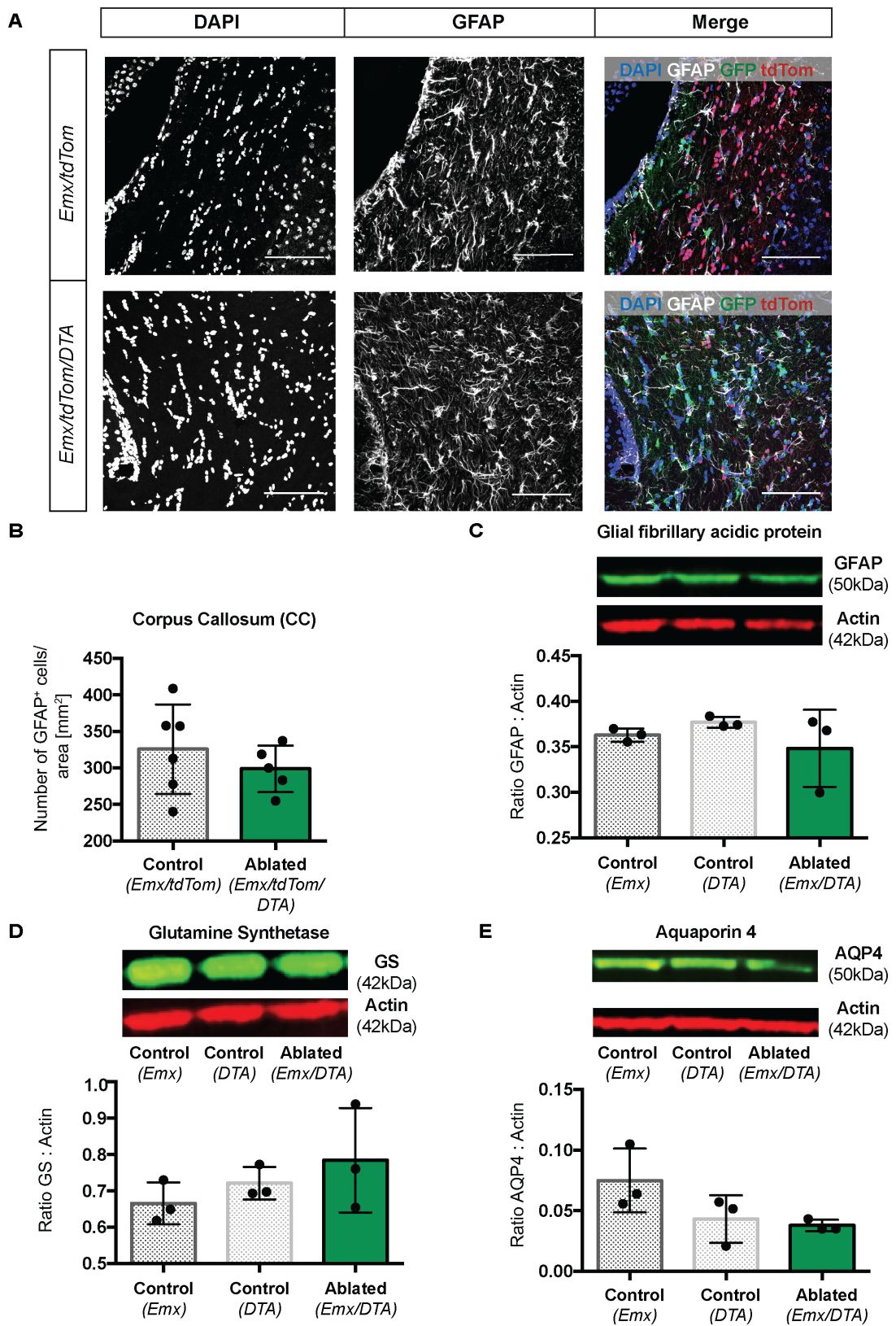


Fig. 4.3 White matter astrocytes are not affected by the DTA ablation model. (A) Representative images of the GFAP IHC staining of the CC in *Emx/tdTom* control and *Emx/tdTom/DTA* ablated animals. (B) Quantification of IHC staining. Percentage of GFAP⁺ cells (out of total DAPI⁺ cells) in *Emx/tdTom* control and *Emx/tdTom/DTA* ablated animals. In ablated animals, there is a trend towards a decreased number of astrocytes (Control: n = 6, Ablated: n = 5, Unpaired t-test). (C, D, E) Western blot analysis of astrocyte marker proteins (Glial fibrillary acidic protein (GFAP, textbfC), Glutamine synthetase (GS, textbfD), Aquaporin 4 (AQU4, textbfE)) of whole brain samples. No difference in astrocyte marker protein expression was detected between control and ablated animals (n = 3, One-way Anova). Scale bar = 100 μ m, IHC = immunohistochemistry

4.5 *Emx1*⁺ cells are present in the spinal cord

The motor system is involved in generating and controlling voluntary movements and reflexes, and can be divided into two parts: (1) the peripheral component (peripheral axon, the neuromuscular junction and muscle) and (2) the central component (brain and spinal cord). More specifically, in the central component movement involves the initiation of action potentials in motor neurons in the motor cortex, which project through the internal capsule to the brain stem and spinal cord. In addition, the basal nuclei and cerebellum act to regulate movement. Therefore, intact neuronal transmission in the brain (motor cortex, basal nuclei, cerebellum) and the spinal cord is crucial for the execution of a motor task. Consequently, an effect of the DTA ablation model on any cell type in the spinal cord, could lead to the locomotor phenotype observed.

To exclude leakiness of the *Emx1-Cre* mouse line in the spinal cord, the number of tdTOMATO⁺ cells in an *Emx/tdTom* control animal was counted. $6.8 \times 10^{-3}\%$ of the total SOX10⁺ OLCs in the spinal cord expressed tdTOMATO, and therefore might be ablated in the *Sox10-DTA/Emx1-Cre* model. As the proportion of *Emx1*⁺ cells in the spinal cord is so small, it is unlikely, but not impossible, to be the underlying cause or contribute to the locomotor phenotype.

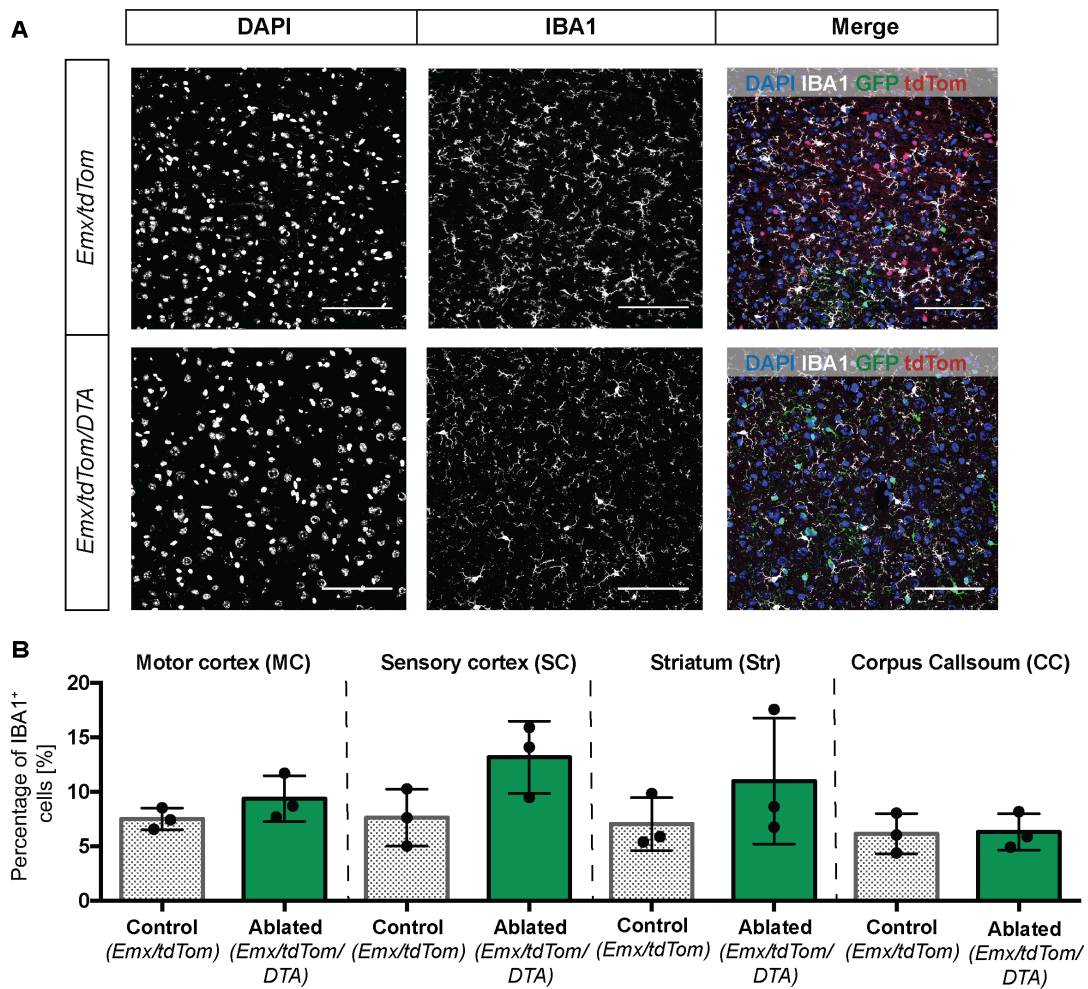


Fig. 4.4 Microglia cells are not affected by the DTA ablation model. (A) Representative images of the IBA1 IHC staining of the MC in *Emx/tdTom* control and *Emx/tdTom/DTA* ablated animals. (B) Quantification of IHC staining. Percentage of IBA1⁺ cells (out of total DAPI⁺ cells) in *Emx/tdTom* control and *Emx/tdTom/DTA* ablated animals. No difference in IBA1⁺ microglia was detected between control and ablated animals (n = 3, Unpaired t-test, except striatum: Mann-Whitney test). Scale bar = 100 μ m, IHC = immunohistochemistry

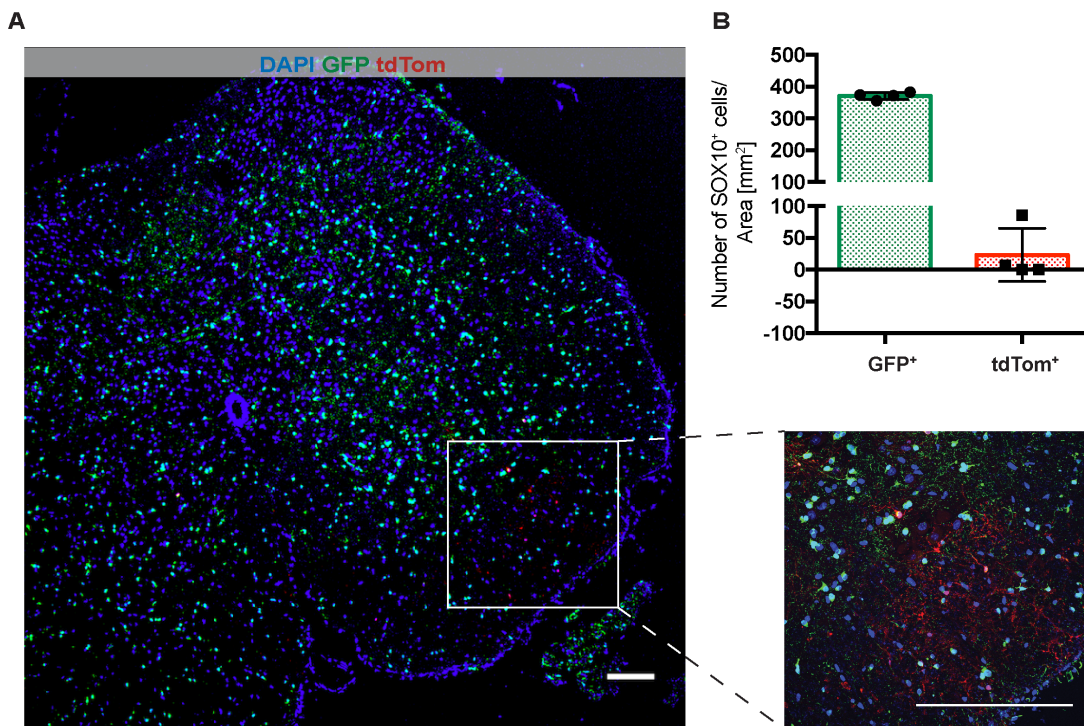


Fig. 4.5 DTA ablation of dorsal OPCs also affects the spinal cord. (A) Representative images of the spinal cord of an *Emx1/tdTom* control animal. (B) Number of GFP⁺ SOX10⁺ and tdTOMATO⁺ SOX10⁺ cells in *Emx1/tdTom* control animals. The proportion of *Emx1*⁺ cells in the spinal cord is very small (Control: n = 2, Ablated: n = 3, no statistics performed due to small n-number). Scale bar = 100 μ m.

4.6 Conclusion and discussion chapter 4

In this chapter, the off-target effects of the DTA-ablation system have been investigated, with no statistically significant effect on neurons, astrocytes and microglia observed. In addition, only a small subset of cells in the spinal cord expressed *Emx1*, which most likely will not account for the locomotor phenotype observed in *Emx1-Cre/Sox10-DTA* animals (see Chapter 3).

The specificity of the ablation mouse model is dependent on the expression of *Emx1* and *Sox10* (Figure 3.1). In order for off-target effects to occur, *Emx1* and *Sox10* need to be expressed within the same cell, but not necessarily at the same time. While *Emx1* only needs to be expressed once to induce Cre-recombination, *Sox10* needs to be continuously active to drive DTA expression. According to the limited available literature, only a subset of astrocytes potentially expresses both transcription factors (Table 4.1 and 4.2). In line with this, a trend towards a reduction of white matter astrocytes in ablated animals was observed (Figure 4.3), indicating that the *Emx1*-

Cre/Sox10-DTA model might affect astrocyte numbers. As variations in the GFAP staining due to the small number of biological replicates prevents a definitive answer, the astrocyte staining using a pan-astrocyte marker in a larger number of animals needs to be repeated. In addition to astrocytes, neural crest derived cells potentially express *Sox10*. Even though no *Emx1* expression of neural crest cells is reported, they might be a target of the DTA ablation. The only neural crest derived cells in the nervous system are Schwann cells, the myelinating cells of the peripheral nervous system, and neurons in the sensory and autonomic ganglia. As alterations in subsets of both cell types can alter the locomotor coordination of animals, the influence of the DTA ablation model on neural crest cells needs to be investigated (see also Discussion 7.5.2).

Besides an off-target effect of the DTA ablation on neurons, a possible trend towards a reduced phosphorylation of neurofilaments in the motor cortex of ablated animals was observed. The phosphorylation status is considered as a surrogate marker of axonal health and has been correlated with neurodegenerative diseases. Both OPCs and oligodendrocytes are in close contact with neurons, significantly modulating their function. Therefore, it is conceivable that a change in the OLC population results in altered axonal health. Hence, to make a final conclusion on the status of axonal health in ablated animals, SMI32 staining in a larger number of animals needs to be repeated as well as other axonal health markers assessed (see Discussion, Section 7.2).

An inflammatory response caused by the ablation of OPCs might result in disruptions of CNS function. The DTA ablation method was proven to cause apoptosis of the target cells, which does not provoke an inflammatory response other than a transient microglia response. Undoubtedly, microglia will be activated in ablated animals, to clear the debris of the apoptotic cells. However, in development the brain is very plastic, which includes the apoptosis of excess neurons as well as synaptic pruning (Buss, Sun, & Oppenheim, 2006; Katz & Shatz, 1996). Therefore, the additional ablation of dorsal OPCs is not expected to cause a significant increase in microglia activation. In an adult animal, no OPCs ablation due to the DTA model is expected because the OPC turn-over in an adult animal is slow, so that remaining dorsal OPCs are not expected to produce many progeny. In accordance, no activation of microglia, an indicator of perturbations of homeostasis in the brain, was detected. This is consistent with another OPC ablation model, likewise detecting microglia activation only short-term in response to ablation (Birey et al., 2015). Therefore, the DTA strategy is a highly efficient means of ablating the target cells, with minimal off target effects.

Sox10	Yes/No	Reference
Astrocytes		
Embryonic/neonatal	No, but some astrocyte precursors (B,SC)	(Y. Zhang et al., 2014) (Masahira et al., 2006) (Glasgow et al., 2014)
Adult	n/a (no expression speculated in literature) (B)	n/a
Neurons		
Embryonic/neonatal	No, but some neuronal precursors (SC)	(Masahira et al., 2006)
Adult	Yes (L2, L4 and L6 neurons) (B)	(Allen Brain Atlas)
Microglia		
Embryonic/neonatal	No (B)	(Y. Zhang et al., 2014)
Adult	No (SC)	(Chiu et al., 2013)
Neural crest cells (Schwann cells, DRGs)		
Embryonic/neonatal	Yes	(Kuhlbrodt, et al., 1998)
Adult	Yes (Schwann cells only)	(Kuhlbrodt, et al., 1998)

Table 4.1 Expression of *Sox10* in the cells of the nervous system.

Emx1	Yes/No	Reference
Astrocytes		
Embryonic/neonatal	Yes (dorsal astrocytes and dorsal astrocyte precursor only) (B)	(Y. Zhang et al., 2014) (Gorski et al., 2002)
Adult	n/a	n/a
Neurons		
Embryonic/neonatal	Yes (only in dorsal excitatory neurons) (B)	(Y. Zhang et al., 2014) (Gorski et al., 2002)
Adult	Yes (pyramidal neurons) (B)	(Chan et al., 2001)
Microglia		
Embryonic/neonatal	Yes (B)	(Y. Zhang et al., 2014)
Adult	n/a	n/a
Neural crest cells (Schwann cells, DRGs)		
Embryonic/neonatal	n/a	n/a
Adult	n/a	n/a

Table 4.2 Expression of *Emx1* in the cells of the nervous system. Assessing the expression profile of *Emx1* and *Sox10* alongside the age of the animal is important, as only expression of *Emx1* before or simultaneously with *Sox10* will cause off-target effects. Similarly, the expression of both transcription factors also needs to be investigated separately in the brain and spinal cord, as an expression in either CNS area does not necessarily indicate an expression in the respective other. B = brain, SC = spinal cord

Chapter 5

Effects of DTA ablation on oligodendrocyte lineage cells

In the CNS, OPC numbers are tightly regulated, remaining steadily at 5-7% of total brain cells (Pringle & Richardson, 1993). Each OPC maintains an exclusive territory through self-repulsion, which allows the OPCs to actively survey its environment. In homeostasis, and in response to a local injury, a loss of self-repulsion by OPC cell death or differentiation triggers the remaining OPCs to proliferate to re-establish the OPC network (Hughes et al., 2013). However, the ablation of dorsal OPCs reduces the OPC number in the forebrain dramatically in the early postnatal weeks (approximately by 40% based on the proportion of dorsal OPCs in the adult animal). Are ventral OPCs capable of compensating for this significant loss of OPCs? Hypomyelination in response to the dorsal OPCs ablation could explain the locomotor disabilities observed *in vivo* (see Chapter 3). Thus, the effect of the DTA ablation system on the oligodendrocyte lineage needs to be established.

5.1 Ablation of dorsal OPCs leads to an expansion of OPCs, but not oligodendrocytes

To identify OPCs, the NG2 antigen was used. As NG2 does not exclusively mark OPCs, SOX10 as an oligodendrocyte lineage marker was used to unambiguously label OPCs. Despite the ablation of more than 85% of the dorsal OPCs, a significant expansion of NG2⁺ SOX10⁺ OPCs was detected in ablated animals. Whilst only 2% of all cortical DAPI⁺ cells were NG2⁺ SOX10⁺ OPCs in control animals, 10% of all DAPI⁺ cells stained positive for SOX10 and NG2 in the cortex of ablated animals.

In comparison to the cortex, more NG2⁺ SOX10⁺ OPCs were detected in the corpus callosum. Nevertheless, a four-fold increase of NG2⁺ SOX10⁺ OPCs was found in the corpus callosum of ablated animals (*Emx/tdTom*: 4.3% versus *Emx/tdTom/DTA*: 16.0%) (Figure 5.1).

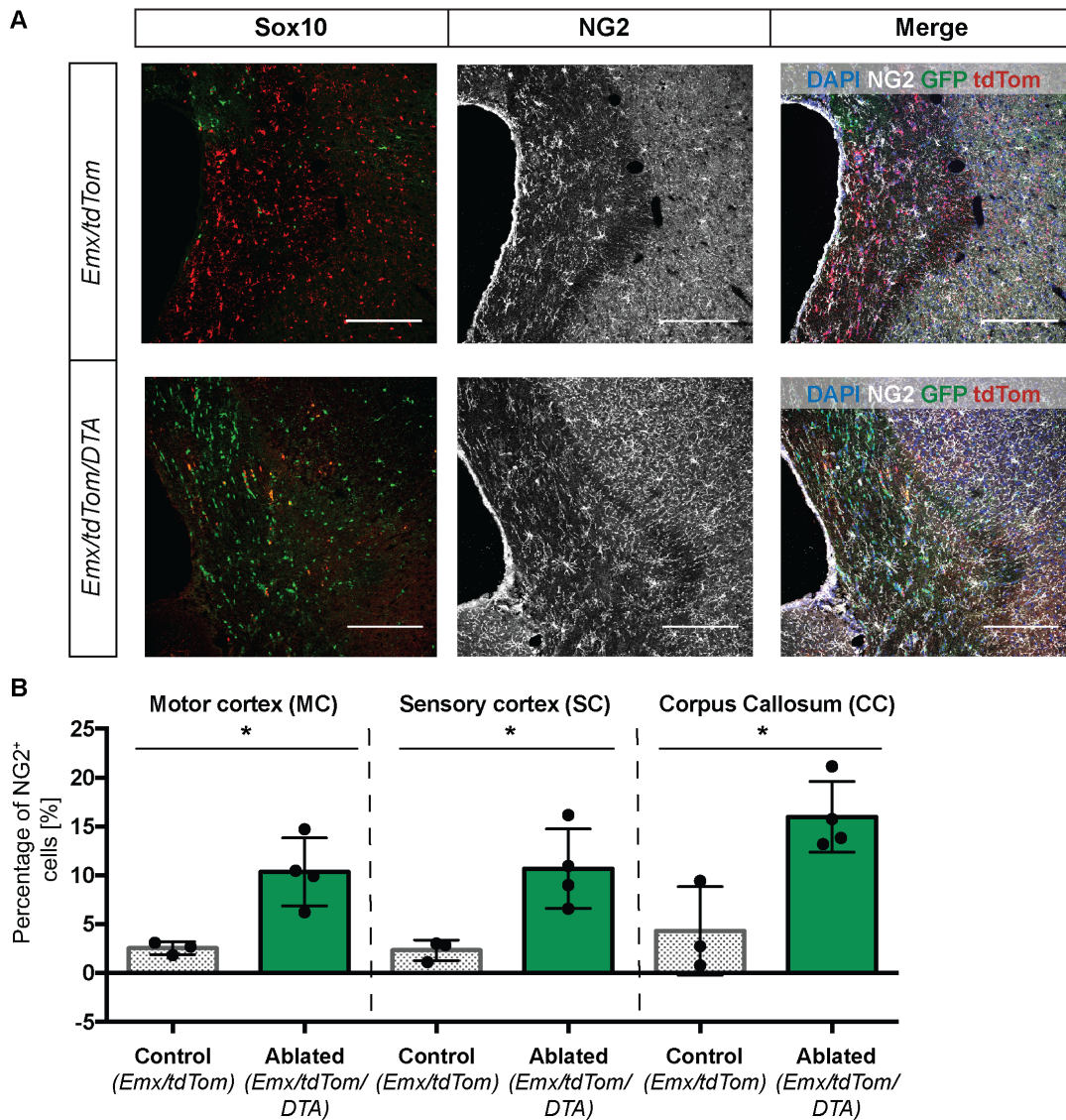


Fig. 5.1 Dorsal OPC ablation leads to an expansion of the OPC pool. (A) Representative images of the NG2 IHC staining of the CC in *Emx/tdTom* control and *Emx/tdTom/DTA* ablated animals. (B) Quantification of IHC staining. Percentage of NG2⁺ SOX10⁺ cells (of total DAPI⁺ cells) in *Emx/tdTom* control and *Emx/tdTom/DTA* ablated animals. The number of NG2⁺ SOX10⁺ cells are significantly increased in ablated animals in all brain areas assessed (n = 3, Unpaired t-test, * = p<0.05). Scale bar = 100μm, IHC = immunohistochemistry, CC= corpus callosum

Mature oligodendrocytes were identified using the marker protein CC1. Significantly more mature oligodendrocytes were detected in the white matter, when compared to all the grey matter areas (white matter: 63.5% versus grey matter: 14.8%). However, in contrast to OPCs, mice ablated of the dorsal OPC population show similar numbers of mature CC1⁺ SOX10⁺ oligodendrocytes when compared to control animals (Figure 5.2 A,B). Oligodendrocyte numbers have been additionally counted using flow cytometry. Consistent with the immunohistochemistry results, the brains of the ablated animals contain the same amount of MOG⁺ SOX10⁺ mature oligodendrocytes as control animals, indicating that ventral OPCs can compensate for the loss of dorsal OPCs, resulting in physiological oligodendrocyte numbers after ablation (Figure 5.2 C,D).

5.2 Ablation of dorsal OPCs does not cause white matter hypomyelination

To determine whether the ventral oligodendrocytes are capable of myelinating the dorsal parts of the telencephalon, magnetic resonance imaging (MRI) was carried out to visualise the myelination status of the full brain. Brain preparation and imaging was performed by Joe Guy (former PhD student in the Franklin laboratory, University of Cambridge).

To assess differences in myelination, the average T2* signal intensity (which decreases with increasing myelination) in a given white matter area was measured between control and ablated animals. Due to space restrictions of the imaging coil, the scanning of all the brains had to be performed in two consecutive experiments. To account for changes that may occur between MRI scans (including coil tuning, electronics temperature, brain temperature, shimming, background RF interference, position of tissue in the coil, and digitisation of the signal) the ratio of the intensity of a given white matter tract divided by intensity of a grey matter area in close proximity was calculated. This method still harbours the drawback of finding truly equivalent areas across different brains, as differences in anatomy or perfusion (to only name a few) will influence the intensity.

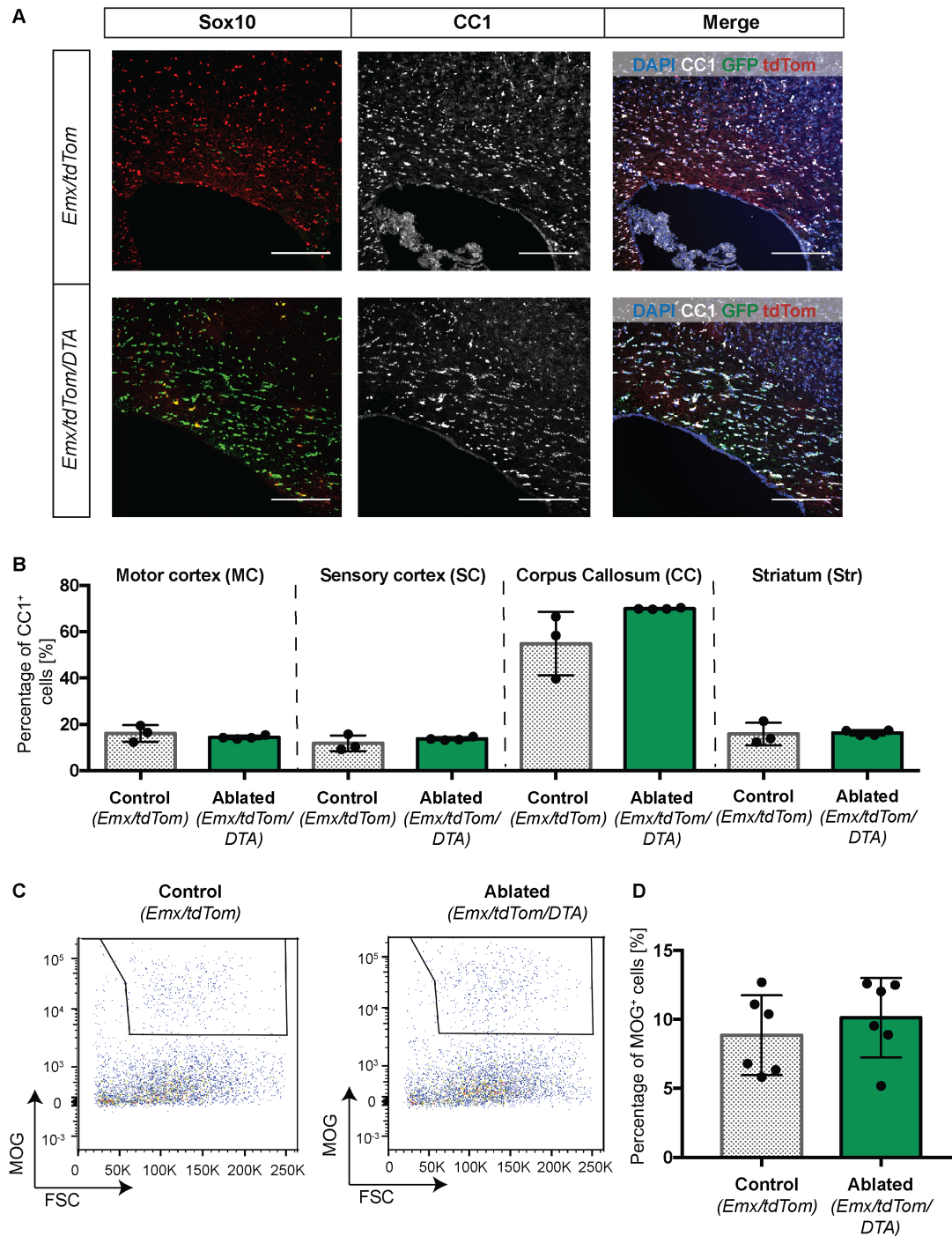


Fig. 5.2 Oligodendrocyte numbers are not affected by the ablation of dorsal OPC.

(A) Representative images of the CC1 IHC staining of the CC in *Emx/tdTom* control and *Emx/tdTom/DTA* ablated animals. (B) Quantification of IHC staining. Percentage of CC1⁺ SOX10⁺ oligodendrocytes (of total DAPI⁺ cells) in *Emx/tdTom* control and *Emx/tdTom/DTA* ablated animals. No significant difference in the number of mature CC1⁺ SOX10⁺ oligodendrocytes were detected between control and ablated animals (n = 3, Unpaired t-test, except corpus callosum: Mann-Whitney test). Scale bar = 100 μ m, IHC = immunohistochemistry, CC= corpus callosum. (C) Representative images of MOG flow cytometry staining. (D) Percentage of MOG⁺ SOX10⁺ mature oligodendrocytes (of the total living DAPI⁺ OLCs) in control and ablated animals. Brains of control and ablated animals showed a similar percentage of MOG⁺ mature oligodendrocytes (n = 6, Unpaired t-test).

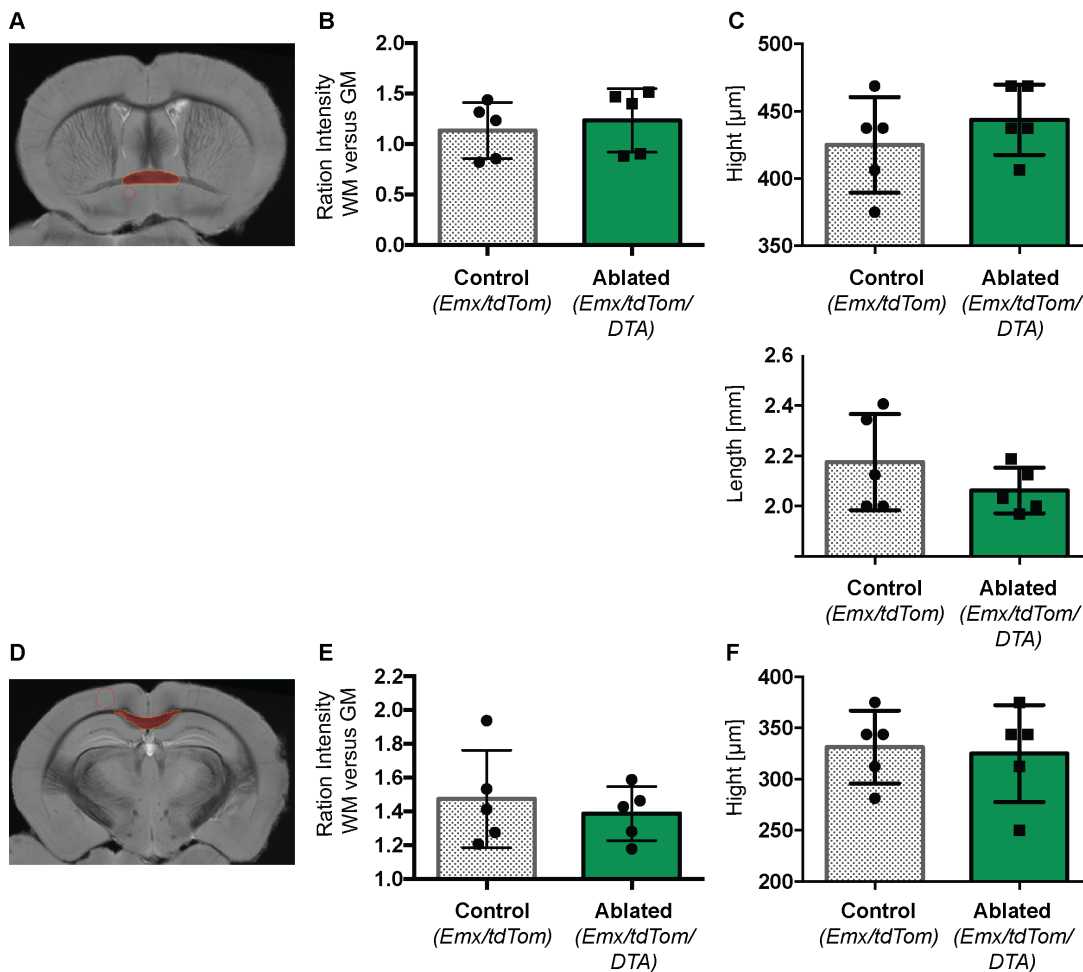


Fig. 5.3 MRI analysis did not detect myelination changes in major white matter tracts following ablation of dorsal OPCs. (A, D) Representative image of *Emx/tdTom* control and *Emx/tdTom/DTA* ablated animals used to calculate the ratio of white matter to grey matter intensity to assess AC (A) and CC (D) myelination. (B, E) MRI was quantified by the ratio of white matter and adjacent grey matter intensity. No significant difference in the myelination levels of the AC (B) or the CC (E) was detected ($n = 5$, Unpaired t-test). (C, F) Average height and lengths of the AC (C) and CC (F) in control and ablated animals. The dimensions of the AC and CC in ablated animals are similar to control animals ($n = 5$, Unpaired t-test). AC = anterior commissure, CC = Corpus callosum

Due to the fact that the anterior commissure (AC) is exclusively populated by ventral OPCs, it was used as an control region for the MRI analysis (Figure 5.3 A). As expected, no difference in the average ratio of intensity was detected in the AC of control and ablated animals (*Emx/tdTom*: 1.1, *Emx/tdTom/DTA*: 1.2) (Figure 5.3 B). In addition to the intensity, the height and length of the AC is measured as an indicator of hypomyelination. With an average height of $440\mu\text{m}$ and width of 2mm, the dimensions of the AC of ablated animals are not significantly different to the

control animals (Figure 5.3 C). Similarly, the ratio of intensity in the corpus callosum (CC) is comparable between groups, with an average ratio of 1.5 and 1.4 in control and ablated animals, respectively (Figure 5.3 D,E). Furthermore, the height of the CC of mice ablated of the dorsal OPC population is not different to the control animals (Figure 5.3 F), indicating that ventral oligodendrocytes are capable of myelinating the CC.

5.3 Conclusion and discussion chapter 5

The effect of dorsal OPC population ablation on the remaining OLCs in the adult brain has been investigated in this chapter. Intriguingly, an increase in the total OPC population was observed, indicating an overcompensation of the remaining OPCs in response to an extensive OPC loss. However, NG2 staining in tissue can be variable depending on the level of fixation of the tissue. In addition, NG2 is not solely labelling OPCs, but also pericytes in an uninjured CNS as well as macrophages and Schwann cells in an injured CNS (McTigue, Tripathi, & Wei, 2006). As there was no sign of inflammation (no increase in microglia numbers, no microglia activation) indicating a potential injury state detected (??), it is improbable that macrophages and Schwann cells will express NG2 in the brain of ablated animals. In addition, as pericytes and macrophages do not express SOX10, it is unlikely that either cell type was counted as false-positive in the experiment described in this chapter (Figure ??). Furthermore, even though Schwann cells express SOX10, it is also unlikely that they were counted due to their distinctive morphology. However, NG2 expression in a cell line of oligodendrocyte progenitor cells was also shown to be increased in response to cytokine treatment mimicking injury *in vitro* (Moransard et al., 2011), which can lead the impression that there is more NG2 reactivity in ablated animals. Still a similar up regulation of NG2 in the dorsal ablation model is not anticipated as adult ablated animals do not show any sign of inflammation (??). Consequently, due to the ambiguity of NG2 as an OPCs marker, the result needs to be confirmed by an independent method. Immunohistochemistry staining with antibodies against A2B5 or PDGFR α can be used. However, the PDGFR α protein expression is decreased with age (see Chapter 6, Figure ?? and Figure ??), potentially not reflecting true OPC numbers. Therefore, RNAScope to visualise PDGFR α mRNA to identify OPCs needs to be used instead. In addition, Scholl analysis of OPCs in tissue as well as cultured *in vitro* should be carried out to reveal the complexity of OPCs processes as it can be hypothesised that the

territories occupied by a single OPC should decrease with an increase in OPC numbers.

The analysis of the number of oligodendrocytes showed comparable rates of OPC differentiation. Together with the MRI analysis, showing that ventrally derived oligodendrocytes can myelinate axons in dorsal areas, this indicates that ventral derived OPCs are capable of compensating for the lack of dorsal OPCs. However, MRI analysis will not reveal subtle changes in myelination, especially in the grey matter, in which axons are only sparsely myelinated. Small changes in the amount of myelination as well as changes in the myelin structure (eg. myelin sheath length or thickness) cannot be visualised by MRI. Therefore, electron microscopy analysis should be carried out in addition to MRI (Chapter 6, Figure 6.4).

The observation that an excess of OPCs is not reflected in oligodendrocyte numbers is intriguing. In the literature, multiple hypotheses on potential induction signals for OPC differentiation are discussed (see Introduction, Section 1.3.1). One hypothesis states that there is simply an internal clock, dictating when an OPC will start differentiating (Hill et al., 2014; Klingseisen & Lyons, 2017). Contact-inhibition of neighbouring OPCs triggers differentiation upon full establishment of the OPC network is suggested in a second hypothesis (Klingseisen & Lyons, 2017). The first two theories would predict a proportional increase in the number of oligodendrocytes, when OPC numbers rise. In contrast, a third hypothesis proposes an axon stimulated mechanism of OPC differentiation, implicating that only so many oligodendrocytes are formed, which are needed for myelination.

Multiple *in vitro* studies support a OPC-driven model of differentiation, as OPCs differentiate without axonal presence (S. Lee et al., 2012; Mei et al., 2014; Bechler et al., 2015; Redmond et al., 2016). However, not all OPCs differentiate into oligodendrocytes *in vivo*, rendering the need for an axonal inductive signal to coordinate OPC differentiation. The observation that the oligodendrocyte numbers are not proportionally increasing with the OPC numbers, would speak to an axon-mediated initiation of OPC differentiation.

Chapter 6

Intrinsic heterogeneity of ventral and dorsal OLCs

The ablation of dorsal OPCs in early development caused a locomotor coordination defect in adult mice, most likely as a result of impaired neuronal conduction. While the mechanisms of impaired neuronal conduction can be various, one working hypothesis is that ventral and dorsal OLCs support neuronal conduction differently. Underlying this hypothesis is the assumption of an intrinsic heterogeneity of OPCs based on their developmental origin, giving rise to functionally heterogeneous OLCs. Therefore, the abnormal dominance of ventral OLCs in otherwise dorsal OLC populated areas, and vice versa, would lead to an impairment in brain function. Investigating the heterogeneity of the developmentally distinct OLC populations will show whether ventral and dorsal OLCs support neuronal conduction differently, revealing a functional importance of developmental OPC heterogeneity in adult brain function.

6.1 Ventral and dorsal OPCs have the same propensity to differentiate

To investigate whether the formation of the oligodendrocyte lineage cells derived from ventral or dorsal origin is comparable during development, a flow cytometry analysis of animals ranging from the age of P5 to 2 months was performed. In this study, OPCs were identified using PDGFR α staining, whilst MOG was used to identify mature oligodendrocytes. To label the remaining cells of the oligodendrocyte lineage, O4 antibody staining was performed, reacting with late OPCs up to mature oligodendrocytes (see Introduction, Section 1.2.1).

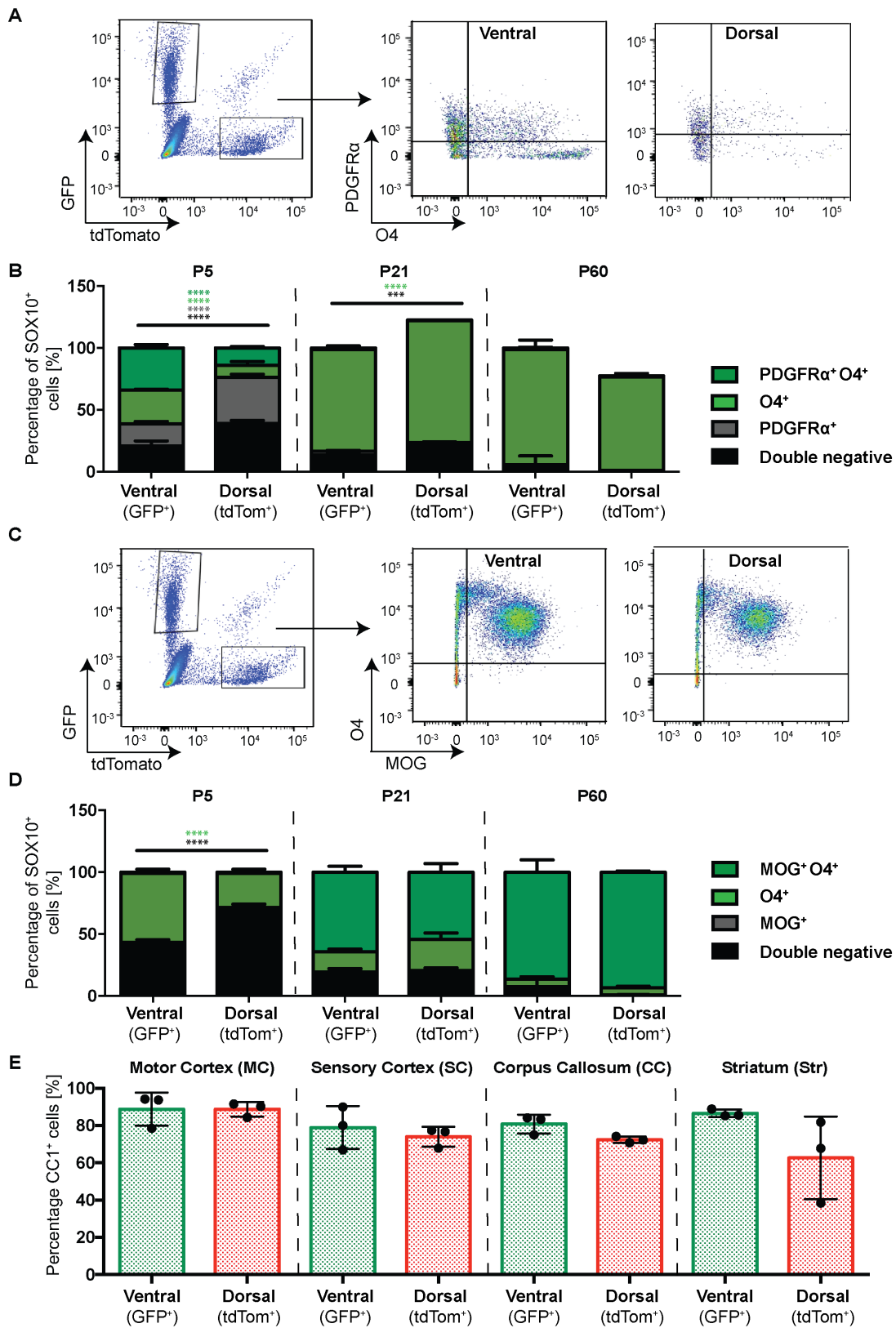


Fig. 6.1 The percentage of ventrally- and dorsally-derived oligodendrocytes is similar in the adult brain. (A-D) Flow cytometry analysis of ventral and dorsal OLC population in the adult brain. (A) Representative image of PDGFR α and O4 staining. (B) Percentage of GFP $^{+}$ (ventral) and tdTOMATO $^{+}$ (dorsal) cells (out of the total living SOX10 $^{+}$ OLCs) expressing PDGFR α and/or O4 in control and ablated animals. At P5, dorsally-derived OLCs are less differentiated as a higher percentage of cells expresses PDGFR α , but lack O4 expression (n = 6, two-way Anova, *** = p<0.001, **** = p<0.0001). (C) Representative image of O4 and MOG staining. (D) Percentage of GFP $^{+}$ (ventral) and tdTOMATO $^{+}$ (dorsal) cells (of the total living SOX10 $^{+}$ OLCs) expressing O4 and/or MOG in control and ablated animals. After an initial delay in dorsal OPC differentiation, the percentage of ventral and dorsal MOG $^{+}$ oligodendrocytes is similar in adults (n = 6, two-way Anova, **** = p<0.0001). (E) Quantification of IHC staining. Percentage of CC1 $^{+}$ GFP $^{+}$ or CC1 $^{+}$ tdTOMATO $^{+}$ oligodendrocytes (out of total SOX10 $^{+}$ cells) in control and ablated animals. Similar percentages of ventral and dorsal CC1 $^{+}$ oligodendrocytes reside in the adult brain (n = 3; MC, CC: Mann-Whitney test; SC, Str: unpaired t-test). MC = motor cortex, SC = sensory cortex, CC = corpus callosum, Str = striatum, IHC = immunohistochemistry

The intrinsic GFP or tdTOMATO fluorescence reflecting SOX10-expression was used to unambiguously identify cells of the oligodendrocyte lineage. In addition, CD11b $^{+}$ microglia have been excluded from the flow cytometry analysis to exclude false positive events due to antibody engulfment (for details of gating strategy see Chapter 3, Figure ?? A).

Early in postnatal development (postnatal day 5), oligodendrocyte lineage cells of the dorsal origin expressed significantly more PDGFR α (GFP $^{+}$ ventral OLCs: 17.8%, tdTom $^{+}$ dorsal OLCs: 37.4%) and less O4 (GFP $^{+}$ ventral OLCs: 27.3%, tdTom $^{+}$ dorsal OLCs: 9.6%) when compared to ventral OLCs, indicating that fewer dorsal OLCs were differentiated at that stage (Figure 6.1 A,B). However, at the age of 2 months no difference between the number of O4 $^{+}$ MOG $^{+}$ oligodendrocytes was detected (Figure 6.1 C,D). Therefore the initial delay in OPC differentiation might reflect the timing of OPC formation in embryonic development, with ventral OPCs arising significantly earlier than dorsal OPCs (ventral OPCs: starting at E12.5, dorsal OPCs: starting at P0 (see Introduction, Section 1.4.1)). In accordance, CC1 staining in adult brain sections revealed no difference in the percentage of mature oligodendrocytes formed by ventral or dorsal OLCs (Figure 6.1 E).

Unfortunately, the flow data can not be used to make any claims about OPCs at later developmental stages as the number of detected PDGFR α cells decreased significantly

from P21 (Figure 6.1 A). A drop in PDGFR α expression of OPCs with increasing age would explain this observation. Indeed, RNA-sequencing and proteomics analysis of purified neonatal (P0-P7), adult (2-4 months) and old (> 9months) OPCs revealed a significant decrease in PDGFR α expression (data adopted from Roey Baror and Alerie Guzman de la Fuente, members of the Franklin laboratory, University of Cambridge) (Figure 6.2 A,B).

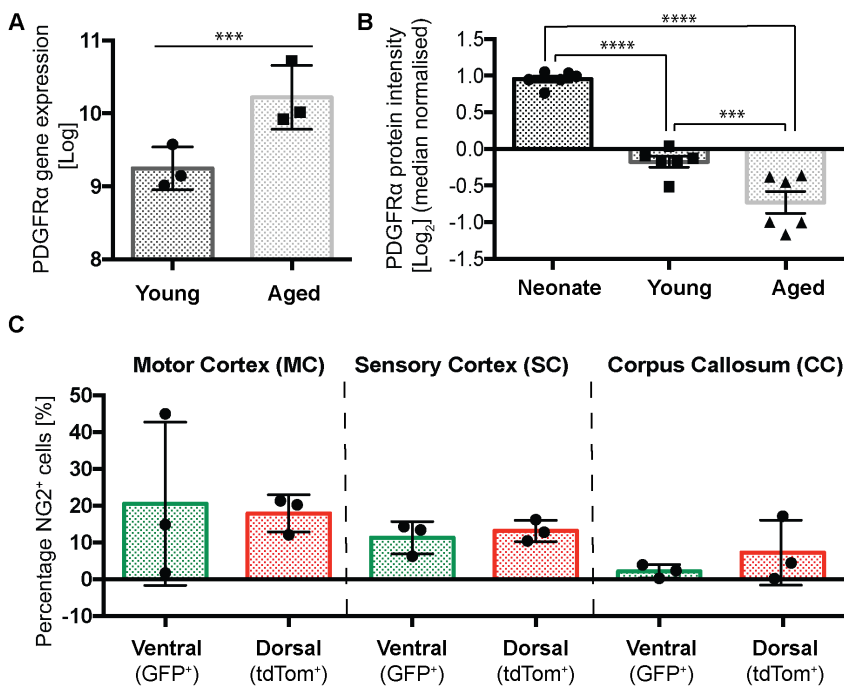


Fig. 6.2 The percentage of ventrally and dorsally derived OPCs is similar in the adult brain. (A) Amount of *Pdgfra* gene expressed in OPCs isolated from young and aged animals ($n = 3$, unpaired t-test, *** = $p < 0.001$). (B) Amount of PDGFR α protein expressed in OPCs isolated from neonatal, young and aged animals ($n = 6$, LIMMA, *** = $p < 0.001$, **** = $p < 0.0005$). (C) Quantification of IHC staining. Percentage of NG2⁺ GFP⁺ or NG2⁺ tdTOMATO⁺ (out of total SOX10⁺ cells) in *Emx/tdTom* control and *Emx/tdTom/DTA* ablated animals. Similar percentages of ventral and dorsal NG2⁺ OPCs reside in the adult brain ($n = 3$, unpaired t-test, except CC: Mann-Whitney test). CC = corpus callosum, IHC = immunohistochemistry.

In order to assess the proportion of OPCs of ventral and dorsal origin in adult animals, immunohistochemistry staining of NG2, an alternative OPC marker, was performed. As NG2 is also reactive to microglia and pericytes, only SOX10-expressing NG2⁺ cells have been counted. No difference in the proportion of NG2⁺ OPCs between the ventral and dorsal oligodendrocyte lineage was detected in the adult brain (Figure 6.2 C).

6.2 Differences in gene expression of ventral and dorsal oligodendrocytes

To uncover molecular differences of the developmentally distinct OLCs, the gene expression profile of ventral and dorsal OLCs isolated from either the motor cortex or the CC have been analysed using single cell Drop-sequencing. The preparation of the cells, the Drop-sequencing and the bioinformatic analysis were performed by Elisa Floriddia and Daniel van Brueggen (laboratory of Goncalo Castelo-Branco, Karolinska Institute, Sweden).

The clustering analysis of all GFP⁺ and tdTOMATO⁺ cells isolated from control *Emx/tdTom* and ablated *Emx/tdTom/DTA* animals revealed that, as expected, the OPCs cluster separately to the oligodendrocyte population (Figure 6.3 A,B). Focussing on the OPC population, OPCs from ventral and dorsal origins cluster together, indicating that individual cells of the ventral and dorsal origin have a similar spread of gene expression profiles (Figure 6.3 A,B). However, in the motor cortex OPCs of the two developmental origins are more separated than in the CC (Figure 6.3 A). Whether this is indicative of significant differences in gene expression needs to be investigated by further comparative gene expression analysis. In addition, OPCs isolated from the *Emx/tdTom/DTA* ablation model, are not distinguishable from the control OPCs. These observations suggest, that OPCs are a homogenous cell population with respect to their gene expression (Figure 6.3 A,B).

In comparison to the OPC population, obvious differences in the clustering of the oligodendrocyte populations can be detected. In the motor cortex seven oligodendrocyte populations (cluster 1-7, Figure 6.3 E) have been identified. One oligodendrocyte population (cluster 7) can be classified as myelin forming oligodendrocytes, whereas the gene expression profiles of the remaining oligodendrocytes is indicative of mature oligodendrocytes (classifications have been done according to (Marques et al., 2016)) (Figure 6.3 C). In control animals, five out of seven oligodendrocyte clusters are composed of cells of the ventral origin (cluster 3-7). One oligodendrocyte subpopulation (cluster 2) is comprised of cells of ventral and dorsal origin, whereas the remaining subpopulation (cluster 1) is formed by cells of the dorsal origin (Figure 6.3 E). Intriguingly, the tdTOMATO specific, dorsal oligodendrocyte clusters (cluster 1) cannot be detected in the *Emx/tdTom/DTA* ablation animals, indicating that ventral OPCs cannot form this particular oligodendrocyte populations. Instead, a population of oligodendrocytes

(cluster 3) appear, which have not been identified in control animals (Figure 6.3 E). This population shows the molecular fingerprint of both myelin-forming and mature oligodendrocytes.

In the corpus callosum a total of four oligodendrocyte populations have been detected by cluster analysis (cluster 1-4, Figure 6.3 F), most of which are mature oligodendrocytes, except for one population (cluster 3) carrying the molecular fingerprint of myelin-forming oligodendrocytes (Figure 6.3 D). In contrast to the motor cortex, dorsal and ventral OPCs generate all the oligodendrocyte subpopulations in *Emx/tdTom* control animals (cluster 4, Figure 6.3 F). Except for subpopulations (cluster 1), the majority of oligodendrocytes (cluster 2) formed in the *Emx/tdTom/DTA* ablation animals exhibit a different transcriptional profile to the *Emx/tdTom* control animals. The gene expression profile of the newly formed oligodendrocyte subpopulation (cluster 2) is reminiscent of mature oligodendrocytes, but clusters closely to newly-formed oligodendrocyte subpopulations (cluster 3) of control animals (Figure 6.3 F).

In summary, even though no difference in gene expression of OPCs was detected, ventral and dorsal oligodendrocytes form distinct subpopulations in the motor cortex, but not in the corpus callosum. In response to dorsal OPC ablation, new oligodendrocyte subpopulations appear in both brain areas which have a distinct transcriptional profile to control cells.

6.3 Ventral and dorsal oligodendrocytes form similar myelin

Neuronal conduction can be accelerated by an initial myelination, but also adjusted through alterations of the myelin structure. Consequently, the observed locomotor phenotype in response to dorsal OPCs ablation might be explained by the formation of distinct myelin structures of ventral and dorsal oligodendrocytes. Myelin sheaths formed by dorsal OPCs might be tailored to support the needs of cortical neuronal circuits, which cannot be achieved by myelination through a ventral oligodendrocyte.

The majority of the myelin sheath is composed of lipids, with a small proportion of proteins interspersed. Whilst little is known about the functional importance of individual lipids in the myelin sheath, the specific role of different myelin proteins have been studied extensively. Any changes of expression of an individual myelin protein can directly translate into a transformation of the myelin structure (see Introduction,

Section 1.2.3). To investigate the myelin protein composition of myelin sheaths formed by ventral and dorsal oligodendrocytes, western blot analysis of protein lysates extracted from whole brain samples of control or ablated mice was performed.

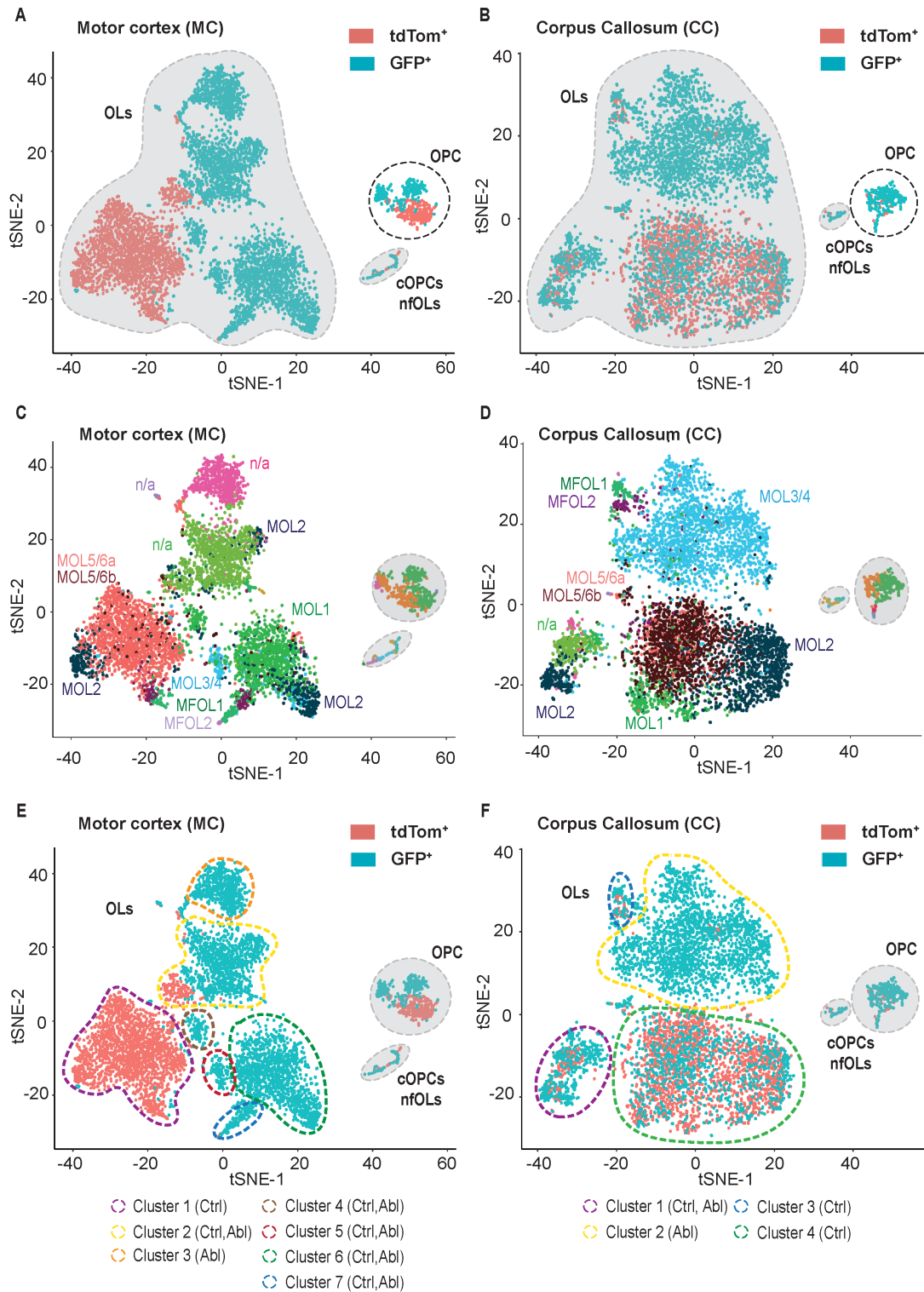


Fig. 6.3 Developmentally heterogeneous oligodendrocytes form distinct oligodendrocyte subpopulations. (A-F) Results of t-SNE gene expression cluster analysis. Each graph represents all cells isolated from control and ablated animals in the motor cortex (A,C,E) or corpus callosum (B,D,F). Each dot represents a cell analysed. (A,B) Whilst the ventral and dorsal OPC clusters show slight separation in the motor cortex, all OPCs are intermingled in the corpus callosum. Regardless of the brain area, OPCs isolated from ablated animals cannot be distinguished from control OPCs. Red = dorsally derived oligodendrocytes, blue = ventrally derived oligodendrocytes, cOPC = committed OPCs, nfMOL = newly formed oligodendrocytes, OL = oligodendrocyte. (C,D) Annotation of different oligodendrocyte populations according to the study of Marques and colleagues (Marques et al., 2016). MFOL = myelin forming oligodendrocyte, MOL = mature oligodendrocyte, n/a = not previously identified. (E) Ventrally and dorsally derived oligodendrocytes form discrete subpopulations in the motor cortex. In the ablated animals, the subpopulation formed by dorsally-derived oligodendrocytes (cluster 1) disappears, while an additionally, previously not annotated subpopulation (cluster 3) appears. (F) In control animals, the gene expression of ventral and dorsal oligodendrocytes cannot be distinguished. Following ablation, a new subpopulation formed by ventral oligodendrocytes (cluster 2) appears. (E,F) Cntr = cluster of oligodendrocytes present in *Emx/tdTom* control animals, Abl = cluster of oligodendrocytes present in *Emx/tdTom/DTA* ablated animals

Due to the high ablation efficiency (see Chapter 3, Figure ?? and Figure ??), the number of myelin sheaths formed by ventral oligodendrocytes in ablated animals is significantly higher, therefore differences between control and ablated brains should be indicative of a distinct composition of myelin structures formed by the two developmentally distinct oligodendrocyte populations. Animals with ablated of dorsal OPCs did not show any changes in the protein expression of the major myelin proteins (Figure 6.4 A,B), including between isoforms of the same protein (Figure 6.4 A,B). More specific western blot analysis of myelin proteins of FACS-sorted ventral and dorsal oligodendrocytes was not feasible due to a low cell yield from the FACS-sorting.

Electron microscopy (EM) is the gold standard technique to assess myelin sheath thickness; an important myelin characteristic in modulating neuronal conduction. By EM, fluorescence cannot be visualised rendering it difficult to distinguish between myelin sheaths formed by the developmentally distinct OLCs. Nevertheless, a potential difference in the myelin sheath thickness formed by ventral and dorsal oligodendrocytes should be measurable by EM, as the proportion of ventrally derived oligodendrocytes is much higher in the corpus callosum of ablated compared to control animals. The CC has been chosen for EM analysis, because it is the only fully myelinated brain area populated by dorsal OLCs in the control animals. Following the

evaluation of more than 400 axons per genotype, there was no difference in the g-ratio between control and ablated animals (Figure 6.4 C,D).

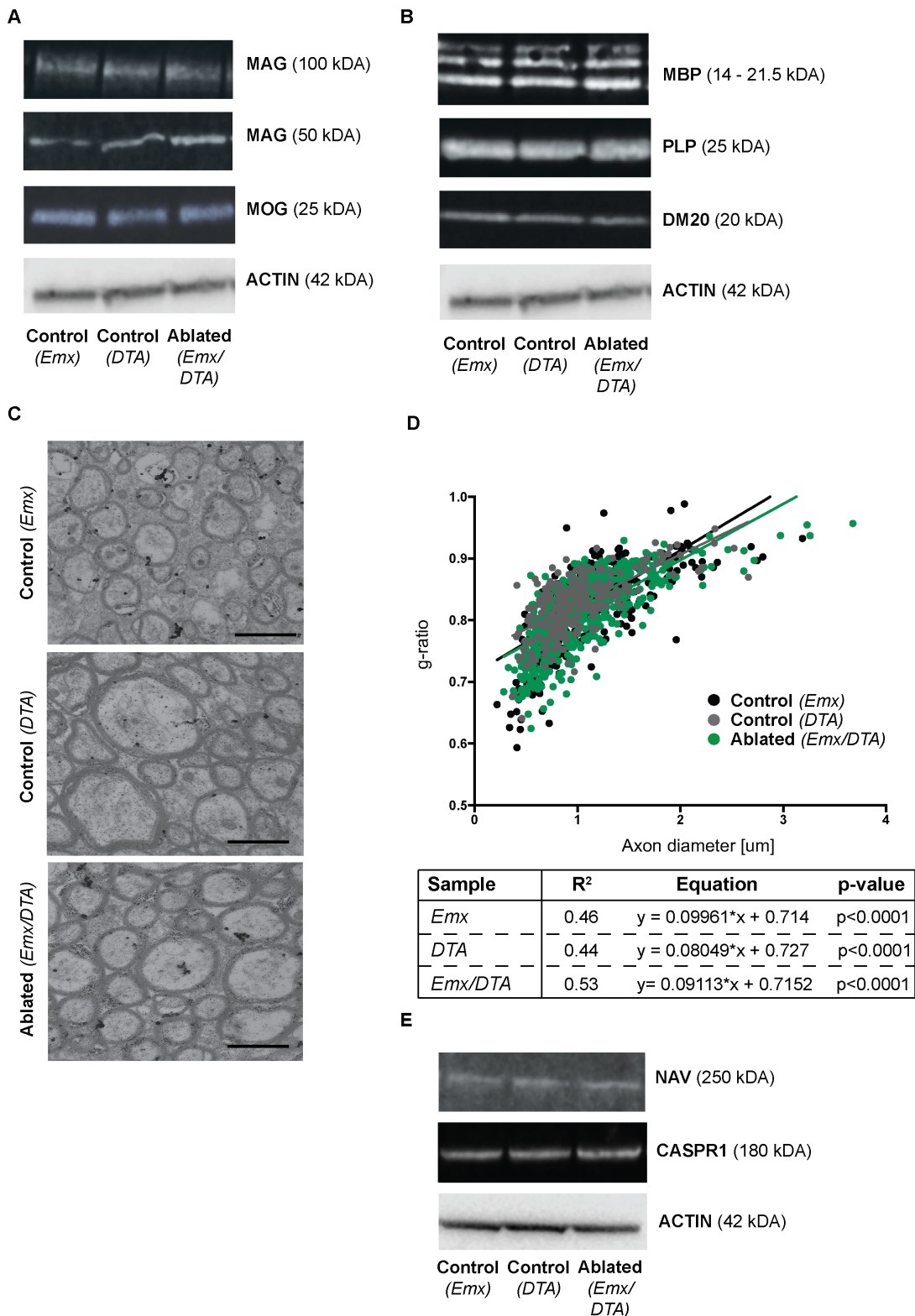


Fig. 6.4 Ventral and dorsal oligodendrocytes form similar myelin. (A,B) Western blot analysis of myelin proteins of whole brain samples. No difference in myelin protein expression was detected between control and ablated animals ($n = 3$, One-way Anova). (C) Representative corpus callosum images of electron microscopy. (D) Electron microscopy was quantified by calculating the g-ratio (ratio of axon diameter to myelin sheath diameter). Axons did not exhibit a difference in g-ratio between control and ablated animals ($n = 3$, One-way Anova). (E) Western blot analysis of nodal/paranodal proteins. No difference in nodal/paranodal protein expression was detected between control and ablated animals. Scale bar = $2\mu\text{m}$.

In addition, the amount of sodium channels (Nav⁺-channel) and contactin-associated protein 1 (CASPR1) was measured in whole brain protein lysate as an approximation of the myelin sheath length. As the amount of paranodal proteins is proportional to the number of nodes and the amount of sodium channels is proportional to nodal length (Rios et al., 2003), changes in the nodal structure will be reflected in the amount of nodal/paranodal proteins. Western blot analysis showed no difference in the amount of total Nav⁺-channel and CASPR1 protein in ablated versus control animals, indicating that ventral and dorsal oligodendrocytes do not form myelin sheaths of different lengths (6.4 E). However, more specific *in vitro* assays designed to assess myelin sheath length need to be performed.

6.4 Ventral and dorsal oligodendrocytes form similar nodal structures

There is compelling evidence that small changes in nodal length can cause significant changes to neuronal conduction, resulting in locomotor disabilities (Schneider et al., 2016; Arancibia-Cárcamo et al., 2017). The paranodal area, the junction of myelin sheath and node of Ranvier, is marked by the expression of specific proteins, including CASPR1. Therefore, measuring the distance between two closely adjacent CASPR1 expression spots along one axon gives a good approximation of the nodal distance. Imaging the dense network of axons and myelin sheaths at high resolution was achieved by using structural interference microscopy (SIM) (carried out by Marcus Fantham, laboratory of Prof Clemens Kaminski, Department of Chemical Engineering and Biotechnology, University of Cambridge) (Figure 6.5 A).

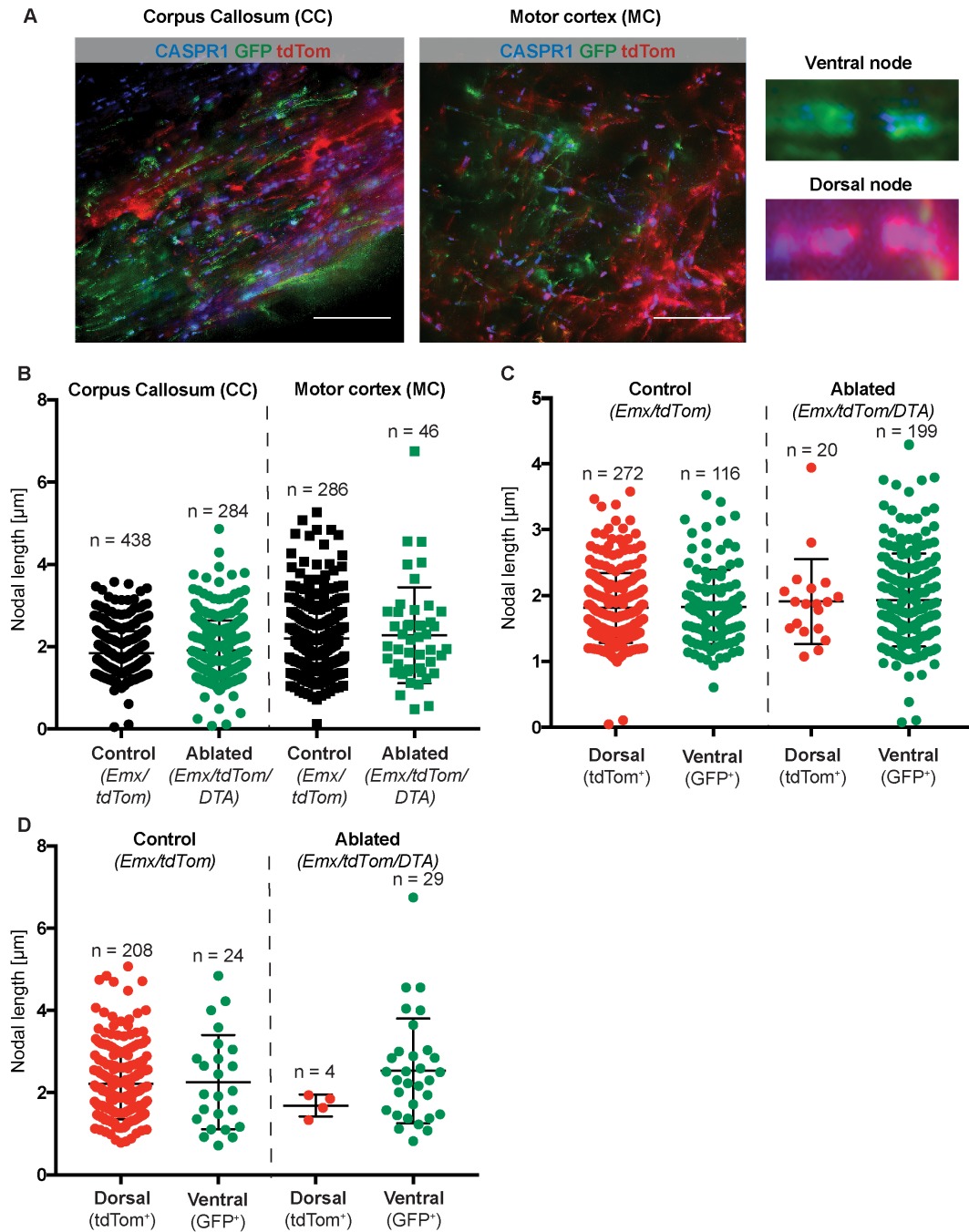


Fig. 6.5 Ventral and dorsal oligodendrocytes form similar nodal structures. (A) Representative images of the corpus callosum and the motor cortex using structural interference microscopy. Magnified images of an example of a node of Ranvier formed by ventral or dorsal oligodendrocytes is depicted. (B-D) Quantification of nodal length by measuring the distance of CASPR1 spots along one axon. (B) No difference in the average nodal length in control and ablated animals was detected ($n = 3$, one-way Anova). (C,D) Ventral and dorsal oligodendrocytes form nodes with similar length in the corpus callosum (C) and motor cortex (D) of both control and ablated animals ($n = 3$, one-way Anova). Scale bar = $20\mu\text{m}$.

Careful measurement of the length of individual nodes showed that the average nodal length in the corpus callosum is $1.84\mu\text{m}$ in control animals and $1.9\mu\text{m}$ in ablated animals. Similarly, in the motor cortex the average length of the nodes of Ranvier is $2.2\mu\text{m}$ in control in comparison to $2.3\mu\text{m}$ in ablated animals, indicating that there is no significant difference in the nodal length between the animal groups, nor between brain areas (Figure 6.5 B). Furthermore, splitting the data into nodes encompassed by either two ventral or two dorsal myelin sheaths along one axon did not reveal any difference in the corpus callosum (Figure 6.5 C) or motor cortex (Figure 6.5 D).

6.5 Conclusion and discussion chapter 6

Since the discovery of the distinct developmental origin of OPCs (Kessaris et al., 2006), the question of whether ventral and dorsal OPCs, and their progeny, are heterogeneous cell populations remains unanswered. In order to investigate differences in the gene expression of ventral and dorsal OLCs, single cell Drop-sequencing was carried out. Whilst clustering analysis of the gene expression data showed no obvious difference between ventral and dorsal OPCs, distinct oligodendrocyte clusters dependent on the developmental origin were identified (Figure 6.3), indicating a heterogeneity in the oligodendrocyte population. The gene expression analysis further revealed that not all oligodendrocyte subpopulations of control animals can be formed in ablated animals, suggesting that ventral OPCs cannot fully compensate for the ablation of dorsal OPCs. For a detailed discussion of the RNA-sequencing results with respect to the OLCs heterogeneity see discussion (see Discussion, Section 7.2). The lack of compensation by ventral OPCs might explain the locomotor phenotype observed in dorsal ablated animals (see Chapter 3). Establishing a list of differentially expressed genes of the ventral and dorsal oligodendrocyte subpopulations might help to uncover the mechanism of the locomotor phenotype defects in the ablated animals.

Simultaneously to the investigation of the molecular heterogeneity, a difference at the cellular level of the developmentally distinct oligodendrocytes was assessed. As the locomotor phenotype is most likely caused by an abnormal conduction or transmission of action potentials, and the myelin sheath is playing an important role in neuronal conduction, various characteristics of myelin sheaths formed by ventral or dorsal oligodendrocytes were compared. The analysis of the thickness of ventral and dorsal formed myelin sheaths showed no difference in the corpus callosum. However, the cortex was not studied, and hence differences may arise here. Furthermore, no

differences in the amount of myelin proteins between control and ablated animals was detected, indicating that ventral and dorsal myelin sheaths are composed of the same proportion of the distinct myelin proteins. However, small differences in the expression of myelin sheath proteins might be masked in the western blot experiment because the analysis was performed with whole brain protein lysates based on the assumption that in ablated animals significantly more myelin sheaths are formed by ventral oligodendrocytes. A better experimental approach would be to analyse the protein expression of isolated ventral and dorsal oligodendrocytes. However, as the cell yield of the FACS sorting was low, western blot analysis of such samples was not possible. Comparative gene expression analysis of ventral and dorsal oligodendrocytes will help to identify differences in myelin genes in ventral and dorsal oligodendrocytes.

The assessment of nodal/paranodal proteins further indicated that the length of ventral and dorsal myelin sheaths is similar. Again it should be emphasised that the western blot analysis of nodal/paranodal proteins is only an approximate measurement and is not direct indication of myelin sheath length. The high density of myelin sheaths in the brain makes the *in vivo* measurement of the myelin sheath length extremely challenging (Figure 6.5). *In vitro* assays designed to measure myelin sheath length (eg. Nanofibre assay) need to be performed to provide a definitive answer to whether ventral and dorsal oligodendrocytes form myelin sheaths with distinct properties. In addition, similar to the western blot experiment with myelin proteins, the shift towards myelination by ventral oligodendrocytes in ablated animals compared to control animals might not be significant enough to detect morphological changes.

Besides modulating myelin sheath properties, oligodendrocytes might also modulate neuronal conduction by altering the nodal lengths. The analysis of nodal length formed by either two oligodendrocytes of ventral or dorsal origin revealed no difference. However, a variety up to 40% of the measurements within a biological replicate was observed. This great variety across multiple axons within one brain area has been observed before, and most likely represents a way of fine tuning neuronal conduction independent of the axon diameter (Arancibia-Cárcamo et al., 2017).

In summary, the results presented in this chapter indicate that ventral and dorsal oligodendrocytes are heterogeneous, but how this heterogeneity is manifested in oligodendrocyte function or myelin sheath morphology has not yet been identified. No evidence of a difference in myelin sheath or nodal properties formed by ventral and dorsal oligodendrocytes was found. A full discussion of the hypothesis that ventral

and dorsal oligodendrocytes form different myelin sheaths and its influence on the locomotor phenotype can be found in the discussion chapter (see Discussion, Section 7.4).

Chapter 7

Discussion

7.1 Importance of studying OLC heterogeneity

Oligodendrocytes play key roles in shaping the CNS environment, actively supporting neuronal function through the modulation of neuronal conduction, neurotransmission and by providing neurotrophic support. OPCs are stem cells in the CNS, capable of forming oligodendrocytes both in development and adulthood. The generation of newly formed oligodendrocytes in adulthood has been shown to be crucial for learning and regeneration (Liu et al., 2012; McKenzie et al., 2014; Franklin & Goldman, 2015). But do OPCs and oligodendrocytes also support brain function in other ways? Do functional subpopulations of OPCs or oligodendrocytes exist? Studying the heterogeneity of the OLCs can reveal new functions of both OPC and oligodendrocyte populations in the CNS. Due to the importance of OLCs to neuronal function, it is not a surprise that primary defects in the OLCs lead to different neurodegenerative and psychiatric diseases. Understanding the underlying cause of disease development, including the basic biology of the hierarchy and heterogeneity of the oligodendrocyte lineage cells, is pivotal to develop treatment strategies.

Heterogeneity in this context describes the observation that a single cell type is distinctly non-uniform with respect to its molecular and/or cellular characteristics, including gene/protein expression, metabolism, morphology, proliferation potential, differentiation potential, motility, and regenerative potential. The gold standard to unambiguously identify heterogeneous populations of a cell type is the proof of functional differences *in vivo*. This should not be confused with the identification of cells at different cell states within a cell population, or cells captured at different points along a linear differentiation/maturation path.

There are two types of heterogeneity that are distinguishable. Extrinsic heterogeneity describes the heterogeneity of a cell population in response to exposure to different environmental signals, eventually resulting in different functions of the cell populations *in vivo*. This definition implies that extrinsically heterogeneous cells would behave similarly when put in an identical environment. In contrast, cells that are intrinsically heterogeneous will exhibit different functional behaviour even in an identical environment. Intrinsic heterogeneity must be hard-wired in the gene expression profile causing different cellular behaviour. As intrinsic heterogeneity is established due to different extrinsic signals, the definition of intrinsic and extrinsic heterogeneity can be blurry. Intrinsic and extrinsic heterogeneity of a cell population are also not mutually exclusive. The mechanism by which an extrinsic heterogeneity transitions to an intrinsic heterogeneity is not fully understood. Will every extrinsic heterogeneity eventually manifest itself in intrinsic heterogeneity?

In the oligodendrocyte lineage, both OPCs and oligodendrocytes can obtain heterogeneity by residing in different environments (extrinsic heterogeneity). Due to the specification of OPCs in different domains of the developing CNS, in which different transcription factor networks are predominant, OPCs have the potential to also acquire intrinsic heterogeneity. In contrast, as oligodendrocytes undergo limited migration and so reside in the same location in the CNS parenchyma, only a local change in the brain environment can cause the acquisition of intrinsic heterogeneity of oligodendrocytes within one brain area. As the local environment can differ for instance due to the heterogeneity of other CNS cell types or the presence of blood vessels, oligodendrocytes are theoretically capable of the acquisition of intrinsic heterogeneity itself. But can a fully differentiated cells acquire long-lasting gene expression changes which still persist when the environment changes? The scenario of acquisition of intrinsic oligodendrocyte heterogeneity does not exclude the possibility that oligodendrocytes can also inherit intrinsic heterogeneity from the OPC.

Distinguishing the two types of heterogeneity is crucial to understanding the importance of lineage hierarchy and thereby the layers of regulation to establish complex organ function. In addition, for disease treatment the discrimination of intrinsic and extrinsic heterogeneity is important as it allows predictions to be made about the cellular response to a treatment option. Extrinsically heterogeneous cells should behave similarly to a treatment, whereas intrinsically heterogeneous cell populations are likely to respond differently due to their distinct expression profiles. The type of functional

heterogeneity also matters in light of cell transplantation treatments, as a specific function carried out by an intrinsically heterogeneous cell population most likely cannot be taken over by the remaining cell population(s).

7.2 Heterogeneity of the oligodendrocyte lineage

7.2.1 Ventral and dorsal oligodendrocytes are functionally heterogeneous

The discovery of the distinct developmental origin of OPCs raised the question of whether ventrally and dorsally derived OPCs are intrinsically heterogeneous, thereby fulfilling different functions in the CNS. Multiple observations from the literature speak for the argument that the developmental origin of OPCs determines their function in the brain: (1) In the adult brain, the developmentally distinct OPC populations show a particular distribution pattern, with dorsal OPCs almost exclusively restricted to the dorsal areas of the telencephalon (eg. cortex and CC) (Kessaris et al., 2006), (2) Ventral and dorsal OPCs need different molecular cues for specification (Cai et al., 2005; Chandran et al., 2003; Vallstedt et al., 2005; Langseth et al., 2010) and (3) A block of dorsal OPCs differentiation caused a reduction in myelination in the dorsal telencephalon (Yue et al., 2006) (see Introduction, Section 1.4.1). However, the functional heterogeneity of ventral and dorsal OPCs has not been convincingly proven in the adult brain so far, with the exception of an injury model. In response to a demyelinating insult, dorsal OPCs show a more pronounced response when compared to ventral OPCs, demonstrating a functional heterogeneity of the two developmentally distinct OPC populations in a disease context (Crawford et al., 2016).

In order to investigate the functional importance of the developmental origin of OLCs on physiological brain function, dorsal OPCs have been ablated using a transgenic mouse model. Careful phenotypic analysis of animals ablated of dorsal OLCs revealed abnormalities in their locomotor coordination. Single cell RNA-sequencing showed that ventrally and dorsally derived oligodendrocytes form distinct subpopulations in the motor cortex, but not in the corpus callosum. Intriguingly, according to the annotation by Marques and colleagues dorsally derived oligodendrocytes give rise to similar OL subpopulations (MOL2, MOL5, MOL6) in the motor cortex and the corpus callosum (Marques et al., 2016). In addition, OL subpopulations with the

gene expression profile of dorsally derived oligodendrocytes cannot be formed after ablation of the dorsal OPCs, which is compensated for by either the formation of a new or a ventrally derived control OL subpopulation. This demonstrates that ventral OPCs cannot functionally compensate for the lack of dorsal OPCs. The combination of gene expression analysis and motor functional testing demonstrate an intrinsic heterogeneity of developmentally distinct OLs, which is important for physiological brain function.

Furthermore, differences in the number of oligodendrocyte clusters were identified between the corpus callosum and the cortex. As the extrinsic environment in white and grey matter is anticipated to be different due to distinct proportions of cell types (eg. more neuronal cell bodies in the cortex) and cellular processes (eg. axonal conduction versus synaptic transmission of electrical signals in the corpus callosum versus the cortex, respectively), the identification of an additional extrinsic heterogeneity was expected. What might be the role of the oligodendrocyte heterogeneity between the corpus callosum and the cortex? In contrast to the white matter, lots of grey matter axons are not, or are only partially myelinated. Thus, OLs might fulfil additional functions in the cortex, rather than only myelination.

7.2.2 How do developmentally distinct oligodendrocytes acquire intrinsic heterogeneity?

Single-cell RNA sequencing uncovered a heterogeneity of ventrally and dorsally derived oligodendrocytes. In contrast, the developmental origin of the OPCs was not reflected in their gene expression profile, indicating that OPCs are a more homogenous cell population. However, gene expression analysis cannot reveal information about the epigenome or splicing. Indeed, ventral and dorsal OPCs might exhibit a distinct epigenetic priming which only becomes apparent once they differentiate into an oligodendrocyte.

Alternatively, developmentally distinct oligodendrocytes might acquire the intrinsic heterogeneity once fully differentiated. In this case ventral and dorsal oligodendrocytes would need to be exposed to distinct environmental cues, for example by specific neuron-oligodendrocyte interaction. But due to the mosaic distribution of the developmentally distinct oligodendrocytes in the brain parenchyma, this scenario is unlikely.

7.3 Functional heterogeneity of other cell lineages in the brain

7.3.1 Heterogeneity of astrocytes

In the mouse embryo, astrocytes are generated from radial glial cells in distinct regions in the ventricular zone of the spinal cord and brain. According to their developmental origin, astrocytes localise into zones in the adult mouse CNS (Tsai et al., 2012). Additionally, neuronal signals refine the regional features of astrocytes to generate highly specialised neuron-glia units in specific neuronal networks. Such region-specific astrocyte functions are required for the maintenance of CNS homeostasis and neuronal survival, as shown by depletion of region-specific astrocytes in the ventral spinal cord resulting in abnormal neuron synaptogenesis which could not be rescued by the migration of adjacent astrocytes (Tsai et al., 2012). Furthermore, astrocytes carry out important roles in the feeding behaviour and metabolic control in the hypothalamus, circadian rhythm regulation and neuron homeostasis. As an example, semaphorine 3a secreted by ventral astrocytes was shown to be required for proper motor and sensory neuron circuit development (Molofsky et al., 2014). Therefore, functional heterogeneity within the astrocyte population exists, and the basis of the heterogeneity is the developmental origin. However, in comparison to the oligodendrocyte lineage, no astrocyte precursor cell has been identified yet. Whether an astrocyte precursor cell is essential for the maintenance of the astrocyte lineage is questionable, as even differentiated astrocytes are capable of proliferation, therefore rendering a stem cell population unnecessary. Therefore, in the case of astrocytes, it cannot be said that stem cell heterogeneity leads to the functional diversity of astrocytes.

7.3.2 Heterogeneity of neurons

In the ventricular zone, radial glial cells can either directly differentiate into neurons or give rise to neuronal progenitor cells, which are capable of self-renewal and differentiation into neurons. Based on the complex expression network of transcription factors in distinct ventricular zone domains, the regional identity of the new-born neurons is specified, and particularly their mode of neurotransmission and general morphology. For example, in the ventral forebrain ventral morphogen signals (such as SHH) activate the expression of ASCL1 resulting in the formation of GABAergic interneurons. In contrast, glutamatergic projection neurons are specified from radial glial cells of the cortex by the activation of WNT/BMP pathway induced dorsal transcription factors (Martyanova,

Drechsel, & Guillemot, 2012). GABAergic interneurons and glutamatergic projection neurons have distinct morphology and function, demonstrating a functional heterogeneity of the neuronal cell population *in vivo*. Therefore, the functional heterogeneity based on the developmental origin of neurons is reminiscent of the oligodendrocyte lineage heterogeneity.

7.3.3 Common developmental origin of neurons and glia cells

The developmental origin as an underlying determinant of functional heterogeneity is common to all main cell types originating in the brain. This might be explained by the developmental origin collectively shared by oligodendrocytes, astrocytes and a subset of neurons. Early in development, neuroepithelial cells differentiate into basal progenitor cells, giving rise to most of the neurons in the ventral telencephalon, and the radial glial cells. Dorsal telencephalon neurons as well as all astrocytes and oligodendrocytes in the developing CNS are derived from radial glial cells residing in the neuroepithelium of the ventricular zone.

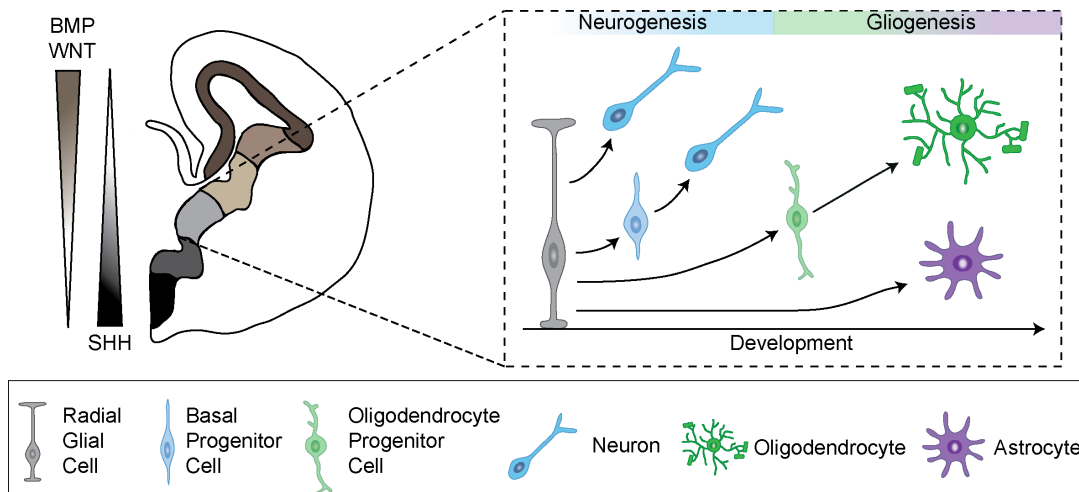


Fig. 7.1 Schematic representation of neurogenesis and gliogenesis in embryonic progenitor zones. In development, neurons, astrocytes and oligodendrocytes develop from a common progenitor population, called radial glial cells. Initially, radial glial cells give rise to neurons, before they switch their fate to gliogenesis, thereafter producing astrocytes and oligodendrocytes. The radial glial cells reside in the ventricular zone, which is organised into different domains based on distinct transcription factor expression governed by morphogens (SHH, BMP, FGF). Amongst others, the organisation of the ventricular zone into different subdomains facilitates the emergence of neuron and glia heterogeneity.

During embryonic development, radial glial cells initially give rise to multiple waves of neurons, before their fate switches to gliogenesis, generating astrocytes and oligodendrocytes (Figure 7.1). Organising signals such as SHH, BMP and FGF, create regional domains in the ventricular zone. Consequently, each ventricular zone domain has a regional-identity defined by the expression of a specific set of transcription factors, leading to the formation of distinct neuron and glia subpopulations based on their developmental origin (Figure 7.1) (reviewed in: (Rowitch & Kriegstein, 2010)).

7.4 Does the heterogeneity of developmentally distinct oligodendrocytes cause the locomotor phenotype?

Stimulation of upper motor neurons, originating in the primary motor cortex, are crucial for the initiation and transmission of information for motor movement. Likewise, commissural neurons in the corpus callosum have been shown to be important in the coordination of asymmetric motor movement. However, to what extent the projection neurons in the corpus callosum are involved in the performance of the locomotor task is difficult to judge. Abnormal neuronal conduction or transmission is most likely the cause for the impairment of locomotor coordination observed in ablated animals. Through myelination, oligodendrocytes can significantly influence neuronal conduction in the brain. Therefore, a change in myelination in the brain may cause the locomotor coordination defects in the animals ablated of dorsal OPCs.

According to the single cell RNA-sequencing results, OL subpopulations resembling dorsally derived oligodendrocytes in the control animals cannot be formed in ablated animals. Instead, the brain of ablated animals is populated by a mix of new and ventrally derived control OL subpopulations. But what is the physiological role of the dorsal oligodendrocytes? Whilst the functions of oligodendrocytes in the brain is multifaceted, the following hypothesis could explain the reason why the absence of a single oligodendrocyte population leads to alterations in neuronal conduction (Figure 7.2):

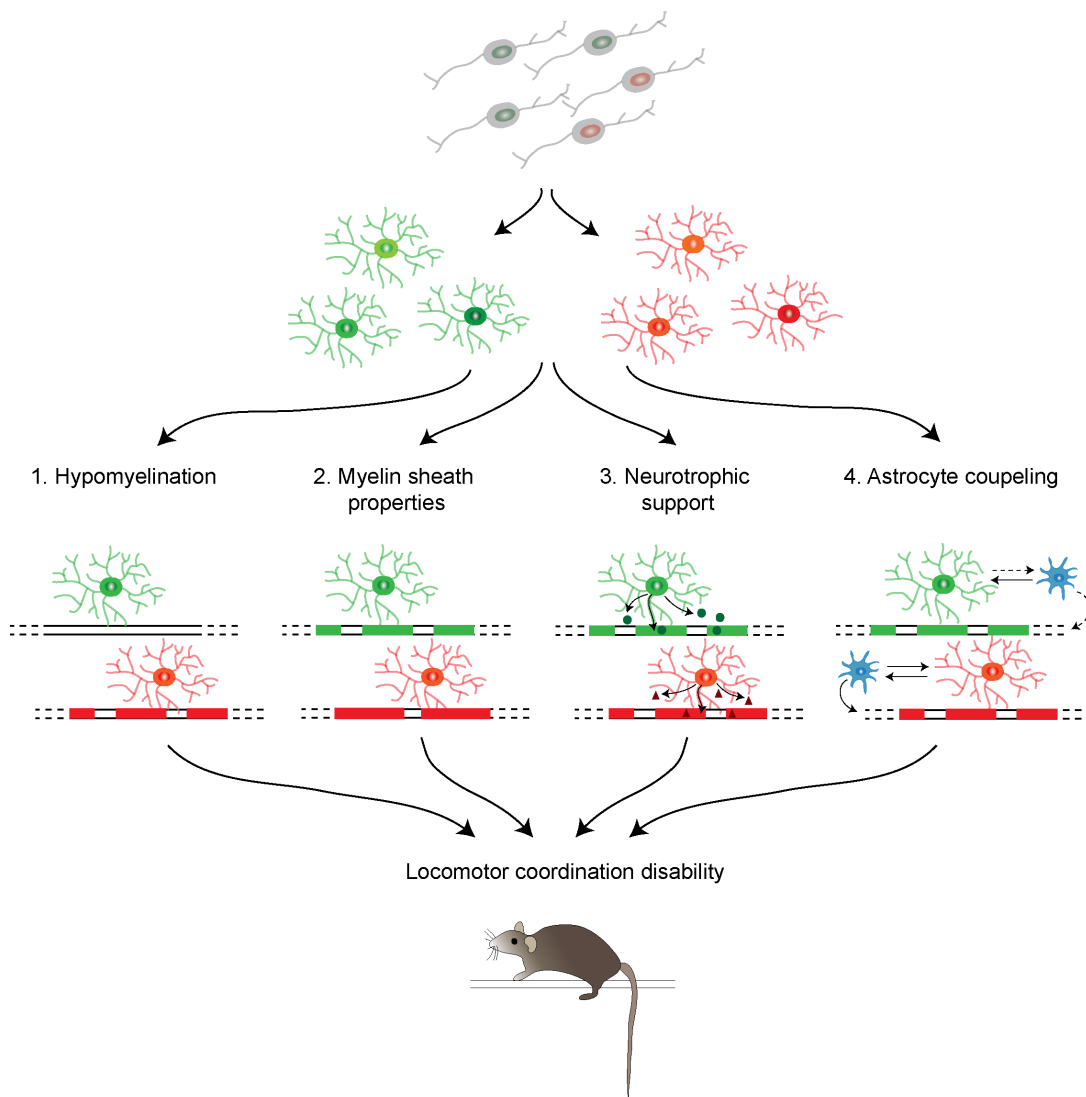


Fig. 7.2 Functional importance of OLCs heterogeneity in physiological brain function. In the adult brain, OL subpopulations can be distinguished based on their developmental origin. Whilst the specific function of exclusively dorsally derived oligodendrocytes needs to be assessed, multiple hypotheses exist: (1) In a particular environment, only dorsal oligodendrocytes can myelinate axons, (2) Ventral and dorsal oligodendrocytes give rise to myelin sheaths with different properties, (3) Ventral and dorsal oligodendrocytes exhibit a distinct mode of axonal support or (4) Ventral and dorsal oligodendrocytes differently communicate with astrocytes, which in turn are important in neuronal support. Regardless of the nature of the functional difference between ventral and dorsal oligodendrocyte subpopulations, dorsal oligodendrocyte subpopulations are crucial for homeostatic brain function. In the absence of dorsal OPCs, ventral OPCs are not capable of forming dorsal oligodendrocyte subpopulations, resulting in a locomotor disability in the ablated animals.

1. Hypothesis: The ablation of dorsal OPCs causes reduced myelination in the motor cortex.

The main function of the myelin sheath wrapped around axons by oligodendrocytes is the acceleration of neuronal conduction. Therefore a lack of myelination causes a significant reduction in neuronal conduction speed, which can lead to abnormalities in locomotor coordination.

In favour of this hypothesis are the observations that (1) the number of nodes of Ranvier (see Chapter 6, Figure 6.5) and (2) the number of SMI32⁺ neurons are decreased in the motor cortex of ablated animals (see Chapter 4, Figure 4.2). SMI32 antibody staining labels unphosphorylated epitopes of the neurofilament heavy chain. In the peripheral nervous system, a reduction in neurofilament phosphorylation has been correlated with demyelination. By comparing myelinated and unmyelinated axons it was discovered that myelination increases the number of neurofilaments and their phosphorylation, and vice versa (de Waegh, Lee, & Brady, 1992; Hsieh et al., 1994; Dashiell, Tanner, Pant, & Quarles, 2002). The existence of an additional pre-myelinating oligodendrocyte population in the motor cortex of ablated animals, while the total numbers of oligodendrocytes is not significantly different between control and ablated animals, hints towards a hypomyelination, thereby further supporting the hypothesis. Why some of the ventral OPCs appear to get stalled along their differentiation pathway in ablated animals remains to be elucidated. It is conceivable that ventral OPCs are not capable of responding to some environmental factors in the cortex, therefore arresting in differentiation. Alternatively, the pre-myelinating oligodendrocyte population could also account for newly-formed oligodendrocytes needed for myelin plasticity. However, as control and ablated animals show similar numbers of oligodendrocytes and are housed in the same environment, it is unlikely that only ablated animals need an additional pre-myelinating oligodendrocyte population.

Magnetic resonance imaging did not reveal the predicted hypomyelination in the motor cortex. However, investigating the level of myelination in the grey matter is complicated by multiple factors. Firstly, not all axons are myelinated in the grey matter and grey matter axons are often only partially myelinated. As the reason for axon selection for myelination is unknown, it cannot be assumed that the myelination is similar between different brain areas and animals. Secondly, as it was found that myelination in adulthood is experience-dependent, the degree of myelination between different animals might vary, depending on their exposure to environmental factors. However, this should be comparable between litter mates. As the identification of a specific cortical area is difficult, an analysis of the whole cortex should be performed.

For instance using light sheet microscopy to efficiently image whole cortices stained for MBP or luxol-fast-blue is an effective method to investigate the myelination level of the motor cortex. Furthermore, immunohistochemistry and flow cytometry analysis for the oligodendrocyte markers CC1 and MOG did not show differences in oligodendrocyte populations between control and ablated animals, as even the less differentiated oligodendrocytes in the ablated animals express CC1 and MOG.

Why would the lack of dorsal OL populations cause reduced myelination and why can this not be compensated for by ventrally derived OL populations? The total number of oligodendrocytes is similar between control and ablated animals, thus excluding the possibility that a simple lack of oligodendrocytes exists after dorsal OPC ablation. Instead, potentially, different OL populations are tailored to support different neuronal subtypes. Thus, secreted factors from distinct neuronal subtypes might specifically induce the differentiation/myelination of the suitable oligodendrocyte populations. As ventral oligodendrocytes have a different gene expression profile, they potentially are unable to respond to the differentiation/myelination signal.

This hypothesis is unlikely to be applicable to the corpus callosum as (1) no hypomyelination was detected and (2) mature oligodendrocytes are residing in the corpus callosum of ablated animals. Nevertheless, a change in neuronal conduction or transmission of motor neurons in the motor cortex may be sufficient to cause abnormalities in locomotor coordination.

2. Hypothesis: Dorsal oligodendrocytes form myelin sheaths with different properties.

The myelin sheath properties as well as node of Ranvier length are important modulators of neuronal conduction, alterations of either could lead to the locomotor phenotype observed in dorsal OPC ablated animals. Potentially, dorsally-derived oligodendrocytes form myelin sheaths with properties that are more adapted to the needs of neuronal circuits located in the dorsal part of the brain. Indeed, the comparison of the myelin sheath properties showed that different neuronal subtypes exhibit a particular pattern of myelination (Micheva et al., 2016)

Analysis of the myelin thickness using EM did not reveal any difference between myelin sheaths formed by ventrally- or dorsally-derived oligodendrocytes in the corpus callosum (see Chapter 6, Figure 6.4). In addition, the nodal length formed either between two ventral or two dorsal derived myelin sheaths was not significantly different.

Accordingly, the nodal length did not change after the ablation of the dorsal OPCs (see Chapter 6, Figure 6.5). Furthermore, western blot analysis of nodal proteins, as an approximation of myelin sheath length, did not show any difference between control and ablated animals (see Chapter 6, Figure 6.4). To confidently state that myelin sheaths formed by ventral and dorsal analysis are indistinguishable, the myelin sheath length needs to be determined. Whilst a nanofibre myelination assay or a oligodendrocyte-neuron co-culture would be most suitable to study myelin sheath length *in vitro*, determining the myelin sheath length *in vivo* is complicated by the density of myelinated fibers in the brain. Because of its lower density of myelinated fibres, any grey matter area is the most suitable starting area.

The hypothesis, that the developmental origin of oligodendrocytes is a determinant of myelin sheath properties, assumes the primary role of oligodendrocytes in determining myelin sheath properties. However, in the current literature, whether the oligodendrocyte or the axon itself regulates myelin sheath thickness and length are still discussed. The strong correlation between myelin sheath thickness and axon diameter was uncovered about 50 years ago (Williams & Wendell-Smith, 1971), indicating that the axon determines the thickness of the myelin sheath. The situation is not so clear for the myelin sheath length. Contradictory results on the correlation of the axon diameter and the myelin sheath length are published (Murray & Blakemore, 1980; Ibrahim, Butt, & Berry, 1995; Ford et al., 2015), leaving an open question as to whether axon diameter and myelin sheath length are proportional. Neuronal signals, including glutamate and GABA, were also shown to negatively correlate with myelin length (Etxeberria et al., 2016; N. B. Hamilton et al., 2017). In addition, regardless of the brain area, the myelin sheath length formed by a single oligodendrocyte varied considerably (Chong et al., 2012), indicating an adaption of each myelin sheath to the needs of the axon. Further studies contradicted these findings, showing that determinants of the myelin sheath length are the regional identity and the density of oligodendrocytes, at least in *in vitro* experiments (Chong et al., 2012; Bechler et al., 2015). Together, these observations indicate that the myelin sheath length is determined by a combination of oligodendrocyte and axon contribution, rendering it possible that the developmental origin of oligodendrocytes determines myelin sheath length. However, great variation in the myelin sheath length per oligodendrocyte in one brain area was noted (Chong et al., 2012), which can only be explained if subpopulations of oligodendrocytes of either developmental origin give rise to myelin sheaths with a distinct length.

3. Hypothesis: Neurotrophic support provided by dorsal oligodendrocytes is

needed for cortical neuronal circuits.

Oligodendrocytes have been shown to support neuronal survival by the provision of nutrients (eg. lactate) as well as survival and growth factors (see Section 1.2.3). Consequently, different neuronal networks might not only require specific adaptation of the conduction speed through myelination, but also might require the supply of distinct neurotrophic factors. It is conceivable that these special needs are facilitated by oligodendrocyte heterogeneity.

An insufficient neurotrophic support of motor cortical neurons in the ablated animals would be an alternative explanation of the trend in altered SMI32 staining (see Chapter 4, Figure 4.2), indicating altered neurofilament heavy chain (NF-H) phosphorylation. The phosphorylation of neurofilaments has been shown to regulate axon calibre and neurofilament transport. Excessive phosphorylation of NF-H leads to their accumulation in the cell body, a common indicator of neurodegenerative diseases (Rudrabhatla, Jaffe, & Pant, 2011). What consequences a decreased phosphorylation of neurofilaments has on neuronal function remains to be elucidated. In the ablated animals, no signs of neuronal cell death have been detected (no reduction of NeuN⁺ cells, no microglial activation), arguing that changes in the phosphorylation of NF-H do not lead to neuronal cell death (see Chapter 4, Section 4.1). Certainly, a reduction in axon calibre due to decreased phosphorylation will reduce conduction speed along the axon. The state of axonal damage should be investigated in more detail by assessing morphological axon characteristics, including the presence of varicosities and spheroid structures, and the presence of amyloid precursor protein (APP). How the neurotrophic support of ventral and dorsal oligodendrocytes, and its subpopulations, might differ will become clear after careful comparative gene expression analysis of ventral and dorsal oligodendrocytes, specifically the dorsal oligodendrocyte population absent in ablated animals.

In general, there is still a debate on the importance of neurotrophic support from oligodendrocytes. Whilst neuronal cell death in response to the knockout of major myelin proteins (eg. CNP and PLP) was attributed to a lack of nutrient supply, no direct proof has been brought forward. With respect to the growth and survival factors, they can also be provided by other brain cell types, questioning what influence the lack of dorsal oligodendrocytes would cause.

4. Hypothesis: Dorsal oligodendrocytes form specific interactions with astrocytes thereby alternating neuronal transmission

Multiple studies demonstrated the importance of astrocytes for OPC migration, OPC differentiation and timing of myelination (Schnädelbach & Fawcett, 2001; Iacobas & Iacobas, 2010; Tress et al., 2012; Camargo et al., 2017) (see Introduction, Section 1.5). However, little is known on the influence of oligodendrocytes on astrocytes. As astrocytes and oligodendrocytes are connected via gap junctions in the adult brain, it is conceivable that oligodendrocytes support astrocyte function by supplying them with nutrients or other growth factors. Potentially, the support of astrocytes facilitated by dorsal oligodendrocytes is different to ventral oligodendrocytes, therefore explaining the trend towards a reduced number of astrocytes in the ablated animals.

The reduced number of astrocytes can also be a direct off-target effect of the DTA ablation system. At this point, it cannot be excluded that a subpopulation of astrocytes do express *Emx1* and *Sox10* during development (see Section 7.5.2 and Chapter 4, Section 4.6). Regardless of the reason, a reduced number of astrocytes can undeniably alter neuronal transmission.

7.5 Can general effects of the ablation model cause the locomotor phenotype?

A heterogeneity in gene expression of the oligodendrocytes based on their developmental origin has been observed (see Chapter 4, Section 6.2). However, differences between control and ablated animals have been identified, including the expansion of the OPC population and a not significant reduction of astrocyte numbers, cannot be attributed to the developmental heterogeneity of OLCs. To what extent can effects caused by the ablation itself explain the locomotor coordination disabilities of ablated animals?

7.5.1 Increase of OPCs might contribute to the locomotor phenotype

In the DTA ablation model the number of OPCs is significantly increased in adult animals (see Chapter 5, Figure 5.1). Can an increase of OPCs have an impact on locomotor coordination? To date, OPCs are mainly seen as the cell of origin of oligodendrocytes in development and adulthood, thereby facilitating developmental

myelination, learning and remyelination. The discovery that OPCs form synapses with neurons opened up the possibility that OPCs also directly modulate neuronal transmission. Consequently, an increase in OPC numbers potentially changes physiological brain function. How such an increase in OPCs would alter neuronal transmission can be only hypothesised because only few physiological roles of OPCs have been described. In normal brain homeostasis, the shedding of the proteoglycan NG2 directly influences neuronal transmission through alterations of the neuronal firing (Sakry et al., 2014). Furthermore, OPCs secrete factors, including FGF2, GDNF and NGF, which were shown to modulate astrocytic and neuronal behaviour *in vitro* (Birey et al., 2015). A change in these or similar signalling cascades due to the increased amount of OPCs, leading to changes in the brain environment and neuronal transmission, may account for the detected abnormalities. In contrast, an abnormal OPC behaviour in ablated animals is unlikely as the gene expression profile of OPCs in ablated animals was similar to controls.

An interesting question is why the excess of OPC numbers is not adjusted to physiological levels by apoptosis? In the CNS the number of OPCs is tightly regulated, with a well-defined territory of each OPC regulated by self-repulsion (Hughes et al., 2013). Comparable OPC ablation approaches in adult animals did not result in a persistent increase of OPCs (Birey & Aguirre, 2015; Schneider et al., 2016). Therefore, the timing of ablation might be important as to whether the OPC number returns to normal levels. Potentially, there is a critical time window in which the number of OPCs and territory size are established. Ablation of OPCs during this critical time window might lead to a pronounced proliferation response in the remaining OPCs, eventually establishing a different equilibrium of OPC numbers in the brain. Netrin-1 has been identified as an important factor in regulating OPC proliferation and morphology, including branch density (Birey & Aguirre, 2015). An abnormal regulation of Netrin-1 signalling in the DTA ablation model might cause the overshoot of OPC proliferation.

To evaluate the impact the expansion of the OPC population on locomotor coordination is difficult because the importance of OPCs on neuronal transmission is not sufficiently studied yet. Furthermore, to validate the fact that there is an excess of OPCs in the brain, further methods identifying OPCs and OPC territories should be carried out (see Chapter 5, Section 5.3).

7.5.2 Off target effects of the DTA ablation system

The specificity of the dorsal OPC DTA ablation model used in this study is based on the expression of the two transcription factors *Emx1* and *Sox10* (see Chapter 3, Figure 3.1). As both transcription factors might also be expressed by subpopulations of other cell types, it cannot be confidently excluded that the locomotor phenotype observed might not stem from off-target effects of the ablation model. Based on the similar cell of origin of OPCs and astrocytes, a subpopulation of dorsal astrocyte might transitionally express *Emx1* and *Sox10* during embryonic development, before undergoing terminal differentiation (see Chapter 4, Section 4.6). A long-term reduction in astrocytes is unlikely, as a compensation by astrocyte proliferation is expected. However, as astrocytes possess a regional identity determining their function (Section 7.3.1), an ablation of a subpopulation of astrocytes might alter neuronal transmission.

In addition to astrocytes, cells of the neural crest might be affected by the DTA ablation model because of their expression of *Sox10*. There is no literature on whether neural crest cells also express *Emx1* at any time during development (see Chapter 4, Section 4.6). In addition, the ablation of Schwann cells or dorsal root ganglia would be expected to result in a strong locomotor phenotype, as the peripheral nervous system is absolutely crucial in locomotion.

7.6 Summary - Working model

In this thesis, differences in the gene expression profile of ventrally and dorsally derived OLs were identified. Intriguingly, ventral OPCs are not capable of differentiating into dorsal-like OLs in response to the ablation of dorsal OPCs. The lack of dorsal OLCs in the brain manifests itself in phenotypic abnormalities of locomotor coordination. Although heterogeneity within the oligodendrocyte lineage has been described before (see Introduction, Sections 1.4.1 and Section 1.4.2), no functional importance of the illustrated differences was convincingly proven. Therefore, this study provides an example of the functional importance of OLC heterogeneity in physiological brain function for the first time.

References

- Aggarwal, S., Snaidero, N., Pähler, G., Frey, S., Sánchez, P., Zweckstetter, M., . . . Simons, M. (2013). Myelin membrane assembly is driven by a phase transition of myelin basic proteins into a cohesive protein meshwork. *PLoS biology*, *11*(6), e1001577.
- Allaman, I., Bélanger, M., & Magistretti, P. J. (2011, February). Astrocyte-neuron metabolic relationships: for better and for worse. *Trends in neurosciences*, *34*(2), 76–87.
- Alliot, F., Godin, I., & Pessac, B. (1999, November). Microglia derive from progenitors, originating from the yolk sac, and which proliferate in the brain. *Brain research. Developmental brain research*, *117*(2), 145–152.
- Almeida, R. G., Czopka, T., Ffrench-Constant, C., & Lyons, D. A. (2011, October). Individual axons regulate the myelinating potential of single oligodendrocytes in vivo. *Development (Cambridge, England)*, *138*(20), 4443–4450.
- Amir, R. E., Van den Veyver, I. B., Wan, M., Tran, C. Q., Francke, U., & Zoghbi, H. Y. (1999, October). Rett syndrome is caused by mutations in X-linked MECP2, encoding methyl-CpG-binding protein 2. *Nature genetics*, *23*(2), 185–188.
- Arancibia-Cárcamo, I. L., Ford, M. C., Cossell, L., Ishida, K., Tohyama, K., & Attwell, D. (2017, January). Node of Ranvier length as a potential regulator of myelinated axon conduction speed. *eLife*, *6*, 521.
- Attwell, D., Buchan, A. M., Charpak, S., Lauritzen, M., Macvicar, B. A., & Newman, E. A. (2010, November). Glial and neuronal control of brain blood flow. *Nature*, *468*(7321), 232–243.
- Back, S. A., Tuohy, T. M. F., Chen, H., Wallingford, N., Craig, A., Struve, J., . . . Sherman, L. S. (2005, September). Hyaluronan accumulates in demyelinated lesions and inhibits oligodendrocyte progenitor maturation. *Nature medicine*, *11*(9), 966–972.
- Badaracco, M. E., Siri, M. V. R., & Pasquini, J. M. (2010, March). Oligodendrogenesis: the role of iron. *BioFactors (Oxford, England)*, *36*(2), 98–102.
- Barres, B. A., Hart, I. K., Coles, H. S., Burne, J. F., Voyvodic, J. T., Richardson, W. D., & Raff, M. C. (1992, July). Cell death and control of cell survival in the oligodendrocyte lineage. *Cell*, *70*(1), 31–46.
- Barres, B. A., Koroshetz, W. J., Swartz, K. J., Chun, L. L., & Corey, D. P. (1990, April). Ion channel expression by white matter glia: the O-2A glial progenitor cell. *Neuron*, *4*(4), 507–524.
- Barres, B. A., & Raff, M. C. (1994, May). Control of oligodendrocyte number in the developing rat optic nerve. *Neuron*, *12*(5), 935–942.
- Barres, B. A., Raff, M. C., Gaese, F., Bartke, I., Dechant, G., & Barde, Y. A. (1994, January). A crucial role for neurotrophin-3 in oligodendrocyte development. *Nature*, *367*(6461), 371–375.
- Bechler, M. E., Byrne, L., & Ffrench-Constant, C. (2015, September). CNS Myelin

- Sheath Lengths Are an Intrinsic Property of Oligodendrocytes. *Current biology* : *CB*, 25(18), 2411–2416.
- Bender, A. R., Völkle, M. C., & Raz, N. (2016, January). Differential aging of cerebral white matter in middle-aged and older adults: A seven-year follow-up. *NeuroImage*, 125, 74–83.
- Bengtsson, S. L., Nagy, Z., Skare, S., Forsman, L., Forsberg, H., & Ullén, F. (2005, September). Extensive piano practicing has regionally specific effects on white matter development. *Nature neuroscience*, 8(9), 1148–1150.
- Bergles, D. E., Roberts, J. D., Somogyi, P., & Jahr, C. E. (2000, May). Glutamatergic synapses on oligodendrocyte precursor cells in the hippocampus. *Nature*, 405(6783), 187–191.
- Birey, F., & Aguirre, A. (2015, April). Age-Dependent Netrin-1 Signaling Regulates NG2+ Glial Cell Spatial Homeostasis in Normal Adult Gray Matter. *The Journal of neuroscience : the official journal of the Society for Neuroscience*, 35(17), 6946–6951.
- Birey, F., Kloc, M., Chavali, M., Hussein, I., Wilson, M., Christoffel, D. J., . . . Aguirre, A. (2015, December). Genetic and Stress-Induced Loss of NG2 Glia Triggers Emergence of Depressive-like Behaviors through Reduced Secretion of FGF2. *Neuron*, 88(5), 941–956.
- Bjartmar, C., Hildebrand, C., & Loinder, K. (1994, July). Morphological heterogeneity of rat oligodendrocytes: Oligodendrocytes: Electron microscopic studies on serial sections. *Glia*, 11(3), 235–244.
- Blumenfeld-Katzir, T., Pasternak, O., Dagan, M., & Assaf, Y. (2011). Diffusion MRI of structural brain plasticity induced by a learning and memory task. *PloS one*, 6(6), e20678.
- Boda, E., Di Maria, S., Rosa, P., Taylor, V., Abbracchio, M. P., & Buffo, A. (2015, February). Early phenotypic asymmetry of sister oligodendrocyte progenitor cells after mitosis and its modulation by aging and extrinsic factors. *Glia*, 63(2), 271–286.
- Boespflug-Tanguy, O., Labauge, P., Fogli, A., & Vauris-Barriere, C. (2008, May). Genes involved in leukodystrophies: a glance at glial functions. *Current neurology and neuroscience reports*, 8(3), 217–229.
- Boyke, J., Driemeyer, J., Gaser, C., Büchel, C., & May, A. (2008, July). Training-induced brain structure changes in the elderly. *The Journal of neuroscience : the official journal of the Society for Neuroscience*, 28(28), 7031–7035.
- Brady, S. T., Witt, A. S., Kirkpatrick, L. L., de Waegh, S. M., Readhead, C., Tu, P. H., & Lee, V. M. (1999, September). Formation of compact myelin is required for maturation of the axonal cytoskeleton. *The Journal of neuroscience : the official journal of the Society for Neuroscience*, 19(17), 7278–7288.
- Briscoe, J., Pierani, A., Jessell, T. M., & Ericson, J. (2000, May). A homeodomain protein code specifies progenitor cell identity and neuronal fate in the ventral neural tube. *Cell*, 101(4), 435–445.
- Bushong, E. A., Martone, M. E., Jones, Y. Z., & Ellisman, M. H. (2002, January). Protoplasmic astrocytes in CA1 stratum radiatum occupy separate anatomical domains. *The Journal of neuroscience : the official journal of the Society for Neuroscience*, 22(1), 183–192.
- Buss, R. R., Sun, W., & Oppenheim, R. W. (2006). Adaptive roles of programmed cell death during nervous system development. *Annual review of neuroscience*, 29(1), 1–35.
- Butt, A. M., Colquhoun, K., Tutton, M., & Berry, M. (1994, August). Three-

- dimensional morphology of astrocytes and oligodendrocytes in the intact mouse optic nerve. *Journal of Neurocytology*, 23(8), 469–485.
- Butt, A. M., Ibrahim, M., Ruge, F. M., & Berry, M. (1995, July). Biochemical subtypes of oligodendrocyte in the anterior medullary velum of the rat as revealed by the monoclonal antibody Rip. *Glia*, 14(3), 185–197.
- Butt, A. M., & Ransom, B. R. (1989). Visualization of oligodendrocytes and astrocytes in the intact rat optic nerve by intracellular injection of lucifer yellow and horseradish peroxidase. *Glia*, 2(6), 470–475.
- Byravan, S., Foster, L. M., Phan, T., Verity, A. N., & Campagnoni, A. T. (1994, September). Murine oligodendroglial cells express nerve growth factor. *Proceedings of the National Academy of Sciences of the United States of America*, 91(19), 8812–8816.
- Cahoy, J. D., Emery, B., Kaushal, A., Foo, L. C., Zamanian, J. L., Christopherson, K. S., ... Barres, B. A. (2008, January). A transcriptome database for astrocytes, neurons, and oligodendrocytes: a new resource for understanding brain development and function. *The Journal of neuroscience : the official journal of the Society for Neuroscience*, 28(1), 264–278.
- Cai, J., Qi, Y., Hu, X., Tan, M., Liu, Z., Zhang, J., ... Qiu, M. (2005, January). Generation of oligodendrocyte precursor cells from mouse dorsal spinal cord independent of Nkx6 regulation and Shh signaling. *Neuron*, 45(1), 41–53.
- Calver, A. R., Hall, A. C., Yu, W. P., Walsh, F. S., Heath, J. K., Betsholtz, C., & Richardson, W. D. (1998, May). Oligodendrocyte population dynamics and the role of PDGF in vivo. *Neuron*, 20(5), 869–882.
- Camargo, N., Goudriaan, A., van Deijk, A.-L. F., Otte, W. M., Brouwers, J. F., Lodder, H., ... Verheijen, M. H. G. (2017, May). Oligodendroglial myelination requires astrocyte-derived lipids. *PLoS biology*, 15(5), e1002605.
- Cammer, W., Zhang, H., & Cammer, M. (1993, August). Glial cell abnormalities in the CNS of the carbonic anhydrase II deficient mutant mouse. *Journal of the neurological sciences*, 118(1), 1–9.
- Chan, C. H., Godinho, L. N., Thomaidou, D., Tan, S. S., Gulisano, M., & Parnavelas, J. G. (2001, December). Emx1 is a marker for pyramidal neurons of the cerebral cortex. *Cerebral cortex (New York, N.Y. : 1991)*, 11(12), 1191–1198.
- Chandran, S., Kato, H., Gerreli, D., Compston, A., Svendsen, C. N., & Allen, N. D. (2003, December). FGF-dependent generation of oligodendrocytes by a hedgehog-independent pathway. *Development (Cambridge, England)*, 130(26), 6599–6609.
- Charles, P., Hernandez, M. P., Stankoff, B., Aigrot, M. S., Colin, C., Rougon, G., ... Lubetzki, C. (2000, June). Negative regulation of central nervous system myelination by polysialylated-neural cell adhesion molecule. *Proceedings of the National Academy of Sciences of the United States of America*, 97(13), 7585–7590.
- Cheepsunthorn, P., Palmer, C., & Connor, J. R. (1998, October). Cellular distribution of ferritin subunits in postnatal rat brain. *The Journal of Comparative Neurology*, 400(1), 73–86.
- Chittajallu, R., Aguirre, A., & Gallo, V. (2004, November). NG2-positive cells in the mouse white and grey matter display distinct physiological properties. *The Journal of physiology*, 561(Pt 1), 109–122.
- Chiu, I. M., Morimoto, E. T. A., Goodarzi, H., Liao, J. T., O’Keeffe, S., Phatnani, H. P., ... Maniatis, T. (2013, July). A neurodegeneration-specific gene-expression signature of acutely isolated microglia from an amyotrophic lateral sclerosis

- mouse model. *Cell reports*, 4(2), 385–401.
- Chomiak, T., & Hu, B. (2009, November). What is the optimal value of the g-ratio for myelinated fibers in the rat CNS? A theoretical approach. *PloS one*, 4(11), e7754.
- Chong, S. Y. C., Rosenberg, S. S., Fancy, S. P. J., Zhao, C., Shen, Y.-A. A., Hahn, A. T., ... Chan, J. R. (2012, January). Neurite outgrowth inhibitor Nogo-A establishes spatial segregation and extent of oligodendrocyte myelination. *Proceedings of the National Academy of Sciences of the United States of America*, 109(4), 1299–1304.
- Christopherson, K. S., Ullian, E. M., Stokes, C. C. A., Mallowney, C. E., Hell, J. W., Agah, A., ... Barres, B. A. (2005, February). Thrombospondins are astrocyte-secreted proteins that promote CNS synaptogenesis. *Cell*, 120(3), 421–433.
- Chung, S. H., Guo, F., Jiang, P., Pleasure, D. E., & Deng, W. (2013, March). Olig2/Plp-positive progenitor cells give rise to Bergmann glia in the cerebellum. *Cell Death and Disease*, 4(3), e546.
- Chung, W. S., Allen, N. J., & Eroglu, C. (2015, February). Astrocytes Control Synapse Formation, Function, and Elimination. *Cold Spring Harbor perspectives in biology*, 7(9), a020370.
- Clarke, L. E., Young, K. M., Hamilton, N. B., Li, H., Richardson, W. D., & Attwell, D. (2012, June). Properties and fate of oligodendrocyte progenitor cells in the corpus callosum, motor cortex, and piriform cortex of the mouse. *The Journal of neuroscience : the official journal of the Society for Neuroscience*, 32(24), 8173–8185.
- Cohen, R. I., Marmur, R., Norton, W. T., Mehler, M. F., & Kessler, J. A. (1996, October). Nerve growth factor and neurotrophin-3 differentially regulate the proliferation and survival of developing rat brain oligodendrocytes. *Journal of Neuroscience*, 16(20), 6433–6442.
- Colello, R. J., Pott, U., & Schwab, M. E. (1994, May). The role of oligodendrocytes and myelin on axon maturation in the developing rat retinofugal pathway. *Journal of Neuroscience*, 14(5 Pt 1), 2594–2605.
- Coull, J. A. M., Beggs, S., Boudreau, D., Boivin, D., Tsuda, M., Inoue, K., ... De Koninck, Y. (2005, December). BDNF from microglia causes the shift in neuronal anion gradient underlying neuropathic pain. *Nature*, 438(7070), 1017–1021.
- Crawford, A. H., Stockley, J. H., Tripathi, R. B., Richardson, W. D., & Franklin, R. J. M. (2014, October). Oligodendrocyte progenitors: adult stem cells of the central nervous system? *Experimental neurology*, 260, 50–55.
- Crawford, A. H., Tripathi, R. B., Richardson, W. D., & Franklin, R. J. M. (2016, April). Developmental Origin of Oligodendrocyte Lineage Cells Determines Response to Demyelination and Susceptibility to Age-Associated Functional Decline. *Cell reports*, 15(4), 761–773.
- Cunningham, C. L., Martínez-Cerdeño, V., & Noctor, S. C. (2013, March). Microglia regulate the number of neural precursor cells in the developing cerebral cortex. *The Journal of neuroscience : the official journal of the Society for Neuroscience*, 33(10), 4216–4233.
- Czopka, T., Ffrench-Constant, C., & Lyons, D. A. (2013, June). Individual oligodendrocytes have only a few hours in which to generate new myelin sheaths in vivo. *Developmental cell*, 25(6), 599–609.
- da Cunha, A., Jefferson, J. A., Jackson, R. W., & Vitković, L. (1993, January). Glial cell-specific mechanisms of TGF-beta 1 induction by IL-1 in cerebral cortex.

- Journal of neuroimmunology*, 42(1), 71–85.
- Dai, X., Lercher, L. D., Clinton, P. M., Du, Y., Livingston, D. L., Vieira, C., ... Dreyfus, C. F. (2003, July). The trophic role of oligodendrocytes in the basal forebrain. *The Journal of neuroscience : the official journal of the Society for Neuroscience*, 23(13), 5846–5853.
- Dai, X., Qu, P., & Dreyfus, C. F. (2001, May). Neuronal signals regulate neurotrophin expression in oligodendrocytes of the basal forebrain. *Glia*, 34(3), 234–239.
- Daneman, R., & Prat, A. (2015, January). The blood-brain barrier. *Cold Spring Harbor perspectives in biology*, 7(1), a020412.
- Dashiell, S. M., Tanner, S. L., Pant, H. C., & Quarles, R. H. (2002, June). Myelin-associated glycoprotein modulates expression and phosphorylation of neuronal cytoskeletal elements and their associated kinases. *Journal of neurochemistry*, 81(6), 1263–1272.
- Dawson, M. R. L., Polito, A., Levine, J. M., & Reynolds, R. (2003, October). NG2-expressing glial progenitor cells: an abundant and widespread population of cycling cells in the adult rat CNS. *Molecular and cellular neurosciences*, 24(2), 476–488.
- De Biase, L. M., Nishiyama, A., & Bergles, D. E. (2010, March). Excitability and synaptic communication within the oligodendrocyte lineage. *The Journal of neuroscience : the official journal of the Society for Neuroscience*, 30(10), 3600–3611.
- de Haas, A. H., Boddeke, H. W. G. M., & Biber, K. (2008, June). Region-specific expression of immunoregulatory proteins on microglia in the healthy CNS. *Glia*, 56(8), 888–894.
- de la Fuente, A. G., Errea, O., van Wijngaarden, P., Gonzalez, G. A., Kerninon, C., Jarjour, A. A., ... Franklin, R. J. M. (2015, December). Vitamin D receptor-retinoid X receptor heterodimer signaling regulates oligodendrocyte progenitor cell differentiation. *The Journal of cell biology*, 211(5), 975–985.
- del Río Hortega, P. (1928, January). Tercera aportación al conocimiento morfológico e interpretación funcional de la oligodendroglía. *Memorias de la Real Sociedad Española de Historia Natural*, XIV, 5–122.
- Deoni, S. C. L., Mercure, E., Blasi, A., Gasston, D., Thomson, A., Johnson, M., ... Murphy, D. G. M. (2011, January). Mapping infant brain myelination with magnetic resonance imaging. *The Journal of neuroscience : the official journal of the Society for Neuroscience*, 31(2), 784–791.
- Desai, A. R., & McConnell, S. K. (2000, July). Progressive restriction in fate potential by neural progenitors during cerebral cortical development. *Development (Cambridge, England)*, 127(13), 2863–2872.
- de Waegh, S. M., Lee, V. M., & Brady, S. T. (1992, February). Local modulation of neurofilament phosphorylation, axonal caliber, and slow axonal transport by myelinating Schwann cells. *Cell*, 68(3), 451–463.
- Dimou, L., Simon, C., Kirchhoff, F., Takebayashi, H., & Götz, M. (2008, October). Progeny of Olig2-expressing progenitors in the gray and white matter of the adult mouse cerebral cortex. *The Journal of neuroscience : the official journal of the Society for Neuroscience*, 28(41), 10434–10442.
- Donaldson, H. H., & Hoke, G. W. (1905, January). On the areas of the axis cylinder and medullary sheath as seen in cross sections of the spinal nerves of vertebrates. *Journal of Comparative Neurology and Psychology*, 15(1), 1–16.
- Dugas, J. C., Cuellar, T. L., Scholze, A., Ason, B., Ibrahim, A., Emery, B., ... Barres, B. A. (2010, March). Dicer1 and miR-219 Are required for normal

- oligodendrocyte differentiation and myelination. *Neuron*, 65(5), 597–611.
- Edgar, J. M., McLaughlin, M., Yool, D., Zhang, S.-C., Fowler, J. H., Montague, P., ... Griffiths, I. R. (2004, July). Oligodendroglial modulation of fast axonal transport in a mouse model of hereditary spastic paraplegia. *The Journal of cell biology*, 166(1), 121–131.
- Emery, B., Agalliu, D., Cahoy, J. D., Watkins, T. A., Dugas, J. C., Mulinyawe, S. B., ... Barres, B. A. (2009, July). Myelin gene regulatory factor is a critical transcriptional regulator required for CNS myelination. *Cell*, 138(1), 172–185.
- Eng, L. F., Vanderhaeghen, J. J., & Gerstl, B. (1970, January). A study of proteins in old multiple sclerosis plaques. *Transactions of the American Society for Neurochemistry*, 1, 42.
- Etxeberria, A., Hokanson, K. C., Dao, D. Q., Mayoral, S. R., Mei, F., Redmond, S. A., ... Chan, J. R. (2016, June). Dynamic Modulation of Myelination in Response to Visual Stimuli Alters Optic Nerve Conduction Velocity. *The Journal of neuroscience : the official journal of the Society for Neuroscience*, 36(26), 6937–6948.
- Fancy, S. P. J., Baranzini, S. E., Zhao, C., Yuk, D.-I., Irvine, K.-A., Kaing, S., ... Rowitch, D. H. (2009, July). Dysregulation of the Wnt pathway inhibits timely myelination and remyelination in the mammalian CNS. *Genes & development*, 23(13), 1571–1585.
- Fancy, S. P. J., Zhao, C., & Franklin, R. J. M. (2004, November). Increased expression of Nkx2.2 and Olig2 identifies reactive oligodendrocyte progenitor cells responding to demyelination in the adult CNS. *Molecular and cellular neurosciences*, 27(3), 247–254.
- Fernández-Gamba, A., Leal, M. C., Maarouf, C. L., Richter-Landsberg, C., Wu, T., Morelli, L., ... Castaño, E. M. (2012, June). Collapsin response mediator protein-2 phosphorylation promotes the reversible retraction of oligodendrocyte processes in response to non-lethal oxidative stress. *Journal of neurochemistry*, 121(6), 985–995.
- Fewou, S. N., Ramakrishnan, H., Büssov, H., Gieselmann, V., & Eckhardt, M. (2007, June). Down-regulation of polysialic acid is required for efficient myelin formation. *The Journal of biological chemistry*, 282(22), 16700–16711.
- Fitzner, D., Schnaars, M., van Rossum, D., Krishnamoorthy, G., Dibaj, P., Bakhti, M., ... Simons, M. (2011, February). Selective transfer of exosomes from oligodendrocytes to microglia by macropinocytosis. *Journal of cell science*, 124(Pt 3), 447–458.
- Flores, A. I., Narayanan, S. P., Morse, E. N., Shick, H. E., Yin, X., Kidd, G., ... Macklin, W. B. (2008, July). Constitutively active Akt induces enhanced myelination in the CNS. *The Journal of neuroscience : the official journal of the Society for Neuroscience*, 28(28), 7174–7183.
- Fogarty, M., Richardson, W. D., & Kessaris, N. (2005, April). A subset of oligodendrocytes generated from radial glia in the dorsal spinal cord. *Development (Cambridge, England)*, 132(8), 1951–1959.
- Foran, D. R., & Peterson, A. C. (1992, December). Myelin acquisition in the central nervous system of the mouse revealed by an MBP-Lac Z transgene. *Journal of Neuroscience*, 12(12), 4890–4897.
- Ford, M. C., Alexandrova, O., Cossell, L., Stange-Marten, A., Sinclair, J., Kopp-Scheinflug, C., ... Grothe, B. (2015, August). Tuning of Ranvier node and internode properties in myelinated axons to adjust action potential timing. *Nature communications*, 6, 8073.

- Fragoso, G., Haines, J. D., Roberston, J., Pedraza, L., Mushynski, W. E., & Almazan, G. (2007, November). p38 mitogen-activated protein kinase is required for central nervous system myelination. *Glia*, 55(15), 1531–1541.
- Franklin, R. J. M., & Ffrench-Constant, C. (2008, November). Remyelination in the CNS: from biology to therapy. *Nature reviews. Neuroscience*, 9(11), 839–855.
- Franklin, R. J. M., & Ffrench-Constant, C. (2017, November). Regenerating CNS myelin - from mechanisms to experimental medicines. *Nature reviews. Neuroscience*, 18(12), 753–769.
- Franklin, R. J. M., & Goldman, S. A. (2015, May). Glia Disease and Repair-Remyelination. *Cold Spring Harbor perspectives in biology*, 7(7), a020594.
- Friedman, B., Hockfield, S., Black, J. A., Woodruff, K. A., & Waxman, S. G. (1989). In situ demonstration of mature oligodendrocytes and their processes: An immunocytochemical study with a new monoclonal antibody, Rip. *Glia*, 2(5), 380–390.
- Fruttiger, M., Karlsson, L., Hall, A. C., Abramsson, A., Calver, A. R., Boström, H., ... Richardson, W. D. (1999, February). Defective oligodendrocyte development and severe hypomyelination in PDGF-A knockout mice. *Development (Cambridge, England)*, 126(3), 457–467.
- Fuzik, J., Zeisel, A., Máté, Z., Calvigioni, D., Yanagawa, Y., Szabó, G., ... Harkany, T. (2016, February). Integration of electrophysiological recordings with single-cell RNA-seq data identifies neuronal subtypes. *Nature biotechnology*, 34(2), 175–183.
- Fyffe-Maricich, S. L., Karlo, J. C., Landreth, G. E., & Miller, R. H. (2011, January). The ERK2 mitogen-activated protein kinase regulates the timing of oligodendrocyte differentiation. *The Journal of neuroscience : the official journal of the Society for Neuroscience*, 31(3), 843–850.
- Garcia, M. L., Lobsiger, C. S., Shah, S. B., Deerinck, T. J., Crum, J., Young, D., ... Cleveland, D. W. (2003, December). NF-M is an essential target for the myelin-directed "outside-in" signaling cascade that mediates radial axonal growth. *The Journal of cell biology*, 163(5), 1011–1020.
- Gard, A. L., Burrell, M. R., Pfeiffer, S. E., Rudge, J. S., & Williams, W. C. (1995, July). Astroglial control of oligodendrocyte survival mediated by PDGF and leukemia inhibitory factor-like protein. *Development (Cambridge, England)*, 121(7), 2187–2197.
- Geers, C., & Gros, G. (2000, April). Carbon dioxide transport and carbonic anhydrase in blood and muscle. *Physiological reviews*, 80(2), 681–715.
- Gibson, E. M., Purger, D., Mount, C. W., Goldstein, A. K., Lin, G. L., Wood, L. S., ... Monje, M. (2014, May). Neuronal activity promotes oligodendrogenesis and adaptive myelination in the mammalian brain. *Science (New York, N.Y.)*, 344(6183), 1252304–1252304.
- Ginhoux, F., Greter, M., Leboeuf, M., Nandi, S., See, P., Gokhan, S., ... Merad, M. (2010, November). Fate mapping analysis reveals that adult microglia derive from primitive macrophages. *Science (New York, N.Y.)*, 330(6005), 841–845.
- Glasgow, S. M., Zhu, W., Stolt, C. C., Huang, T.-W., Chen, F., LoTurco, J. J., ... Deneen, B. (2014, October). Mutual antagonism between Sox10 and NFIA regulates diversification of glial lineages and glioma subtypes. *Nature neuroscience*, 17(10), 1322–1329.
- Goddard, D. R., Berry, M., Kirvell, S. L., & Butt, A. M. (2001, November). Fibroblast growth factor-2 inhibits myelin production by oligodendrocytes in vivo. *Molecular and cellular neurosciences*, 18(5), 557–569.

- Goebbels, S., Oltrogge, J. H., Kemper, R., Heilmann, I., Bormuth, I., Wolfer, S., . . . Nave, K.-A. (2010, June). Elevated phosphatidylinositol 3,4,5-trisphosphate in glia triggers cell-autonomous membrane wrapping and myelination. *The Journal of neuroscience : the official journal of the Society for Neuroscience*, 30(26), 8953–8964.
- Goebbels, S., Wieser, G. L., Pieper, A., Spitzer, S., Weege, B., Yan, K., . . . Nave, K.-A. (2017, January). A neuronal PI(3,4,5)P3-dependent program of oligodendrocyte precursor recruitment and myelination. *Nature neuroscience*, 20(1), 10–15.
- Gordon, G. R. J., Howarth, C., & Macvicar, B. A. (2011, April). Bidirectional control of arteriole diameter by astrocytes. *Experimental physiology*, 96(4), 393–399.
- Gorski, J. A., Talley, T., Qiu, M., Puellas, L., Rubenstein, J. L. R., & Jones, K. R. (2002, August). Cortical excitatory neurons and glia, but not GABAergic neurons, are produced in the Emx1-expressing lineage. *The Journal of neuroscience : the official journal of the Society for Neuroscience*, 22(15), 6309–6314.
- Gould, R. M., & Dawson, R. M. (1976, March). Incorporation of newly formed lecithin into peripheral nerve myelin. *The Journal of cell biology*, 68(3), 480–496.
- Grabert, K., Michoel, T., Karavolos, M. H., Clohisey, S., Baillie, J. K., Stevens, M. P., . . . McColl, B. W. (2016, March). Microglial brain region-dependent diversity and selective regional sensitivities to aging. *Nature neuroscience*, 19(3), 504–516.
- Griffiths, I., Klugmann, M., Anderson, T., Yool, D., Thomson, C., Schwab, M. H., . . . Nave, K. A. (1998, June). Axonal swellings and degeneration in mice lacking the major proteolipid of myelin. *Science (New York, N.Y.)*, 280(5369), 1610–1613.
- Guo, F., Maeda, Y., Ma, J., Xu, J., Horiuchi, M., Miers, L., . . . Pleasure, D. (2010, September). Pyramidal Neurons Are Generated from Oligodendroglial Progenitor Cells in Adult Piriform Cortex. *Journal of Neuroscience*, 30(36), 12036–12049.
- Haines, J. D., Fragoso, G., Hossain, S., Mushynski, W. E., & Almazan, G. (2008, May). p38 Mitogen-activated protein kinase regulates myelination. *Journal of molecular neuroscience : MN*, 35(1), 23–33.
- Hamilton, N. B., & Attwell, D. (2010, April). Do astrocytes really exocytose neurotransmitters? *Nature reviews. Neuroscience*, 11(4), 227–238.
- Hamilton, N. B., Clarke, L. E., Arancibia-Cárcamo, I. L., Kougoumtzidou, E., Matthey, M., Káradóttir, R., . . . Attwell, D. (2017, February). Endogenous GABA controls oligodendrocyte lineage cell number, myelination, and CNS internode length. *Glia*, 65(2), 309–321.
- Hamilton, S. P., & Rome, L. H. (1994, August). Stimulation of in vitro myelin synthesis by microglia. *Glia*, 11(4), 326–335.
- Hardy, R. J., Lazzarini, R. A., Colman, D. R., & Friedrich, V. L. (1996, October). Cytoplasmic and nuclear localization of myelin basic proteins reveals heterogeneity among oligodendrocytes. *Journal of neuroscience research*, 46(2), 246–257.
- Harris, J. J., & Attwell, D. (2012, January). The energetics of CNS white matter. *The Journal of neuroscience : the official journal of the Society for Neuroscience*, 32(1), 356–371.
- Hattori, T., Shimizu, S., Koyama, Y., Emoto, H., Matsumoto, Y., Kumamoto, N., . . . Ito, A. (2014). DISC1 (disrupted-in-schizophrenia-1) regulates differentiation of oligodendrocytes. *PloS one*, 9(2), e88506.
- He, Y., Dupree, J., Wang, J., Sandoval, J., Li, J., Liu, H., . . . Casaccia-Bonnel, P. (2007, July). The transcription factor Yin Yang 1 is essential for oligodendrocyte

- progenitor differentiation. *Neuron*, 55(2), 217–230.
- Hikida, T., Jaaro-Peled, H., Seshadri, S., Oishi, K., Hookway, C., Kong, S., ... Sawa, A. (2007, September). Dominant-negative DISC1 transgenic mice display schizophrenia-associated phenotypes detected by measures translatable to humans. *Proceedings of the National Academy of Sciences of the United States of America*, 104(36), 14501–14506.
- Hill, R. A., Patel, K. D., Goncalves, C. M., Grutzendler, J., & Nishiyama, A. (2014, November). Modulation of oligodendrocyte generation during a critical temporal window after NG2 cell division. *Nature neuroscience*, 17(11), 1518–1527.
- Hill, R. A., Patel, K. D., Medved, J., Reiss, A. M., & Nishiyama, A. (2013, September). NG2 cells in white matter but not gray matter proliferate in response to PDGF. *The Journal of neuroscience : the official journal of the Society for Neuroscience*, 33(36), 14558–14566.
- Hines, J. H., Ravanelli, A. M., Schwindt, R., Scott, E. K., & Appel, B. (2015, May). Neuronal activity biases axon selection for myelination in vivo. *Nature neuroscience*, 18(5), 683–689.
- Hochstim, C., Deneen, B., Lukaszewicz, A., Zhou, Q., & Anderson, D. J. (2008, May). Identification of positionally distinct astrocyte subtypes whose identities are specified by a homeodomain code. *Cell*, 133(3), 510–522.
- Hodgkin, A. L., & Huxley, A. F. (1990). *A quantitative description of membrane current and its application to conduction and excitation in nerve*. 1952. (Vol. 52).
- Howng, S. Y. B., Avila, R. L., Emery, B., Traka, M., Lin, W., Watkins, T., ... Popko, B. (2010, February). ZFP191 is required by oligodendrocytes for CNS myelination. *Genes & development*, 24(3), 301–311.
- Hsieh, S. T., Kidd, G. J., Crawford, T. O., Xu, Z., Lin, W. M., Trapp, B. D., ... Griffin, J. W. (1994, November). Regional modulation of neurofilament organization by myelination in normal axons. *Journal of Neuroscience*, 14(11 Pt 1), 6392–6401.
- Hughes, E. G., Kang, S. H., Fukaya, M., & Bergles, D. E. (2013, June). Oligodendrocyte progenitors balance growth with self-repulsion to achieve homeostasis in the adult brain. *Nature neuroscience*, 16(6), 668–676.
- Iacobas, S., & Iacobas, D. A. (2010, August). Astrocyte proximity modulates the myelination gene fabric of oligodendrocytes. *Neuron glia biology*, 6(3), 157–169.
- Ibrahim, M., Butt, A. M., & Berry, M. (1995, November). Relationship between myelin sheath diameter and internodal length in axons of the anterior medullary velum of the adult rat. *Journal of the neurological sciences*, 133(1-2), 119–127.
- Jabs, R., Kirchhoff, F., Kettenmann, H., & Steinhäuser, C. (1994, February). Kainate activates Ca(2+)-permeable glutamate receptors and blocks voltage-gated K⁺ currents in glial cells of mouse hippocampal slices. *Pflugers Archiv : European journal of physiology*, 426(3-4), 310–319.
- Kang, S. H., Fukaya, M., Yang, J. K., Rothstein, J. D., & Bergles, D. E. (2010, November). NG2+ CNS glial progenitors remain committed to the oligodendrocyte lineage in postnatal life and following neurodegeneration. *Neuron*, 68(4), 668–681.
- Káradóttir, R., Hamilton, N. B., Bakiri, Y., & Attwell, D. (2008, April). Spiking and nonspiking classes of oligodendrocyte precursor glia in CNS white matter. *Nature neuroscience*, 11(4), 450–456.
- Katz, L. C., & Shatz, C. J. (1996, November). Synaptic activity and the construction of cortical circuits. *Science (New York, N.Y.)*, 274(5290), 1133–1138.
- Keller, T. A., & Just, M. A. (2009, December). Altering cortical connectivity:

- remediation-induced changes in the white matter of poor readers. *Neuron*, *64*(5), 624–631.
- Keren-Shaul, H., Spinrad, A., Weiner, A., Matcovitch-Natan, O., Dvir-Szternfeld, R., Ulland, T. K., . . . Amit, I. (2017, June). A Unique Microglia Type Associated with Restricting Development of Alzheimer's Disease. *Cell*, *169*(7), 1276–1290.e17.
- Kessaris, N., Fogarty, M., Iannarelli, P., Grist, M., Wegner, M., & Richardson, W. D. (2006, February). Competing waves of oligodendrocytes in the forebrain and postnatal elimination of an embryonic lineage. *Nature neuroscience*, *9*(2), 173–179.
- Kettenmann, H., Blankenfeld, G. V., & Trotter, J. (1991). Physiological properties of oligodendrocytes during development. *Annals of the New York Academy of Sciences*, *633*, 64–77.
- Kierdorf, K., Erny, D., Goldmann, T., Sander, V., Schulz, C., Perdiguero, E. G., . . . Prinz, M. (2013, March). Microglia emerge from erythromyeloid precursors via Pu.1- and Irf8-dependent pathways. *Nature neuroscience*, *16*(3), 273–280.
- Kim, C. H., Hvoslef-Eide, M., Nilsson, S. R. O., Johnson, M. R., Herbert, B. R., Robbins, T. W., . . . Mar, A. C. (2015, November). The continuous performance test (rCPT) for mice: a novel operant touchscreen test of attentional function. *Psychopharmacology*, *232*(21–22), 3947–3966.
- Kim, J. G., & Hudson, L. D. (1992, December). Novel member of the zinc finger superfamily: A C2-HC finger that recognizes a glia-specific gene. *Molecular and cellular biology*, *12*(12), 5632–5639.
- Kinney, H. C., Brody, B. A., Kloman, A. S., & Gilles, F. H. (1988, May). Sequence of central nervous system myelination in human infancy. II. Patterns of myelination in autopsied infants. *Journal of neuropathology and experimental neurology*, *47*(3), 217–234.
- Klingseisen, A., & Lyons, D. A. (2017, April). Axonal Regulation of Central Nervous System Myelination: Structure and Function. *The Neuroscientist : a review journal bringing neurobiology, neurology and psychiatry*, *15*, 1073858417703030.
- Kondo, T., & Raff, M. (2000, July). Basic helix-loop-helix proteins and the timing of oligodendrocyte differentiation. *Development (Cambridge, England)*, *127*(14), 2989–2998.
- Kotter, M. R., Li, W.-W., Zhao, C., & Franklin, R. J. M. (2006, January). Myelin impairs CNS remyelination by inhibiting oligodendrocyte precursor cell differentiation. *The Journal of neuroscience : the official journal of the Society for Neuroscience*, *26*(1), 328–332.
- Koudelka, S., Voas, M. G., Almeida, R. G., Baraban, M., Soetaert, J., Meyer, M. P., . . . Lyons, D. A. (2016, June). Individual Neuronal Subtypes Exhibit Diversity in CNS Myelination Mediated by Synaptic Vesicle Release. *Current biology : CB*, *26*(11), 1447–1455.
- Kuhlbrodt, K., Schmidt, C., Sock, E., Pingault, V., Bondurand, N., Goossens, M., & Wegner, M. (1998, September). Functional analysis of Sox10 mutations found in human Waardenburg-Hirschsprung patients. *The Journal of biological chemistry*, *273*(36), 23033–23038.
- Kukley, M., Capetillo-Zarate, E., & Dietrich, D. (2007, March). Vesicular glutamate release from axons in white matter. *Nature neuroscience*, *10*(3), 311–320.
- Kukley, M., Nishiyama, A., & Dietrich, D. (2010, June). The fate of synaptic input to NG2 glial cells: neurons specifically downregulate transmitter release onto differentiating oligodendroglial cells. *The Journal of neuroscience : the official*

- journal of the Society for Neuroscience*, 30(24), 8320–8331.
- Lalancette-Hébert, M., Gowing, G., Simard, A., Weng, Y. C., & Kriz, J. (2007, March). Selective ablation of proliferating microglial cells exacerbates ischemic injury in the brain. *The Journal of neuroscience : the official journal of the Society for Neuroscience*, 27(10), 2596–2605.
- Landry, C. F., Ivy, G. O., Dunn, R. J., Marks, A., & Brown, I. R. (1989, December). Expression of the gene encoding the beta-subunit of S-100 protein in the developing rat brain analyzed by in situ hybridization. *Brain research. Molecular brain research*, 6(4), 251–262.
- Langseth, A. J., Munji, R. N., Choe, Y., Huynh, T., Pozniak, C. D., & Pleasure, S. J. (2010, October). Wnts influence the timing and efficiency of oligodendrocyte precursor cell generation in the telencephalon. *The Journal of neuroscience : the official journal of the Society for Neuroscience*, 30(40), 13367–13372.
- Lappe-Siefke, C., Goebbels, S., Gravel, M., Nicksch, E., Lee, J., Braun, P. E., ... Nave, K.-A. (2003, March). Disruption of *Cnp1* uncouples oligodendroglial functions in axonal support and myelination. *Nature genetics*, 33(3), 366–374.
- Laursen, L. S., Chan, C. W., & Ffrench-Constant, C. (2011, March). Translation of myelin basic protein mRNA in oligodendrocytes is regulated by integrin activation and hnRNP-K. *The Journal of cell biology*, 192(5), 797–811.
- Lawson, L. J., Perry, V. H., Dri, P., & Gordon, S. (1990). Heterogeneity in the distribution and morphology of microglia in the normal adult mouse brain. *Neuroscience*, 39(1), 151–170.
- Lee, S., Leach, M. K., Redmond, S. A., Chong, S. Y. C., Mellon, S. H., Tuck, S. J., ... Chan, J. R. (2012, September). A culture system to study oligodendrocyte myelination processes using engineered nanofibers. *Nature methods*, 9(9), 917–922.
- Lee, Y., Morrison, B. M., Li, Y., Lengacher, S., Farah, M. H., Hoffman, P. N., ... Rothstein, J. D. (2012, July). Oligodendroglia metabolically support axons and contribute to neurodegeneration. *Nature*, 487(7408), 443–448.
- Lendahl, U., Zimmerman, L. B., & McKay, R. D. (1990, February). CNS stem cells express a new class of intermediate filament protein. *Cell*, 60(4), 585–595.
- Li, Q., Brus-Ramer, M., Martin, J. H., & McDonald, J. W. (2010, July). Electrical stimulation of the medullary pyramid promotes proliferation and differentiation of oligodendrocyte progenitor cells in the corticospinal tract of the adult rat. *Neuroscience letters*, 479(2), 128–133.
- Lin, S.-C., Huck, J. H. J., Roberts, J. D. B., Macklin, W. B., Somogyi, P., & Bergles, D. E. (2005, June). Climbing fiber innervation of NG2-expressing glia in the mammalian cerebellum. *Neuron*, 46(5), 773–785.
- Linnington, C., Webb, M., & Woodhams, P. L. (1984, September). A novel myelin-associated glycoprotein defined by a mouse monoclonal antibody. *Journal of neuroimmunology*, 6(6), 387–396.
- Liu, J., Dietz, K., DeLoyht, J. M., Pedre, X., Kelkar, D., Kaur, J., ... Casaccia, P. (2012, December). Impaired adult myelination in the prefrontal cortex of socially isolated mice. *Nature neuroscience*, 15(12), 1621–1623.
- López-Otín, C., Blasco, M. A., Partridge, L., Serrano, M., & Kroemer, G. (2013, June). The hallmarks of aging. *Cell*, 153(6), 1194–1217.
- Lu, Q. R., Sun, T., Zhu, Z., Ma, N., Garcia, M., Stiles, C. D., & Rowitch, D. H. (2002, April). Common developmental requirement for Olig function indicates a motor neuron/oligodendrocyte connection. *Cell*, 109(1), 75–86.
- Lyons, D. A., Naylor, S. G., Scholze, A., & Talbot, W. S. (2009, July). Kif1b

- is essential for mRNA localization in oligodendrocytes and development of myelinated axons. *Nature genetics*, 41(7), 854–858.
- Madden, D. J., Bennett, I. J., & Song, A. W. (2009, December). Cerebral white matter integrity and cognitive aging: contributions from diffusion tensor imaging. *Neuropsychology review*, 19(4), 415–435.
- Makinodan, M., Okuda-Yamamoto, A., Ikawa, D., Toritsuka, M., Takeda, T., Kimoto, S., ... Kishimoto, T. (2013). Oligodendrocyte plasticity with an intact cell body in vitro. *PloS one*, 8(6), e66124.
- Makinodan, M., Rosen, K. M., Ito, S., & Corfas, G. (2012, September). A critical period for social experience-dependent oligodendrocyte maturation and myelination. *Science (New York, N.Y.)*, 337(6100), 1357–1360.
- Mangin, J.-M., Kunze, A., Chittajallu, R., & Gallo, V. (2008, July). Satellite NG2 progenitor cells share common glutamatergic inputs with associated interneurons in the mouse dentate gyrus. *The Journal of neuroscience : the official journal of the Society for Neuroscience*, 28(30), 7610–7623.
- Mangin, J.-M., Li, P., Scafidi, J., & Gallo, V. (2012, September). Experience-dependent regulation of NG2 progenitors in the developing barrel cortex. *Nature neuroscience*, 15(9), 1192–1194.
- Marin-Husstege, M., Muggironi, M., Liu, A., & Casaccia-Bonnel, P. (2002, December). Histone deacetylase activity is necessary for oligodendrocyte lineage progression. *The Journal of neuroscience : the official journal of the Society for Neuroscience*, 22(23), 10333–10345.
- Markham, J. A., Herting, M. M., Luszpak, A. E., Juraska, J. M., & Greenough, W. T. (2009, September). Myelination of the corpus callosum in male and female rats following complex environment housing during adulthood. *Brain research*, 1288, 9–17.
- Marques, S., Zeisel, A., Codeluppi, S., van Bruggen, D., Mendanha Falcão, A., Xiao, L., ... Castelo-Branco, G. (2016, June). Oligodendrocyte heterogeneity in the mouse juvenile and adult central nervous system. *Science (New York, N.Y.)*, 352(6291), 1326–1329.
- Marshall, G. P., Demir, M., Steindler, D. A., & Laywell, E. D. (2008, December). Subventricular zone microglia possess a unique capacity for massive in vitro expansion. *Glia*, 56(16), 1799–1808.
- Martynoga, B., Drechsel, D., & Guillemot, F. (2012, October). Molecular control of neurogenesis: a view from the mammalian cerebral cortex. *Cold Spring Harbor perspectives in biology*, 4(10), a008359–a008359.
- Masahira, N., Takebayashi, H., Ono, K., Watanabe, K., Ding, L., Furusho, M., ... Ikenaka, K. (2006, May). Olig2-positive progenitors in the embryonic spinal cord give rise not only to motoneurons and oligodendrocytes, but also to a subset of astrocytes and ependymal cells. *Developmental biology*, 293(2), 358–369.
- McFarland, H. F., & Martin, R. (2007, September). Multiple sclerosis: a complicated picture of autoimmunity. *Nature immunology*, 8(9), 913–919.
- McKenzie, I. A., Ohayon, D., Li, H., de Faria, J. P., Emery, B., Tohyama, K., & Richardson, W. D. (2014, October). Motor skill learning requires active central myelination. *Science (New York, N.Y.)*, 346(6207), 318–322.
- McKinnon, R. D. (1993, June). A role for TGF-beta in oligodendrocyte differentiation. *The Journal of cell biology*, 121(6), 1397–1407.
- McKinnon, R. D., Matsui, T., Dubois-Dalcq, M., & Aaronson, S. A. (1990, November). FGF modulates the PDGF-driven pathway of oligodendrocyte development. *Neuron*, 5(5), 603–614.

- McTigue, D. M., Tripathi, R., & Wei, P. (2006, April). NG2 colocalizes with axons and is expressed by a mixed cell population in spinal cord lesions. *Journal of neuropathology and experimental neurology*, 65(4), 406–420.
- Mei, F., Fancy, S. P. J., Shen, Y.-A. A., Niu, J., Zhao, C., Presley, B., . . . Chan, J. R. (2014, August). Micropillar arrays as a high-throughput screening platform for therapeutics in multiple sclerosis. *Nature medicine*, 20(8), 954–960.
- Mensch, S., Baraban, M., Almeida, R., Czopka, T., Ausborn, J., El Manira, A., & Lyons, D. A. (2015, May). Synaptic vesicle release regulates myelin sheath number of individual oligodendrocytes in vivo. *Nature neuroscience*, 18(5), 628–630.
- Merzbacher, L. (1910, January). Eine eigenartige familiär-hereditäre Erkrankungsform. *Zeitschrift für die gesamte Neurologie und Psychiatrie*.
- Micheva, K. D., Wolman, D., Mensch, B. D., Pax, E., Buchanan, J., Smith, S. J., & Bock, D. D. (2016, July). A large fraction of neocortical myelin ensheathes axons of local inhibitory neurons. *eLife*, 5, 3347.
- Mills, E. A., Davis, C.-h. O., Bushong, E. A., Boassa, D., Kim, K.-Y., Ellisman, M. H., & Marsh-Armstrong, N. (2015, August). Astrocytes phagocytose focal dystrophies from shortening myelin segments in the optic nerve of *Xenopus laevis* at metamorphosis. *Proceedings of the National Academy of Sciences of the United States of America*, 112(33), 10509–10514.
- Miron, V. E., Boyd, A., Zhao, J.-W., Yuen, T. J., Ruckh, J. M., Shadrach, J. L., . . . Ffrench-Constant, C. (2013, September). M2 microglia and macrophages drive oligodendrocyte differentiation during CNS remyelination. *Nature neuroscience*, 16(9), 1211–1218.
- Miyata, T., Kawaguchi, A., Saito, K., Kawano, M., Muto, T., & Ogawa, M. (2004, July). Asymmetric production of surface-dividing and non-surface-dividing cortical progenitor cells. *Development (Cambridge, England)*, 131(13), 3133–3145.
- Molofsky, A. V., Kelley, K. W., Tsai, H.-H., Redmond, S. A., Chang, S. M., Madireddy, L., . . . Rowitch, D. H. (2014, May). Astrocyte-encoded positional cues maintain sensorimotor circuit integrity. *Nature*, 509(7499), 189–194.
- Montag, D., Giese, K. P., Bartsch, U., Martini, R., Lang, Y., Blüthmann, H., . . . Nave, K. A. (1994, July). Mice deficient for the myelin-associated glycoprotein show subtle abnormalities in myelin. *Neuron*, 13(1), 229–246.
- Monteiro, R. A. (1983, August). Do the Purkinje cells have a special type of oligodendrocyte as satellites? *Journal of anatomy*, 137 (Pt 1)(Pt 1), 71–83.
- Moransard, M., Dann, A., Staszewski, O., Fontana, A., Prinz, M., & Suter, T. (2011, May). NG2 expressed by macrophages and oligodendrocyte precursor cells is dispensable in experimental autoimmune encephalomyelitis. *Brain : a journal of neurology*, 134(Pt 5), 1315–1330.
- Murray, J. A., & Blakemore, W. F. (1980, February). The relationship between internodal length and fibre diameter in the spinal cord of the cat. *Journal of the neurological sciences*, 45(1), 29–41.
- Murtie, J. C., Macklin, W. B., & Corfas, G. (2007, August). Morphometric analysis of oligodendrocytes in the adult mouse frontal cortex. *Journal of neuroscience research*, 85(10), 2080–2086.
- Nait Oumesmar, B., Vignais, L., Duhamel-Clérin, E., Avellana-Adalid, V., Rougon, G., & Baron-Van Evercooren, A. (1995, March). Expression of the highly polysialylated neural cell adhesion molecule during postnatal myelination and following chemically induced demyelination of the adult mouse spinal cord. *The*

- European journal of neuroscience*, 7(3), 480–491.
- Nave, K.-A. (2010, November). Myelination and support of axonal integrity by glia. *Nature*, 468(7321), 244–252.
- Nawaz, S., Sánchez, P., Schmitt, S., Snaidero, N., Mitkovski, M., Velte, C., . . . Simons, M. (2015, July). Actin filament turnover drives leading edge growth during myelin sheath formation in the central nervous system. *Developmental cell*, 34(2), 139–151.
- Neusch, C., Rozengurt, N., Jacobs, R. E., Lester, H. A., & Kofuji, P. (2001, August). Kir4.1 potassium channel subunit is crucial for oligodendrocyte development and in vivo myelination. *The Journal of neuroscience : the official journal of the Society for Neuroscience*, 21(15), 5429–5438.
- Neymeyer, V., Tephly, T. R., & Miller, M. W. (1997, August). Folate and 10-formyltetrahydrofolate dehydrogenase (FDH) expression in the central nervous system of the mature rat. *Brain research*, 766(1-2), 195–204.
- Nguyen, M. V. C., Felice, C. A., Du, F., Covey, M. V., Robinson, J. K., Mandel, G., & Ballas, N. (2013, November). Oligodendrocyte lineage cells contribute unique features to Rett syndrome neuropathology. *The Journal of neuroscience : the official journal of the Society for Neuroscience*, 33(48), 18764–18774.
- Nicholas, R. S., Stevens, S., Wing, M. G., & Compston, D. A. (2002, March). Microglia-derived IGF-2 prevents TNF α induced death of mature oligodendrocytes in vitro. *Journal of neuroimmunology*, 124(1-2), 36–44.
- Nicholas, R. S., Wing, M. G., & Compston, A. (2001, March). Nonactivated microglia promote oligodendrocyte precursor survival and maturation through the transcription factor NF-kappa B. *The European journal of neuroscience*, 13(5), 959–967.
- Noctor, S. C., Martínez-Cerdeño, V., Ivic, L., & Kriegstein, A. R. (2004, February). Cortical neurons arise in symmetric and asymmetric division zones and migrate through specific phases. *Nature neuroscience*, 7(2), 136–144.
- Norenberg, M. D. (1979, March). Distribution of glutamine synthetase in the rat central nervous system. *The journal of histochemistry and cytochemistry : official journal of the Histochemistry Society*, 27(3), 756–762.
- Ogawa, Y., Eins, S., & Wolff, J. R. (1985, June). Oligodendrocytes in the pons and middle cerebellar peduncle of the cat. *Cell and Tissue Research*, 240(3), 541–552.
- Osanai, Y., Shimizu, T., Mori, T., Yoshimura, Y., Hatanaka, N., Nambu, A., . . . Ikenaka, K. (2017, January). Rabies virus-mediated oligodendrocyte labeling reveals a single oligodendrocyte myelinates axons from distinct brain regions. *Glia*, 65(1), 93–105.
- Ottersen, O. P., Zhang, N., & Walberg, F. (1992). Metabolic compartmentation of glutamate and glutamine: morphological evidence obtained by quantitative immunocytochemistry in rat cerebellum. *Neuroscience*, 46(3), 519–534.
- Pajevic, S., Basser, P. J., & Fields, R. D. (2014, September). Role of myelin plasticity in oscillations and synchrony of neuronal activity. *Neuroscience*, 276, 135–147.
- Paolicelli, R. C., Bolasco, G., Pagani, F., Maggi, L., Scianni, M., Panzanelli, P., . . . Gross, C. T. (2011, September). Synaptic pruning by microglia is necessary for normal brain development. *Science (New York, N.Y.)*, 333(6048), 1456–1458.
- Pelizaeus, F. (1985, January). Ueber eine eigenthümliche Form spastischer Lähmung mit Cerebralerscheinungen auf hereditärer Grundlage. *European Archives of Psychiatry and Clinical*.
- Pelvig, D. P., Pakkenberg, H., Stark, A. K., & Pakkenberg, B. (2008, November).

- Neocortical glial cell numbers in human brains. *Neurobiology of aging*, 29(11), 1754–1762.
- Poduslo, S. E., & Norton, W. T. (1972, March). Isolation and some chemical properties of oligodendroglia from calf brain. *Journal of neurochemistry*, 19(3), 727–736.
- Poulsen, K. T., Armanini, M. P., Klein, R. D., Hynes, M. A., Phillips, H. S., & Rosenthal, A. (1994, November). TGF beta 2 and TGF beta 3 are potent survival factors for midbrain dopaminergic neurons. *Neuron*, 13(5), 1245–1252.
- Pringle, N. P., Mudhar, H. S., Collarini, E. J., & Richardson, W. D. (1992, June). PDGF receptors in the rat CNS: during late neurogenesis, PDGF alpha-receptor expression appears to be restricted to glial cells of the oligodendrocyte lineage. *Development (Cambridge, England)*, 115(2), 535–551.
- Pringle, N. P., & Richardson, W. D. (1993, February). A singularity of PDGF alpha-receptor expression in the dorsoventral axis of the neural tube may define the origin of the oligodendrocyte lineage. *Development (Cambridge, England)*, 117(2), 525–533.
- Psachoulia, K., Jamen, F., Young, K. M., & Richardson, W. D. (2009, November). Cell cycle dynamics of NG2 cells in the postnatal and ageing brain. *Neuron glia biology*, 5(3-4), 57–67.
- Qi, Y., Cai, J., Wu, Y., Wu, R., Lee, J., Fu, H., ... Qiu, M. (2001, July). Control of oligodendrocyte differentiation by the Nkx2.2 homeodomain transcription factor. *Development (Cambridge, England)*, 128(14), 2723–2733.
- Raff, M. C., Abney, E. R., Cohen, J., Lindsay, R., & Noble, M. (1983, June). Two types of astrocytes in cultures of developing rat white matter: differences in morphology, surface gangliosides, and growth characteristics. *The Journal of neuroscience : the official journal of the Society for Neuroscience*, 3(6), 1289–1300.
- Raff, M. C., Lillien, L. E., Richardson, W. D., Burne, J. F., & Noble, M. D. (1988, June). Platelet-derived growth factor from astrocytes drives the clock that times oligodendrocyte development in culture. *Nature*, 333(6173), 562–565.
- Raff, M. C., Miller, R. H., & Noble, M. (1983, June). A glial progenitor cell that develops in vitro into an astrocyte or an oligodendrocyte depending on culture medium. *Nature*, 303(5916), 390–396.
- Ramón y Cajal, S. (n.d.). *Histologie du systeme nerveux de l'homme et des vertebres*. Paris: Maloine.
- Ransohoff, R. M., & El Khoury, J. (2015, September). Microglia in Health and Disease. *Cold Spring Harbor perspectives in biology*, 8(1), a020560.
- Rasband, M. N., & Peles, E. (2015, September). The Nodes of Ranvier: Molecular Assembly and Maintenance. *Cold Spring Harbor perspectives in biology*, 8(3), a020495.
- Raz, N., Lindenberger, U., Rodrigue, K. M., Kennedy, K. M., Head, D., Williamson, A., ... Acker, J. D. (2005, November). Regional brain changes in aging healthy adults: general trends, individual differences and modifiers. *Cerebral cortex (New York, N.Y. : 1991)*, 15(11), 1676–1689.
- Readhead, C., & Hood, L. (1990, March). The dysmyelinating mouse mutations shiverer (shi) and myelin deficient (shimld). *Behavior genetics*, 20(2), 213–234.
- Redmond, S. A., Mei, F., Eshed-Eisenbach, Y., Osso, L. A., Leshkowitz, D., Shen, Y.-A. A., ... Chan, J. R. (2016, August). Somatodendritic Expression of JAM2 Inhibits Oligodendrocyte Myelination. *Neuron*, 91(4), 824–836.
- Redwine, J. M., & Armstrong, R. C. (1998, November). In vivo proliferation of oligodendrocyte progenitors expressing PDGFalphaR during early remyelination.

- Journal of neurobiology*, 37(3), 413–428.
- Remahl, S., & Hildebrand, C. (1982, April). Changing relation between onset of myelination and axon diameter range in developing feline white matter. *Journal of the neurological sciences*, 54(1), 33–45.
- Rios, J. C., Rubin, M., St Martin, M., Downey, R. T., Einheber, S., Rosenbluth, J., ... Salzer, J. L. (2003, August). Paranodal interactions regulate expression of sodium channel subtypes and provide a diffusion barrier for the node of Ranvier. *The Journal of neuroscience : the official journal of the Society for Neuroscience*, 23(18), 7001–7011.
- Rivers, L. E., Young, K. M., Rizzi, M., Jamen, F., Psachoulia, K., Wade, A., ... Richardson, W. D. (2008, December). PDGFRA/NG2 glia generate myelinating oligodendrocytes and piriform projection neurons in adult mice. *Nature neuroscience*, 11(12), 1392–1401.
- Rothman, D. L., De Feyter, H. M., de Graaf, R. A., Mason, G. F., & Behar, K. L. (2011, October). ¹³C MRS studies of neuroenergetics and neurotransmitter cycling in humans. *NMR in biomedicine*, 24(8), 943–957.
- Rowitch, D. H., & Kriegstein, A. R. (2010, November). Developmental genetics of vertebrate glial–cell specification. *Nature*, 468(7321), 214–222.
- Roy, K., Murtie, J. C., El-Khodor, B. F., Edgar, N., Sardi, S. P., Hooks, B. M., ... Corfas, G. (2007, May). Loss of erbB signaling in oligodendrocytes alters myelin and dopaminergic function, a potential mechanism for neuropsychiatric disorders. *Proceedings of the National Academy of Sciences of the United States of America*, 104(19), 8131–8136.
- Ruckh, J. M., Zhao, J.-W., Shadrach, J. L., van Wijngaarden, P., Rao, T. N., Wagers, A. J., & Franklin, R. J. M. (2012, January). Rejuvenation of regeneration in the aging central nervous system. *Cell stem cell*, 10(1), 96–103.
- Rudrabhatla, P., Jaffe, H., & Pant, H. C. (2011, November). Direct evidence of phosphorylated neuronal intermediate filament proteins in neurofibrillary tangles (NFTs): phosphoproteomics of Alzheimer's NFTs. *FASEB journal : official publication of the Federation of American Societies for Experimental Biology*, 25(11), 3896–3905.
- RUSHTON, W. A. H. (1951, September). A theory of the effects of fibre size in medullated nerve. *The Journal of physiology*, 115(1), 101–122.
- Saab, A. S., Tzvetavona, I. D., Trevisiol, A., Baltan, S., Dibaj, P., Kusch, K., ... Nave, K.-A. (2016, July). Oligodendroglial NMDA Receptors Regulate Glucose Import and Axonal Energy Metabolism. *Neuron*, 91(1), 119–132.
- Sakry, D., Neitz, A., Singh, J., Frischknecht, R., Marongiu, D., Binamé, F., ... Mittmann, T. (2014, November). Oligodendrocyte precursor cells modulate the neuronal network by activity-dependent ectodomain cleavage of glial NG2. *PLoS biology*, 12(11), e1001993.
- Salami, M., Itami, C., Tsumoto, T., & Kimura, F. (2003, May). Change of conduction velocity by regional myelination yields constant latency irrespective of distance between thalamus and cortex. *Proceedings of the National Academy of Sciences of the United States of America*, 100(10), 6174–6179.
- Sampaio-Baptista, C., Khrapitchev, A. A., Foxley, S., Schlagheck, T., Scholz, J., Jbabdi, S., ... Johansen-Berg, H. (2013, December). Motor skill learning induces changes in white matter microstructure and myelination. *The Journal of neuroscience : the official journal of the Society for Neuroscience*, 33(50), 19499–19503.
- Sánchez, I., Hassinger, L., Paskevich, P. A., Shine, H. D., & Nixon, R. A. (1996,

- August). Oligodendroglia regulate the regional expansion of axon caliber and local accumulation of neurofilaments during development independently of myelin formation. *Journal of Neuroscience*, *16*(16), 5095–5105.
- Schafer, D. P., Lehrman, E. K., Kautzman, A. G., Koyama, R., Mardinly, A. R., Yamasaki, R., . . . Stevens, B. (2012, May). Microglia sculpt postnatal neural circuits in an activity and complement-dependent manner. *Neuron*, *74*(4), 691–705.
- Schlegel, A. A., Rudelson, J. J., & Tse, P. U. (2012, August). White matter structure changes as adults learn a second language. *Journal of cognitive neuroscience*, *24*(8), 1664–1670.
- Schnädelbach, O., & Fawcett, J. W. (2001). Astrocyte influences on oligodendrocyte progenitor migration. *Progress in brain research*, *132*, 97–102.
- Schneider, S., Gruart, A., Grade, S., Zhang, Y., Kröger, S., Kirchhoff, F., . . . Dimou, L. (2016, December). Decrease in newly generated oligodendrocytes leads to motor dysfunctions and changed myelin structures that can be rescued by transplanted cells. *Glia*, *64*(12), 2201–2218.
- Scholz, J., Klein, M. C., Behrens, T. E. J., & Johansen-Berg, H. (2009, November). Training induces changes in white-matter architecture. *Nature neuroscience*, *12*(11), 1370–1371.
- Schulz, C., Gomez Perdiguero, E., Chorro, L., Szabo-Rogers, H., Cagnard, N., Kierdorf, K., . . . Geissmann, F. (2012, April). A lineage of myeloid cells independent of Myb and hematopoietic stem cells. *Science (New York, N.Y.)*, *336*(6077), 86–90.
- See, J., Zhang, X., Eraydin, N., Mun, S.-B., Mamontov, P., Golden, J. A., & Grinspan, J. B. (2004, August). Oligodendrocyte maturation is inhibited by bone morphogenetic protein. *Molecular and cellular neurosciences*, *26*(4), 481–492.
- Seidl, A. H., Rubel, E. W., & Barría, A. (2014, April). Differential conduction velocity regulation in ipsilateral and contralateral collaterals innervating brainstem coincidence detector neurons. *The Journal of neuroscience : the official journal of the Society for Neuroscience*, *34*(14), 4914–4919.
- Shen, S., Liu, A., Li, J., Wolubah, C., & Casaccia-Bonnel, P. (2008, March). Epigenetic memory loss in aging oligodendrocytes in the corpus callosum. *Neurobiology of aging*, *29*(3), 452–463.
- Shen, S., Sandoval, J., Swiss, V. A., Li, J., Dupree, J., Franklin, R. J. M., & Casaccia-Bonnel, P. (2008, September). Age-dependent epigenetic control of differentiation inhibitors is critical for remyelination efficiency. *Nature neuroscience*, *11*(9), 1024–1034.
- Sim, F. J., Zhao, C., Penderis, J., & Franklin, R. J. M. (2002, April). The age-related decrease in CNS remyelination efficiency is attributable to an impairment of both oligodendrocyte progenitor recruitment and differentiation. *The Journal of neuroscience : the official journal of the Society for Neuroscience*, *22*(7), 2451–2459.
- Simeone, A., Gulisano, M., Acampora, D., Stornaiuolo, A., Rambaldi, M., & Boncinelli, E. (1992, July). Two vertebrate homeobox genes related to the *Drosophila* empty spiracles gene are expressed in the embryonic cerebral cortex. *The EMBO journal*, *11*(7), 2541–2550.
- Smith, C. M., Cooksey, E., & Duncan, I. D. (2013, February). Myelin loss does not lead to axonal degeneration in a long-lived model of chronic demyelination. *The Journal of neuroscience : the official journal of the Society for Neuroscience*, *33*(6), 2718–2727.

- Smith, M. E., & Eng, L. F. (1965, December). The turnover of the lipid components of myelin. *Journal of the American Oil Chemists' Society*, 42(12), 1013–1018.
- Snaidero, N., Möbius, W., Czopka, T., Hekking, L. H. P., Mathisen, C., Verkleij, D., ... Simons, M. (2014, January). Myelin membrane wrapping of CNS axons by PI(3,4,5)P3-dependent polarized growth at the inner tongue. *Cell*, 156(1-2), 277–290.
- Snaidero, N., Velte, C., Myllykoski, M., Raasakka, A., Ignatev, A., Werner, H. B., ... Simons, M. (2017, January). Antagonistic Functions of MBP and CNP Establish Cytosolic Channels in CNS Myelin. *Cell reports*, 18(2), 314–323.
- Sobel, R. A., Greer, J. M., Isaac, J., Fondren, G., & Lees, M. B. (1994, January). Immunolocalization of proteolipid protein peptide 103-116 in myelin. *Journal of neuroscience research*, 37(1), 36–43.
- Somjen, G. G. (1988). Nervenkitz: notes on the history of the concept of neuroglia. *Glia*, 1(1), 2–9.
- Sommer, I., & Schachner, M. (1981, April). Monoclonal antibodies (O1 to O4) to oligodendrocyte cell surfaces: an immunocytological study in the central nervous system. *Developmental biology*, 83(2), 311–327.
- Sontheimer, H., Trotter, J., Schachner, M., & Kettenmann, H. (1989, February). Channel expression correlates with differentiation stage during the development of oligodendrocytes from their precursor cells in culture. *Neuron*, 2(2), 1135–1145.
- Sortwell, C. E., Daley, B. F., Pitzer, M. R., McGuire, S. O., Sladek, J. R., & Collier, T. J. (2000, October). Oligodendrocyte-type 2 astrocyte-derived trophic factors increase survival of developing dopamine neurons through the inhibition of apoptotic cell death. *The Journal of Comparative Neurology*, 426(1), 143–153.
- Stankoff, B., Aigrot, M.-S., Noël, F., Wattilliaux, A., Zalc, B., & Lubetzki, C. (2002, November). Ciliary neurotrophic factor (CNTF) enhances myelin formation: a novel role for CNTF and CNTF-related molecules. *The Journal of neuroscience : the official journal of the Society for Neuroscience*, 22(21), 9221–9227.
- Steinhäuser, C., Jabs, R., & Kettenmann, H. (1994, February). Properties of GABA and glutamate responses in identified glial cells of the mouse hippocampal slice. *Hippocampus*, 4(1), 19–35.
- Sternberger, N. H., Itoyama, Y., Kies, M. W., & Webster, H. D. (1978, May). Myelin basic protein demonstrated immunocytochemically in oligodendroglia prior to myelin sheath formation. *Proceedings of the National Academy of Sciences of the United States of America*, 75(5), 2521–2524.
- Sternberger, N. H., Quarles, R. H., Itoyama, Y., & Webster, H. D. (1979, March). Myelin-associated glycoprotein demonstrated immunocytochemically in myelin and myelin-forming cells of developing rat. *Proceedings of the National Academy of Sciences of the United States of America*, 76(3), 1510–1514.
- Stevens, B., Allen, N. J., Vazquez, L. E., Howell, G. R., Christopherson, K. S., Nouri, N., ... Barres, B. A. (2007, December). The classical complement cascade mediates CNS synapse elimination. *Cell*, 131(6), 1164–1178.
- Stolt, C. C., Rehberg, S., Ader, M., Lommes, P., Riethmacher, D., Schachner, M., ... Wegner, M. (2002, January). Terminal differentiation of myelin-forming oligodendrocytes depends on the transcription factor Sox10. *Genes & development*, 16(2), 165–170.
- Stolt, C. C., Schlierf, A., Lommes, P., Hillgärtner, S., Werner, T., Kosian, T., ... Wegner, M. (2006, November). SoxD proteins influence multiple stages of oligodendrocyte development and modulate SoxE protein function. *Develop-*

- mental cell*, 11(5), 697–709.
- Sugiarto, S., Persson, A. I., Munoz, E. G., Waldhuber, M., Lamagna, C., Andor, N., ... Petritsch, C. (2011, September). Asymmetry-defective oligodendrocyte progenitors are glioma precursors. *Cancer cell*, 20(3), 328–340.
- Suh, S. W., Bergher, J. P., Anderson, C. M., Treadway, J. L., Fosgerau, K., & Swanson, R. A. (2007, April). Astrocyte glycogen sustains neuronal activity during hypoglycemia: studies with the glycogen phosphorylase inhibitor CP-316,819 ([R-R*,S*]-5-chloro-N-[2-hydroxy-3-(methoxymethylamino)-3-oxo-1-(phenylmethyl)propyl]-1H-indole-2-carboxamide). *The Journal of pharmacology and experimental therapeutics*, 321(1), 45–50.
- Takeuchi, H., Sekiguchi, A., Taki, Y., Yokoyama, S., Yomogida, Y., Komuro, N., ... Kawashima, R. (2010, March). Training of working memory impacts structural connectivity. *The Journal of neuroscience : the official journal of the Society for Neuroscience*, 30(9), 3297–3303.
- Tanaka, H., Ma, J., Tanaka, K. F., Takao, K., Komada, M., Tanda, K., ... Ikenaka, K. (2009, July). Mice with altered myelin proteolipid protein gene expression display cognitive deficits accompanied by abnormal neuron-glia interactions and decreased conduction velocities. *The Journal of neuroscience : the official journal of the Society for Neuroscience*, 29(26), 8363–8371.
- Tanaka, Y., Tozuka, Y., Takata, T., Shimazu, N., Matsumura, N., Ohta, A., & Hisatsune, T. (2009, September). Excitatory GABAergic activation of cortical dividing glial cells. *Cerebral cortex (New York, N.Y. : 1991)*, 19(9), 2181–2195.
- Taubert, M., Draganski, B., Anwander, A., Müller, K., Horstmann, A., Villringer, A., & Ragert, P. (2010, September). Dynamic properties of human brain structure: learning-related changes in cortical areas and associated fiber connections. *The Journal of neuroscience : the official journal of the Society for Neuroscience*, 30(35), 11670–11677.
- Tomassy, G. S., Berger, D. R., Chen, H.-H., Kasthuri, N., Hayworth, K. J., Vercelli, A., ... Arlotta, P. (2014, April). Distinct profiles of myelin distribution along single axons of pyramidal neurons in the neocortex. *Science (New York, N.Y.)*, 344(6181), 319–324.
- Toyama, B. H., Savas, J. N., Park, S. K., Harris, M. S., Ingolia, N. T., Yates, J. R., & Hetzer, M. W. (2013, August). Identification of long-lived proteins reveals exceptional stability of essential cellular structures. *Cell*, 154(5), 971–982.
- Trapp, B. D., Nishiyama, A., Cheng, D., & Macklin, W. (1997, April). Differentiation and death of premyelinating oligodendrocytes in developing rodent brain. *The Journal of cell biology*, 137(2), 459–468.
- Tremblay, M.-È., Lowery, R. L., & Majewska, A. K. (2010, November). Microglial interactions with synapses are modulated by visual experience. *PLoS biology*, 8(11), e1000527.
- Tress, O., Maglione, M., May, D., Pivneva, T., Richter, N., Seyfarth, J., ... Willecke, K. (2012, May). Panglial gap junctional communication is essential for maintenance of myelin in the CNS. *The Journal of neuroscience : the official journal of the Society for Neuroscience*, 32(22), 7499–7518.
- Trevisiol, A., Saab, A. S., Winkler, U., Marx, G., Imamura, H., Möbius, W., ... Hirrlinger, J. (2017, April). Monitoring ATP dynamics in electrically active white matter tracts. *eLife*, 6, 27.
- Tripathi, R. B., Clarke, L. E., Burzomato, V., Kessaris, N., Anderson, P. N., Attwell, D., & Richardson, W. D. (2011a, May). Dorsally and ventrally derived oligodendrocytes have similar electrical properties but myelinate preferred tracts. *The*

- Journal of neuroscience : the official journal of the Society for Neuroscience*, 31(18), 6809–6819.
- Tripathi, R. B., Clarke, L. E., Burzomato, V., Kessar, N., Anderson, P. N., Attwell, D., & Richardson, W. D. (2011b, May). Dorsally and Ventrally Derived Oligodendrocytes Have Similar Electrical Properties but Myelinate Preferred Tracts. *The Journal of neuroscience : the official journal of the Society for Neuroscience*, 31(18), 6809–6819.
- Tsai, H.-H., Li, H., Fuentealba, L. C., Molofsky, A. V., Taveira-Marques, R., Zhuang, H., . . . Rowitch, D. H. (2012, July). Regional astrocyte allocation regulates CNS synaptogenesis and repair. *Science (New York, N.Y.)*, 337(6092), 358–362.
- Tsai, H.-H., Niu, J., Munji, R., Davalos, D., Chang, J., Zhang, H., . . . Fancy, S. P. J. (2016, January). Oligodendrocyte precursors migrate along vasculature in the developing nervous system. *Science (New York, N.Y.)*, 351(6271), 379–384.
- Tse, K.-H., & Herrup, K. (2017, January). DNA damage in the oligodendrocyte lineage and its role in brain aging. *Mechanisms of ageing and development*, 161(Pt A), 37–50.
- Tustison, N. J., Avants, B. B., Cook, P. A., Zheng, Y., Egan, A., Yushkevich, P. A., & Gee, J. C. (2010, June). N4ITK: improved N3 bias correction. *IEEE transactions on medical imaging*, 29(6), 1310–1320.
- Tyler, W. A., Gangoli, N., Gokina, P., Kim, H. A., Covey, M., Levison, S. W., & Wood, T. L. (2009, May). Activation of the mammalian target of rapamycin (mTOR) is essential for oligodendrocyte differentiation. *The Journal of neuroscience : the official journal of the Society for Neuroscience*, 29(19), 6367–6378.
- Uchida, T., Pappenheimer, A. M., & Harper, A. A. (1972, February). Reconstitution of diphtheria toxin from two nontoxic cross-reacting mutant proteins. *Science (New York, N.Y.)*, 175(4024), 901–903.
- Vallstedt, A., Klos, J. M., & Ericson, J. (2005, January). Multiple dorsoventral origins of oligodendrocyte generation in the spinal cord and hindbrain. *Neuron*, 45(1), 55–67.
- van den Berg, C. J., & Garfinkel, D. (1971, June). A simulation study of brain compartments. Metabolism of glutamate and related substances in mouse brain. *The Biochemical journal*, 123(2), 211–218.
- Viganò, F., Möbius, W., Götz, M., & Dimou, L. (2013, October). Transplantation reveals regional differences in oligodendrocyte differentiation in the adult brain. *Nature neuroscience*, 16(10), 1370–1372.
- Vinet, J., Lemieux, P., Tamburri, A., Tiesinga, P., Scafidi, J., Gallo, V., & Sik, A. (2010, February). Subclasses of oligodendrocytes populate the mouse hippocampus. *The European journal of neuroscience*, 31(3), 425–438.
- Wang, S., Sdrulla, A. D., diSibio, G., Bush, G., Nofziger, D., Hicks, C., . . . Barres, B. A. (1998, July). Notch receptor activation inhibits oligodendrocyte differentiation. *Neuron*, 21(1), 63–75.
- Weng, Q., Chen, Y., Wang, H., Xu, X., Yang, B., He, Q., . . . Lu, Q. R. (2012, February). Dual-mode modulation of Smad signaling by Smad-interacting protein Sip1 is required for myelination in the central nervous system. *Neuron*, 73(4), 713–728.
- Weruaga-Prieto, E., Egger, P., & Celio, M. R. (1996, January). Topographic variations in rat brain oligodendrocyte morphology elucidated by injection of Lucifer Yellow in fixed tissue slices. *Journal of Neurocytology*, 25(1), 19–31.
- Wilkins, A., Chandran, S., & Compston, A. (2001, October). A role for oligodendrocyte-derived IGF-1 in trophic support of cortical neurons. *Glia*, 36(1), 48–57.

- Wilkins, A., Majed, H., Layfield, R., Compston, A., & Chandran, S. (2003, June). Oligodendrocytes promote neuronal survival and axonal length by distinct intracellular mechanisms: a novel role for oligodendrocyte-derived glial cell line-derived neurotrophic factor. *The Journal of neuroscience : the official journal of the Society for Neuroscience*, 23(12), 4967–4974.
- Williams, P. L., & Wendell-Smith, C. P. (1971, September). Some additional parametric variations between peripheral nerve fibre populations. *Journal of anatomy*, 109(Pt 3), 505–526.
- Windrem, M. S., Osipovitch, M., Liu, Z., Bates, J., Chandler-Militello, D., Zou, L., . . . Goldman, S. A. (2017, August). Human iPSC Glial Mouse Chimeras Reveal Glial Contributions to Schizophrenia. *Cell stem cell*, 21(2), 195–208.e6.
- Wyllie, D. J., Mathie, A., Symonds, C. J., & Cull-Candy, S. G. (1991, January). Activation of glutamate receptors and glutamate uptake in identified macroglial cells in rat cerebellar cultures. *The Journal of physiology*, 432, 235–258.
- Xiao, L., Ohayon, D., McKenzie, I. A., Sinclair-Wilson, A., Wright, J. L., Fudge, A. D., . . . Richardson, W. D. (2016, September). Rapid production of new oligodendrocytes is required in the earliest stages of motor-skill learning. *Nature neuroscience*, 19(9), 1210–1217.
- Xie, F., Fu, H., Zhang, J.-C., Chen, X.-F., Wang, X.-L., & Chen, J. (2014, July). Gene profiling in the dynamic regulation of the lifespan of the myelin sheath structure in the optic nerve of rats. *Molecular medicine reports*, 10(1), 217–222.
- Xie, F., Liang, P., Fu, H., Zhang, J.-C., & Chen, J. (2014, July). Effects of normal aging on myelin sheath ultrastructures in the somatic sensorimotor system of rats. *Molecular medicine reports*, 10(1), 459–466.
- Xie, F., Zhang, J.-C., Fu, H., & Chen, J. (2013, November). Age-related decline of myelin proteins is highly correlated with activation of astrocytes and microglia in the rat CNS. *International journal of molecular medicine*, 32(5), 1021–1028.
- Yamada, J., & Jinno, S. (2014, August). Age-related differences in oligodendrogenesis across the dorsal-ventral axis of the mouse hippocampus. *Hippocampus*, 24(8), 1017–1029.
- Yamaizumi, M., Mekada, E., Uchida, T., & Okada, Y. (1978, September). One molecule of diphtheria toxin fragment A introduced into a cell can kill the cell. *Cell*, 15(1), 245–250.
- Ye, F., Chen, Y., Hoang, T., Montgomery, R. L., Zhao, X.-h., Bu, H., . . . Lu, Q. R. (2009, July). HDAC1 and HDAC2 regulate oligodendrocyte differentiation by disrupting the beta-catenin-TCF interaction. *Nature neuroscience*, 12(7), 829–838.
- Young, K. M., Psachoulia, K., Tripathi, R. B., Dunn, S.-J., Cossell, L., Attwell, D., . . . Richardson, W. D. (2013, March). Oligodendrocyte dynamics in the healthy adult CNS: evidence for myelin remodeling. *Neuron*, 77(5), 873–885.
- Yuan, X., Eisen, A. M., McBain, C. J., & Gallo, V. (1998, August). A role for glutamate and its receptors in the regulation of oligodendrocyte development in cerebellar tissue slices. *Development (Cambridge, England)*, 125(15), 2901–2914.
- Yue, T., Xian, K., Hurlock, E., Xin, M., Kernie, S. G., Parada, L. F., & Lu, Q. R. (2006, January). A critical role for dorsal progenitors in cortical myelination. *The Journal of neuroscience : the official journal of the Society for Neuroscience*, 26(4), 1275–1280.
- Zatorre, R. J., Fields, R. D., & Johansen-Berg, H. (2012, March). Plasticity in gray and white: neuroimaging changes in brain structure during learning. *Nature neuroscience*, 15(4), 528–536.

- Zawadzka, M., Rivers, L. E., Fancy, S. P. J., Zhao, C., Tripathi, R., Jamen, F., ... Franklin, R. J. M. (2010, June). CNS-resident glial progenitor/stem cells produce Schwann cells as well as oligodendrocytes during repair of CNS demyelination. *Cell stem cell*, 6(6), 578–590.
- Zhang, X., Surguladze, N., Slagle-Webb, B., Cozzi, A., & Connor, J. R. (2006, December). Cellular iron status influences the functional relationship between microglia and oligodendrocytes. *Glia*, 54(8), 795–804.
- Zhang, Y., Argaw, A. T., Gurfein, B. T., Zameer, A., Snyder, B. J., Ge, C., ... John, G. R. (2009, November). Notch1 signaling plays a role in regulating precursor differentiation during CNS remyelination. *Proceedings of the National Academy of Sciences of the United States of America*, 106(45), 19162–19167.
- Zhang, Y., Chen, K., Sloan, S. A., Bennett, M. L., Scholze, A. R., O’Keeffe, S., ... Wu, J. Q. (2014, September). An RNA-sequencing transcriptome and splicing database of glia, neurons, and vascular cells of the cerebral cortex. *The Journal of neuroscience : the official journal of the Society for Neuroscience*, 34(36), 11929–11947.
- Zhang, Y., Sloan, S. A., Clarke, L. E., Caneda, C., Plaza, C. A., Blumenthal, P. D., ... Barres, B. A. (2016, January). Purification and Characterization of Progenitor and Mature Human Astrocytes Reveals Transcriptional and Functional Differences with Mouse. *Neuron*, 89(1), 37–53.
- Zhao, C., Li, W.-W., & Franklin, R. J. M. (2006, September). Differences in the early inflammatory responses to toxin-induced demyelination are associated with the age-related decline in CNS remyelination. *Neurobiology of aging*, 27(9), 1298–1307.
- Zhao, C., Ma, D., Zawadzka, M., Fancy, S. P. J., Elis-Williams, L., Bouvier, G., ... Franklin, R. J. M. (2015, August). Sox2 Sustains Recruitment of Oligodendrocyte Progenitor Cells following CNS Demyelination and Primes Them for Differentiation during Remyelination. *The Journal of neuroscience : the official journal of the Society for Neuroscience*, 35(33), 11482–11499.
- Zhou, Q., & Anderson, D. J. (2002, April). The bHLH transcription factors OLIG2 and OLIG1 couple neuronal and glial subtype specification. *Cell*, 109(1), 61–73.
- Zhou, Q., Wang, S., & Anderson, D. J. (2000, February). Identification of a novel family of oligodendrocyte lineage-specific basic helix-loop-helix transcription factors. *Neuron*, 25(2), 331–343.
- Zhu, Q., Whitemore, S. R., Devries, W. H., Zhao, X., Kuypers, N. J., & Qiu, M. (2011, June). Dorsally-derived oligodendrocytes in the spinal cord contribute to axonal myelination during development and remyelination following focal demyelination. *Glia*, 59(11), 1612–1621.
- Zhu, Q., Zhao, X., Zheng, K., Li, H., Huang, H., Zhang, Z., ... Qiu, M. (2014, February). Genetic evidence that Nkx2.2 and Pdgfra are major determinants of the timing of oligodendrocyte differentiation in the developing CNS. *Development (Cambridge, England)*, 141(3), 548–555.
- Ziskin, J. L., Nishiyama, A., Rubio, M., Fukaya, M., & Bergles, D. E. (2007, March). Vesicular release of glutamate from unmyelinated axons in white matter. *Nature neuroscience*, 10(3), 321–330.

Appendix 1

Perfusion: Paraformaldehyde (PFA)

Component	Vendor	Amount
PFA	Sigma	40g
1x PBS	n/a	1l

Table 7.1 **Formulation of PFA.**

800ml 1x PBS were heated up to 50-60°C, before 40g PFA (Sigma) were added. Solution was stirred continuously on a hot plate at a temperature below 60°C until fully dissolved. PFA solution was cooled down to RT and the pH was adjusted to 7.2-7.4. Next, the PFA solution was filled up to a litre and filtered through a Whatman paper (Sigma). PFA solution was stored at 4°C until use. PFA not be used for longer than 7 days.

Perfusion: Glutaraldehyde

Component	Vendor	Amount
Glutaraldehyde (25%)	Agar Scientific	4%
Calcium chloride (CaCl) (1%)	Sigma	0.008%
PBS	n/a	n/a

Table 7.2 **Formulation of glutaraldehyde.**

Chemical	μm	MW	mg/5l
Amino Acids			
Glycine	400	75.07	150.1
L-Alanine	22	89.09	9.8
L- Arginine hydrochloride	483	174.2	420.7
L-Asparagine-H ₂ O	5.5	150.13	4.1
L-Cysteine hydrochloride-H ₂ O	7.7	313.2	12.1
L-Histidine hydrochloride-H ₂ O	200	209.6	209.6
L-Isoleucine	802	131.2	526.1
L-Leucine	802	131.2	526.1
L-Lysine hydrochloride	798	146.2	583.3
L-Methionine	201	149.2	149.9
L-Phenylalanine	400	165.2	330.4
L-Proline	67	115.1	38.6
L-Serine	400	105	210
L-Threonine	798	119	474.8
L-Tryptophan	78	204.2	79.6
L- Tyrosine disodium salt dihydrate	398	181.2	360.6
L-Valine	803	117.2	470.6
Vitamines			
Choline chloride	28	139.6	19.6
D-Calcium pantothenate	8	238.3	9.5
Niacinamide	30	122	18.3
Pyridoxine hydrochloride	20	206	20.6
Thiamine hydrochloride	10	337	16.9
i-Inositol	40	180.2	36
Inorganic salts			
Ferric nitrate (Fe(NO ₃) ₃ 9H ₂ O)	0.25	404	0.5
Potassium chloride (KCl)	5360	74.6	1997.9
Sodium Bicarbonate (NaHCO ₃)	880	84	369.6
Sodium chloride (NaCl)	89000	58	25810
Sodium phosphate dibasic (Na ₂ HPO ₄) anhydrous	906	120	543.6
Zinc sulfate (ZnSO ₄ 7H ₂ O)	0.67	287.6	0.96
Other components			
D-Glucose	25000	180.2	22525
Sodium pyruvate	227	110	124.9
MOPS	10000	269.3	12465

Table 7.3 **Formulation of Half.** All chemicals were purchased from Sigma. Formulation was developed by Björn Neumann (Franklin laboratory, University of Cambridge).

Cell isolation: Transport medium

Component	Vendor	Amount
Half	made in house	n/a
B27	Gibco	2%
Pen/Strep	Gibco	1%
NAC	Sigma	500nM

Table 7.4 **Formulation of transport medium.****Cell isolation: Dissociation solution**

Component	Vendor	Amount
Half	made in house	n/a
Papain	Worthington	24mg/ml
DNase 1 Type IV	Sigma	160 μ g/ml
NAC	Sigma	500nM

Table 7.5 **Formulation of dissociation solution.****Cell isolation: Trituration solution**

Component	Vendor	Amount
Half	made in house	n/a
B27	Gibco	2%
Sodium pyruvate	Gibco	1%
NAC	Sigma	500nM

Table 7.6 **Formulation of trituration solution.****Mounting medium: Mowiol**

Component	Vendor	Amount
Mowiol	Calbiochem	133.3 g/l
Glycerol	Sigma	333.3 g/l
0.2M Tris (pH 8.5)	Sigma	66.6%
DABCO	Sigma	2.5%
dH ₂ O	n/a	n/a

Table 7.7 **Formulation of mowiol.**

The mowiol and glycerol were mixed, before added to the water and Tris, and agitated for 12hrs at RT to dissolve. The solution was heated to 50°C for 10min whilst stirring continuously. Centrifugation at 800g for 20min was performed to clarify the solution. The DABCO was added, the solution aliquoted and stored at -20°C.

Resin Embedding: Resin

Component	Vendor	Amount
Resin	TAAB Laboratories	50%
Dodecyl succinic anhydride (DDSA)	TAAB Laboratories	34%
Methyl nadic anhydride (MNA)	TAAB Laboratories	16%
2,4,6-Tris(dimethylaminomethyl)phenol (DMP-30)	TAAB Laboratories	2%

Table 7.8 **Formulation of resin.**

DMP-30 is a chelator, hence it always needs to be added last. Resin must always be prepared freshly.

Western Blot: Running buffer

Component	Vendor	Amount
Bolt™ MOPS buffer (20x)	Thermo Fisher	5%
dH ₂ O	n/a	n/a

Table 7.9 **Formulation of western blot running buffer.**

Western Blot: Transfer buffer

Component	Vendor	Amount
Bolt™ transfer buffer (20x)	Thermo Fisher	5%
Methanol	Sigma	10%
Bolt™ Antioxidant	Thermo Fisher	0.1%
dH ₂ O	n/a	n/a

Table 7.10 **Formulation of western blot transfer buffer.**